ELECTRICAL RESPONSES OF NEURAL UNITS IN THE ANTEROVENTRAL COCHLEAR NUCLEUS OF THE CAT

by

Terrance Raymond Bourk

B.A.Sc., University of British Columbia
(1967)

S.M., Massachusetts Institute of Technology
(1970)

SUBMITTED IN PARTIAL FULFILLMENT OF THE

REQUIREMENTS FOR THE DEGREE OF

DOCTOR OF PHILOSOPHY

at the

MASSACHUSETTS INSTITUTE OF TECHNOLOGY

September 1976

VOL. I

Signature of Author .....
Department of Electrical Engineering and
Computer Science, June 30, 1976

Certified by .....
Thesis Supervisor

Accepted
Chairman, Departmental Committee on Graduate Students

ELECTRICAL RESPONSES OF NEURAL UNITS IN THE ANTEROVENTRAL COCHLEAR NUCLEUS OF THE CAT

by

Terrance Raymond Bourk

Submitted to the department of Electrical Engineering and Computer Science on June 30, 1976 in partial fulfillment of the requirements for the Degree of Doctor of Philosophy

ABSTRACT

Single unit activity was recorded in the anteroventral cochlear nucleus (AVCN) of barbiturate-anesthetized cats. Spike waveforms were carefully examined to determine the presence or absence of prepotentials and their waveforms. Categories of units were established based on prepotential characteristics. A second set of categories is based on response patterns to tone bursts and continuous tone. These two categorizations of the units were found to be strongly related, in that units exhibiting a prepotential almost always have response patterns resembling those of auditory nerve units.

The usefulness of the prepotential and response pattern distinctions is enhanced by the fact that many other physiological characteristics of units are correlated with the categories.

The categories show strong correlations with the unit locations in the nucleus. In many cases the unit categories seem to correspond with morphologically distinguishable cell types. Units that exhibit a prepotential appear to be bushy cells that receive inputs from auditory nerve fibers via end-bulbs. Units that do not exhibit a prepotential may be stellate cells that receive small endings from the auditory nerve fibers. Further correlations with anatomy were obtained by electrically stimulating the output tracts and projection sites of AVCN cells. A farily complete description of the AVCN, consistent with all the empirical data, is presented in this thesis.

THESIS SUPERVISOR: William T. Peake

TITLE: Professor of Electrical Engineering and Computer Science

ACKNOWLEDGMENTS

Throughout my thesis research Dr. Nelson Y.S. Kiang has been a major influence. He has provided, both personally and through his administering of the Eaton-Peabody Laboratory, an environment in which the readily available advice and assistance made my research more enjoyable and, at times, even made it seem feasible. Many of the particular topics examined in this study are based on the earlier research of Nelson Kiang, his former students and colleagues. Nelson must also receive credit for having braved the first draft of the thesis - a formidable task.

I would like to thank Professor William T. Peake for his continuing support through my many years at M.I.T.; both his efforts to sustain my financial support and his careful criticism and thoughtful enquiry into my findings are much appreciated.

Many of the people affiliated with the Eaton-Peabody Laboratory contributed to my research and education. Dr. Donald A. Godfrey provided a careful introduction to experimental techniques for single unit recording and localization of recording sites in the cochlear nucleus. Barbara E. Norris performed a major role in the documentation and analysis of the experimental results. She prepared the histological material and taught and assisted me in the interpretation of the histology. Without Barbara's conscientious and knowledgeable assistance in the analysis of the data, many aspects of the present results would not have been examined. The involved surgical preparation for the experiments was ably performed by

Elizabeth M. Marr, Catherine L. Pike and Susan M. Liberman. The thesis figures were prepared by Elizabeth M. Marr and Susan M. Liberman. Numerous other people at Eaton-Peabody Laboratory contributed to my research; Drs. Don H. Johnson, Edwin C. Moxon and John J. Guinan, Jr. were particularly helpful.

I would like to thank Dr. Joe C. Adams for urging me to try antidromic stimulation from the inferior colliculus and for subsequently providing anatomical findings that helped in the interpretation of the physiological data.

The discussions and anatomical data freely offered by Drs. D. Kent Morest, W. Bruce Warr and Nell B. Cant are greatly appreciated. I am particularly grateful to Kent Morest for his helpful instruction on the recognition of the AVCN subdivisions and for the time he spent determining the complete set of cochlear nucleus subdivision boundaries for the block model sections. Bruce Warr generously shared his unpublished data and ideas on projections from the cochlear nucleus and on axonal populations of the trapezoid body.

I would like to thank Professors H. Steven Colburn and Lawrence S. Frishkopf for their helpful criticisms of the thesis.

I gratefully acknowledge the fellowship which the Grass Instrument Company provided during a time period in which my research assistantship had lapsed.

TABLE OF CONTENTS

Page

LIST of FIGURES

LIST of TABLES

CHAPTER I

INTRODUCTION

The cochlear nucleus (CN) is an essential link in the ascending auditory pathway of mammals. Acoustic stimuli are converted by the cochlea to neural discharges in fibers of the auditory nerve (AN) all of which enter and terminate within the nucleus. The information carried by these fibers is therefore available to the central nervous system (CNS) only through the outputs of CN cells. Many of these cells send their axons to other parts of the central nervous system including, for example, the superior olivary complex, the nuclei of the lateral lemniscus, and the inferior colliculus. Cells in these regions, in turn, provide ascending projections to more central structures as well as descending projections to the CN and more peripheral structures.

As a part of any systematic study of the auditory system it is necessary to know how cells in the CN respond to acoustic stimuli and what their detailed functional connections are to the other parts of the central nervous system. These two goals guided much of the present study.

In a broader context, however, this study has implications for general neurophysiology in that the CN provides a collection of well-studied neurons with interconnections that appear to be simple enough to begin a detailed analysis at the present time yet sufficiently complicated so that the principles of organization might be realistically applicable to other areas of the mammalian CNS. As an experimental preparation, the cat CN has the advantage of being a superficial, accessible and well-defined protrusion from the lateral edge of the brainstem. A number of classical, as well as more recent, anatomical

studies have described the structural composition of the CN in terms of endings, cell types and connections. The early anatomical studies divided the CN into two main parts, the dorsal cochlear nucleus (DCN) and the ventral cochlear nucleus (VCN). The DCN is generally considered to be more complex, both anatomically and physiologically. For the VCN, however, a fairly complete picture of the neuronal circuitry is beginning to emerge.

In the VCN, there is an array of cell types organized to some extent from anterior to posterior through the VCN. There is also a variety of physiological types which are thought to correspond, at least in part, to the cell types. Whether the variety of response characteristics originates in variations in the types of endings of the AN, cellular morphologies in the CN or neuronal circuitry is uncertain at present. Part of the interest in the present study derives from the possibility that the cells in the CN might provide "test cases" for attempts to determine how these factors influence the behaviour of neurons. Since the cells in the VCN receive much of their synaptic input from the AN, this array of cell types has the same input in some respects but produces different outputs. Thus, the VCN presents an opportunity to formulate hypothetical input-output relations for each cell type and then to test the generality of the formulations with systematic changes in controlled stimuli. An assumption of this approach is that the major afferent input to these cells can be accurately specified (albeit statistically) by the discharge patterns of the AN fibers.

The VCN is often divided into two parts, the posteroventral cochlear nucleus (PVCN) and the anteroventral cochlear nucleus (AVCN). A survey of the physiology of the PVCN is available in Godfrey et al. (1975a), but what evidence there is of the physiology of the AVCN is either piecemeal or sketchy. Although the physiology of the VCN has been the subject of many studies in the past decade, there are few data which are specific with respect to location within the AVCN.

Anatomical studies of the AVCN have shown a variety of cellular morphologies and types of innervation. The systematic variations in these structural properties with location within the AVCN suggest that any study of the physiology that does not take account of the structural order will probably be needlessly complicated by the overall heterogeneity. Most of the previous physiological studies have not included the histological controls necessary to specify the location of units within the AVCN. Such studies can serve to define general categories for the physiology, but the data cannot resolve issues at the level of cell types. Of the few studies that have histologically verified the locations of units in the AVCN, all have been deficient in that either the unit locations were not determined and/or documented to the extent that the locations with respect to the AVCN subdivisions could be ascertained, the sampling was limited to only a small portion of the AVCN, or the data sample was too small to provide a regional characterization of the AVCN.

This thesis represents part of a continuing effort to determine the

input-output properties of the cells of the AVCN. As a working hypothesis, it is assumed that the anatomically distinct components of the AVCN will exhibit distinct physiological properties. By determining the distinguishing properties of each cell type, we would then be able to study the physiology of groups of units with similar structure. The main goal of this thesis is to try to define unit types, i.e., collections of units whose physiological properties are relatively homogeneous, and to determine any spatial segregations so as to suggest correlations between the unit types and particular anatomical features. Two aspects of the single unit physiology were used for the major categorizations of units. The data processing relevant to these categorizations is described in the Methods chapter, section 4.2 (for prepotentials) and 4.4 (for responses to tone burst and continuous tone). Most of the conclusions of the thesis are based on the relationship of these categorizations to each other and to the anatomy. Sections 2, 3 and 4 of the Results chapter present these categorizations and their interrelationship. Other aspects of the unit physiology were examined and are shown in sections 5 through 9 of Results to reinforce the generality of the unit types defined by the prepotential and response type categorizations. Since the data presented in these sections are mainly corroborative, it is not essential that the reader study them in detail. Asterisks were placed beside the section numbers to indicate that these sections could be by-passed on an initial reading.

The procedures used to determine the recording sites and relate these sites to an equivalent location in the model cochlear nucleus are presented in section 5 of Methods. Sections 5.6.1 and 5.6.2 have

been marked with asterisks to indicate that these sections can also be examined cursorily on an initial reading. In section 10 of Results, the spatial distribution of the various unit categories is used to infer anatomical correlates of the unit types.

The main conclusions of the thesis, which relate the proposed unit types to the anatomically defined cell types of the AVCN, are presented in sections 1, 2 and 3 of the Discussion.

CHAPTER II

BACKGROUND

The purpose of this chapter is to review the anatomy and physiology of the AVCN. Emphasis will be placed on the relatively few systematic studies in which the descriptions of the AVCN can be related to the more recent anatomical subdivision schemes for the cat cochlear nucleus.

1. Anatomy

The CN, which is situated on the dorso-lateral edge of the brainstem receives the central terminations of the auditory nerve (AN). Most anatomical studies have described the AN as terminating only within the CN (Powell and Cowan, 1962; Stotler, 1963; Feldman and Harrison, 1969). The CN in turn provides outputs to many other parts of the central nervous system via three fiber tracts: a ventral pathway, the trapezoid body and two dorsal pathways, the dorsal and intermediate acoustic striae.

The AN in cat consists of about 50,000 axons which are the central processes of the spiral ganglion cells. The peripheral processes innervate the organ of Corti providing synaptic terminals under the hair cells. Within the organ of Corti, these peripheral processes exhibit two main innervation patterns, namely the radial and longitudinal fibers (Lorente de Nó, 1937). A third type has recently been described by Lorente de Nó (1976).

Figure II-1 Primary innervation of the ventral cochlear nucleus

Reproduced from Ramón y Cajal (Figure 330, 1909), this drawing of the Golgi impregnated fibers and endings of the auditory nerve from a newborn dog shows the fibers entering the cochlear nucleus (A), bifurcating (center) and the two branches providing terminals in the PVCN (lower half) and the AVCN (upper half). At D the descending branch fibers turn at the posterior edge of the PVCN to enter the DCN (not shown). Note the approximately parallel course of the fibers and the large terminals in the AVCN. The fibers labelled E are part of the vestibular nerve. The plane of sectioning is probably approximately sagittal (tilted toward horizontal) with anterior up and dorsal (and medial) to the left.

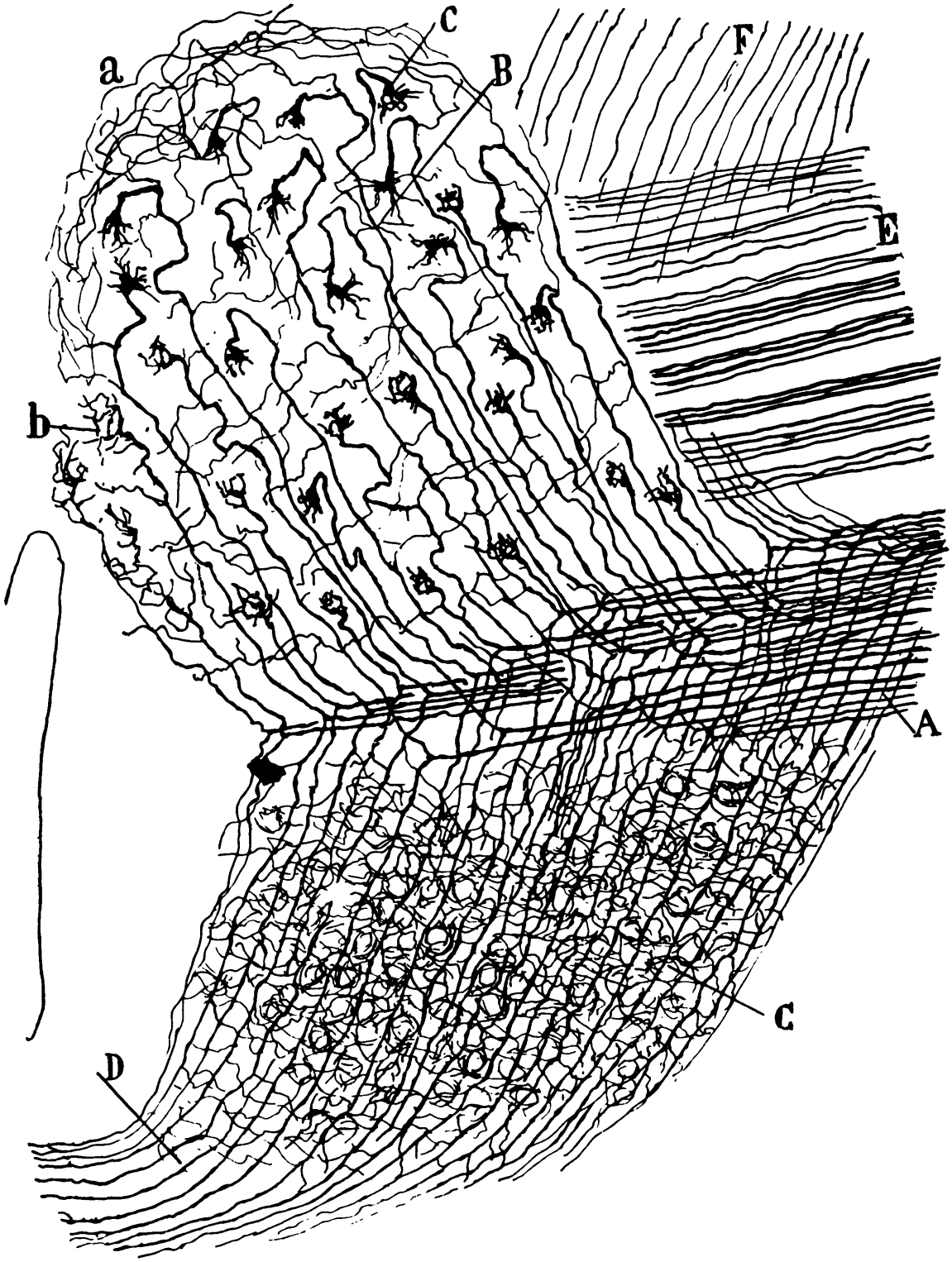
a
C
B
F
E
b
A
c
D

After entering the CN, the auditory nerve fibers bifurcate, giving rise to the ascending and descending branches (Figure II-1). The descending branch courses through the posterior ventral cochlear nucleus (PVCN) innervating that region and then turns dorso-rostrally to innervate the dorsal cochlear nucleus (DCN). The ascending branches run through the AVCN giving off endings along their course. Following the definition of Brawer et al. (1974), the AVCN will be considered to include not only the region innervated by the ascending branch but also the wedge shaped region in which the bifurcations occur (called interstitial nucleus (n.i.) by Lorente de Nó (1933b) and PV by Brawer et al. (1974)).

1.1 Subdivisions

A number of anatomical studies of the CN have proposed schemes for subdividing it. These studies differed in several ways:

(1) the anatomical techniques,

(2) the cellular elements emphasized (i.e., presynaptic endings, cell bodies, dendrites, axons, etc.), and/or

(3) the criteria used to define the regions.

In spite of these differences, there is a remarkable similarity between the resulting subdivisions of the AVCN. Table II-1 and Figure II-2 summarize some of the major schemes. Since the subdivisions defined by Brawer et al. (1974) will be used as the main anatomical reference in this study, their nomenclature will be adopted. Lorente de Nó (1933b), working with Golgi preparations of mouse, rat and cat divided his "ganglion ventrale" into three

Table II-1 Approximate correspondences of AVCN subdivisions

Lorente de Nó (1933b)	Osen (1969b)	Harrison and Irving (1965)	Brawer et al. (1974)
g.v. III	large spherical cell area	III	AA
-	-	-	APD
g.v. II	small spherical cell area	I	AP
g.v. I	multipolar cell area	II	PD
interstitial nucleus	globular cell area	II	PV
-	small cell cap	-	part of granular region plus ?

Figure II-2 Comparison of AVCN subdivisions

Diagrammatic "sagittal" sections show the subdivisions of three studies of the cat cochlear nucleus (Osen, 1969b; Lorente de Nó, 1933b; and Brawer et al., 1974) and a study of the rat cochlear nucleus (Harrison and Irving, 1965). The subdivisions in PVCN and DCN of Brawer et al. (1974) are not shown except for the fusiform cell layer (dashed lines). General orientation of the sections is labelled on the Harrison and Irving drawing. Relevant abbreviations:

(1) "Brawer, Morest and Kane" section: G, Granular region; for all other labels within the subdivisions, the first letter stands for the division and the second and third for the part of the division, e.g., APD is the posterodorsal part of the anterior division.

(2) "Osen" section: l. sph. c. a., large spherical cell area; s. sph. c.a., small spherical cell area; gl. c. a., globular cell area; cap, small cell cap (x's represent small cell distribution); co. f. cochlear fiber; n. vest., vestibular nerve.

(3) "Lorente de Nó" section: g.v., ganglion ventrale; n.i., interstitial nucleus; F.C., cochlear fiber.

(4) "Harrison and Irving" section: G, granular area; TB, trapezoid body; VN, vestibular nerve; AN, auditory nerve; ANN, auditory nerve nucleus. The ascending and descending branches of the auditory nerve are labelled ab or AB and db or DB respectively.

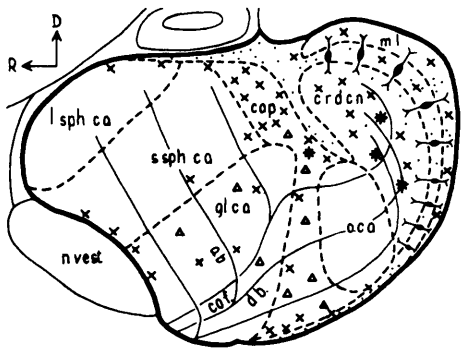

OSEN

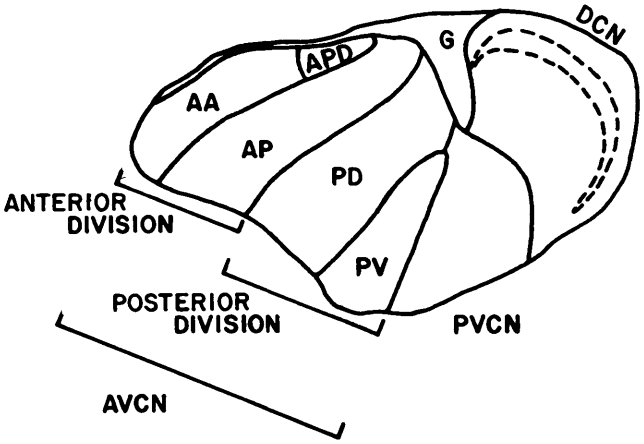

BRAWER, MOREST & KANE

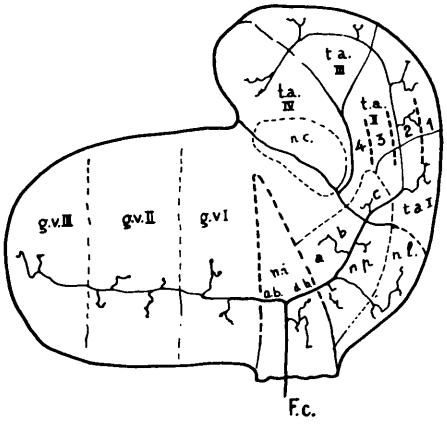

LORENTE de NÓ

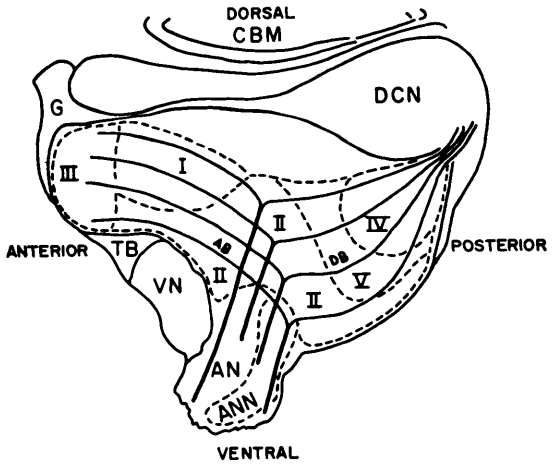

HARRISON & IRVING

parts at approximately equal intervals along the course of the ascending branch fibers from interstitial nucleus out to the rostral limit of the nucleus. Having no details of his criteria and only a diagrammatic representation of the boundaries, we must exercise some caution in comparing his scheme with the others. Harrison and Irving (1965) have proposed a subdivision of the rat VCN on the basis of Nissl and Protargol stained material. Their subdivisions have shapes that are somewhat similar to those in the cat studies and their criteria, although not directly comparable, do have some components that are equivalent. Osen (1969b) proposed a subdivision of the CN of cat based on Nissl and Glees preparations. Using cell size, shape (soma plus primary dendritic structure) and Nissl pattern as the main measures of the cell morphology, Osen defined types and mapped their occurrence. Figure II-2 shows a diagrammatic summary of her subdivisions which are named for the predominant cell type. Brawer et al. (1974) subdivided the part of AVCN rostral to PV (interstitial nucleus) on the basis of Nissl-stained sections of the cat CN. Using cell body size, staining density and packing density of cells, they defined four regions plus the granular region. PV was distinguished from PD on the basis of the myelinated fascicles of the auditory nerve root in PV and the more densely woven axonal plexus in PD.

The three cat studies, Lorente de Nó (1933b), Osen (1969b), and Brawer et al. (1974), have very similar subdivisions of AVCN. The treatment of the dorsal portion of AVCN appears to be the main discrepancy between these three schemes. Brawer et al. (1974) have a

rostral subdivision APD which probably represents the antero-dorso-medial part of Osen's small spherical cell area. Osen's small cell cap is represented in the Brawer et al. (1974) scheme partly in their granular region but probably more in the dorsal parts of AP and PD. Lorente de Nó (1933b) appears to define only the main subdivisions. According to Osen (1970) the most rostral subdivision, the large spherical cell region, does not receive input from the AN fibers originating in the basal most part of the cochlea. A further (and somewhat minor) variation between the subdivision schemes is whether the region of the primary bifurcations is considered to be a separate subdivision. Lorente de Nó (1933b) and Brawer et al. (1974) explicitly recognize it, Osen (1969b) shows it (dotted in Figure II-2) but includes it as part of her globular cell area and Harrison and Irving (1965) do not consider the cells or endings in it to be unique.

Several other anatomical studies of the CN have defined subdivisions of the AVCN that are either less extensive or essentially similar to those already described. Powell and Erulkar (1962); Rasmussen (1967) and van Noort (1969) have subdivided AVCN into two parts which probably correspond to the anterior and posterior divisions of Brawer et al. (1974). Pirsig (1968) has applied the Harrison and Irving (1965) system to the guinea pig and Osen's scheme has been used in the description of the kangaroo rat CN by Caspary (1968) and Webster et al. (1968).

1.2 Cell types

It is generally agreed that each of the AVCN subdivisions contains more than one cell type. Harrison and Irving (1965) identified a large number of cell types in the AVCN of the rat, whereas Brawer et al. (1974) using Golgi preparations of the cat CN identified only two main types in AVCN, the bushy cell and the stellate cell. Drawings of examples of the stellate and bushy cells are reproduced in Figure II-3. The bushy cells usually have spherical cell bodies and one or two short dendrites which terminate in a profuse ramification. The stellate cells have a multipolar soma with several large dendrites extending in different directions. In contrast to the regional concentrations of cell types described by Osen and Harrison and Irving, the two types described in Brawer et al. (1974) and Lorente de Nó (1976) are found throughout AVCN. Brawer et al. (1974) describe two other cell types. The infrequently occurring giant cell and the commonly occurring small cell are illustrated by the examples in Figure II-3. The small cell has a shape similar to that of the stellate cells but a smaller size.

Based on the descriptions of the cell types identified in the various studies, it is possible to suggest a tentative correlation as summarized in Table II-2. Since the most rostral subdivision of the AVCN is generally described to be populated predominantly by a single cell type, this region provides an opportunity to relate the various studies. The cells in rostral AVCN are fairly large (20 - 30 μm diameter) with a few small dendrites coming from the round cell body. This cell has been called "c" in rat (Harrison

Table II-2 Tentative correspondences of AVCN cell types

Osen (1969b)	Harrison and Irving (1965)	Brawer et al. (1974)
large spherical	c (bulbs of Held)	~ bushy
small spherical	i (pale bulbs of Held) plus small cells	?
multipolar	d,e,f,	stellate
globular	g (modified bulbs of Held)	~ bushy
giant	h	giant
small	j and small cells	small
granule	granule	granule

Figure II-3 Golgi impregnated cell types of the AVCN

Reproduced from Brawer et al. (1974) and Brawer and Morest (1975), these drawings of Golgi impregnated cells illustrate their cell categories. Below each cell type is the name. The drawing in the lower right of the figure shows an end-bulb contacting a bushy cell. The scales are approximately constant except for the drawing in the lower right.

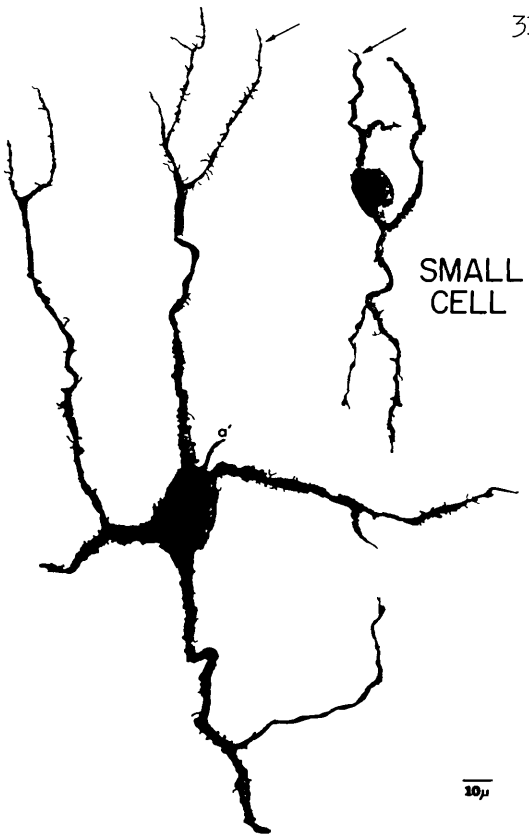

STELLATE CELL

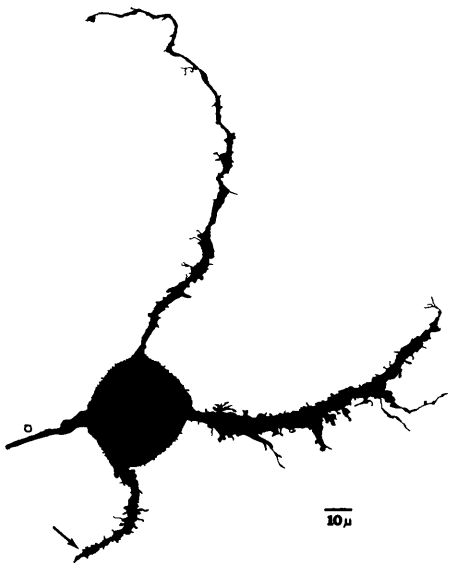

GIANT CELL

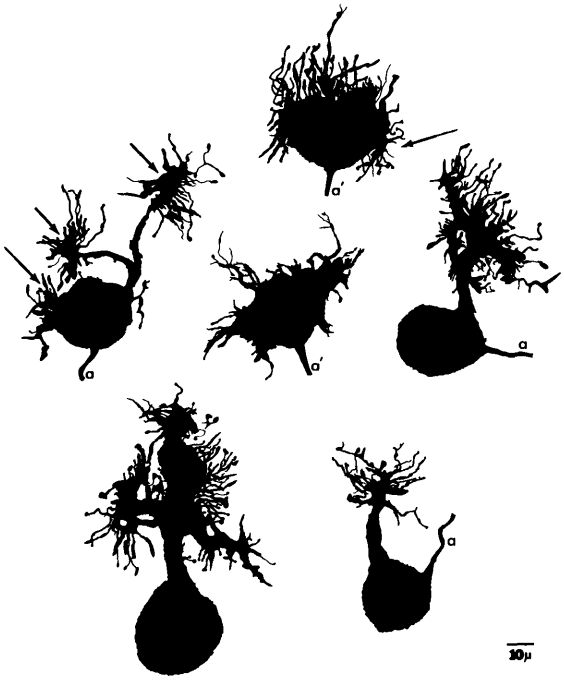

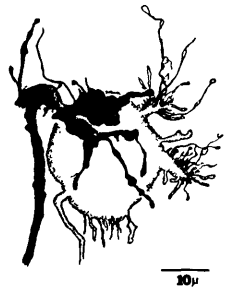

BUSHY CELLS

and Irving, 1965), large spherical in cat (Osen, 1969b), principal in cat and chinchilla (McDonald and Rasmussen, 1971) and bushy in cat (Brawer et al., 1974). The less common cells of the rostral division have been called spindle by McDonald and Rasmussen (1971) and stellate by Brawer et al. (1974). Osen (1969b) speculates that in addition to the large spherical cells in rostral AVCN there may be some of what she has called small spherical cells. Region AP or the small spherical cell area, however, appears to be less homogeneous than AA and less easily resolved between the different studies. Subdivision PD is usually described to contain at least four cell types. The main types in cat are bushy and stellate according to Brawer et al. (1974) and globular and multipolar according to Osen (1969b) with both sets of investigators describing, in addition, the occurrence of giant cells particularly in dorsal AVCN and small cells in most regions. PV according to Osen contains mainly globular cells in addition to some small and multipolar cells. The globular cell which is described as receiving the large endings of the auditory nerve called modified bulbs of Held by Harrison and Irving (1965) is probably equivalent to the bushy cell (Brawer et al., 1974) in PV and PD. The bushy cell has short dendrite(s) like the globular cell and received modified end-bulbs (Brawer and Morest, 1975).

1.3 Primary innervation

The details of the course of the AN fibers through AVCN and the types of synaptic terminations provided by the AN fibers and their collaterals are shown in such Golgi studies as those of Held (1893), Ramón y Cajal (1909), Lorente de Nó (1933b), Feldman and Harrison

(1969) and Brawer and Morest (1975). Two types of endings are found throughout AVCN: the end-bulbs of Held and small boutons. When the cochlea is destroyed the end-bulbs degenerate, whereas many of the bouton endings remain (e.g., Stotler, 1963; Reese, 1966; Harrison and Irving, 1966). These boutons of non-primary origin presumably arise from the axonal ramifications of cells located within the CN (Lorente de Nó, 1933b) and of cells in other parts of the central nervous system (e.g., Rasmussen, 1967).

The end-bulbs in the posterior division (PD and PV) are generally described as smaller than those of the anterior division. Ramón y Cajal (1909) in dog, Feldman and Harrison (1969) in rat and Brawer and Morest (1975) in cat noted this variation in Golgi preparations as did Harrison and Irving (1965) from their Protargol-stained material. Brawer and Morest (1975) measured the areas of the silhouettes of Golgi impregnated end-bulbs. They found the average area in the posterior division to be about 200 μm^2 and in the anterior division to be about 450 μm^2.

In Golgi studies of cat (Brawer and Morest, 1975; Lorente de Nó, 1976) and rat (Feldman and Harrison (1969) it has been noted that in contrast to the general view expressed earlier by Lorente de Nó (1933b), some AN fibers do not provide end-bulbs in the rostral half of AVCN but usually send a fine collateral to the rostral limit of AVCN. Lorente de Nó (1976) has suggested that those which do not provide an end-bulb in rostral AVCN represent the central projections of the longitudinal fibers in the cochlea.

An interesting property of the end-bulbs is that they are seen by Brawer and Morest (1975) and Lorente de Nó (1933b, 1976) to end in apposition to bushy cells. We note too that Harrison and Irving (1965) observed in their Progargol preparations of the rat CN that the end-bulbs appeared to contact only certain cell types (cf. Table II-2). In their study of the "rostral one-third" of AVCN (presumably AA) in the chinchilla and cat, McDonald and Rasmussen (1971) noted that the end-bulbs made synaptic contact with the round soma "principal neurons" but not with the spindle-shaped neurons scattered among the principal cells. In fact, the "spindle cells" which probably represent the stellate cells of AA (Brawer et al., 1974) rarely received any synaptic contacts on the soma. Thus the stellate cells probably receive only bouton terminations whereas the bushy cells receive end-bulbs and boutons from the AN fibers.

The convergence of several end-bulbs on cells of the AVCN has been noted in many anatomical studies (e.g., Ramón y Cajal, 1909; Harrison and Irving, 1965; Feldman and Harrison, 1969). The difficulties in confirming the synaptic contact of the end-bulb with a cell and the simultaneous confirmation that the various processes on the cell originate from separate AN fibers limit the reliability of the estimated convergence ratios. The general conclusion, however is that 2 or 3 end-bulbs are commonly found on each cell. More recently Lorente de Nó (1976) has described the cells of rostral AVCN as receiving only one large end-bulb.

From the drawings of the Golgi impregnated end-bulbs (e.g., Brawer and Morest, 1975) we see that the smaller are 5 μm or greater along at least one dimension whereas many are 10 to 20 μm with several lobes. Feldman and Harrison (1969) show three cases from their Golgi study of the rat CN in which two end-bulbs from the same AN fiber could be contacting a single cell. Thus it is possible for one AN fiber, with or without convergence, to provide processes which would cover a significant portion of a bushy cell's surface (diameter of 20 to 30 μm). Lenn and Reese (1966) have noted that in a single section through an end-bulb it is possible to see a 20 μm length of apposition with a cell on which the ending makes up to 14 synaptic contacts. Thus over the surface of the end-bulb there would be a large number of synaptic contacts which are controlled by a single AN fiber.

1.4 Ascending projections

The cells of AVCN are reported to project via the association fibers of Lorente de Nó (1933b) to the ipsilateral DCN and via the trapezoid body to parts of the superior olivary complex, lateral lemniscus and inferior colliculus on both sides of the brain. These relations are summarized in Figure II-4 taken from Kiang (1976).

Before presenting some of the data and hypotheses concerning the cells of origin of these projections we must consider the fiber components of the trapezoid body. When the cochlear nuclei were bilaterally ablated, Brownell (1975) found that most of the trapezoid body axons crossing the midline degenerated. According to van

Figure II-4 Schematic diagram of output pathways of the cochlear nucleus

The cochlea is represented by a spiral, the cochlear nucleus by an idealized sagittal section, and the inferior colliculus by an idealized transverse section in a more rostral plane. Solid lines, pathways considered to be well documented; dotted lines, pathways for which some evidence exists, but not of a conclusive nature. To simplify the drawing, the pathways are not strictly correct in all anatomic details (such as the relative position of various fiber components in the trapezoid body). AVCN, anteroventral cochlear nucleus; CNIC, central nucleus of the inferior colliculus; DCN, dorsal cochlear nucleus; DNLL, dorsal nucleus of the lateral lemniscus; HLSO, dorsal hilus of the lateral superior olivary nucleus; IN, interstitial nucleus of the cochlear nucleus; INSH, interstitial nucleus of the stria of Held; LNTB, lateral nucleus of the trapezoid body; LSO, lateral superior olivary nucleus; MNTB, medial nucleus of the trapezoid body; MSO, medial superior olivary nucleus; Pgl, lateral paragigantocellular nucleus; POal, anterolateral periolivary nucleus; POdl, dorsolateral periolivary nucleus; POdm, dorsomedial periolivary nucleus; POp, posterior periolivary nucleus; POpv, posteroventral periolivary nucleus; POvl, ventrolateral periolivary nucleus; POvm, ventromedial periolivary nucleus; PVCN, posteroventral cochlear nucleus; VNLL, ventral nucleus of the lateral lemniscus; VNTB, ventral nucleus of the trapezoid body.

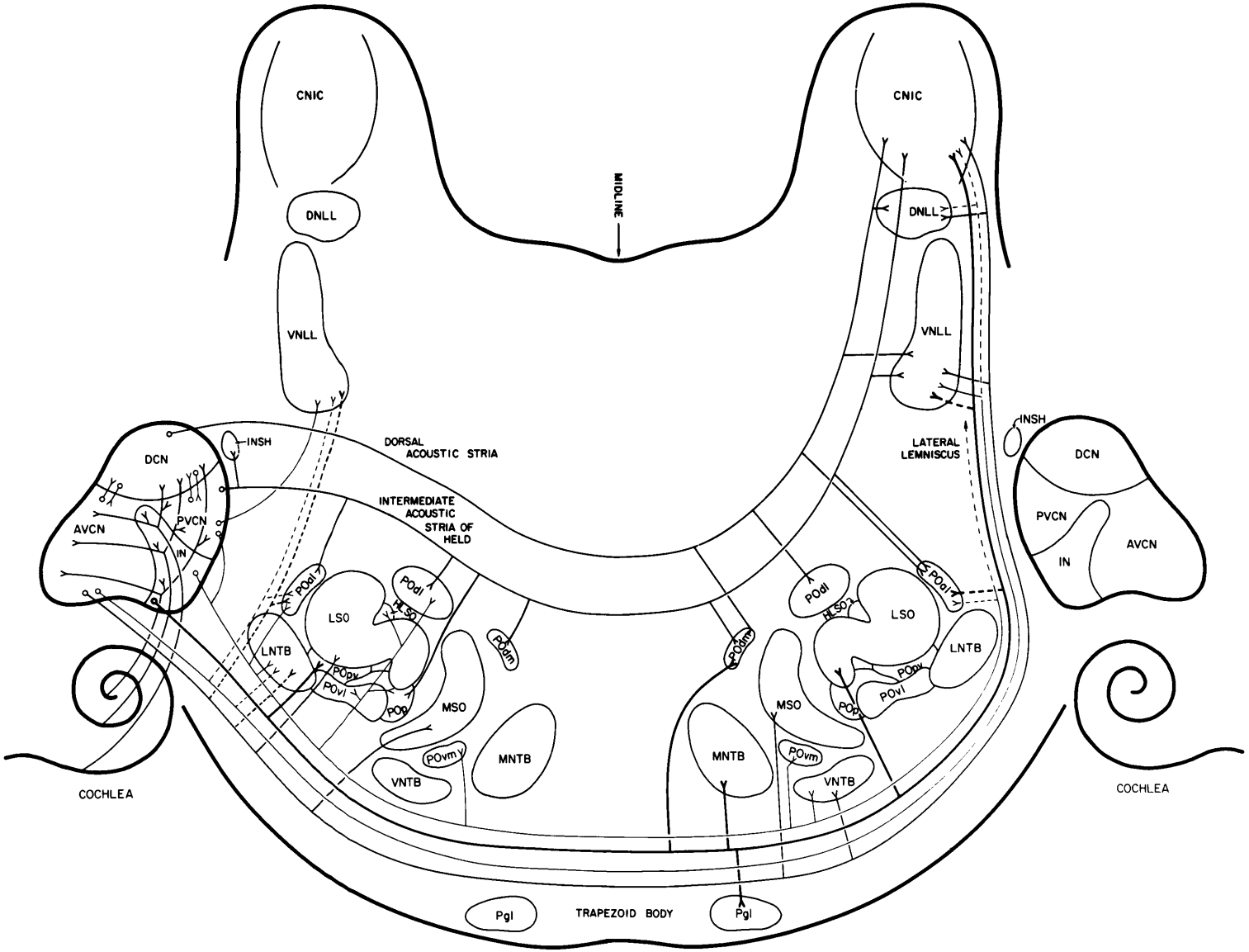
CNIC
CNIC
MIDLINE
DNLL
DNLL
VNLL
VNLL
INSH
INSH
DCN
DCN
AVCN
PVCN
IN
DORSAL
ACOUSTIC STRIA
INTERMEDIATE
ACOUSTIC
STRIA OF
HELD
LATERAL
LEMNISCUS
PVCN
AVCN
IN
POal
POdl
HL
LSO
LSO
LNTB
LNTB
POdm
POdm
POpv
POvl
POp
MSO
MSO
POvm
MNTB
MNTB
VNTB
VNTB
COCHLEA
COCHLEA
Pgl
TRAPEZOID BODY
Pgl

Noort (1969) there are some descending fibers among the thin fibers in the ventral part of the trapezoid body. Thus at the midline the trapezoid body is probably predominantly composed of the axons of CN cells. The three main groups of axons (Ramón y Cajal, 1909; van Noort, 1969; Brownell, 1975) as characterized in terms of their diameters and locations within a cross-section (sagittal) of the trapezoid body are:

(1) the medium-sized fibers (4 μm) which occupy approximately the dorsal 1/3 of the trapezoid body,

(2) the thick fibers (8-12 μm) which are ventral to the medium-sized axons, and

(3) the thin axons (1-4 μm) which are mixed in with the thick axons and which increase in concentration toward the ventral surface of the trapezoid body.

The diameters quoted above come from van Noort (1969). These three components are diagrammatically represented in Figure II-4 with different line widths; the dorsal-ventral arrangement of the components was not preserved, however.

One of the most distinctive projections from the AVCN is represented by the thick axons of the trapezoid body. These axons originate from cells in the central region of the VCN (Harrison and Warr, 1962; Harrison and Irving, 1964; Irving and Harrison, 1965; Warr, 1972) and are seen to give rise to the calyciform endings on the principal cells of the contralateral medial nucleus of the trapezoid body (MNTB) (Ramón y Cajal, 1909; Harrison and Warr, 1962; Morest, 1968). The cells of origin have been described to be the

g-cells in rat (Harrison and Warr, 1962). Osen (1969b) has traced the large axons of globular cells "far into the trapezoid body". These thick axons are also reported to provide collaterals to a periolivary nucleus (Warr, 1972) and some collaterals to the lateral lemniscus (van Noort, 1969).

The medium-sized axons provide terminals to the ipsilateral superior olive (LSO) and medial superior olive (MSO) and the contralateral MSO (Ramón y Cajal, 1909). Large numbers of these axons degenerate when the rostral two-thirds of the AVCN is lesioned (Warr, 1966). In addition to the medium-sized axons in the dorsal trapezoid body, however, finer axons in the ventral part of the trapezoid body also degenerate after lesioning of the cochlear nucleus. Osen (1969a) has suggested that the projections to both MSO's originate in the large spherical cell area (presumably bushy cells in AA) and that the projection to the LSO originates in the small spherical cell area. Harrison and Irving (1966), however, attribute both projections to their region III. The relationship of the bushy and stellate cells in AP to the components of the trapezoid body and to the innervations of the LSO and MSO are uncertain at present.

The inferior colliculus, generally considered to be the most rostral auditory center to which the CN projects (Barnes et al., 1943; Warr, 1966) give rise to degenerating axons and terminals in the ipsilateral and contralateral IC. Both the dorsal (medium-sized) and ventral (thin) components of the trapezoid body seem to project to the IC. Lesions of the caudal AVCN produce degeneration of fine axons in the contralateral IC (Warr, 1972). Van Noort (1969) claims

that some of the thick axons of the trapezoid body project to the contralateral IC.

1.5 Non-primary inputs

In addition to the synapses from the auditory nerve fibers on the AVCN cells there are inputs from DCN (Lorente de Nó, 1933b) and higher auditory centers (Rasmussen, 1960, 1967). According to Rasmussen (1960) the largest group of recurrent fibers arises in the ipsilateral LSO. Another pathway is the olivocochlear bundle which provides terminations in the AVCN in addition to those in the cochlea (Rasmussen, 1946, 1960). The complex patterns of termination of the various non-primary fibers in AVCN are currently under study (Cant and Morest, 1975).

2. Physiology

Throughout much of this study the AN discharge characteristics are taken as a reference both explicitly in some of the direct comparisons and implicitly in the definition of many of the categories for AVCN units. Much of the relevant physiology of the AN is described in Kiang et al. (1965a).

The discussion of the physiology of the AVCN will be restricted mainly to those experiments in which unit recordings have been localized to AVCN. Some of the unlocalized "CN" or "VCN" data will be considered only where more specific data are not available.

The early physiological studies of the CN described some of the properties of CN units and presented various classification

procedures. Rose et al. (1959) demonstrated the systematic change in the most sensitive or characteristic frequency (CF) of the single or multiple units recorded along microelectrode penetrations of the CN. This "tonotopic organization" was generally found to be discontinuous at the borders between the three major subdivisions of the CN (AVCN, PVCN and DCN).

2.1 Unit classifications

The introduction of the interval and PST histograms (Gerstein and Kiang, 1960) as analytical tools allowed the correlation of the discharge properties of single units with gross subdivision of the CN (Kiang et al., 1965b; Pfeiffer and Kiang, 1967). In Rodieck et al. (1962) and Pfeiffer and Kiang (1965) the shapes of interval histograms (IH's) of spontaneous and continuously stimulated activity were described and categorized; in Kiang et al. (1965b) and Pfeiffer (1966a) the PST histograms for tone burst stimulation at CF were categorized. Most of their data for the AVCN were probably from the rostral part. Posterior AVCN was not specifically discussed. The categories, however, are useful and have been used in many later studies (although sometimes with definitions that do not correspond to the original ones, e.g., Caspary, 1972; Britt and Starr, 1976a,b).

The IH shapes were characterized by the time of the mode, the symmetry about the mode and the shape of the IH beyond the mode (the "decay"). Since the decay of most IH's is close to exponential, the IH's were plotted on semilogarithmic coordinates and the devia-

tions from linearity classified according to whether the curvature was convex down or up. These two deviations were called Slower-than-Exponential and Faster-than Exponential respectively.

The tone burst stimulation utilized two basic paradigms, the short tone burst (STB; 25 msec burst at 10/sec) and the long tone burst (LTB; 900 msec burst at 1/sec). Based on the PST histograms of the responses to these tone bursts at the unit's CF (STBCF and LTBCF) they defined four main categories for the responses to each paradigm. On the basis of the PST histogram shapes as a function stimulus level, it was possible to characterize the complete profile for many units in the CN, particularly those in the VCN. Figure II-5 taken from Godfrey et al. (1975a) shows data for four VCN units which illustrate the main STBCF categories. The names of the categories are given above each column of PST histograms. The third histogram from the top in each column illustrates the prototype PST shape that characterizes the unit type. The LTBCF categories almost parallel the STBCF categories. There is an On type with responses only at the onset, a Primarylike type with a slow decay from the initial peak, a Dip type with a dip or broad minimum just after the initial peak and a Build-up type with a long latency and slow build up of activity. (Idealized PST histograms illustrating these forms are shown in Pfeiffer (1966a) and the first three are illustrated in Figure IV-16.) Godfrey (1972; Godfrey et al., 1975 a,b) has extended and refined the STBCF categories, particularly for the units of PVCN and DCN. One major limitation of this scheme, which places strong emphasis on the response to STBCF,

is the lack of applicability to units with a CF that is so low that the spike discharges are strongly phase-locked. All of the categories appear to become phase-locked at low frequencies; thus when the CF is low the only response pattern found is a sequence of phase-locked peaks.

Kiang et al. (1965b) describe the behaviour of the "only type of unit" found in the "anterodorsal portion" of the AVCN. This type of unit has:

(1) a response to tone bursts which is Primarylike,

(2) IH's with a short mode and Faster-than-Exponential decay and

(3) a spike waveform with a positive or "P" component preceding the normal extracellular spike (negative peak). Pfeiffer (1966b) described the spike waveforms of these units and suggested that the positive component (which shall be referred to as the prepotential) was presynaptic originating from the discharge of the large endings in this region, i.e., the end-bulbs of Held. A similar spike waveform was recorded in the MNTB (Guinan et al., 1972a) where there is strong evidence that the positive prepotential is of presynaptic origin (Li and Guinan, 1971).

The region of AVCN from which Pfeiffer recorded the units with a positive prepotential most likely includes AA and perhaps AP and APD. More than one cell type is found in rostral AVCN and hence one might expect to find units with other characteristics. How frequently such units occur and what their characteristics are is unclear from previous work.

Figure II-5 PST histogram patterns for four response categories

Each column shows the PST histograms of the responses to STBCF stimulation at four different intensities. The "unit type" is given above the upper histogram of each column. The figure comes from Godfrey et al. (1975a). Unit DG8-12 which was located in the AVCN exhibits a "notch" at the highest intensity shown. The other units were located in PVCN.

UNIT NUMBER:	DG53 - 31	DG8-12	DG69-22	DG65-12
CF (THRESHOLD):	5.50 kHz (-98 dB)	7.09 kHz (-106 dB)	3.71 kHz (-74 dB)	9.90 kHz (-113 dB)
UNIT TYPE:	"ON"	"PRIMARYLIKE"	"CHOPPER"	"PAUSER"

STIMULUS LEVEL IN DB RE THRESHOLD

+8		-4	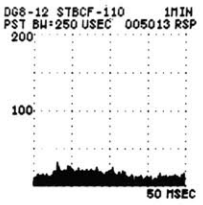	+4	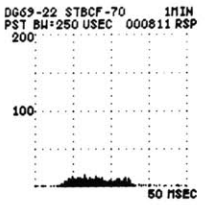	+13	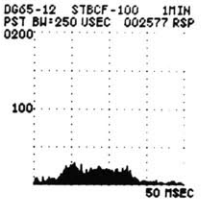
+28		+6	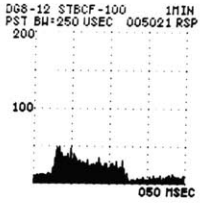	+14	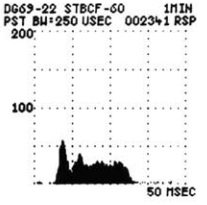	+43	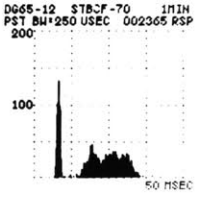
+58		+16	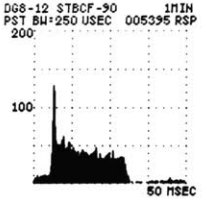	+24	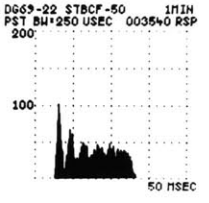	+83	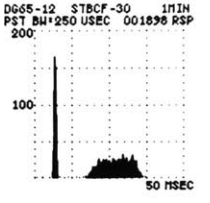
+88		+26	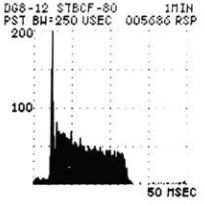	+44	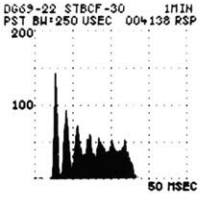	+103	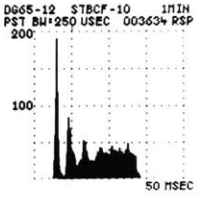

The physiology of units in interstitial nucleus or PV is described in Kiang et al. (1965b) along with their recordings from PVCN. Godfrey (1972), however, describes units localized to PV alone and also some in "posterior AVCN" (probably PD). From both of these studies we find that PV contains mainly Primarylike and Chopper units; Godfrey has 19 classified units: 7 Primarylike, 7 Chopper, 2 On type units and 3 with a broad dip after an initial peak in the STBCF response. Localized to "posterior AVCN" Godfrey has 11 classified units: 10 Chopper and 1 Phase-locked. Kiang et al. (1965b) note that the IH's from units of PV and PVCN usually have an exponential decay in contrast to the Faster-than-Exponential for the units of rostral AVCN.

Goldberg and Brownell (1973) studied single units in AVCN and DCN of the cat. Of the 61 units they localized to the "spherical cell region", 33 were in the "large-celled zone" and 28 were in the "small-celled zone"; they noted that about half of the units recorded in the spherical cell region had the complex spike waveform as noted by Pfeiffer. Most units in the spherical cell region had primarylike response patterns to tone burst. Since Goldberg and Brownell used 200 msec tone bursts and 5 msec bin widths in their PST histograms many Chopper units would have a primarylike PST histogram shape. Of the 34 units with spontaneous activity that were tested for single tone suppression of background activity only 3 units were found to have inhibitory sidebands. Their examination of IH's generally agreed with the conclusions of Pfeiffer and Kiang (1965) in that the units with long mode symmetric IH's are usually

found in DCN, whereas the units in rostral AVCN have asymmetric IH's with short modes.

Evans and Nelson (1973) have proposed a classification scheme for CN units which focusses on suppression of background activity both during and after tonal stimuli. Most of the units located in the AVCN were in their first two categories, both of which show no suppression effects during the tone presentation. This observation was relatively independent of whether the animal was anaesthetized or not. The number of units sampled from the AVCN for each of their preparations was, however, never more than 30 and was as low as 9.

A study of the CN of the cat reported in van Gisbergen et al. (1975a) used, as the major categorization scheme, a modification of the Evans and Nelson (1973) scheme. The first two categories of Evans and Nelson were represented in Type A (only activation during the tone burst. Type AS units exhibited activation and suppression by tonal stimuli of different frequencies (Evans and Nelson, types 3 and 4) and Type S exhibited only suppression (Evans and Nelson, type 5). Units with a low rate of spontaneous activity cannot be practically analyzed in such a system and so were assigned to the non-committal A(S) type. This restriction, as we shall see in the Results chapter, would, a priori, cause a large percentage of the units in AVCN to fall into the unanalyzable A(S) category. In addition to the Evans and Nelson scheme, van Gisbergen categorized some units according to a modified form of the Kiang et al. (1965b) and Pfeiffer (1966a) system. He identified:

(1) "transient" units (On type),

(2) "sustained" units (Primarylike and Chopper types),

(3) "build up" units (Build-up type), and

(4) "complex" units (Pauser type plus others?).

By counting the localized units shown in van Gisbergen et al. (1975a, Fig. 6), we find that of the approximately 44 units in AVCN, 23 had a spontaneous rate greater than 5 spikes/sec and so were tested for suppression. More than half of these units showed suppression of their background activity by tonal stimuli outside the excitatory region. Evans and Nelson (1973) found that less than 10% of all AVCN units showed suppression. The sample size in both studies is small and the studies probably have regional sampling biases. In the spherical cell region, Goldberg and Brownell (1973) found only 3 of the 34 units with spontaneous activity to exhibit inhibitory sidebands, and van Gisbergen et al. (1975a) appear to have 4 out of 12. The use of dot displays and systematic sampling of a range of frequencies is suggested in van Gisbergen et al. (1975a) as the possible reason for their more frequent observation of suppression than found by Evans and Nelson. Most of the A type units were localized to the spherical cell area. Most of the "sustained", AS and A(S) units were found in the globular cell area and many of these units exhibited "chopping". The "complex" units were not found in the globular cell area but a relatively large number (7) in the spherical cell area. This is of course somewhat surprising considering that Kiang et al. (1965b) and Goldberg and Brownell (1973) found the units of rostral AVCN to have predominantly a primarylike response. A tentative resolution of this discrepancy will be considered in the Discussion chapter.

The study of the kangaroo rat CN done by Caspary (1972) offers little that is relevant to this study. The interpretation of his results and integration with the other data is difficult. Since the recordings were made with fine-tipped pipette microelectrodes, some of the units were probably recorded from axons of the auditory nerve, CN cells and descending inputs to the CN. Furthermore, the "quasi-intracellular" recording conditions would have compromised the response properties and reliability of the dye-marking of the cells. Because of the large discrepancies between Caspary's data and the recordings of other experimenters using extracellular (Kiang et al., 1965a; Goldberg and Brownell, 1973; Godfrey et al., 1975a,b) and intracellular (Romand, 1976) techniques in the AVCN of the cat, further consideration of these results will be left to the Discussion.

2.2 Phase-locked responses to low frequency tones

Although many studies make reference to phase-locking, only a few have systematically studied it and tried to quantify the extent of phase-locking exhibited by the CN units. Auditory nerve fibers appear to be relatively uniform in their degree of phase-locking (Rose et al., 1967; Anderson et al., 1971; Johnson, 1974). The only exception is a trend for units with the lower spontaneous rates to have a slightly higher maximum "synchronization index" (Johnson, 1974). Moushegian and Rupert (1970 a,b; Rupert and Moushegian, 1970) report a range of phase-locking which is probably comparable to that of AN fibers in other animals (e.g., Kiang et

al., 1967a; Rose et al., 1967), whereas others they categorize as "non-phase-lockers"; that is, units for which the IH's of their response to tonal stimuli do not have significant peaks at multiples of the stimulus period.

Lavine (1971) studied phase-locking in the cat CN and shows, for a number of units, the systematic decrease in "vector strength" as the frequency of the stimulating tone is increased. All stimuli were delivered at levels between 70 and 80 dB SPL. The units localized to the AVCN (6 in all) had "high" values of "vector strength" whereas the units with "low" values (0 to 0.3) were localized to the DCN. Goldberg and Brownell (1973) in their study of AVCN and DCN chose the single frequency of 1.5 kHz at which to compare "vector strengths" from their sample of units, thereby controlling for the frequency dependence of synchrony. Lavine's observation of the difference between the AVCN and the DCN was generally confirmed by Goldberg and Brownell although they found 4 out of 35 units in the AVCN to have a "vector strength" of less than 0.3. All of these AVCN units with low synchrony had "diphasic" spike waveforms, i.e., the units did not have an obvious positive prepotential. Rose et al. (1974) also report recording from many units in the AVCN of the cat that have synchronization comparable to that of AN units.

2.3 Trapezoid body recordings

The trapezoid body represents the major (probably the only) pathway through which the AVCN neurons project out of the cochlear nucleus. Hilali and Whitfield (1953) have recorded from the trape-

zoid budy, but more recently, Brownell (1975) has tried to relate recordings from the trapezoid body axons (at the midline) to the major subdivisions of the axonal population. He found mainly primarylike activity in the region of the "medium diameter population", the fiber group that has been suggested to arise from the spherical cell region (Warr, 1966) which also has primarylike response properties. Most of the units recorded in the "large diameter population" also had a primarylike response to tone bursts at CF, but often exhibited inhibitory sidebands (8 of the 10 tested). A small number of non-primarylike units ("Chopper" and "Onset") were recorded in the "large diameter population" region. As in the Goldberg and Brownell (1973) study, the tone burst responses were obtained in a manner that would have caused many AVCN Chopper units to appear Primarylike.

2.4 Efferent effects

In addition to the auditory nerve input to the CN there are several known efferent pathways as were described in the anatomy section. Although there is no direct knowledge of the discharge properties of the particular efferent inputs to AVCN, some effects of both electrical stimulation of certain sites in brain and acoustic stimulation of the contralateral ear have been investigated. These studies provide an indication of the possible influence of the efferent pathways on the activity of AVCN units. In most cases the non-primary inputs to the CN have been shown to have a more distinct influence on units in the DCN. Starr and Wernick (1968)

have studied CN activity while stimulating the crossed olivocochlear bundle (OCB) at the decussation just under the floor of the fourth ventricle. The AVCN units exhibited the least effects on spontaneous activity with only 4% showing an increase in rate. The 32% that exhibited a decrease may have done so as a result of the decrement in auditory nerve activity which would occur if there was background acoustic stimulation (Wiederhold and Kiang, 1970). With tone evoked activity, however, 35% of the AVCN units exhibited increases or "complex" effects of the OCB stimulation. Comis and Whitfield (1966, 1968), Comis and Davis (1969) and Comis (1970) have presented evidence for excitatory effects in AVCN following stimulation of the medial region of the ipsilateral LSO, possibly due to activation of the recurrent bundle of Rasmussen (1960). In the same experiments Comis and Whitfield suggested the ventral nucleus of the lateral lemniscus as another source of excitatory input to AVCN.

Suppression and activation via contralateral acoustic stimulation has been demonstrated in the DCN of the chinchilla by Mast (1973, 1970). He has not, however, systematically studied the AVCN. A number of earlier reports have described suppression of spontaneous activity or responses to ipsilateral stimulation (e.g., Pfalz, 1962; Klinke et al., 1969). Pirsig and Pfalz (1967) have reported suppression of unit activity in the VCN of guinea pig and Hochfeld (1973), in a limited sampling of the AVCN, found two units which exhibited suppression to contralateral tonal stimulation.

The effects of efferent inputs to the AVCN of the (anaesthetized) cat appear to be found for only a sub-population of the cells in the AVCN. When effects are found, they are often relatively weak, have a long latency (50 msec to several hundred msec) for natural stimulation and have long time-constants for onset and cessation of the effect. The efferents, therefore, most likely do not play an important role in determining the patterns of response to such stimuli as STB or clicks although they could certainly be involved in producing a slowly adapting response to a long duration tone burst.

CHAPTER III

METHODS

1. Preparation of the Animal

The experiments were performed on healthy adult cats selected for clean external ear canals and body weights between 1.2 and 4.3 kg with 85% of the cats weighing between 2 and 3.5 kg.

Before surgery the cats were anesthetized with dial-urethane (75 mg/kg) injected intraperitoneally. Additional injections were given later in the experiment whenever a withdrawal reflex could be elicited by pinching the animal's toes. After a cannula was inserted into the trachea, the animal was placed in a headholder, the external meati cut near the tympanic membranes, and the bulla and septum opened widely to expose the cochlea and middle-ear of both sides. For all but seven experiments, the tendons of the middle-ear muscles were cut. The posterior fossa was opened bilaterally as close to the tentorium as possible. After reflection of the dura, the cerebellum overlying the cochlear nucleus (CN) was aspirated to expose the dorsal and posterior surface of the CN.

During many of the experiments a stimulating electrode was placed in either the superior olivary complex or the inferior colliculus. To facilitate placement of the electrode in the superior olivary complex, the floor of the IVth ventricle in the region of the genu of the facial nerve was exposed by aspiration of the cerebellum at the midline. For experiments involving electrical stimulation of the inferior

colliculus (IC), the posterior surface of the IC was exposed by aspirating the overlying portion of the cerebellum. Table III-1 summarizes some of the general information for each experiment including the sites that were electrically stimulated.

2. Stimulus Generation and Delivery

2.1 Acoustic stimulation

After surgery the cat was placed in a chamber which was acoustically isolated and electrically shielded. Earphone-probe tube assemblies (Kiang et al.,1965a) were sealed into the cut external ear canals. The sound source was a 1 inch Brüel and Kjaer condenser microphone (4131) and the probe-tube microphone was a Brüel and Kjaer ¼ inch microphone (4136). In order to be able to specify stimuli in sound pressure level (dB re .0002 dynes/cm^2) at the tympanic membrane the transfer function of voltage applied to the earphone amplifier to sound pressure level (SPL) was determined at the beginning of each experiment and checked two or three times during the experiment. The procedure for calibrating the acoustic source was first to calibrate the probe tube and probe-microphone combination by means of a calibrated ¼ inch microphone in a small cavity. After the assembly was sealed into the external auditory meatus, the probe-microphone output was measured in response to a constant amplitude sinusoidal input to the earphone amplifier at a set of frequencies from 0.1 to 40 kHz. From this measurement and the probe-tube calibration the sound pressure level at the probe tip was then computed at each sample frequency.

Table III-1 General format of experiments

Experiment Numbers	VDL		Middle-ear Muscles	Histology of CN		Electrical Stimulation		
	Start	End	Cut	Sagittal	Special Transverse	Cochlea	Trapezoid Body	Inferior Colliculus
20	79	75	X	X				
36	80	82		X				
37	84	85		X				
38	80	85		X				
39	87	87		X				
40	55	55	X	X		C		
42	87	89	X	X			T	
44	84	82	X	X			T	
45	80	80	X	X			T	
47	77	78	X				T	
48	88	90	X	X			T	
51	80	83	X	X			T	
52	80	70	X	X			T	
53	80	80	X	X			T	
54	88	87	X	X			T	
57	86	76	X	X			T	
59	90	92	X		X		T	
61	78	80	X		X		T	
62	73	64	X		X		T	
63	75	70	X		X		T	
65	78	72	X		X		T	
66	79	69	X		X		T	
71	79	82	X		X		T	
72	83	83	X		X		T	
73	80	65	X		X		T	
74	75	67	X		X		T	
75	77	78	X		X		T	
76	74	82	X	X				
79	88	92	X	X			T	

Table III-1 (continued)

80	74	76			X			
81	83	83	X	X			T	
82	68	70	X			C	T	
83	92	88		X				I
84	80	90	X	X		C	T	
85	75	75		X				I
86	86	89	X	X			T	
87	85	87	X	X			T	
88	80	80	X	X			T	
89	80	82	X	X			T	
90	80	85	X	X			T	
92	82	85	X	X			T	
94	70	72	X	X				I
95	85	76	X	X				I
96	82	87	X	X			T	
97	74	79	X	X				I
98	80	75	X	X				I
100	83	75	X	X				I
102	84	89	X	X		C		
103	84	80	X	X		C	T	
104	75	82	X	X				I
105	79	81	X	X				
Total 51			44	37	11	5	33	8

Figure III-1 Typical transfer ratio of the acoustic system: acoustic calibration for experiment B104

The computed magnitude and phase angle of the sound pressure at the probe tube tip (nominally at the tympanic membrane) are plotted for a sinusoidal input to the earphone amplifier with an amplitude equal to the reference (maximum) level. The magnitude is given in sound pressure level (dB re 0.0002 dynes/cm^2) and the phase in periods with respect to the voltage applied to the earphone amplifier. Phase lag is negative. There are 50 points per decade.

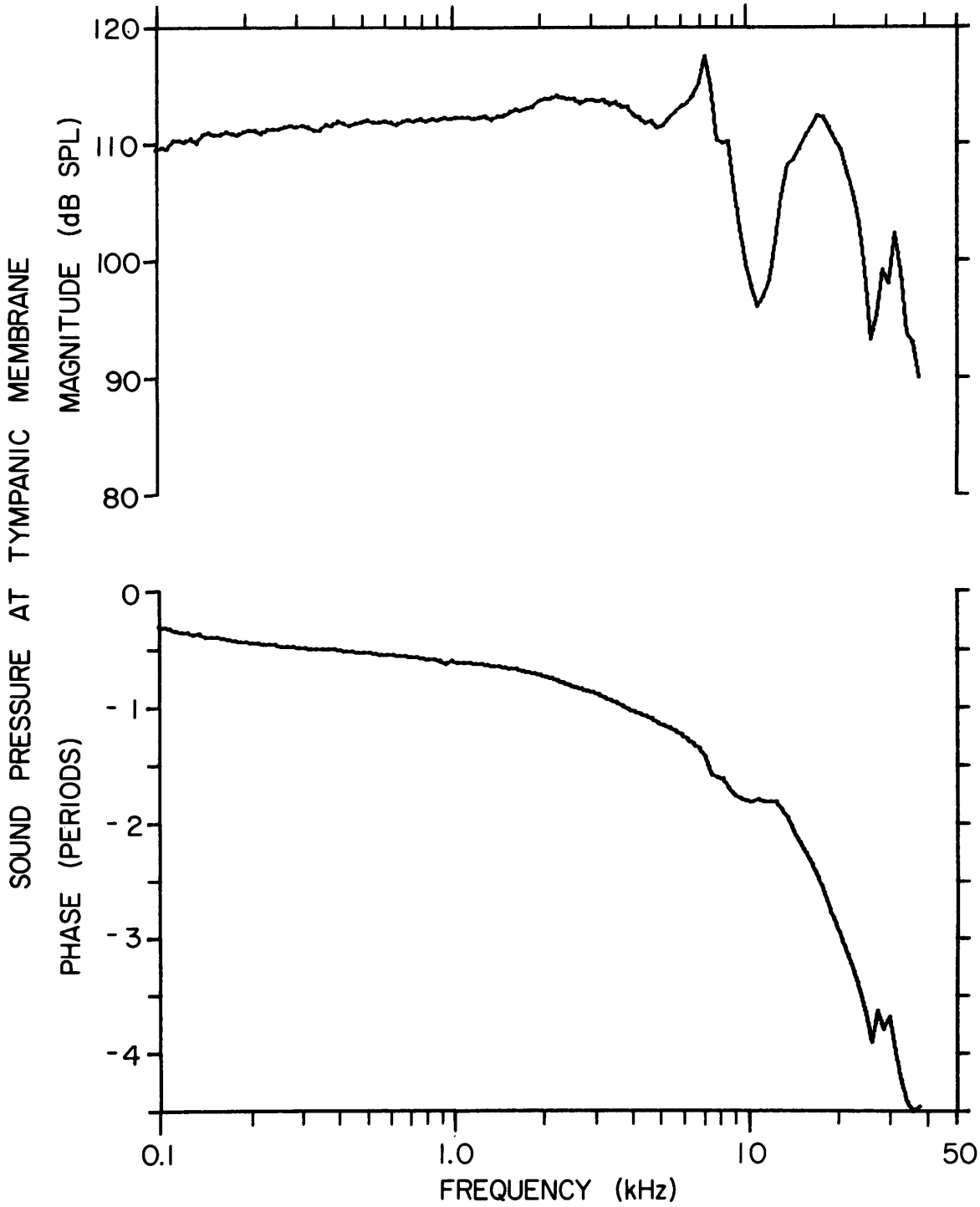
SOUND PRESSURE AT TYMPANIC MEMBRANE
MAGNITUDE (dB SPL)
120
110
100
90
80
PHASE (PERIODS)
0
-1
-2
-3
-4
0.1
1.0
10
50
FREQUENCY (kHz)

A typical calibration transfer ratio of sound pressure at the probe tube tip in magnitude (dB/SPL) and phase produced by a tone at the reference level is shown in Figure III-1. The phase characteristic was not always measured. For frequencies at which the probe tip is acoustically close to the tympanic membrane, the calibration curve represents the sound pressure level at the tympanic membrane.

For all of the experiments a standard set of acoustic stimuli was available. A block diagram of the stimulus timing and generation equipment is contained in Figure III-2. The stimuli, which are specified in terms of the electrical waveform delivered to the earphone amplifier were:

(a) Click - a rectangular pulse with a duration of 100 μsec and a reference amplitude equal to the peak value of the reference tone level. Both rarefaction (RC) or condensation (CC) clicks were available.

(b) Tone - a sinusoid with a total harmonic distortion of .01% (General Radio 1310-A) and reference level of 200 V peak to peak into the 1 inch condenser earphone.

(c) Tone burst - a gated sinusoid with an envelope with a rise-fall characteristic which was adjusted so that a tangent to the half-amplitude point would intersect the zero level at 2.5 msec and the full amplitude level at 5.0 msec. The duration (between the half-amplitude points) and the repetition rate were commonly:

25 msec at 10/sec.(short tone burst, STB)

or 900 msec at 1/sec.(long tone burst, LTB)

The normal tone burst envelope was timed so that a positive zero-crossing of the ungated sinusoid occurred at the burst zero time. In a few cases which will be clearly identified, the timing of the envelope was purposely made asynchronous with respect to the sinusoid being gated.

(d) short noise burst (SNB) - a broad-band noise (20 Hz to 50 kHz) gated with an envelope having the same characteristics as that of the short tone burst. The reference level for the noise was chosen to be the level at which the broad-band rms voltage of the ungated noise was equal to the rms voltage of the reference level for tones. The SNB stimulus was also delivered at 10/sec.

2.2 Electric shock stimuli

Many of the experiments incorporated one or more types of shock stimulation in addition to the acoustic stimuli described above. Each shock was generated by a monophasic rectangular voltage pulse delivered to the stimulating electrodes. The amplitude, duration and polarity of the pulse could be varied. The duration was usually 50 or 100 μsec. The most general stimulus was a burst of shocks for which the timing was determined in one of two ways:

1. the shock(s) could either precede or follow an acoustic stimulus by a variable time, or
2. the shock(s) could be generated at a variable delay after an action potential.

Figure III-2 Schematic diagram for the stimulus generation and signal processing

The stimulus generating components are contained mainly in the upper half of the figure and the signal processing components in the lower half. The timing controls for both acoustic and shock stimuli are contained in the box formed by dashed lines. The diagonal dashed line represents the ganged switch, coupling the selection of the stimulus waveform with the appropriate timing pulse. The two electrodes just above the cat are the microelectrode (conical) and the artifact recording electrode (heavy line). The LINC (Laboratory Instrument Computer) at the lower left receives timing pulses and pulses triggered from spikes and controls the frequency and intensity of the automatic tuning curve tone bursts generated by the blocks at the bottom of the figure.

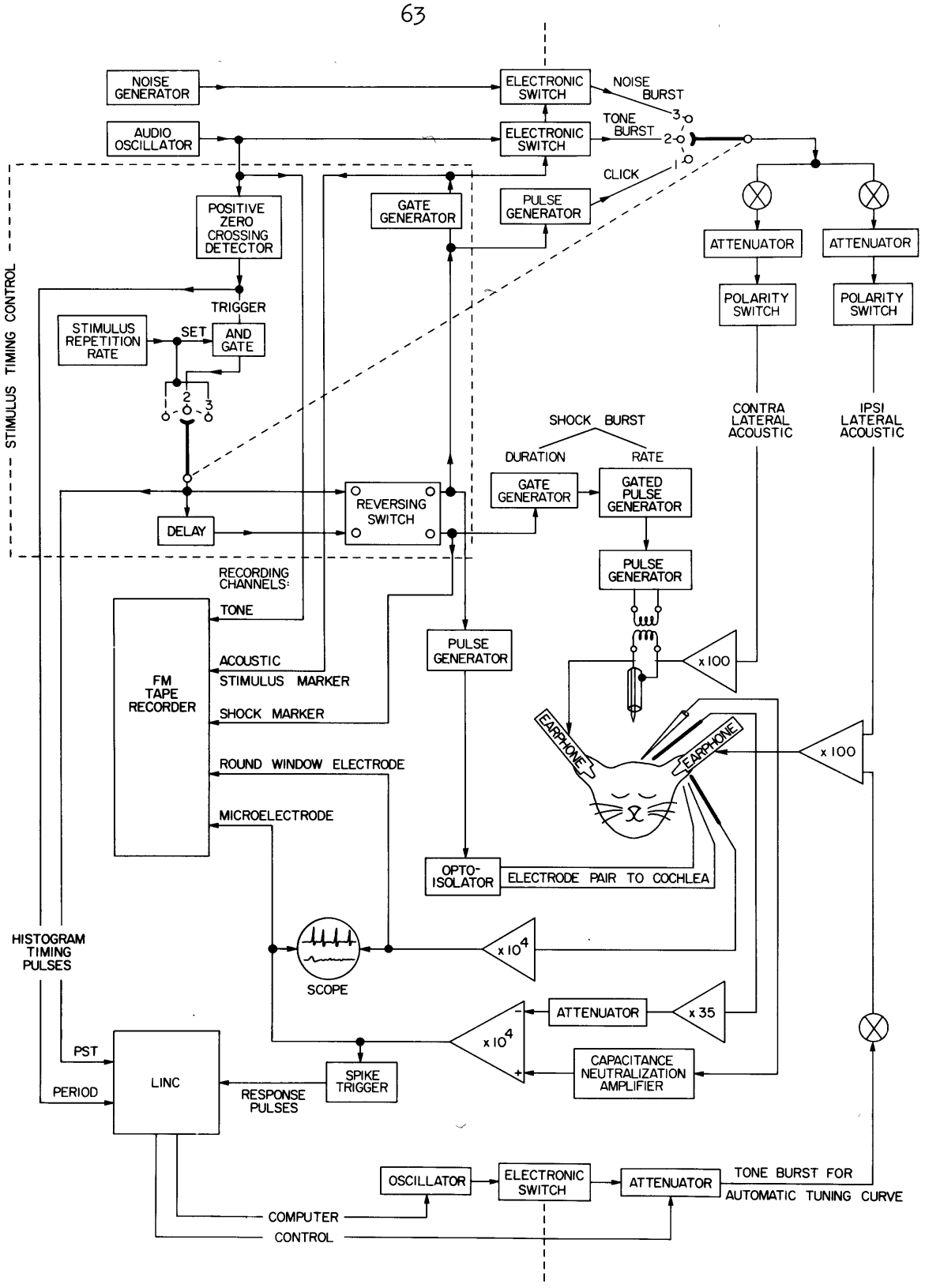
NOISE GENERATOR
ELECTRONIC SWITCH
NOISE BURST
AUDIO OSCILLATOR
ELECTRONIC SWITCH
TONE BURST
CLICK
PULSE GENERATOR
GATE GENERATOR
POSITIVE ZERO CROSSING DETECTOR
STIMULUS TIMING CONTROL
TRIGGER
STIMULUS REPETITION RATE
SET
AND GATE
ATTENUATOR
ATTENUATOR
POLARITY SWITCH
POLARITY SWITCH
CONTRA LATERAL ACOUSTIC
IPSI LATERAL ACOUSTIC
SHOCK BURST
DURATION
RATE
GATE GENERATOR
GATED PULSE GENERATOR
REVERSING SWITCH
DELAY
PULSE GENERATOR
RECORDING CHANNELS:
TONE
ACOUSTIC STIMULUS MARKER
SHOCK MARKER
FM TAPE RECORDER
PULSE GENERATOR
x100
EARPHONE
EARPHONE
x100
ROUND WINDOW ELECTRODE
MICROELECTRODE
OPTO-ISOLATOR
ELECTRODE PAIR TO COCHLEA
HISTOGRAM TIMING PULSES
SCOPE
x10^4
ATTENUATOR
x35
x10^4
CAPACITANCE NEUTRALIZATION AMPLIFIER
PST
PERIOD
LINC
RESPONSE PULSES
SPIKE TRIGGER
OSCILLATOR
ELECTRONIC SWITCH
ATTENUATOR
TONE BURST FOR AUTOMATIC TUNING CURVE
COMPUTER CONTROL

Figure III-3 A schematic representation of the positions of the recording and stimulating electrodes

Two diagrammatic transverse sections through the brainstem illustrate the electrical recording and stimulation sites used in the experiments. The gross cochlear potential recordings were made with the wire electrodes adjacent to the round windows (labelled on the right). The microelectrode recording from the left (ipsilateral) cochlear nucleus was differential whenever shock stimuli were being delivered; the potential recorded from the gross electrode placed near the cochlear nucleus was used to cancel some of the shock evoked-response and artifact. The ipsilateral cochlea was electrically stimulated in some experiments (see Table III-1) via a cotton wick electrode on the round window and a wire electrode on the surface of the cochlea away from the round window. In most experiments (see Table III-1) a concentric stimulating electrode was placed either into the trapezoid body near the contralateral MSO or into the contralateral inferior colliculus.

The insert (upper left) shows a cross-sectional view of a typical stimulating electrode tip and a microelectrode tip to the same scale. Abbreviations: auditory nerve, AN; anteroventral cochlear nucleus, AVCN; dorsal cochlear nucleus, DCN; lateral superior olive, LSO; medial superior olive, MSO; medial nucleus of the trapezoid body, MNTB; central nucleus of the inferior colliculus, CNIC.

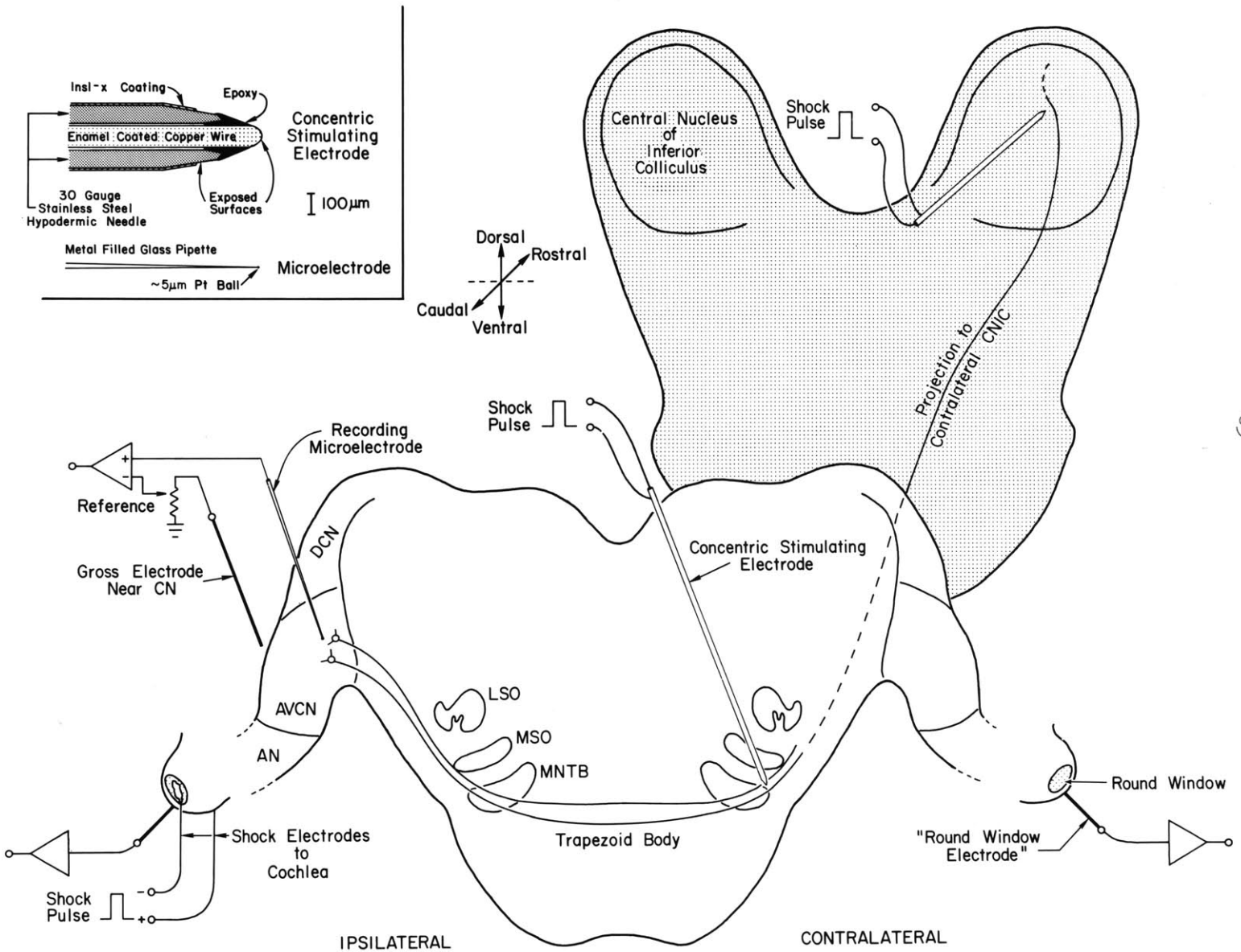
Insl-x Coating
Epoxy
Enamel Coated Copper Wire
Concentric Stimulating Electrode
30 Gauge Stainless Steel Hypodermic Needle
Exposed Surfaces
100μm
Metal Filled Glass Pipette
~5μm Pt Ball
Microelectrode
Dorsal
Rostral
Caudal
Ventral
Central Nucleus of Inferior Colliculus
Shock Pulse
Projection to Contralateral CNIC
Shock Pulse
Recording Microelectrode
Reference
Gross Electrode Near CN
DCN
Concentric Stimulating Electrode
AVCN
AN
LSO
MSO
MNTB
Trapezoid Body
Round Window
"Round Window Electrode"
Shock Electrodes to Cochlea
Shock Pulse
IPSILATERAL
CONTRALATERAL

Within Figure III-2 are shown the components used to control the timing of shocks and acoustic signals. For condition (2) above the delay module was triggered by the pulses triggered from the single unit spikes.

The technique for delivering shocks to the cochlea was the same as that used by Moxon (1967). The voltage pulse was coupled via an optical isolator to an electrode pair. The negative electrode was a cotton wick moistened with saline, placed in contact with the round window membrane. The positive electrode was a wire in contact with the periosteum over the surface of the cochlea. These two electrodes are shown diagrammatically in Figure III-3 at the left cochlea. For electric stimulation of the sites in the brain, rectangular pulses were transformer-coupled to a concentric bipolar electrode shown diagrammatically in Figure III-2 above the cat and in Figure III-3 in the brain stem of IC. A sketch of the tip dimensions of a typical bipolar electrode is also shown in Figure III-3. The shank, insulated down to the tip, was a #30 hypodermic needle etched to the shape shown. During the experiment, this electrode was mounted on an hydraulic microdrive so that it could be moved along this trajectory from outside the experimental chamber. Current flow through the stimulating electrodes was monitored with a current probe.

Some of the interpretations of the single unit responses to electrical stimulation will depend on the particular structures the current pulses are assumed to have stimulated. We shall therefore consider some evidence concerning the spread of current from a stimulating electrode. In a review article on electrical stimulation of

neural elements in the mammalian CNS, Ranck (1975) has examined data from 10 different studies on the relationship between the distance from the stimulus electrode to the site of nerve excitation and the threshold current amplitude. This function is called a "current-distance relationship." These data come from many different experimental situations and have all been computationally adjusted by Ranck to apply to pulses of a 200 μsec duration. Following the same procedure we have adjusted the data to refer to a pulse duration of 50 μsec. The scatter of the different experimental results is essentially encompassed by the dotted region on Figure III-4, with the median represented by the heavy line through the center, labelled "50 μsec, monopolar." The slope of this line is consistent with a square-law relationship as would be expected for a point source in a uniform medium. It is of interest to note that some theoretical formulations (e.g., Bean, 1974) do not predict a square-law relationship.

In the present study, we used a 50 μsec pulse delivered through a bipolar electrode. The current-distance relationship for a bipolar electrode is more difficult to predict and as reported by Ranck, there is little empirical evidence for establishing such a relationship.

One application of these considerations is to the question of whether axons on the ipsilateral side of the brain were stimulated by the shock pulses delivered in the region of the contra-lateral MSO. We note that the distance from the midline was usually about 3 mm. The horizontal band across the top of Figure III-4 shows the range of distance (2 to 4 mm) to the midline. The concentric bipolar electrode was oriented so that the dipole axis was approximately parallel to the

Figure III-4 Current-distance relationship for electrical stimulation

A. The diagonal, lightly dotted band with the median line labelled "50 μsec, monopolar" represents the expected current-distance relationship for a current pulse 50 μsec wide and delivered from a monopolar electrode. This band was estimated from the data gathered together by Ranck (1975) and is largely empirical, requiring theoretical considerations only to convert the data to an effective pulse width of 50 μsec. The vertical axis represents the distance from the stimulating electrode tip to the neural structure stimulated by the current pulse. The line labelled "50 μsec, bipolar" is based on a simple theoretical formulation for a dipole with 200 μm pole separation (see text). The 2 to 4 mm distance range is dotted to illustrate the usual experimental distance between the stimulating electrode and the midline during the trapezoid body stimulation.

B. The lower plot is a histogram of the current levels used to elicit a presumed antidromic response from AVCN units during the trapezoid body stimulation.

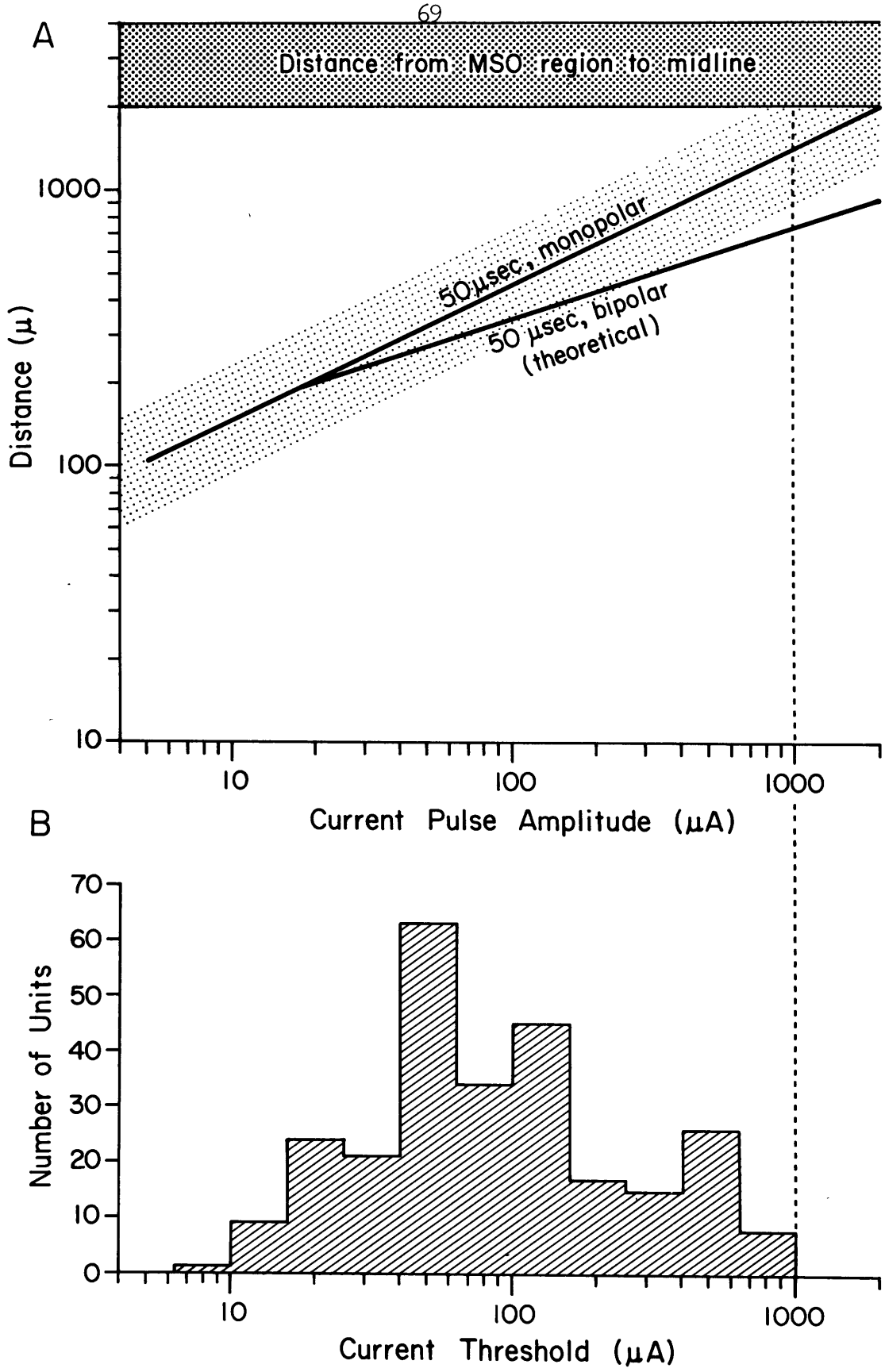
A
Distance from MSO region to midline
1000
100
10
Distance (μ)
50 μsec, monopolar
50 μsec, bipolar
(theoretical)
10
100
1000
Current Pulse Amplitude (μA)
B
70
60
50
40
30
20
10
0
Number of Units
10
100
1000
Current Threshold (μA)

midline (see Figure III-3), particularly when the electrode path was close to the midline. The relevant distance (electrode to midline) is the distance perpendicular to the electrode.

As an estimate of the possible current-distance relation for a bipolar electrode, we shall compare the field strength resulting from a point source of current with a dipole source-sink combination passing the same current as the point source. For a point source the field strength is given by,

$$|E| = \frac{I}{4\pi\sigma} \quad \frac{1}{d_m^2} \qquad 3.1$$

where I = current, σ = conductivity, and d_m = distance from the source. For a dipole source with a pole separation of ℓ, the maximum field strength at a perpendicular distance d_B from the axis of the dipole is given by,

$$|E|_{max} < \frac{I}{4\pi\sigma} \quad \frac{\ell}{d_B^3} \qquad \text{if } d_B >> \ell \qquad 3.2$$

Near either pole the field strength is the same as that of a point source. If we require that the bipolar and monopolar electrodes create the same field strength magnitude in order to stimulate the axons, then by equating field strengths and currents:

$$d_B = (\ell\, d_m^2)^{1/3}, \text{ if } d_B >> \ell$$

and

$$d_B = d_m, \text{ if } d_B << \ell \qquad 3.3$$

Using a pole separation of ℓ = 200 μm (a typical distance for the stimulating electrodes as shown in Figure III-3, insert) we obtain the "bipolar" relationship in Figure III-4. The lower half of the figure shows a histogram of the current levels used to stimulate AVCN units. Only at the upper limit (1 mA) is it likely that axons could have been stimulated on the ipsilateral side of the brain; at 100 μA or less the current spread is relatively small (only 1/5 of the distance to the midline).

3. Recording Prodecures

As is shown in Figure III-2, an analog tape recorder was used to record many of the relevant signals during the experiments. The purpose of the tape recorder was both to provide a back-up record of all responses processed during the experiment (except for tuning curves) and also to record data that could not be processed on-line. Normally the signals recorded were:

(a) the amplified signal recorded with the microelectrode,

(b) the amplified signal recorded with the gross round window electrode,

(c) a gate to mark the time of presentation of transient stimuli and also the duration of the tone or noise bursts,

(d) a time marker for each shock pulse,

(e) the oscillator signal used for the continuous tone or tone burst stimulation.

The tape recorder was normally operated in FM mode with a 0 to 5 kHz bandwidth. For many units a more accurate record of the spike waveform was obtained by recording a short segment of spontaneous activity or continuous tone response with a 10 kHz bandwidth.

3.1 Round window electrode

The tip of a wire electrode was placed onto the periosteum just ventral to the round window. The gross cochlear potentials (cochlear microphonic and neural components) recorded between this electrode and the headholder were used as a monitor of the sensitivity of the cochlea. A routine test that was used throughout the course of each experiment as a check on the stability of the cochlea was to determine the visual detection level (VDL). The VDL was taken to be the lowest rarefaction click level at which the gross neural potential could be visually detected on an oscilloscope display of the round window electrode signal.

Table III-1 lists the VDL's for each of the 51 experiments from which usable data were obtained. Only those units recorded when the VDL was -70 or lower were used for data on acoustic response or spontaneous activity. Shock responses were used even when the VDL was as high as -65 dB. Spike waveforms were analyzed from all experiments.

3.2 Stimulating electrode

As the concentric stimulating electrode was first advanced into

the brain, the potentials recorded from the center conductor were monitored. The gross responses to SNB and STB were used to aid in localizing the stimulating electrode tip (see also section 5.7).

3.3 Microelectrode

The recordings from the cochlear nucleus were obtained by means of platinum-tipped microelectrodes (Gesteland et al., 1959; Kiang, 1965). This type of microelectrode has been used in a number of previous studies of the cochlear nucleus (e.g., Kiang et al., 1965b; Pfeiffer, 1966a,b; Goldberg and Brownell, 1973). The glass pipettes are metal filled and the tip is formed by a porous platinum-black blob of approximately 5 μm diameter (range 3 to 10 μm). The size of the tip seems to make recording from primary axons unlikely (Kiang, 1965). The electrical signal from the microelectrode was buffered by a unity gain amplifier having a high input impedance and capacitance neutralization. The signal was then brought out of the chamber to a high gain differential amplifier. The reference electrode was the headholder.

During the shock stimulation, the negative input to the differential amplifier was used to partially cancel electrical artifact. The signal from a wire electrode placed near the microelectrode, but on the temporal bone or cerebellum, was adjusted in amplitude so that most of the electrical artifact and the evoked response to the shock would be cancelled. This arrangement is shown in both Figure III-2 and Figure III-3.

During the recordings, the position of the microelectrode was controlled by a calibrated hydraulic manipulator from outside the chamber. While advancing the microelectrode a search stimulus was always used. When the approximate characteristic frequency (CF) of the region being recorded from was known, short tone bursts were the search stimulus; otherwise noise bursts were used.

4. Processing Microelectrode Recordings

The signals recorded with the microelectrode were of two main classes:

1) gross evoked responses which represent the summated activity of many neural elements responding to the stimulus. The gross responses have stable amplitudes, shapes and latencies which are graded functions of the stimulus intensity.

2) single unit action potentials or spikes which represent the discharges of individual cells. They are all-or-none in shape and amplitude with probabilistic times of occurrence. Their shorter duration (lasting only a few tenths of a millisecond) usually distinguishes the spikes from gross response. Some punctate stimuli, such as acoustic clicks or shock pulses, when delivered at suprathreshold levels can produce a large, fast evoked response and at the same time strongly synchronized spikes such that even the largest of single

unit spikes merge with the gross response. Only by reducing the intensity of the stimulus could the spikes be recognized by their all-or-none amplitudes and variable timing near threshold.

4.1 Single unit criteria

When the microelectrode was positioned so as to record the spikes of one single unit with an amplitude and/or shape which were clearly distinguishable from those of any other unit being recorded, the discharge characteristics of that unit were studied. The times of occurrence of the spikes were registered for computer processing by means of a level-crossing detector. Thus most of the units studied had to satisfy the more stringent requirement that the spike amplitude be greater than that of all other potentials in the recording. In a few instances, the spikes from a pair of simultaneously recorded units were discriminated through the use of two level-crossing detectors and a spike height discrimination algorithm. Different spike polarities were also used to separate simultaneous units.

The criteria for deciding that a train of action potentials was from a single unit were:

(1) The amplitudes and shapes of the spikes were constant except for the occasional spikes which occurred within approximately 1 msec of a preceding spike.

(2) The amplitude and shape of all spikes changed uniformly when the microelectrode was moved.

(3) Very short intervals (< .5 msec) did not occur.

(4) When antidromic responses were elicited with shock stimuli, the interaction of the orthodromic and antidromic spikes occurred for all the spike shapes exhibited by the unit.

The first three tests were evaluated for every unit with criterion (4) applied to some of the units.

To each unit that was entered in the protocol a rating was assigned. The ratings were made up of a letter and optional + or - sign which indicated position within the category. The main categories were:

(1) "A" rating: a single unit with spikes clearly larger than other unitary activity in the background and larger than any gross response. For these units a level-crossing detector registers the timing of spikes accurately.

(2) "B" rating: a single unit recorded under conditions that would cause the level-crossing detector to miss some spikes and/or to be triggered by gross response or background activity.

(3) "C" rating: unitary activity which ranged from a single unit with spikes that were so small that many extra and/or lost triggers would result if a level-crossing detector were used (C+) through to recordings which were almost assuredly from several units (C-).

Histograms that were computed when the rating was C+ or worse were

discarded in the final analysis.

4.2 Spike waveform and prepotentials

During the experiments certain aspects of the spike waveforms were noted. A brief description of the shapes of the spikes associated with each single unit usually included:

(1) whether they were predominantly mono-, di-, or triphasic

(2) the polarity of the largest peak

(3) the width of the largest peak (approximate half-amplitude width)

(4) where the waveforms showed inflection points

(5) if the waveform appeared to fractionate into two or more components.

The most systematically examined aspect of the spike waveforms was a deflection which is frequently found to precede the spike itself, the prepotential (pp) (Pfeiffer, 1966b). For most of the single units used in this study, a decision was made as to whether or not there was a detectable prepotential (pp) associated with the spike. Since the pp's can be smaller than the noise level of the recordings, the detection of the pp's can be difficult. A unit was said to not exhibit a pp only after negative results were obtained throughout a sequence of tests to be described in the remainder of this section.

The tests applied during the experiments detected many of the units that had a pp. When the pp was large it was obvious on the oscilloscope display of the microelectrode signal. Even when the pp amplitude

was at or below the noise level, the existence of the pp could often be demonstrated by triggering the oscilloscope sweep in the positive region of the noisy baseline activity. The presence of a positive pp results in a distinct superposition of spikes at about 0.5 msec after the trigger point.

Each unit which was not positively identified during the experiment as having a prepotential was reprocessed from the analog tape records. By using a display that was time-locked to the spike and yet showed the microelectrode record for one millisecond preceding the spike (pre-spike display), a more sensitive examination could be made. Early in the study, this display was obtained by playing the tapes in reverse; later, a digital delay line with free running sampling at 50 kHz was used. The delay line allowed a display of both positive and negative time with respect to the triggering point and could be used during the experiments. Large and intermediate size prepotentials were immediately obvious on inspection of the pre-spike display. Because of the persistence of the oscilloscope traces, small prepotentials could be inferred from consistent displacements of the background noise of the recording. When a pp could not be seen in the individual spike waveforms, an average was computed. In some cases after only 10 to 100 spikes had been averaged, the average showed a clear pp-like component at about 0.5 msec before the spike. For many other units, the average was allowed to progress to beyond 1000 spike triggers while the baseline became less and less "noisy". No significant component other than the spike itself was found.

When testing for the presence of a pp, stimulus conditions that would produce strong inter-unit correlations had to be avoided. Spontaneous activity was the preferred condition with low intensity continuous tone or noise as the second choice. Clicks, shock stimuli and high intensity low frequency tones that might result in strongly synchronized responses from many units were never used to elicit discharges that would be examined for a pp.

4.3 Tuning curves

Two procedures were used to obtain tuning curves (TC). The most general type of TC was taken manually with the experimenter making the detection judgment for each point on the TC by a combination of audio and visual cues in the monitoring of the discharges. The other type of TC was measured in an automated way (Kiang et al., 1970). These automatic tuning curves were determined by a computer program which controlled the tone burst frequency and intensity via the oscillator and attenuator shown at the bottom of Figure III-2. The single unit responses were registered via the PST histogram inputs to the LINC. Although the threshold criterion of an automatic tuning curve can be stated with a precision which is lacking for the manual tuning curves, the appropriateness of the algorithm as a measure of the threshold of the various types of CN units with different response properties is uncertain.

Manual TC's were determined by finding the frequency range(s) over which the unit would respond to short tone bursts at a certain

level (in voltage to the earphone). The amplitude was then varied in 5 or 10 dB increments to cover a 30 to 100 dB range. The boundaries of the response region were taken to be the stimulus conditions giving rise to a "just detectable" correlate on the audio playback and/or the oscilloscope display of the spike discharges. The task of detecting a response to the 10/sec tone-bursts varied considerably with the spontaneous discharge rate and the type of unit. When the spontaneous rate was high, a threshold response produced a just detectable 10/sec modulation on the audio monitor. When the spontaneous rate was very low, a more concerted effort was made to count spikes during a sequence of 20 to 50 tone bursts. Examination of the intensity function was used to establish an approximate number of tone bursts over which a few spikes would be taken as a threshold response. A criterion could usually be set to yield a threshold within a few dB of the maximum level at which no detectable response would occur over a 10 second sample (100 tone bursts). For units with a low rate of spontaneous activity and a steep intensity function threshold determinations were reliable with only a few tone bursts. Some of the units with an On type of response had intensity functions with exceptionally low slopes; these units required criteria that set the threshold response to be one spike in about 20 tone bursts.

The particular measure of stimulus intensity which is used to specify a tuning curve can affect the shape of the tuning curve and consequently the CF (Kiang et al., 1967). Also, since the on-line stimulus intensity was specified in terms of voltage to the earphone,

the on-line CF for a high CF unit (particularly above about 12 kHz) could be different from the CF determined when pressure at the tympanic membrane is the measure of stimulus level. The CF, of course, would be different again if other measures such as stapes displacement or velocity were used. The on-line CF's are seldom much higher, but often somewhat lower, than the CF measured from a tuning curve plotted in terms of sound pressure.

4.4 Computer processing of spike times

4.4.1 PST, IH

The times of occurrence of the spikes as indicated by the pulses from a level-crossing detector were processed by the digital clock and LINC to yield histograms of the frequency of occurrence of spikes in time intervals (bins) following either the stimulus presentation marker pulse (PST) or the preceding spike (IH). Usually these histograms were computed during the experiment.

4.4.2 Time-varying interval statistics

For most CN units, it is during the initial 10 to 50 msec of the response to tone and noise burst stimuli that some of the most characteristic response properties are exhibited. Previously these responses have been characterized by means of:

(1) dot displays which are, however, qualitative and insensitive to subtle changes in response pattern,

(2) PST histograms which provide an estimate (average) of the instantaneous rate of discharge and hence an incomplete description of the time-varying stochastic process governing the spike train, and
(3) interval histograms of the discharges during the response.
The interval between discharges is an important parameter in the generation of responses of a neuron. The interval statistics are, however, ignored in the PST computation and often blurred in the overall IH as in (3) above. A computer program (INSTAT) was written to compute simultaneously a regular PST histogram, a mean interval histogram (MIH) and a standard deviation of intervals histogram (SIH). The PST histogram divides post stimulus time into bins and the interspike intervals were assigned to the particular bin in which the spike that defined the start of the interval fell. Only the mean and standard deviation were computed for the intervals assigned to each bin, thereby creating two histograms (MIH and SIH) in addition to the PST histogram. The MIH and SIH have to be interpreted cautiously because of possible biased estimation. For example, near the end of a stimulus, the mean and standard deviation will be based on a combination of the responses to the stimulation and the following "spontaneous" activity. Also, if the mean interval changes significantly during the time span of a bin, the standard deviation will contain an erroneous component that is proportional to the magnitude of the change in the mean interval over the bin width of the PST histogram.

4.4.3 Period histograms

Low-frequency tonal stimuli (frequency $\lesssim$ 5 kHz) often elicit responses from CN units that have an instantaneous rate of discharge with a significant periodic component at the stimulus frequency. A PST histogram synchronized to the individual cycles of the stimulus, known as a positive zero-crossing (PZC) or period histogram, yields an estimate of the instantaneous rate over one cycle of the tone. When the stimulus frequency was below 2 kHz, the period histogram had between 100 and 200 bins, the number varying with the frequency. For frequencies above 2 kHz, the bin width was always 5 μsec.

As a quantitative measure of the extent to which the discharges occur at a preferred phase of the tone, the commonly used synchronization index (Anderson et al., 1971; Littlefield et al, 1972; Johnson, 1974) or vector strength (Goldberg and Brown, 1969) was computed from each period histogram. The synchronization index (S) was obtained by computing the coefficient of the fundamental component in a Fourier series expansion of the period histogram and then normalizing by the number of responses in the histogram. The resulting measure yielded values ranging from 0 (flat histogram) to 1 (all responses in a single bin). The computation is expressed by:

(see next page)

$$S = \frac{\left\{ \left[\sum_{i=1}^{N} h_i \cos \frac{2\pi Bi}{T} \right]^2 + \left[\sum_{i=1}^{N} h_i \sin \frac{2\pi Bi}{T} \right]^2 \right\}^{\frac{1}{2}}}{\sum_{i=1}^{N} h_i} \qquad 3.4$$

where, h_i = contents of i^{th} bin of the period histogram, and

N = number of bins of the period histogram which contained 1 period of the stimulus.

B = bin width of period histogram

T = period of stimulus .

All period histograms, unless otherwise noted, were computed from the discharges to a continuous tone stimulus of 30 seconds duration or longer. For a number of units the synchronized discharge was also measured during the last half of the response to a 25 msec tone burst. The initial 10 msec of the response was not used in the computation in order to exclude the initial transient response which is particularly strong for some CN units.

Since the measured time of occurrence of each spike is determined by a level-crossing detector, additional components of the microelectrode signal can affect the time at which the individual spikes cross the level. Some of the implications of this problem were considered by Moxon (1973) and further analyzed by Johnson (1974). There are two main types of this effect. (1) Spurious signals uncorrelated with the stimulus will produce jitter in the measured spike times, therefore reducing the measured synchronization to stimulus tone. (2) A baseline component related to the stimulus, such as cross-talk from the

stimulus signal or gross evoked potentials, can produce systematic displacements of the measured spike times thereby introducing a stimulus related component in the measured instantaneous rate. Johnson (1974) has analyzed the effect of a Gaussian zero-mean noise added to the microelectrode signal. The reduction in the measured synchrony is significant only for frequencies above 3 KHz even for his "noisy" spike case. Although the signal to noise ratio of some of the spike sequences recorded in this study were worse than Johnson's "noisy" spike case, the spikes recorded with the metal electrodes had a rise-time which was generally 1/2 to 1/3 that estimated by Johnson (200 μsec) for his KCl pipette recordings. The overall effect of having a higher noise level but faster spikes would approximately cancel in most situations. It appears from empirical observations that the time jitter introduced by the background noise becomes serious only under conditions that were already rejected because of poor triggering.

Stimulus related gross responses can be recorded throughout the CN in response to most stimuli. For tones in particular, the sinusoidal gross response or frequency following response (FFR) can become comparable to the amplitude of some spikes recorded with the metal electrodes used in this study. In the absence of spurious components, the level-crossing detector triggered by the spikes would yield a set of times $\{ t_i \}$ as the solutions to the equations,

$$\left\{ \begin{array}{l} v\ (t_i) = V_T \\ \dot{v}\ (t_i) > 0 \end{array} \right\} \qquad 3.5$$

where, $v(t)$ = the voltage from the microelectrode

and V_T = the threshold level of the level-crossing detector.

However, with a sinusoidal waveform superimposed on the spike recording the times become $\{\tilde{t}_i\}$ as solutions to,

$$\begin{aligned} & v(\tilde{t}_i) + A\cos(2\pi f\tilde{t}_i) = V_T \\ & \dot{v}(\tilde{t}_i) - 2\pi fA\sin(2\pi f\tilde{t}_i) > 0 \end{aligned} \qquad 3.6$$

For the case of a spike train with no synchronization of its instantaneous rate and with spikes that are approximately linear about the nominal trigger point, equations 3.6 can be solved to yield the same result as derived by Johnson (1974). The final formula can be rewritten as:

$$\text{Synchronization index} = S = \pi\gamma f T_R \quad (\text{for } S \leq .5) \qquad 3.7$$

where, γ = ratio of the peak-to-peak amplitude of the baseline sinusoid to the spike height (Figure III-5, inset on lower graph)

T_R = "rise-time", defined to be the ratio of the spike height to the slope of the spike at the trigger point or equivalently the "baseline to peak" time for a tangent to the trigger point.

f = frequency of the stimulus.

The parameter γ is a dimensionless amplitude ratio which was estimated during the recordings. In a few cases γ was as large as 0.1, a situation which is easily detectable on the oscilloscope display and in the audio monitor of the microelectrode signal. No situations with $\gamma \geq 0.2$ were even recorded. When γ approaches 0.2 not only is the synchrony measurement compromised but often the triggering quality is significantly degraded.

The spike rise-times were found to be relatively constant within a given category of spike waveform. Some typical averaged spike waveforms are shown at the top of Figure III-5 with their derivatives directly below. The scale to the right of the derivatives provides a direct conversion to rise-time from any particular derivative value. The minimum rise-time values for the recorded spikes were typically:

(i) $50 \lesssim T_R \lesssim 80$ μsec ; triphasic spikes (B)

(ii) $80 \lesssim T_R \lesssim 110$ μsec; diphasic spikes without pp (C, D)

(iii) $T_R \sim 100$ μsec ; spikes of pp units (E)

(iv) $T_R \sim 50$ μsec ; some very narrow spikes (F)

Waveform (A) of Figure III-5 is one of the three broadest spikes recorded in this study. The rise-time for these units was around 150 μsec.

When γ approaches 0.1 the presence of the FFR is obvious. Thus an interesting value of γ at which to examine the synchrony produced by an FFR is for $\gamma = 0.1$. This will be a "worst case" for unsuspected FFR effects. The lower half of Figure II-5 shows a plot of the synchronization index versus the frequency of a sinusoidal baseline with

Figure III-5 The effect of typical spike rise-times and a baseline sinusoid on the measurement of synchronized activity

The upper part of the figure shows six examples of averaged spike waveforms and directly below the computed derivative. All spikes are normalized to the same amplitude so that the derivatives could be directly converted to rise-time on the scale at the right. Rise-time (T_R) and γ are defined in the inset of the lower plot.

Three typical values of T_R were used to plot the theoretical estimate (from equation 3.7) of the synchronization that would be produced by a baseline sinusoid with a peak-to-peak value of one-tenth of the spike amplitude ($\gamma = 0.1$).

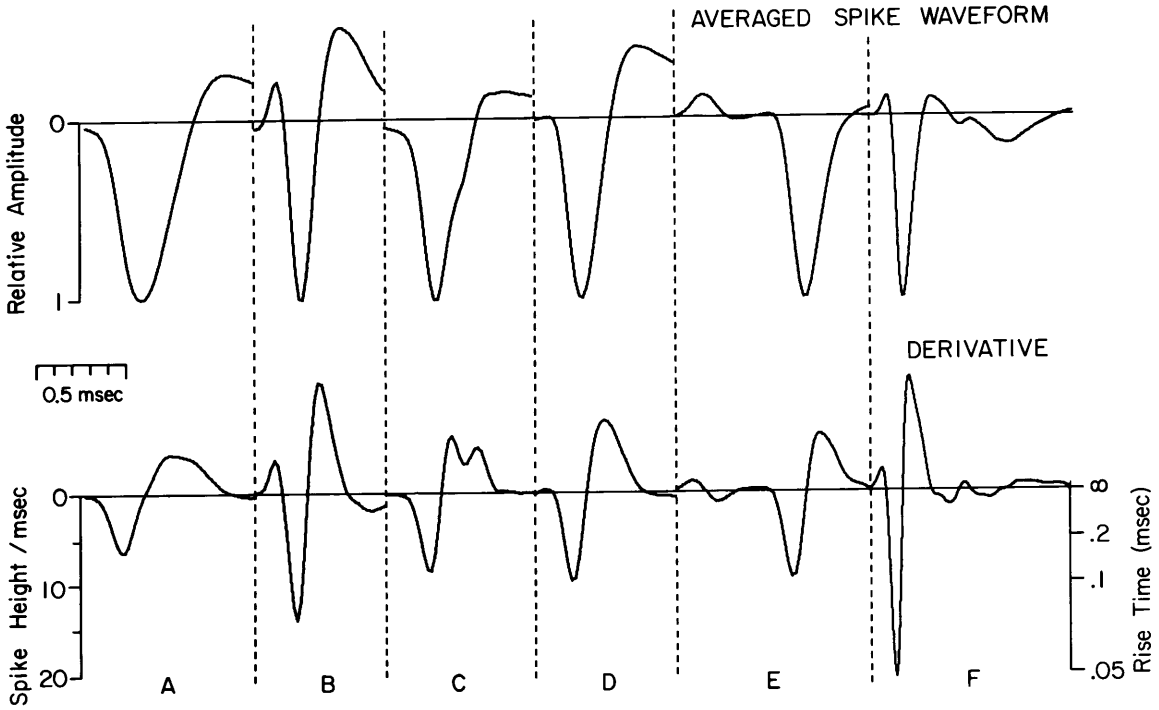
AVERAGED SPIKE WAVEFORM
Relative Amplitude
0
1
0.5 msec
DERIVATIVE
Spike Height / msec
0
10
20
∞
.2
.1
.05
Rise Time (msec)
A
B
C
D
E
F

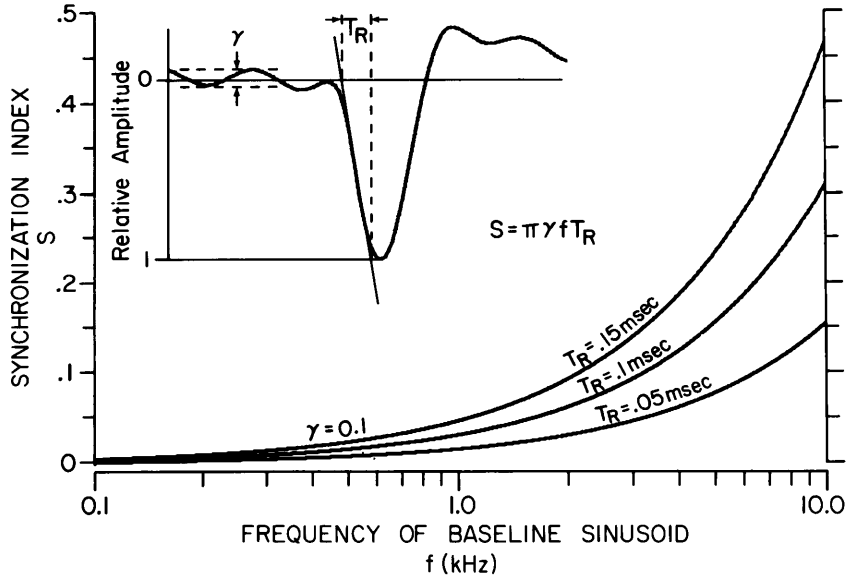
SYNCHRONIZATION INDEX
S
.5
.4
.3
.2
.1
0
Relative Amplitude
γ
T_R
0
1
$S = \pi \gamma f T_R$
T_R = .15msec
T_R = .1msec
T_R = .05msec
γ = 0.1
0.1
1.0
10.0
FREQUENCY OF BASELINE SINUSOID
f (kHz)

$\gamma = 0.1$ and a range of rise-time values typical of the AVCN recordings. When an FFR is noticed, it can be reduced by filtering and/or by addition of a cancelling tone which could reduce the size of γ to 0.05 or less, thereby halving the synchrony values of the curves in Figure III-5.

Although the presence of an FFR can be a source of significant error when computing a period histogram to tonal stimuli above 1 kHz, if carefully controlled for, the effect can be negligible. For most of the sample sizes (the number of spikes), a synchronization index of less than 0.1 is not statistically significant. With $\gamma \leq 0.05$, the synchronization index is below 0.1 for most spike shapes. For frequencies above 3 kHz, the smaller gross response further reduces the problem.

5. Electrode Localization and Mapping of Unit Locations

The remainder of this chapter is concerned with the histological determination of the recording and stimulating sites within the CNS. The precision of the localizations was influenced both by the objectives of the particular experiment and by the amount of histological evidence that was recovered. In most of the experiments, the protocol was constrained to facilitate the subsequent histological verification of the single unit recording sites in the CN. The ultimate objective in the estimation of a single unit location was to determine the equivalent position in a standard three dimensional map of the CN. In some cases, the histological evidence was inadequate to assign an equivalence within the 80 μm cubes of the map, but the AVCN subdivision could at least

be specified.

5.1 Block model

The three dimensional map of the CN, known as the block model, was initially defined by Kiang et al. (1975) and used by Godfrey et al. (1975 a, b) in a study of the posterior CN. The block model is a quantized representation of a particular cochlear nucleus which was selected for the quality of histological preparation and typical appearance of the cochlear nuclei. The procedures used in preparing the model brain differ somewhat from those used in the present study. The following features of preparation of the model cat (TB-20) should be noted:

(1) A posterior craniotomy was performed, but there was no retraction or aspiration of the cerebellum.

(2) The fixative was Bodian's fixative No. 2 (Bodian, 1937) made with tertiary-butyl alcohol.

(3) The plane of sectioning was transverse.

The model was constructed by taking every fourth transverse section (80 μm apart), making drawings of each section from enlarged photographs, aligning these drawings, and digitizing the boundaries of each drawing on a grid with a spacing equivalent to 80 μm on the histological sections.

As a part of the present study, the block model was updated to include the AVCN subdivisions and some new PVCN subdivisions as reported in Brawer et al. (1974). In consultation with D. K. Morest, a series

of drawings of the TB-20 sections were made with the subdivision boundaries as defined in Brawer et al. (1974). The present form of the block model was entered into a computer by tracing the boundaries with an X-Y digitizer. The atlas can now be recreated at any plane of sectioning. In addition to the standard sagittal and horizontal planes, the model has been reconstructed in several oblique planes. The more important of these for the present study is a set of sections for a special transverse plane that is tilted 40^{o} from the standard transverse toward horizontal. This set was needed for part of the experimental series to be described later. Sample sections from the block model are shown in Figure IV-40.

5.2 Experimental procedures

In each experiment an otoscope with a calibrated eyepiece was positioned so as to allow observation of the exposed CN surface. A sketch of the exposed CN outline, the adjacent temporal bone and cerebellum was used as a map on which to record the location of the microelectrode penetrations. This record was used in the experiment to ensure that the microelectrode penetrations were kept sufficiently far apart to be distinguishable in the histological sections.

The surgical exposure of the postero-dorsal surface of the CN also allowed the stereotaxic prediction of electrode locations based on the block model. The otoscope was oriented so that the line of sight would coincide, as closely as possible, with the intersection of the parasagittal and transverse planes. This orientation of the

otoscope made the observed posterior and postero-lateral edges of the CN coincide with the corresponding limits for the block model. Thus a given distance rostral to the posterior edge is equivalent to a particular transverse level in the block model. The equivalent lateral-medial position in the block model is similarly estimated by measuring the distance from the exposed lateral edge of the experimental CN. The correspondence of the lateral edge of the experimentally viewed CN and the absolute lateral limit of the CN holds mainly for the posterior third of the CN where the lateral limit is not obscured by the overlying temporal bone. But this portion is generally adequate to establish a lateral-medial correspondence. For each microelectrode pass, the lateral-ventral and rostro-caudal coordinates at which the microelecrode first contacted the surface were measured with respect to the CN limits. From a knowledge of the point of entry and the orientation of the microelectrode, the trajectory through the block model could be predicted.

The microelectrode manipulator was always oriented so that the electrode trajectory was close to the proposed plane of histological sectioning. Although this correspondence was not essential, it simplified the later reconstruction of the microelectrode tracks.

In addition to maintaining records of the point of entry and orientation of each pass, it was necessary to establish one or more reference points along each track. These points would later be used to relate the electrode movements along the pass to distance along the histological sections. The CN surface was very often one of the

reference points for the passes that entered the brain at the exposed CN surface. In these cases the microelectrode was brought just to the CN surface by a combination of visual and auditory cues. The convergence of the image of the microelectrode tip with its reflection from the CN surface was observed through the otoscope, and, at the same time, an audio monitor of the microelectrode signal would exhibit a sudden drop in the 60 Hz pickup when the electrode contacted the fluid layer over the surface of the brain.

Other reference points were established along the tracks by creating small lesions of about 100 μm diameter. At one to four positions along each track, radio-frequency current was passed through the microelectrode to create lesions. The passing of this current was generally done near the end of the recording time of each pass because the lesioning usually damaged the microelectrode.

The lesions were intended to mark positions along the track. The relationship of these lesions or reference points to the locations of the unit recordings is, however, subject to any changes in the position of the CN with respect to the manipulator that occur between the time of the recordings and the creation of the lesion(s). Since most of the lesions were made near the end of the passes several hours usually elapsed between the first unit recording and the final lesioning. As the microelectrode was withdrawn, opportunities to obtain controls on the relative position of the microelectrode and CN were sought. Similar units and the location of a CF jump at the DCN to VCN border were usually found to be within 50 μm of the earlier recording sites.

When the manipulator is brought back to its starting location it is usually within 50 to 100 μm of the surface.

5.3 Histological preparation

At the end of each experiment for which histology was required, the animal was perfused intracardially with a 0.9% saline solution (100 cc) followed by a 10% formalin fixative solution (1000 cc), both of which were heated to body temperature. The head was removed, immersed in 10% formalin, and stored in a refrigerator. Later, the brain was carefully removed from the skull and placed, ventral surface down, on a macrotome (Rasmussen, 1931). The macrotome served to guide cuts through the brain isolating the portions of interest and defining the plane of sectioning for each piece. First the CN was isolated. For those CN's to be sectioned along a parasagittal plane, a cut parallel to the midline and perpendicular to the base of the macrotome was made just medial to the CN. If the contralateral SOC was also to be examined, it was then isolated by making two cuts through the remaining brainstem along a plane perpendicular to the midline, 55^{o} from the base of the macrotome. When the CN was to be sectioned in the special transverse plane, the brain was cut along a plane perpendicular to the midline and 40^{o} from the base of the macrotome. If a stimulating electrode track through the SOC was to be histologically verified, the SOC was included in the block containing the CN. The SOC was sectioned along with the CN even though the resulting sections were 15^{o} different from the plane of the stimulating electrode path. For histology of the

inferior colliculus (IC), isolation was achieved with a parasagittal cut. The isolated blocks of tissue were embedded in paraffin and sectioned, parallel to the defining cut, into 20 μm thick sections. Alternate sections were stained with protargol and cresyl violet.

5.4 Examination of histological sections

There were usually three steps in the examination of the stained CN sections. The first step was an initial survey to identify the histological evidence of the microelectrode passes. The cresyl violet stained (Nissl) series containing the AVCN and the adjacent parts of DCN and PVCN were examined for lines of stained leukocytes which usually define a microelectrode track and/or densely clustered group of leukocytes which mark lesion sites. The intervening protargol stained sections were usually used to identify or confirm lesion sites since the lesions often showed up clearly as holes in the darkly stained tissue. Lesions were usually 50 to 100 μm in diameter.

The purpose of the second and third steps is to determine the location of the tracks within the subdivisions of AVCN. As stated previously, the objective is to specify each unit's location in the block model. A full reconstruction of the CN, as was done for the model CN, was not attempted for the experimental cats, but rather an abbreviated description of the subdivision boundaries was made. The description has been broken into two parts to form steps 2 and 3. In step 2 we specify one coordinate of the electrode track, namely the position along the dimension perpendicular to the plane of sectioning.

Since this coordinate can be specified in terms of the section numbers from the histological series, the function of step 2 was to describe the location of the subdivisions through the series of sections. The general approach was to determine the pair of sections that bounded or limited the extent of each subdivision. Since some of these "subdivision limits" were difficult to determine and/or were redundant (because they coincided with others), a particular set of subdivision limits, easily and reliably defined and approximately uniformly spaced across the range of AVCN, were chosen to serve as reference planes at intervals through the histological sections. Step 3 involved the preparation of detailed drawings of the AVCN subdivision boundaries for the sections in the vicinity of each useful track. The subdivision boundaries were drawn according to the cytoarchitectonic criteria as described in Brawer et al.(1974).

For certain boundaries the criteria were particularly difficult to apply. Some of the uncertainty is attributed to peculiarities of the particular CN being examined, such as poor staining, experimental or histological deformation of the tissue and a paucity of neurons in the vicinity of a boundary. To some extent these aberrations could be compensated for by a more comprehensive examination of the entire AVCN. There were additional problems, however, that are attributed to the inherent limitations of a subdivision scheme itself. The non-disjoint, qualitative definition of the regional traits combined with overlapping spatial distributions of the characteristic cells made the choice of a dividing line somewhat arbitrary in many cases.

In subdividing AVCN, PV is easily outlined. The rostral half of AA is highly characteristic and easily recognized. As can be seen from the example sagittal section from the block model shown in Figure II-2, it is the determination of AP that essentially completes the subdivision of AVCN; however, this task is generally difficult. The three most common problems are as follows:

(1) The transition from the large densely packed cells of AA to the smaller more widely distributed cells of AP is often gradual having the appearance of clusters of cells in AP of the type typically seen in AA. A compromise is generally necessary in trying to keep these cells in AA and yet not eliminate AP.

(2) The postero-dorsal region of AVCN has a cellular composition that is not readily subdivided according to the criteria applicable to the remainder of the AVCN. When the AP boundaries are extrapolated into this region, what is taken to be AP is sometimes seen to be more densely packed, like APD. Both AP and PD were difficult to define in the dorsal (and lateral) regions just ventral to the granule cell layer.

(3) The choice of the lateral AP limit in the sagittal sections requires another difficult judgment. AP is distinguished from the adjacent AA and PD mainly by a lack of larger cells. This criterion is a negative one, and hence difficult to demonstrate unequivocally especially in the

more lateral sections where the width of AP becomes very small.

5.5 Reconstruction of the track

Once the locations of the tracks and lesions had been recorded on drawings of the CN sections, it was possible to reconstruct the tracks, associate them with the microelectrode passes and estimate the recording sites for each of the single units. Some of the steps in this procedure are summarized for a particular pass in Figure III-6. Rarely was a track contained in only one of the 20 μm thick sections. Thus in order to reconstruct the track, drawings of several sections usually had to be superimposed to obtain what will be referred to as a composite track. Measurements of relative electrode position taken during the experiment were matched with the reconstructed track in the "composite" (Figure III-6, center).

The critical factor in constructing the composite track was the alignment of the sections. With the cochlear nuclei sectioned in the special transverse plane, there were registration holes made by pins placed through the brain stem before the sectioning. The sagittal sections had no such objective criterion for alignment; the CN and adjacent structures of the brain were all that were available. However, this problem was not usually serious either because there were only a few sections to align, or the boundaries of the CN and other structures changed very little over the range involved. For the lateral third of the CN, the sagittal sections do change relatively rapidly

Figure III-6 Reconstruction of the unit locations along an electrode track

The steps in the reconstruction are illustrated from left to right. Drawings (left) of two sagittal sections (numbers 98 and 100) which contain representative features of the track are superimposed in the center to form a composite section. The interpolated unit locations are shown along the estimated center of the track in this composite. The final versions of sections 98 and 100 containing the unit locations and subdivision boundaries are shown of the right.

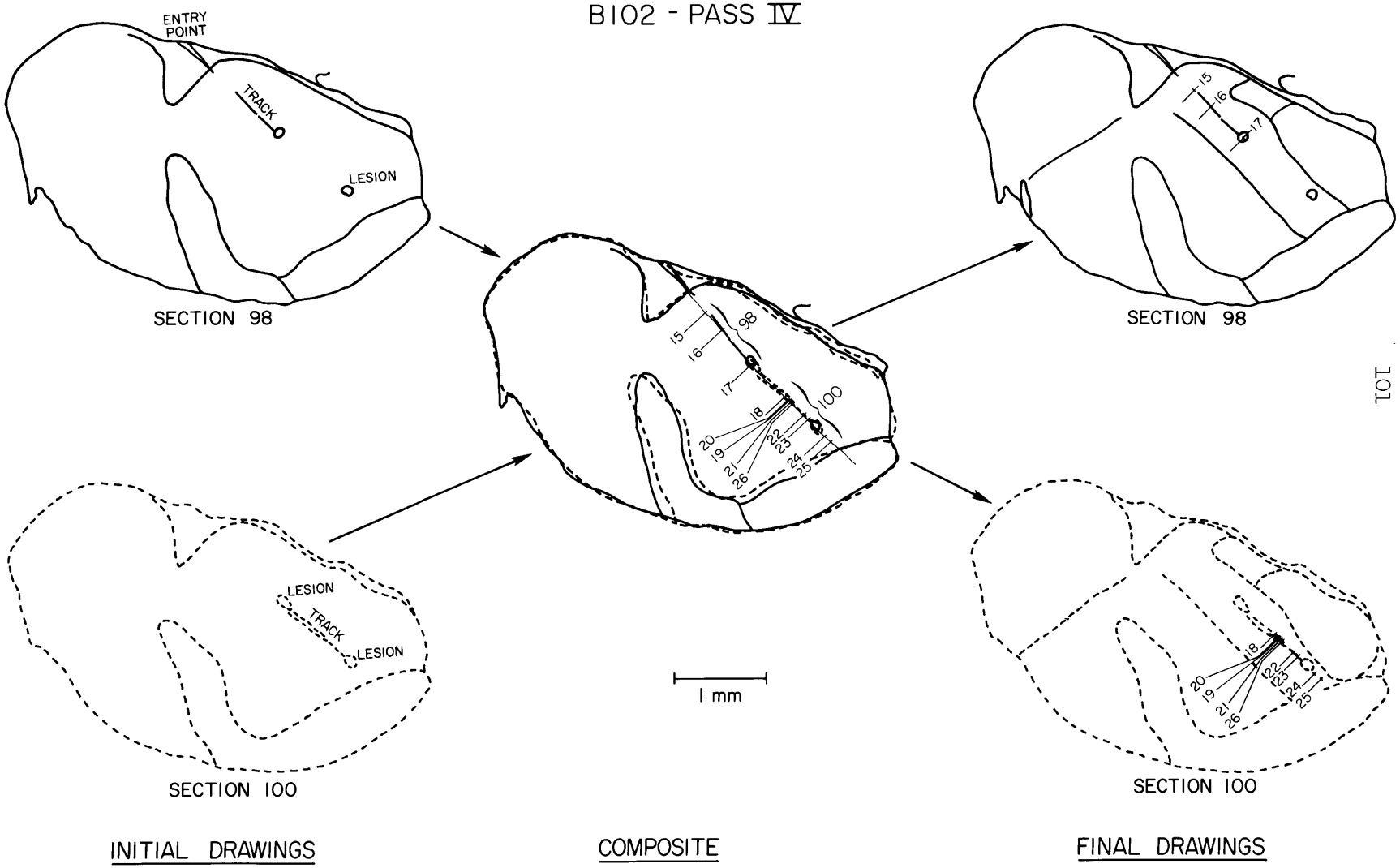
B102 - PASS IV
ENTRY POINT
TRACK
LESION
SECTION 98
LESION
TRACK
LESION
SECTION 100
15
16
17
98
100
18
20
19
21
26
22
23
24
25
1 mm
INITIAL DRAWINGS
COMPOSITE
FINAL DRAWINGS

in both area and shape. The block model served as a guide to the general arrangement of the lateral sections. Whenever several different alignments were tried for the more doubtful composites, the unit locations changed by about 100 μm or less. In only two cases were units not localized because of uncertainties caused by questionable registration of the lateral sagittal sections.

The association of each microelectrode pass made during the experiment with a histological track was based on the experimental record of the microelectrode orientation and point of entry. The relative positions of the tracks plus the different configurations of lesions along the tracks served to resolve ambiguities when the number of tracks found was unaccountably less than the number of passes.

Single unit locations were plotted along the estimated path of the track. Distance along the track was related to the micrometer settings of the hydraulic manipulator by using the reference points (lesions or point of entry at the brain surface). If two or more reference points were recovered for the track, then linear interpolation was used between them. In cases where only one reference point was recovered, the unit locations were usually plotted using an average interpolation factor from other tracks. When there were no reference points available, the particular subdivision could sometimes be assigned if the track was clearly restricted to one region.

The composite shown in the center of Figure III-6 indicates the interpolated unit locations. The interpolation in this case was based

on the estimated centers of the two lesion sites and the point of entry at the CN surface. An estimated center course of the track is shown as a fine line and along the line are indicated the unit locations. After the unit locations are plotted along the composite track, the locations are transferred back to the relevant sections. In addition to the unit locations, we introduce the subdivision boundaries obtained from the examination of the histological material (step 3) as shown in the drawings on the right of Figure III-6.

5.6 Unit locations in the block model

With the completion of the procedure described in section 5.5, the recording sites of the units are described in terms of their position within the experimental cochlear nuclei. By establishing a correspondence between the experimental cochlear nuclei and the block model, we can assign each localized unit a coordinate location in the block model. Pooling of the distributional information from the 48 experiments with histological preparations is immediately available when the units are located in the block model.

The transferring of single unit locations from the experimental CN to the block model was done in two steps. The overall objective was to assign each single unit to a position in the block model which had the same relative position with respect to the subdivision boundaries as the unit had in the sections of the CN to which it was localized. The first step was to choose the block model section that was most comparable to the histological section containing the unit location.

Then, as a second step, these equivalent sections were aligned so that the boundaries coincided in an average sense. With the sections overlaid in this manner, each unit was assigned the coordinates of the coincident block model cube. An inherent assumption of this procedure is that the model CN had the same shape as the experimental cochlear nuclei with the same distribution of subdivisions. The two part aspect of the procedure further assumes that the planes of sectioning are similar. Several comparisons of the block model with the experimental cochlear nuclei were made in checking these assumptions. Most of the deviations were of a form that could be compensated for within the procedure.

The practical problems associated with applying the procedure described above were different for the two planes of sectioning, sagittal and special transverse. Since sagittal sectioning was used more commonly, the procedure will be described in detail for it and then the procedure for the special transverse series will be briefly summarized.

* 5.6.1 Sagittal sections

The first step in mapping unit locations into the block model is to choose a function to relate section numbers in the experimental histology to the sagittal section numbers in the block model. Ideally this function would be linear of the form:

$$S_{BM} = A\ S_E + B \qquad 3.8$$

where S_{BM} = section number in block model,

S_E = section number in experimental histology,

and A and B are constants for a given CN. The constant A would nominally be 1/4 since the block model sections are 80 μm apart and the histological sections are 20 μm thick. The parameter B depends on the particular starting point of the sectioning. In view of the principle that the mapping of units into the block model should maintain the relative positions of the units within the subdivisions, the objective in choosing B (and A?) is to have the subdivision limits of the experimental CN map to the corresponding limits in the block model. A particular set of subdivision limits (lateral PV, lateral PD, lateral AP, medial AA and the most medial subdivision of AVCN) were used to define the lateral-medial location of AVCN. There was considerable variation between the various experimental cochlear nuclei as to whether the most medial point of the AVCN was near the dorsal or ventral border of the CN. An estimate of the medial AVCN limit was made in both the dorsal and ventral regions. Since the medial edge of the AVCN in the block model is essentially vertical, there is only one limit for the block model. The average of the dorsal and ventral estimates of medial AVCN were compared with block model limit.

Figure III-7 shows a comparison of the subdivision limits of experimental cochlear nuclei transformed by equation 3.8 with A = 1/4 (nominal value) and B chosen for each CN so that the lateral PD limits coincided. Some scatter is of course expected. The large variations

Figure III-7 AVCN subdivision limits in the sagittal sections of the block model and the experimental cochlear nuclei

The key on the right lists the 6 subdivision limits estimated for each cochlear nucleus in the experimental series using sagittal sectioning. The experiment number is shown in the column on the left. Each row represents the distances from lateral PD to the other boundaries in the histology of the various experiments. The same distances estimated from the block model are shown at the top of the figure along the sagittal coordinate scale for the block model (the units are 80 μm increments).

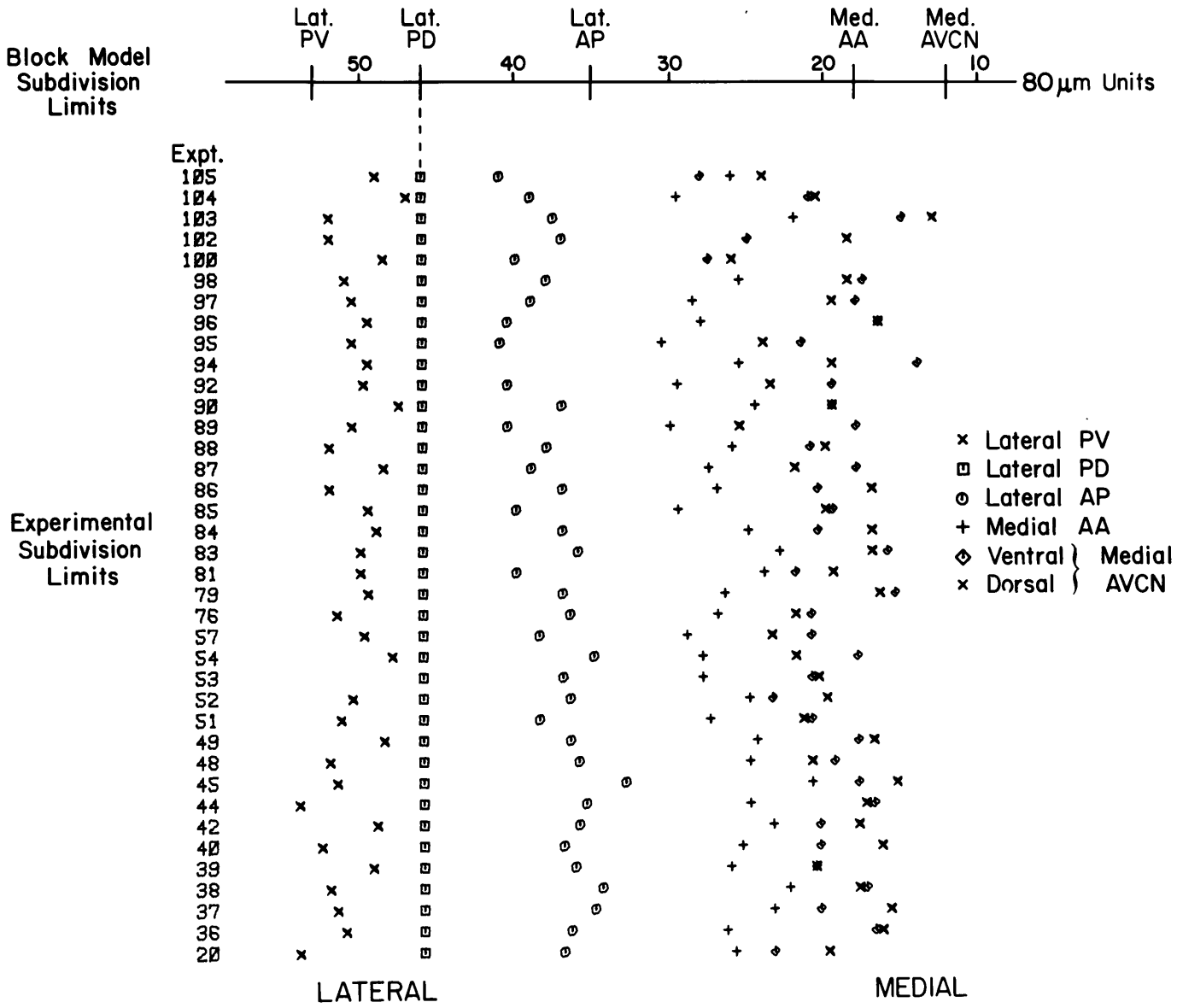
Block Model Subdivision Limits
Lat. PV
Lat. PD
Lat. AP
Med. AA
Med. AVCN
50
40
30
20
10
80 μm Units
Expt.
105
104
103
102
100
98
97
96
95
94
92
90
89
88
87
86
85
84
83
81
79
76
57
54
53
52
51
49
48
45
44
42
40
39
38
37
36
20
Experimental Subdivision Limits
× Lateral PV
□ Lateral PD
⊙ Lateral AP
+ Medial AA
◇ Ventral } Medial
× Dorsal } AVCN
LATERAL
MEDIAL

in the size of the nuclei (eg. Experiment 100 compared to 103) and the consistently smaller size compared to the block model require that A (as well as B) has to be chosen for each CN.

Before letting A be a parameter, some of the differences between the experimental cochlear nuclei and the block model were examined. Figure III-8 B shows a histogram of the distance from Lateral PD to Medial AVCN ("AVCN width"). The arrow labelled "Block Model" shows that the AVCN width for the block model is over 25% larger than the experimental mean (small arrow at horizontal axis). Part A of Figure III-8 illustrates that the smaller width of AVCN as compared to the block model is somewhat weakly correlated with a similar deviation for the posterior part of the cochlear nuclei. Discrepancies between the block model which is based on a CN that was sectioned transversely, and the experimental cochlear nuclei which were sectioned sagittally, might arise from a tendency for the parasagittal macrotome cut to move away from the midplane as it progresses ventrally. To simulate such an effect, the block model was sectioned at a plane 10^{o} from "true" sagittal. The AVCN and PVCN widths changed as shown in Figure III-8 A and B. Although this transformation produces an AVCN width for the block model that is less "extreme", the resulting PVCN width becomes more "extreme". Thus, this difference in sectioning angle of the block model does not account for the width discrepancy. The tentative conclusion from such comparisons of the experimental cochlear nuclei with the block model is that the block model is larger in the lateral-medial direction, often larger in the dorsal-ventral direction but, as found

Figure III-8 Comparison of the experimental cochlear nuclei with the block model

A. Scatter plot of PVCN width versus AVCN width. Width is defined to be the distance between the most lateral and the most medial sections in a sagittal series. In order to make the two measures comparable, PV was not included in the AVCN width. The X's were measured from the experimental cochlear nuclei that were sectioned sagittally. The point labelled (10° Tilt) was obtained from a set of block model sections generated by "sectioning" the model at 10° from the standard sagittal plane. The tilted plane deviated from the midplane as it went ventral. The scales were chosen so that equal percentage deviations from the means, shown by dashed lines, would represent the same distance on the plots. Unit distance in the block model (BMU) is 80 μm. No shrinkage correction was applied to any measurements.

B. Histogram of AVCN width. The same data points as in part A are plotted as a histogram (80 μm bin width). The small arrows at the length scales show the mean of the distribution.

C. Scatter plot of posterior cochlear nucleus (PCN) length versus AVCN length. The distance between the most posterior section containing cochlear nucleus and the most anterior containing AA was subdivided at the posterior limit of PD into a PCN length and an AVCN length. The X's were measured from the experimental cochlear nuclei that were sectioned in the special transverse plane. The point labelled "Block Model (40°-O)" is the comparable measurement from the block model. The other points are

labelled according to the angle of sectioning with respect to the standard transverse plane and the sagittal shifting modification of the block model.

D. Scatter plot of two measures of cochlear nucleus shape. The vertical scale shows the number of special transverse sections between the most rostral fusiform cells in DCN and the caudal limit of AA. The horizontal scale is the distance over which both AP and PV are present in the sections. The symbols are the same as for C. The dashed line is a least-mean-square-error fit to the experimental data points.

E. Histogram of the distance between the transverse sections containing the lateral and medial extremes of the PV to PVCN boundary. These distances were measured from 16 cochlear nuclei sectioned in the standard transverse plane. The arrows represent the equivalent distances for the normal block model (at zero) and for the block model when the sagittal sections are displaced by 1 unit in 3 or 1 unit in 4 as illustrated in part F.

F. Illustration of the sagittal shift modification of the block model. On the left is the normal horizontal section, H45, with the subdivisions of the ventral cochlear nucleus labelled and the PV to PVCN border emphasized with a solid line. On the right is the corresponding section after shifting the sagittal sections with respect to each other by 1 block model unit every 4 sagittal sections.

SAGITTAL SECTIONING

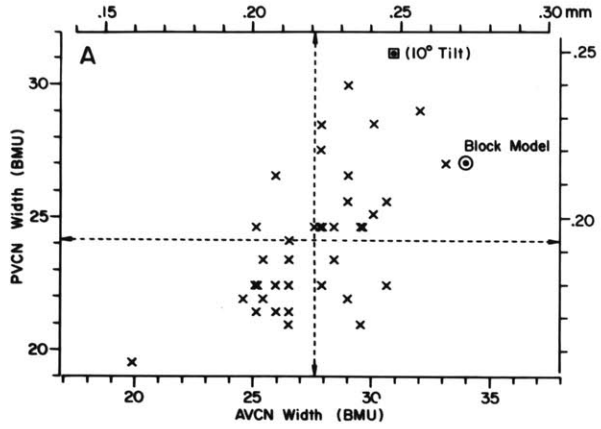

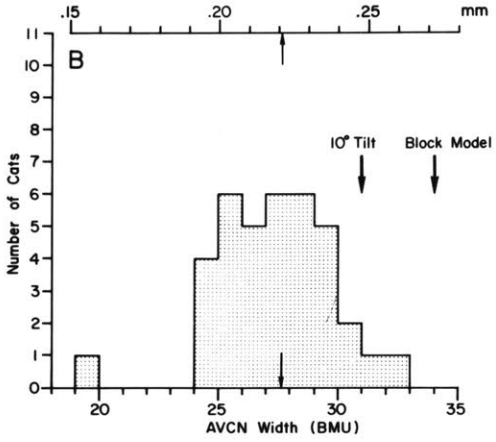

SPECIAL TRANSVERSE SECTIONING

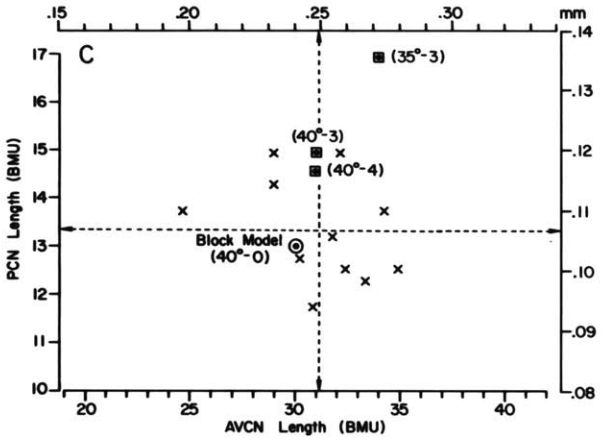

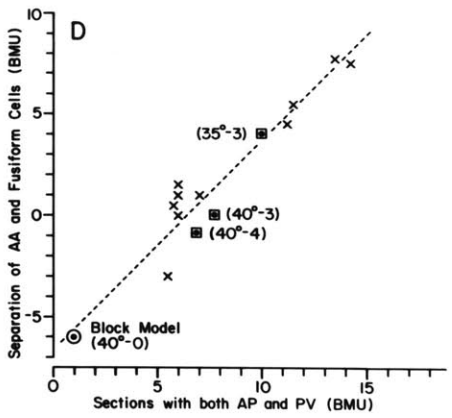

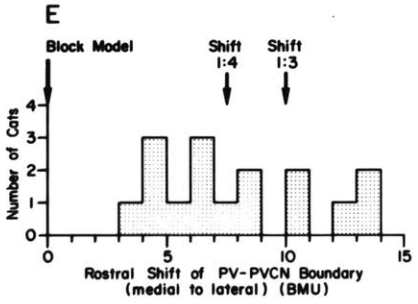

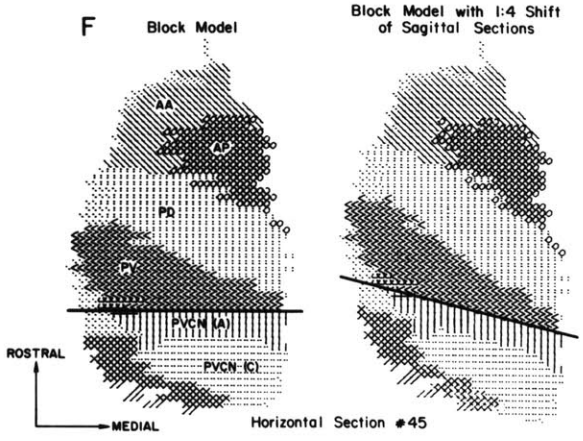

by Godfrey (1971), of a similar length in the rostral-caudal direction.

As the next level of complexity in relating distance in the experimental CN to the block model, the parameter A in equation 3.8 was allowed to vary. For each experimental CN, A and B were chosen according to a least-mean-square-error (LMSE) criterion for the correspondence of the set of subdivision limits with those of the block model. This LMSE fit matched some of the subdivision limits quite well, but others deviated systematically, revealing that the distances between the subdivision limits (inter-limit distances) were in different proportions in the block model than in the experimental cochlear nuclei. Generalizing equation 3.8 to a second-order function did not completely compensate for this deviation. The inter-limit distances were, therefore, taken as the basis of the final matching procedure for the sagittally sectioned cochlear nuclei. The inter-limit distances were averaged across the experimental cochlear nuclei and taken as the basis of a set of "average subdivision limits" (bottom of Figure III-9) to which the experimental subdivision limits were fit by the first-order (equation 3.8) LMSE procedure. The resulting choices of A and B provided the correspondences shown in the center of Figure III-9. The lateral AP limit was given less weight in the mean-square-error computation because of the greater uncertainty in this boundary. The weights are shown just above the "Average Subdivision Limits" line.

The choice of A and B in equation 3.8 determines the mapping from section number in the histology of the particular experimental CN to the "average subdivision limits" axis (lower axis in Figure III-9).

As the final step, we have to relate distance along the "average subdivision limits" axis to the sagittal coordinate of the block model. This transformation, identical for all of the cochlear nuclei, was performed with a fifth-order interpolation polynomial which maps the five average subdivision limits (vertical lines in Figure III-9) to those of the block model (upper axis). Equation 3.8 plus the polynomial were used to plot the relationship of section number in each CN with section number in the block model. An example of one of these graphs is shown in Figure III-10. The deviation from linearity is not large but is systematic. Each of the graphs, and to some extent the assumptions of the procedure were checked by comparing the predicted equivalent sagittal sections of the model and the experimental CN. The main criterion for assessing equivalence was that the two sections have the same distribution of subdivisions; that is, the subdivisions occupy the same percentages of the sections and have the same positional relation to one another. In a few cases the graph was modified to improve the equivalence. The resulting graph was not usually changed by more than one or two model sections at any point.

The selection of the block model section which best represents the particular experimental section establishes one coordinate of the unit locations. The remaining two coordinates were determined by matching the sections. As the continuation of Figure III-6, in which we saw the construction of the composite track and subsequent plotting unit locations for B102-Pass IV, we shall follow section 98 through the remaining steps. In the upper right of Figure II-10 is shown the graph obtained from the LMSE fit procedure. From this graph we read

Figure III-9 AVCN subdivision limits fit to the block model limits

The data points of Figure II-6 were fit by a least-mean-square-error criterion to the average interboundary limits shown at the bottom of the figure. The weights used in the fit are above the average boundaries. The dotted lines from the average boundary lines to the block model limits represent a 5 point linear interpolation to the block model limits.

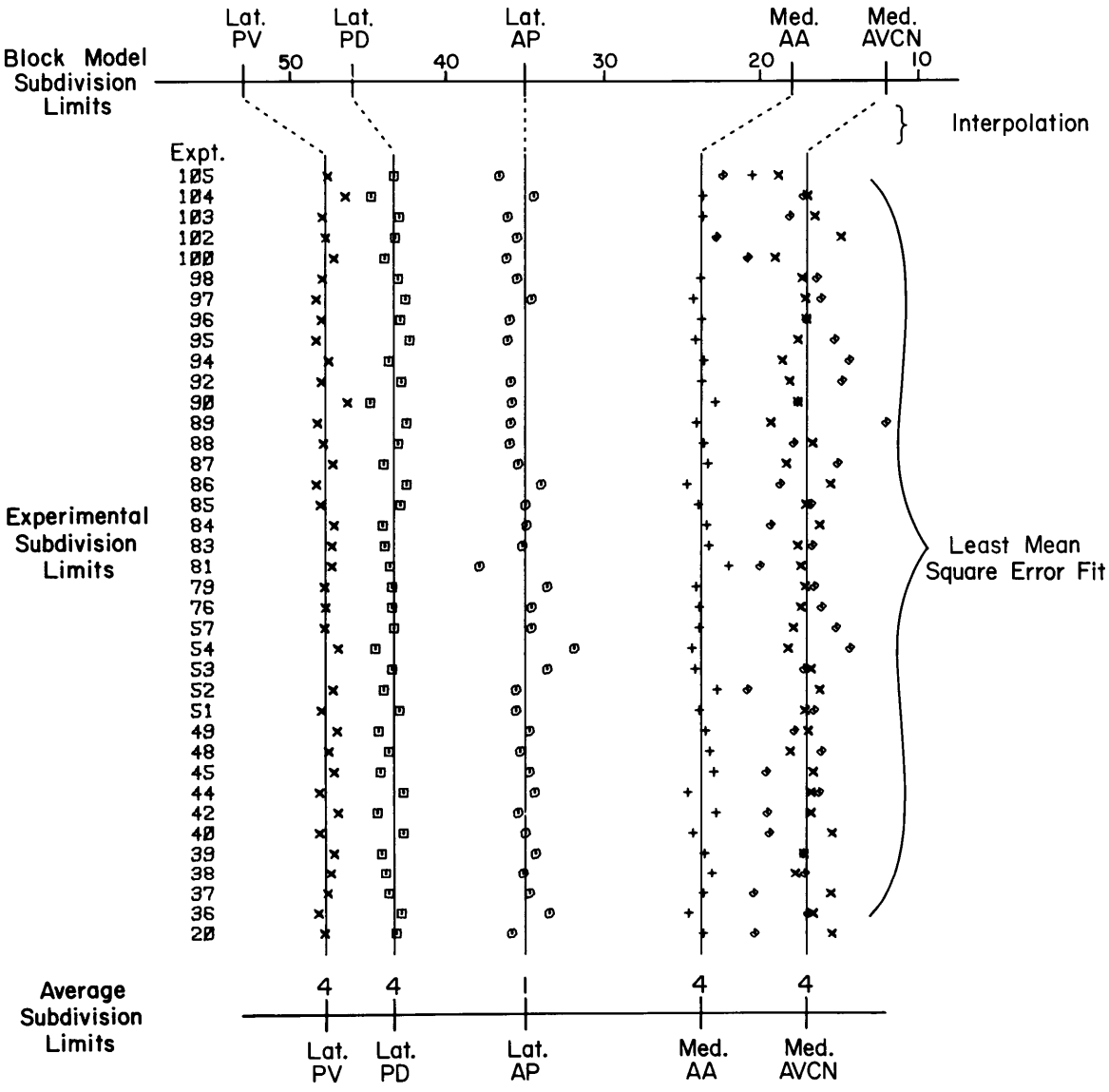
Block Model Subdivision Limits
Lat. PV
Lat. PD
Lat. AP
Med. AA
Med. AVCN
50
40
30
20
10
Interpolation
Expt.
105
104
103
102
100
98
97
96
95
94
92
90
89
88
87
86
85
84
83
81
79
76
57
54
53
52
51
49
48
45
44
42
40
39
38
37
36
20
Experimental Subdivision Limits
Least Mean Square Error Fit
Average Subdivision Limits
4
4
1
4
4
Lat. PV
Lat. PD
Lat. AP
Med. AA
Med. AVCN

Figure III-10 The final step in determining unit locations in the block model

On the right is shown a drawing of section 98 from B102 as it was traced into the computer. The labelling was added for the purposes of the figure. The graph (upper right) is the predicted mapping of the B102 histology to the block model sagittal sections. Section 98 was transformed to allow a direct correspondence with the predicted block model section, S27. The units localized to section 98 (15, 16 and 17) were assigned to the block model coordinates of S27 as summarized in the lower right of the figure. The block model units are 80 μm and the original drawing (right) of section 98 was done at the same scale.

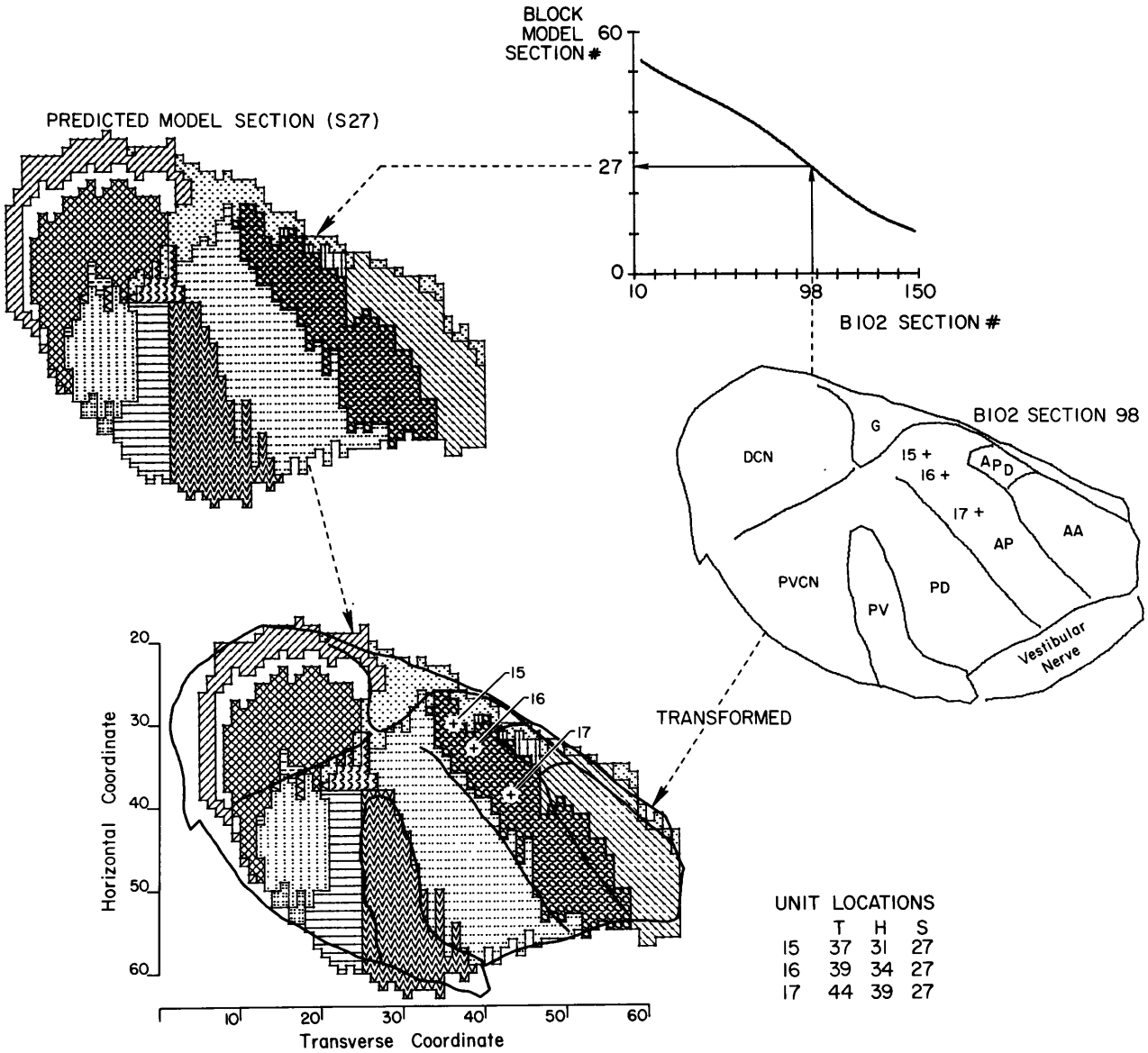
BLOCK MODEL SECTION #
60
27
0
10
98
150
B102 SECTION #
PREDICTED MODEL SECTION (S27)
B102 SECTION 98
DCN
G
15 +
16 +
17 +
AP
D
AA
PVCN
PV
PD
Vestibular Nerve
TRANSFORMED
15
16
17
20
30
40
50
60
Horizontal Coordinate
10
20
30
40
50
60
Transverse Coordinate
UNIT LOCATIONS
T H S
15 37 31 27
16 39 34 27
17 44 39 27

off the block model section, S-27, which is shown at the upper left. The final step is to align S-27 with section 98 from B102.

The experimental sections were drawn on the same scale as the block model sections so that they could be directly superimposed. In a few cases the sections were almost identical so that a translation and rotation were all that was required to bring the boundaries into correspondence. In most cases, however, the experimental sections were smaller than those of the block model. For about half of the sections matched to the block model the shapes were sufficiently different that an acceptable match could not be obtained even after a magnification.

In an effort to characterize the shape differences between the experimental CN sections and the block model, a detailed comparison was made. In addition to all of the CN sections drawn as part of the localization procedures, a complete set of drawings (every 80 μm) was made for three of the experimental cochlear nuclei. From these drawings and further microscopic study, three types of shape differences from the block model were identified. The first discrepancy was characterized as a rotation of the vestibular nerve (labelled in Figure III-10) about its contact point with PV. The CN regions above the vestibular nerve were consequently displaced by proportionally greater distances, the farther from PV they were situated. The second type of shape difference was characterized as a different proportion of length (rostral-caudal) to depth (dorsal-ventral). The third type of discrepancy was unfortunately present to some extent in most sections from the experimental cochlear nuclei. The dorsal surface of the AVCN

is, in the block model, slightly concave near DCN but predominantly convex over the remainder, whereas many experimental cochlear nuclei were distinctly concave for the whole dorsal surface of AVCN. There were concomitant changes in the internal shape as well.

The shape differences described above were grouped into the three types only for convenience in deciding on the methodology for compensation. They may, in fact, represent different aspects of a more general difference between the experimental cochlear nuclei and the block model. For instance the third type, by virtue of its curvature, results in differences similar to those which characterize the first and second types, namely a rotation of the vestibular nerve with respect to PV and an elongation along one direction.

As a first step in dealing with these shape differences the individual section drawings were entered into the computer via a graphical input device. The line segments making up a given section could then be displayed on an oscilloscope screen for comparison with the block model section and transformed by a combination of:

(A) an overall scaling,

(B) a stretching which was area-preserving by including a perpendicular compensating compression, and

(C) a mapping that would straighten a presumed curvature by transforming polar coordinates to rectilinear with area preservation.

The type 1 discrepancy was significant for only three tracks, and was handled by simply sliding the two sections. The other shape deviations

were transformed with (A), (B) and (C) above. When the transformed experimental section matched the block model section, the experimental section was plotted out with the unit locations also transformed. Section 98 in Figure III-10 was transformed by (A), (B) and (C) above in an iterative interactive manner to change the shape and overall size to obtain the correspondence shown in the overlay in the lower left. The unit locations were then specified as coordinates of S-27.

*5.6.2 Special transverse sections

For the cochlear nuclei that were sectioned in the special transverse plane, the procedure used to transfer single unit locations to the block model had, of course, the same objective as for the sagittal sections: to maintain the relative position within the subdivisions. The problems encountered were, however, quite different. Once an equivalent section from the block model was chosen, the matching procedure was straightforward, requiring at most an overall scaling. However, the sections from most of the experimental cochlear nuclei could not be matched with sections from the block model sectioned at the predicted angle of 40^{o} from the transverse plane (the special transverse sections). The experimental cochlear nuclei were therefore compared in detail with the block model in an effort to clarify the nature of this discrepancy. The most obvious manifestation of the difference occurred in the sections containing both PV and AP. In the special transverse sections of the block model, there are only a few sections containing both of these subdivisions. As PV is reaching

its most anterior extent at the lateral border of AVCN, AP is just beginning at the medial edge. In many of the cochlear nuclei, however, there is a large range of coincidence, with some sections having almost equal areas of PV, PD, and AP occupying the lateral, central, and medial thirds respectively of AVCN's lateral to medial extent. Thus the experimental cochlear nuclei seem to show a rostral displacement of lateral AVCN with respect to the medial edge. The displacement (with respect to the block model) appears to develop across the span of AVCN giving rise to the increased coexistence of PV and AP in the sections. In Figure III-8 D is plotted the number of sections containing both AP and PV against a measure selected for its sensitivity to the angle between the plane of sectioning and the orientation of the CN. The strong correlation of these parameters and the extreme location of the standard block model ("40^{o}-0") graphically represents the problem encountered.

Based on this correlation, an additional correlate of the discrepancy was predicted to be a more rostral disposition of the lateral edge of the PV-PVCN border as compared to its medial edge. In the block model, there is no such variation. As a test of this prediction, an earlier experimental series of cochlear nuclei which were sectioned in the standard transverse plane was examined. The results are shown in Figure III-8E. The block model is shown by the arrow at the origin. With this confirmation that the shift is evident in another series, it was decided to re-section the block model after applying a correction. The correction took the form of a progressively increasing displacement

of the sagittal sections along the rostral-caudal direction such that every third or fourth section was shifted by one block model unit. When viewed in a horizontal section this shifting produced a slope of 1:3 or 1:4 of the PV-PVCN border (as shown in Figure III-8 F).

This modification of the block model significantly improved the correspondence with the experimental histological sections. In Figure III-8 D, for example, the two slopes yield points, (40^{o}-4) and (40^{o}-3), which are within the range of the experimental cochlear nuclei. These versions of the block model were, however, not adequate for all of the experimental sections.

The shape differences that were seen in the sagittal series and discussed in Section 5.6.1 indicate that the AVCN in the experimental cochlear nuclei had a different orientation than it does in the block model. As compensation for this discrepancy, the model was re-sectioned at 35^{o} and 30^{o} instead of the predicted 40^{o} from the standard transverse. The modification provided improved agreement between the experimental CN shapes and the block model as is shown by the point (35^{o}-3) in Figure III-8 D.

The effect of the modifications of the block model on the "length" of AVCN and PCN are shown in Figure III-8 C. As more and more movement along Figure III-8 D is obtained, the model coordinate moves up and to the right in Figure III-8 C. It is interesting that the uppermost point occupies a similar position with respect to the experimental points as the block model points in Figure III-8 A. It should be noted also that both of the modifications for the special transverse sections

have no effect on the sagittal sections.

For each CN it was necessary to select the most appropriate transformation of the model. Based on a comparison of the experimental subdivision limits with those of the three versions of the model, the selection process was reinforced by a section by section comparison of the experimental CN with the selected version. The procedure from this point on followed the general principle of determining the unit location by relative placement within the particular subdivisions. The experimental and block model sections were overlaid and each unit assigned to the closest block model coordinate which was in the same subdivision as the unit.

5.7 Stimulating electrode localization

Most stimulating electrode tracks were histologically verified. When the stimulating electrode had been directed into the trapezoid body the brainstem was sectioned either (1) parallel to the stimulating electrode plane (a transverse plane 55^{o} from the ventral surface of the brain) when the CN was being sectioned sagittally or (2) along with the CN when the special transverse sectioning was used for the CN. Even though the special transverse plane is 15^{o} out of the plane of the stimulating electrode, the track was obvious because of the large diameter of the electrode and the lesions created in the regions where the electrical stimulation was performed. The IC was always cut in the sagittal plane.

The particular sites of stimulation along the tracks were difficult to determine because of the lack of reliable reference points

Figure III-11 Localization of the stimulating electrode pass in B54

Left: Amplitude of the gross response caused by noise burst stimulation (-40dB) of the right ear (X's) and left ear (circles) as a function of distance from the floor of the IVth ventricle. The recordings were made from the center conductor of the stimulating electrode (solid line) as it was advanced into the brainstem and also from an earlier micro-electrode pass (dashed line). The arrows indicate the gross response "cross-over" locations.

Right: Drawing of a histological section showing the stimulating electrode track as it passes through the superior olivary complex. The vertical dashed line is the midline which terminates dorsally at the floor of the IVth ventricle. The position along the track to which the "cross-over" (from stimulating electrode) was assumed to correspond is shown by an arrow. A 20% shrinkage of the histological preparation was assumed in relating electrode movement to distance on the sections. LSO, lateral superior olivary complex; MSO, medial superior olivary complex; MNTB, medial nucleus of the trapezoid body.

B54 - Stimulating Electrode Pass

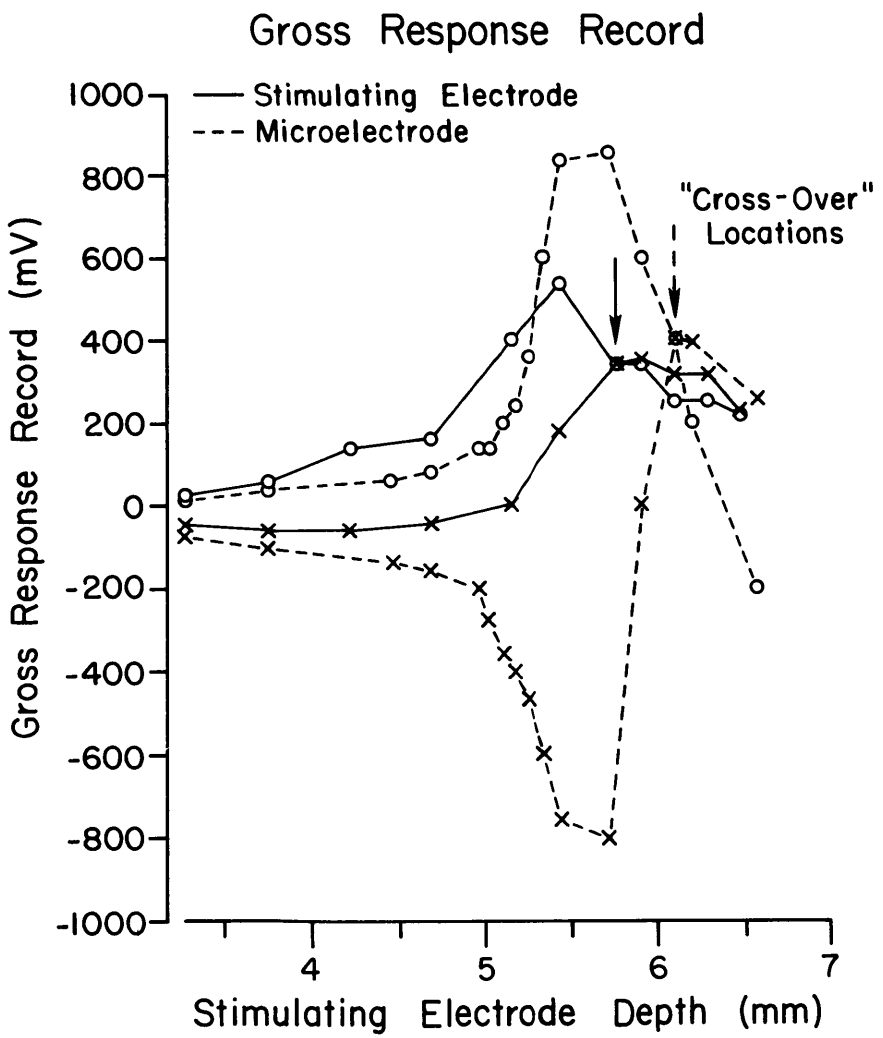

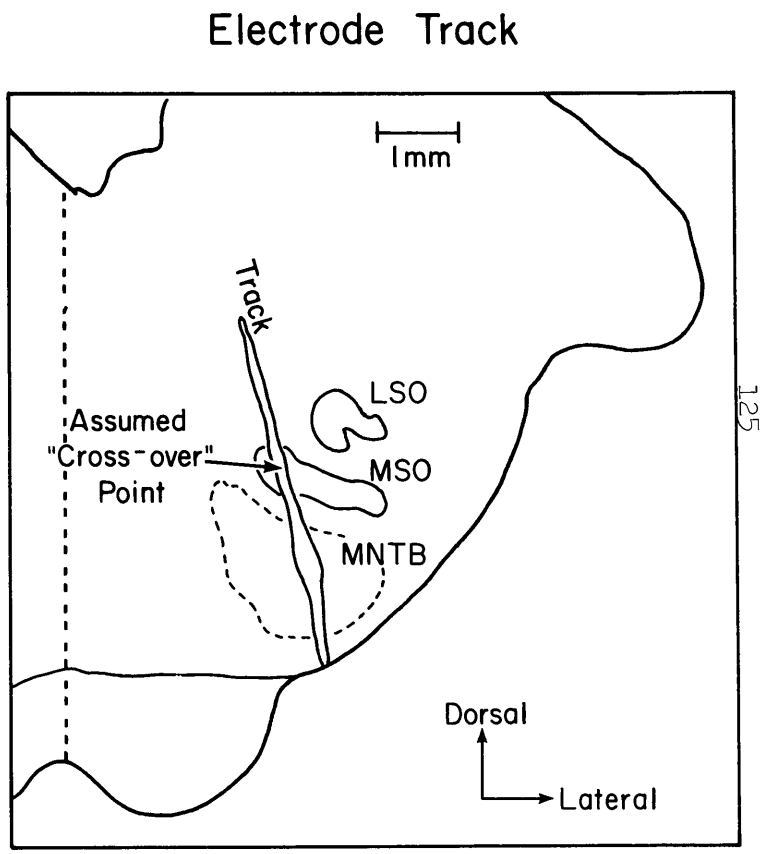

and the deformation of the tissue caused by the stimulating electrode. For the IC passes the points of entry were useful as references since they were always on the surface of the IC, relatively close to the stimulation sites. For the trapezoid body passes the entry points of the electrodes (on the floor of the fourth ventricle) were too far from the trapezoid body to be useful. Physiological evidence of the location of the electrode tip was, however, available for some of the passes that went through the superior olivary complex. The gross evoked response recorded from the center conductor of the stimulating electrode was monitored in response to noise bursts delivered to either the right or left ear as the electrode was first advanced into the brain. Figure III-11 shows an example of a stimulating electrode pass that went through the MSO. The amplitudes of the gross response recorded with the stimulating electrode (solid lines) is compared with those recorded in an earlier microelectrode pass (dashed lines). The microelectrode recordings exhibit a typical "cross-over" (eg. Guinan et al., 1972b; Tsuchitani and Boudreau, 1964). The stimulating electrode recordings also intersect at about the same depth (250 to 300 um different in this case) but the "crossing" is not as sharply defined. For the passes that went through the MSO the gross response "cross-over" from the stimulating electrode records was used as an expedient approximation to the "cross-over" recorded with a microelectrode. The "cross-over" position was then taken to correspond to the intersection of the track with the midline of the MSO (Guinan et al., 1972b). Additional depth information was obtained when positive prepotential units were recorded with the stimulating electrode.

The electrode tip was then presumed to be in the MNTB where such units are common (Guinan, et al., 1972b).

CHAPTER IV

RESULTS

1. Introduction

The first half of this chapter will be devoted to an analysis of certain aspects of the physiology of the single units recorded in AVCN. Based on the more differentiating aspects of the physiology, sets of unit categories were formulated. The two categorization schemes that were found to be most effective in predicting the other properties of the units are defined in sections 2 and 3; in section 2, the prepotential categories based on the presence or lack of a prepotential in the spike waveform, and in section 3, the response types based on the discharge pattern to tone bursts and continuous tone. Since these two categorization schemes form the underlying organization for much of the subsequent data presentation, their relationship will be examined in section 4 before considering any of the other physiological properties. Sections 5 through 9 explore other aspects of the single unit behavior such as spontaneous activity and the responses to continuous tone, long tone bursts and clicks. The objective through most of these sections is to sketch the general characteristics of the units, emphasizing their relationship to the proposed single unit categories. A systematic study of the detailed physiology of the units can be pursued in the future once a general framework to organize the data is made available.

With the various aspects of the physiological data represented in categorization schemes, the relationships of these categories to the unit locations within AVCN could be explored. Section 10 presents the localization-dependent data such as the tonotopic organization of the AVCN, the relationship of the unit types to the AVCN subdivisions, and the detailed spatial distributions of the units.

The final two sections of this chapter deal with the responses of the AVCN units to electric shocks delivered to either the trapezoid body or the inferior colliculus. The data on antidromic activation from these sites can be used to obtain information on the projections from the AVCN to higher centers. This data can be related to anatomical observations on the projections of the cell types in the AVCN, thereby providing another link between unit types (physiology) and cell types (anatomy).

2. Prepotential Categories

The spike waveforms of most of the single units in this study were examined for the presence of a prepotential. The initial definition of the prepotential (pp) by Pfeiffer (1966b) was expanded to include some other forms. Based on the tests described in section 4.2 of Methods, each unit was assigned to a category according to the confidence with which a pp could be identified.

Four categories were initially defined:

a) PP1 - a unit with a clear pp discernable by superposing individual records.

b) PP2 - a unit which probably has a pp. The small size and/or infrequent appearance of the pp creates doubt about its existence.

c) PP3 - a unit which probably does not have a pp. All of the tests were negative.

d) PP4 - a unit for which the presence or lack of a pp could not be determined because of such problems as insufficient recording time, poorly isolated spikes or contamination with gross responses.

The detailed description of these categories, the range of waveforms they represent and the need for an additional category (PP0) will be described in the remainder of this section.

(PP1)

By definition, the units that were assigned to the PP1 category had a pp that was unequivocally observed without the need for averaging. For about 90% of the PP1 units it was possible to demonstrate the pp by triggering the oscilloscope display from the pp; with the other 10% of the PP1 units the pre-spike display had to be used because the amplitude of the pp was close to the noise level of the recordings. It is obvious that the noise level of the recordings sets a limit on how large a pp must be to satisfy the PP1 criteria. It may seem that factors such as the distance of the electrode tip from the cell might, therefore, influence the category of a unit. In practice, it appears that the requirement that the spikes be isolatable during stimulation with STBCF (necessary to obtain the CF and threshold) and be clearly isolated for the pp

tests ensured a minimal spike size for the units tested. The observation that only 10% of the units in the PP1 category had a pp small enough to require the use of the pre-spike display suggests that the majority, at least, were above the noise level.

A selection of the various spike waveforms exhibited by the PP1 units is shown in Figure IV-1. Each unit is represented by a superposition of individual spikes triggered at an arbitrary point on the waveform. The three examples on the left have similar shapes but different overall amplitudes (note the noise levels and voltage calibrations). The examples on the right illustrate a variety of shapes varying from unit B81-26 for which both the pp and the 2nd(or negative) component have similar amplitudes to unit B75-2 which has a very small 2nd component. The fractionation of the 2nd component of B58-21 into two parts is similar to an example shown by Pfeiffer (1966b). He suggested that the two parts of the 2nd component may represent initial segment discharge versus soma-dendritic discharge or postsynaptic potential versus spike. The waveforms on the left plus that of B75-2 represent the most commonly recorded shapes.

Although it is mainly the units with spike waveforms like those of B81-26 that can be confidently confirmed to have a 1 to 1 relationship of the pp and the 2nd component, the other PP1 units generally had waveforms which appeared to be invariant (within the limits set by the noise-level and for a particular position of the electrode). The exceptions appear to be either: (1) the fractionation of the 2nd component as exhibited by B58-21, (2) the occasional lack of the 2nd component whenever a pp occurred during or

Figure IV-1 Spike waveforms recorded from PP1 units

Each of the six plots shows superposed spike waveforms recorded from a PP1 unit. The spike waveforms were sampled at 10 μsec intervals and stored under computer control via a 9 bit analog-to-digital converter and digital delay line. The examples on the left were triggered from a point on the positive prepotentials. The horizontal calibration line applies for all of the units. The vertical calibration lines shown below each unit number represent 200 μV. Positivity at the microelectrode is upward in all plots of spike waveforms.

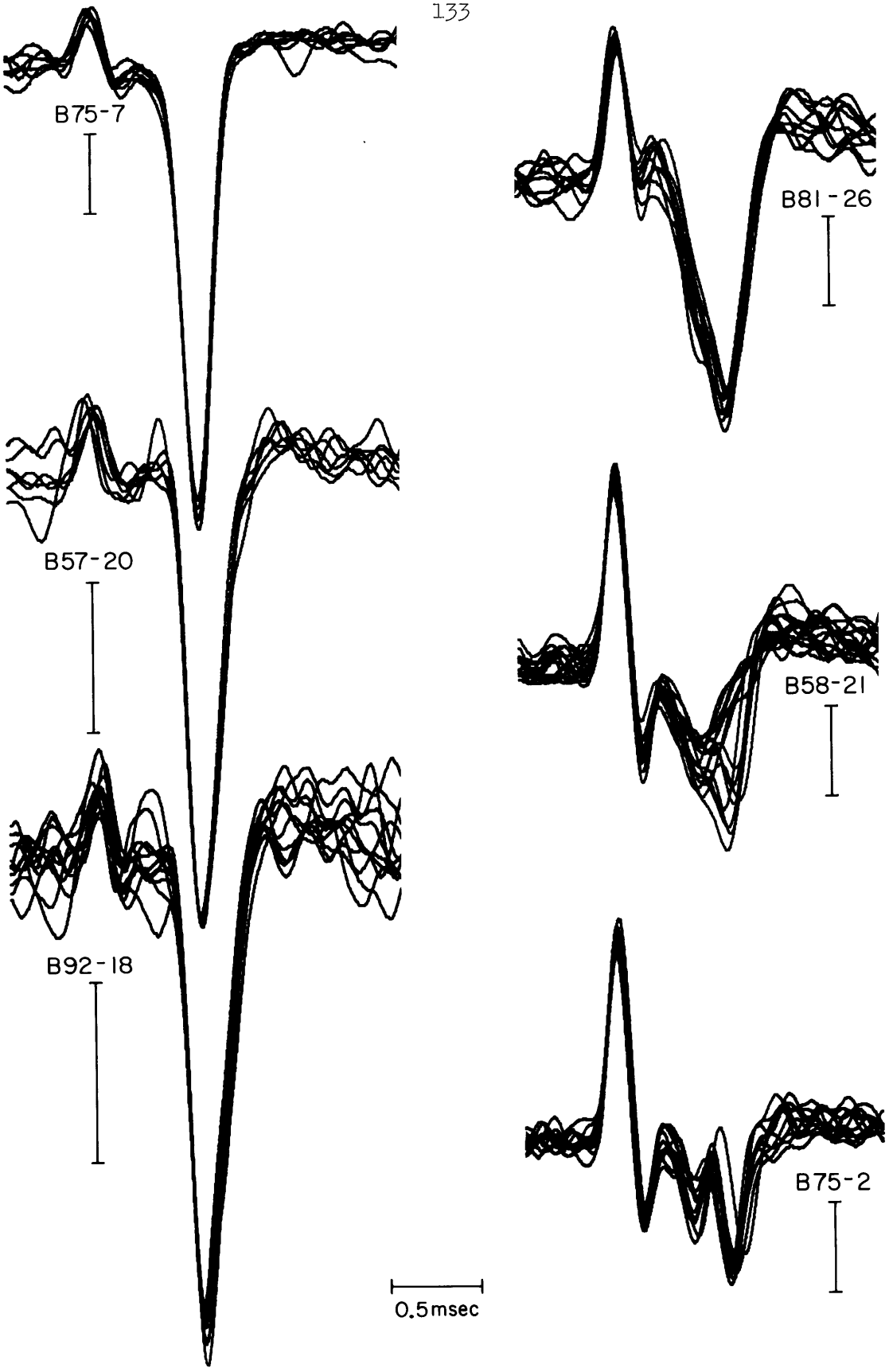
B75-7
B57-20
B92-18
B81-26
B58-21
B75-2
0.5msec

Figure IV-2 Two PPl units with "giant" spikes

The spike waveforms of units B66-10 and B52-16 were sampled in the same manner as described for Figure IV-1. The solid and dotted lines were used to emphasize the two sizes of prepotential and associated sets of waveforms. The spikes of B52-16 were triggered on the rising edge of the dominant positive excursion. The solid and dotted spikes of B66-10 were shifted so that the prepotentials were at a similar position. The horizontal calibration applies to both plots; the vertical calibration lines represent 500 μV. In the B66-10 plot, the negative component of a closely preceding spike shows at the beginning of one of the solid lines. Following this spike a large prepotential precedes a spike for which the biphasic component failed to occur (arrow).

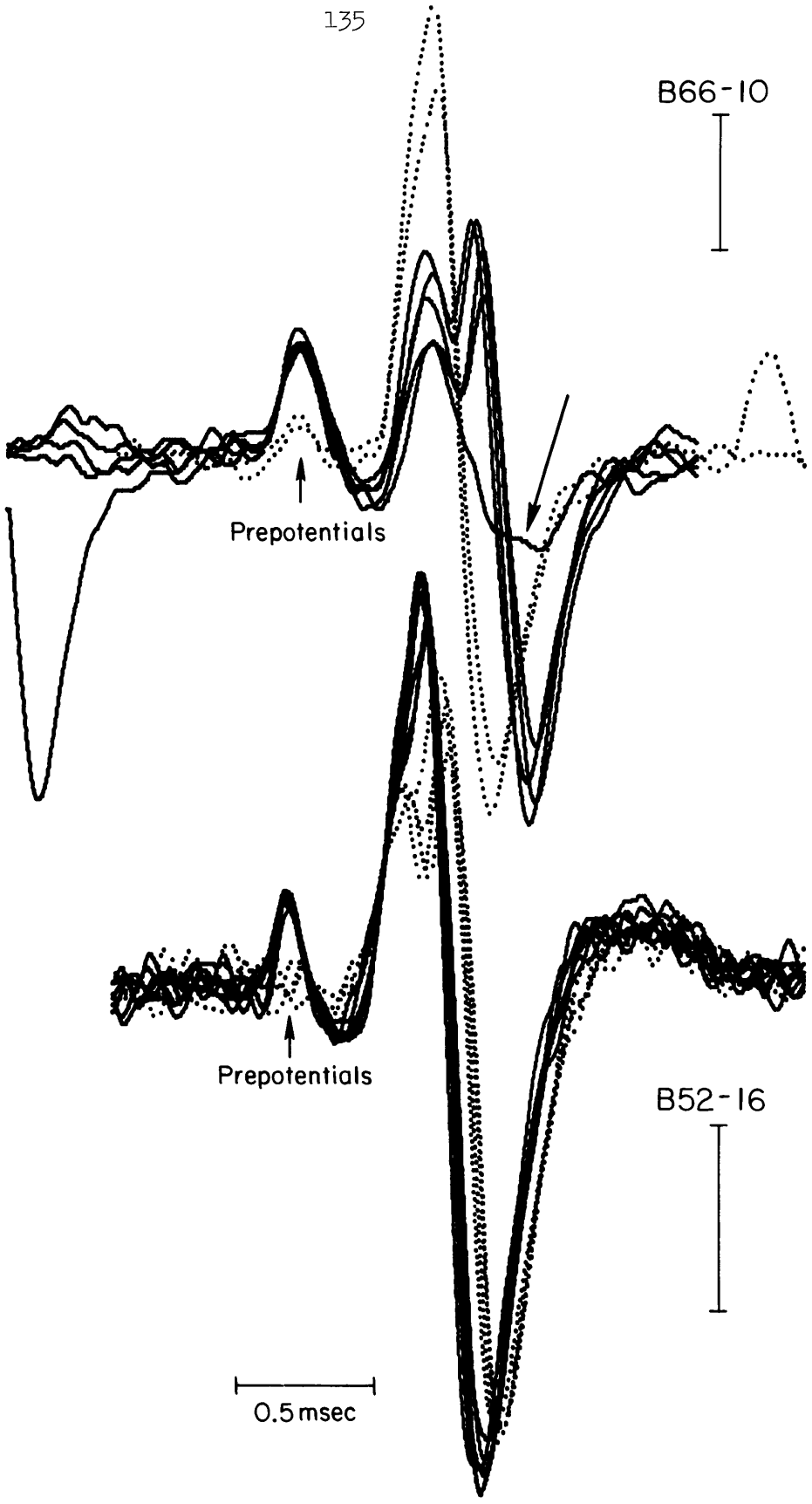
B66-10
Prepotentials
Prepotentials
B52-16
0.5 msec

just after a previous 2nd component (presumably these failures are due to refractory effects) or (3) the infrequent occurrence of two or more distinguishable pp sizes and/or shapes.

Multiple sizes (and shapes) of pp were found only during a special recording situation in which the PP1 unit exhibited a "giant" spike. The "giant" spike is generally assumed to occur when the electrode tip is pressing on the cell (Svaetchin, 1951; Terzuolo and Araki, 1961). Advancing the electrode results in the sudden loss of the 2nd component (see further Figure 3 of Pfeiffer, 1966b). In the majority of such recording situations there was a set of spike shapes associated with at least two sizes of pp as is shown for the two examples in Figure IV-2. The solid and dotted lines were used to reveal the waveforms associated with the large pp (solid) and the small pp (dotted).

(PP2)

For some units it was necessary to average the spike waveform (pre-spike average) in order to demonstrate a prepotential-like potential variation preceding the spike. These units were placed in the PP2 category because of the uncertainty as to whether the pre-potential-like component is a pp. In such instances, an average demonstrates a potential variation 0.4 to 0.6 msec before a spike, but two important aspects commonly observed for the pp's of PP1 units are not verified, the all-or-none nature of the pp and the invariant presence of a pp before the spike. Thus the character of the "prepotential" of PP2 units may be different from that of the PP1 units.

The defining characteristic of the PP2 units is that examination of the pre-spike display will not reveal the sustained presence of a pp although there is a clear "prepotential" in an averaged waveform. Figure IV-3 shows some examples of PP2 units. Unit B92-21, for instance, represents the boundary between the PP1 and PP2 categories in that a pp component can barely be seen in the superpositions. The left-hand column in Figure IV-4 also shows some PP2 units with the pre-spike region magnified 20X. The averages of all but two PP2 units had pp components with an amplitude of less than 1/20 of the spike height. For some of the PP2 units an extended observation of the individual traces revealed occasional prepotentials that were more variable in latency (up to $\pm$ 0.2 msec) with respect to the spike, than those of PP1 units. The pp of most of these units had an amplitude comparable to the noise level and so the observation was usually equivocal. In Figure IV-3 is shown a set of waveforms from unit B71-31; the three spikes with a pp were the only examples in a 1 minute sample. The other waveforms were included for reference.

(PP3)

When the search for a pp was consistently negative over many samples of the recorded discharges of a particular unit, it was assigned to the third category, PP3. Some examples of units placed in the PP3 category are shown in Figure IV-4, contrasted with a representative sample of PP2 units. The center column illustrates how smooth the pre-spike region of the PP3 units can be made by averaging a large number of spikes. The right-hand column shows

Figure IV-3 Spike waveforms recorded from PP2 units

The three superpositions of individual spike waveforms shown on the left illustrate the common range of pp sizes for the PP2 units. To the right of each plot are the averages obtained from a large number of spike waveforms; each average exhibits a pp. B92-21 has a pp which is almost discernible in the superposed traces but not sufficiently to assign the unit to the PP1 category. B71-31 (far right) is an example of one of the PP2 units which exhibited a distinct pp infrequently and with variable latency. Three of the clearest pp waveforms were chosen; the majority of the spikes recorded from this unit did not exhibit a discernible pp. The horizontal calibration applies to all plots. The vertical calibration lines represent 200 μV.

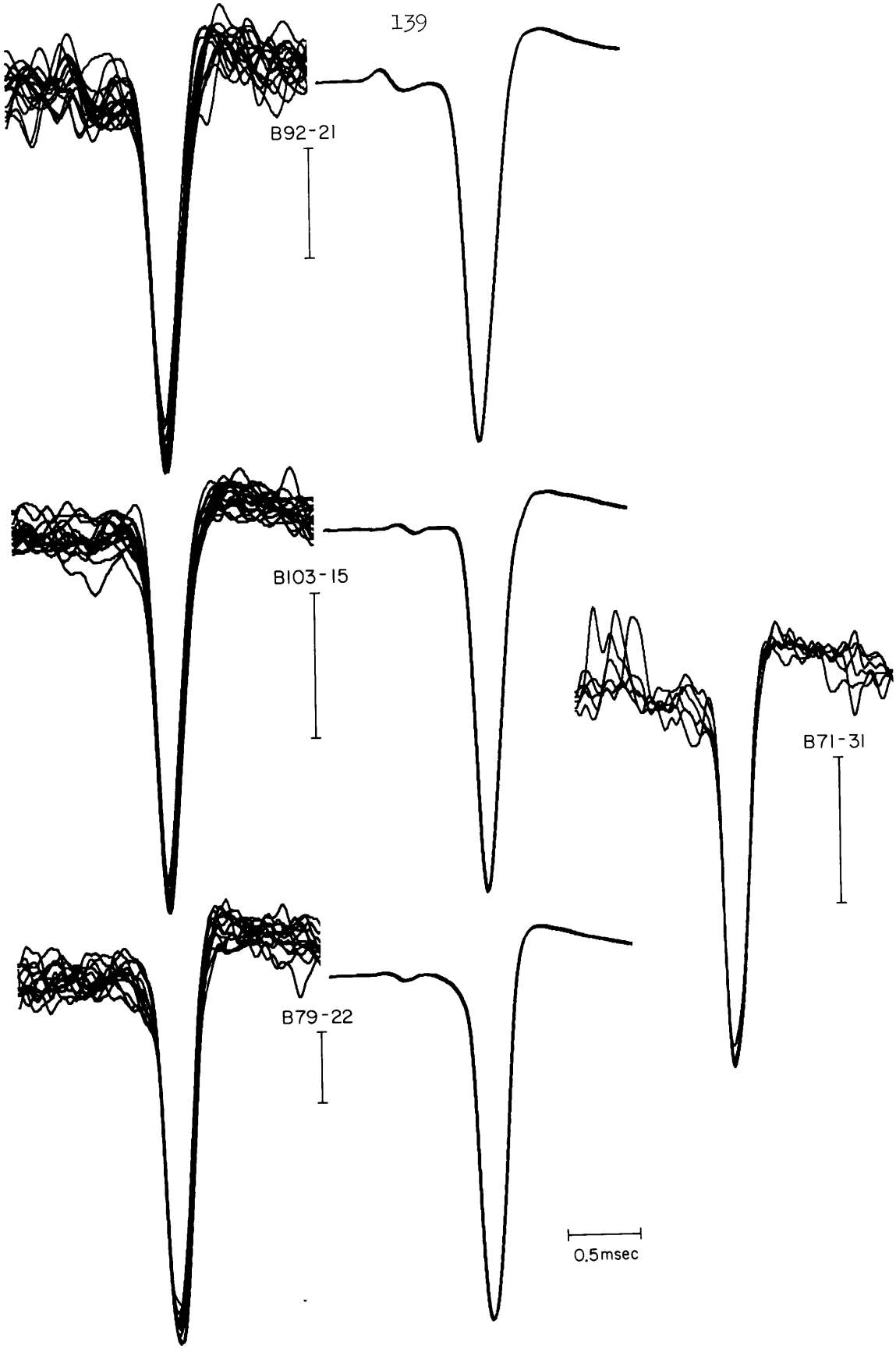
B92-21
B103-15
B71-31
B79-22
0.5msec

Figure IV-4 Averaged spike waveforms for PP2 and PP3 units

Each unit is represented by an averaged spike waveform (dotted line) which has been normalized by the baseline-to-peak amplitude. Superimposed on each average is a plot of the initial portion of the average magnified 20 times (solid lines). The prepotentials of the PP2 units are easily seen at this scale. The averages were aligned by the "trigger point" on the leading edge of the major negative excursion. The dashed lines are 0.6 msec before the "trigger point". The spikes were sampled at 20 μsec intervals (150 points across each plot).

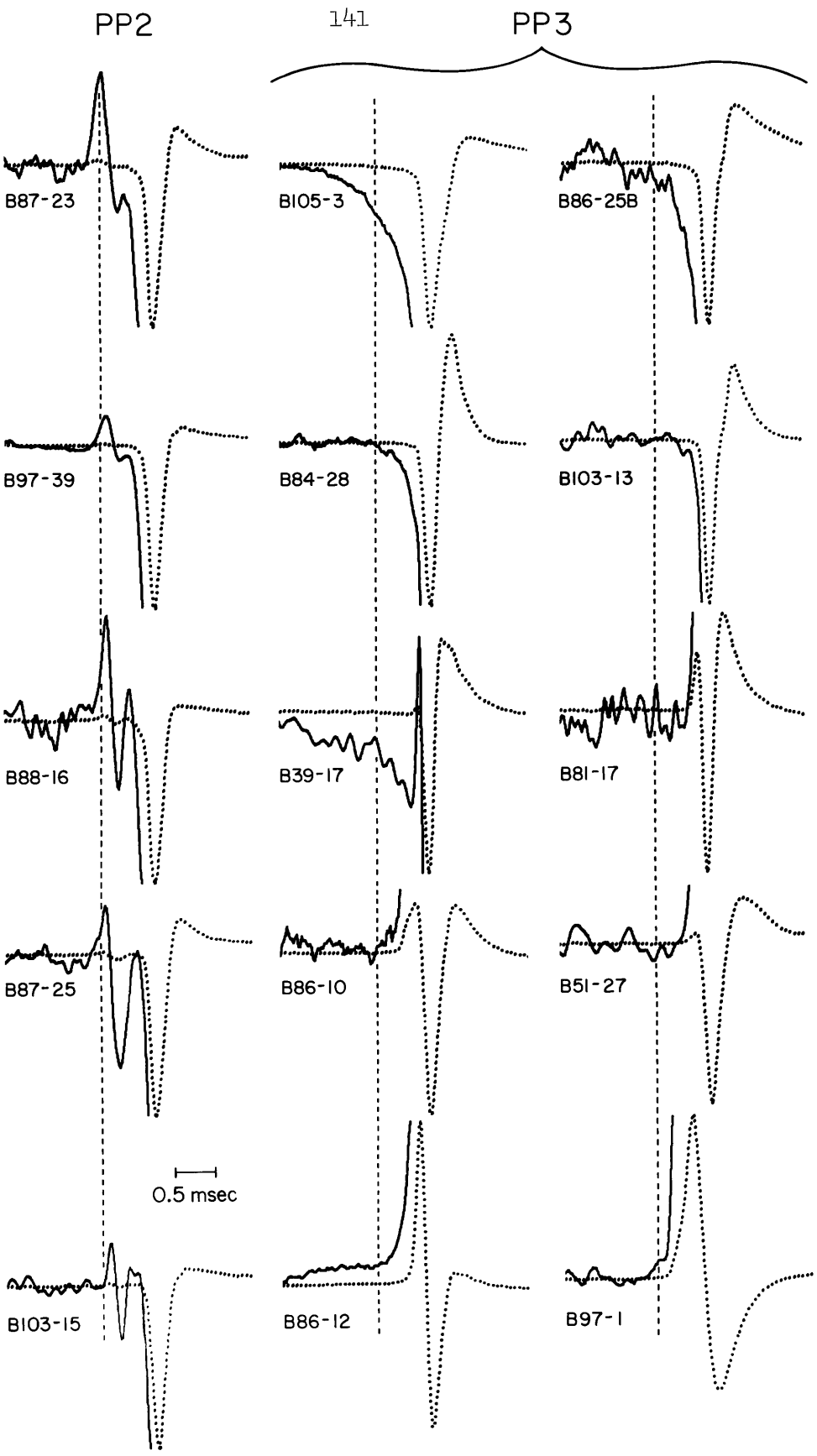
PP2
PP3
B87-23
B105-3
B86-25B
B97-39
B84-28
B103-13
B88-16
B39-17
B81-17
B87-25
B86-10
B51-27
0.5 msec
B103-15
B86-12
B97-1

some "noisy" averages based on fewer spike samples. The examples of small pp's in the PP2 column were not common; most PP2 units had a larger pp. There does not appear to be a clear break between the PP2 and PP3 units both because very small pp's can be found and the available records of the PP3 units set a limit on the size of pp that could be identified. The present averaging technique, however, has probably identified most of the PP2 units, for as will be shown in later sections the PP2 and PP3 units form essentially disjoint populations with respect to some other physiological properties.

(PP4)

The fourth category, PP4, was used for the units about which a decision could not be made. There were two major reasons for a unit being classified as PP4: either the unit had spikes which were too small to be reliably distinguished from the background activity and/or the tape recorded sample of the unit's activity was inadequate. For a small number of units in the PP4 category, the averaged spike waveform had a small, atypical potential variation which may have been a pp or just "noise"; these units were therefore placed in the PP4 category because of the uncertainty.

(PP0)

The four categories were intended to cover the entire range of possibilities. However, a few striking examples of an unusual spike waveshape forced a re-examination. A new category, PP0, was established for what will be referred to as the negative prepotential

units. Initially, a prepotential could not be found for these units because the negative prepotential was thought to be a postsynaptic spike. These PPO units were subsequently recognized by the very fast deflection whose amplitude was often critically sensitive to microelectrode movement.

Figure IV-5 shows a sample of PPO units. The second component varied from unit to unit, but in most cases was close to the noise-level of the recordings. When the second component is very small it is possible to confuse a PPO unit with the PP3 units. Unit B40-21 in Figure IV-5 illustrates a sequence occasionally encountered for the PPO units. As the microelectrode was advanced, the spike waveforms of B40-21 changed from a positive prepotential (A) to biphasic (B) and then to the unusual negative prepotential form (C). Further movement of the microelectrode (either advancement of withdrawal) gave rise to forms (B) and (A) in succession.

The detailed shapes of the spike waveforms should not be taken from the present data. The bandpass characteristics of the amplifiers and tape recorder were observed to cause negligible changes in the spike waveforms but the transfer characteristic of the microelectrode is uncertain. The high frequency cut-off of the microelectrodes as affected by the capacitance neutralization feature of the headstage was observed to cause significant changes in the amplitude of the spike of B102-11 (Figure IV-5). This adjustment was not usually optimized because it generally had no noticeable effect on the majority of the spikes (that is, of categories PP1, PP2, and PP3).

Figure IV-5 Spike waveforms recorded from PPO units

The center and right-hand columns show the individual waveforms and averages from four typical PPO units. All averages show a component after the negative pp. B40-21 (left) is one of the few examples found of a reversible change from a positive pp waveform (A), much like the waveform of B75-2 in Figure IV-1, into a negative pp waveform. Movement of the electrode from the position that corresponded to (C) caused the waveforms in (B) and then in (A) to be recorded. The horizontal calibration applies to all plots; the vertical calibration lines indicate 100 μV for B40-21 and 200 μV for the units in the center column.

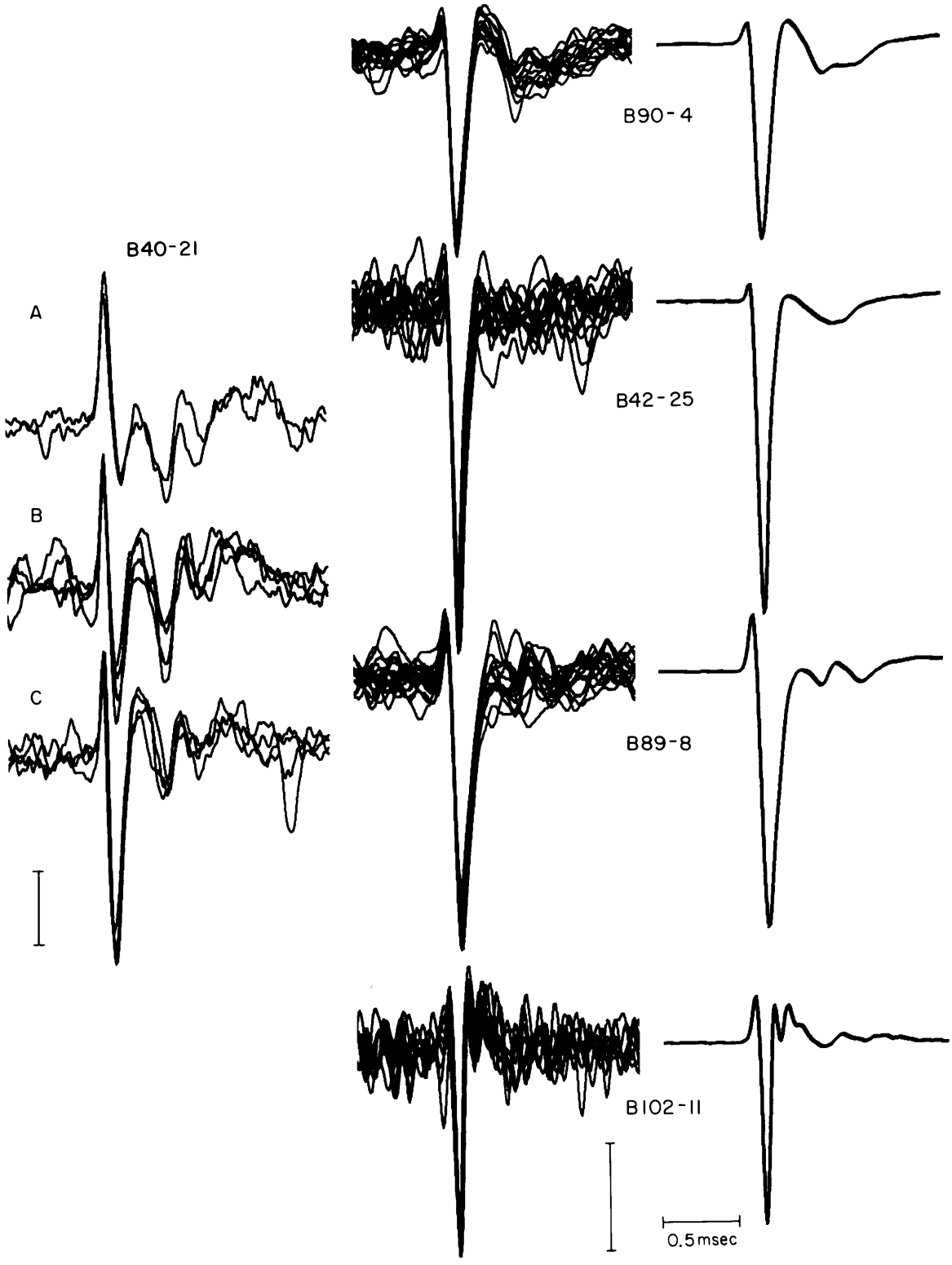
B40-21
A
B
C
B90-4
B42-25
B89-8
B102-11
0.5msec

3. Response Type Categories

Most of the units encountered in AVCN were studied with acoustic stimulation of the ipsilateral ear. For about half of the units localized to AVCN, a profile of the response characteristics to several types of stimuli was determined. This group of units formed the basis for defining the response type categories proposed for the AVCN single units. The categories follow the general format described by Kiang et al. (1965b) and Pfeiffer (1966a) and elaborated on by Godfrey et al. (1975 a and b) for the units of the PVCN and DCN.

All of the response type categories were based primarily on the responses to continuous tone and tone burst at CF. First and foremost in the study of each unit was an examination of the PST histogram of the first 20 msec of the response to tone burst. Since bin widths as small as 1/4 msec were required to resolve the fine structure in the variations of instantaneous rate for some units, a large number of tone burst repetitions (often more than 300) were required to obtain sufficient statistics. As a compromise between off-time and repetition rate, the short tone burst (STB) paradigm has 25 msec on and 75 msec off. Although an off-time of only 75 msec results in some rate reductions for primary and CN units, the general form of response of the AVCN units is seldom changed as the off-time is further increased. To this extent, the response to the STBCF stimulus provides a representation of the response at the onset of a CF tone. The characterization of each unit's response generally required the use of several levels, ranging from below threshold to around 20 to 40 dB above threshold.

The other stimulus paradigm that played a major role in the definition of the response type categories was continuous tone at CF (CTCF). The rate of discharge as a function of the level of the CTCF stimulus aided in the characterization of some of the response type categories. The rate estimates were usually based on 30 or 60 second samples. Any initial adaptations in rate were excluded from the sample.

The long tone burst at CF (LTBCF), another commonly used stimulus, was not routinely used in defining the response type categories. The relatively short off-time (100 msec) following a 900 msec presentation can markedly affect the form of response to the next tone burst, hence the LTBCF paradigm is viewed as a special case and will be considered under a separate classification scheme in section 5 of this chapter. In a few cases, the response to LTBCF was used to confirm that the decreasing rate observed in an STBCF response was indeed followed by a cessation of the response with extended presentation of the tonal stimulus.

The general decision sequence used in placing units into the response type categories is shown in Figure IV-6. The first node in Figure IV-6 (node "a") represents the major partitioning of the units into two classes based on a comparison of the initial discharge rate with the steady-state rate. One class has a "transient" (phasic) response and is represented by the On group. The other class is formed by the more "sustained" (tonic) response types, Primarylike, Chopper and Pauser. The two categories on the upper right, Composite and Unusual, represent a small number of units whose unique properties excluded these units from the major subdivision at node "a". The

Figure IV-6 Decision tree for the response type categories

The decision sequence used to assign units to the various response type categories is diagrammatically represented in this figure. The entry point is at the top and the nodes represent decisions described in the text. Each response type is shown as a box with the name or abbreviation within it. Above each box is the number of units finally placed in that category. The overall totals for the Chopper and On groups as given at nodes c and f, respectively, include the undifferentiated Chop-? and On-? units.

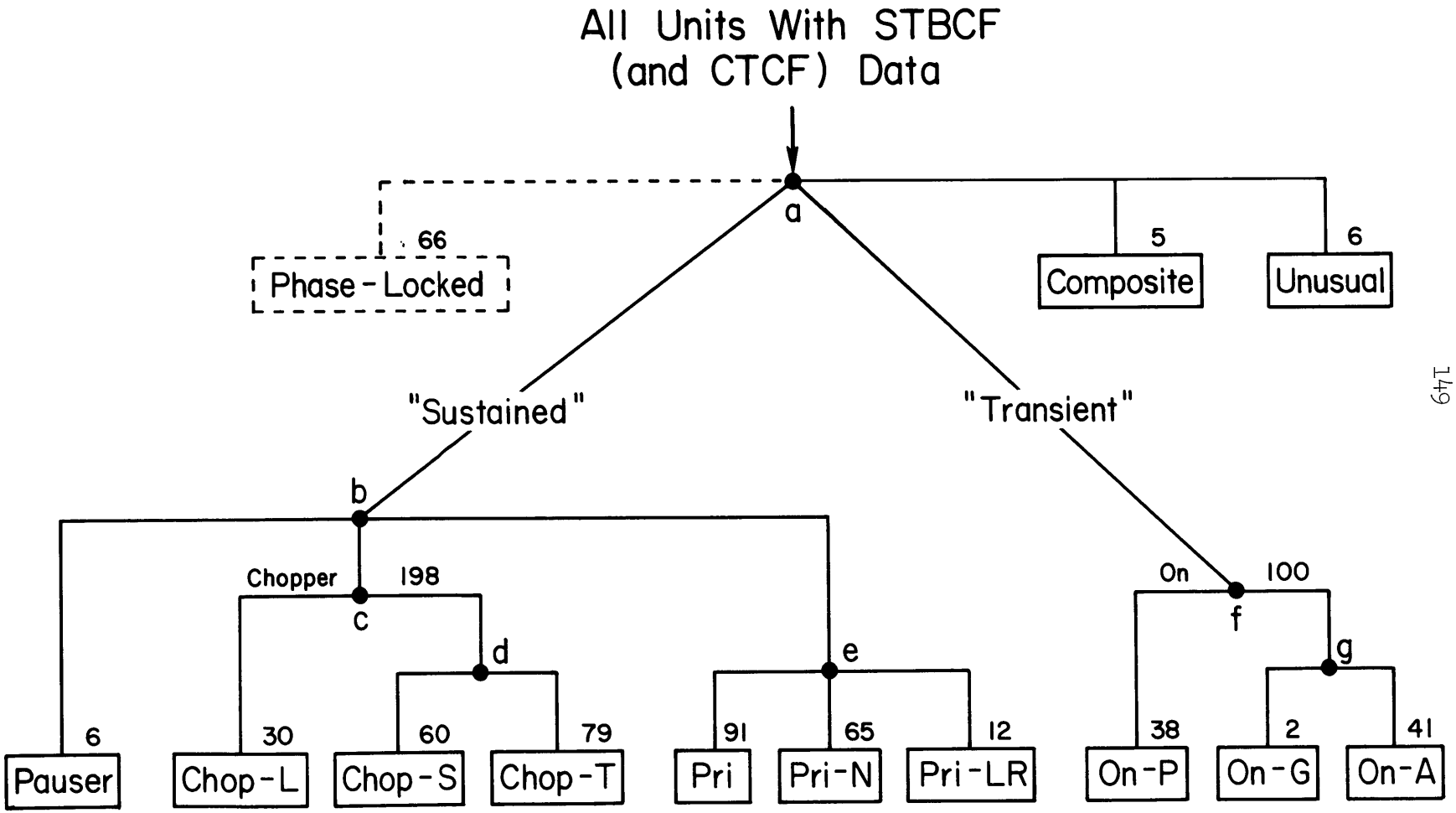
All Units With STBCF
(and CTCF) Data
a
66
Phase-Locked
5
Composite
6
Unusual
"Sustained"
"Transient"
b
Chopper
198
c
d
e
On
100
f
g
6
Pauser
30
Chop-L
60
Chop-S
79
Chop-T
91
Pri
65
Pri-N
12
Pri-LR
38
On-P
2
On-G
41
On-A

dashed line from node "a" represents the units rejected from the classification scheme because their response to a level series of STBCF was dominated by phase-locking to the low frequency (CF) tone. Seventeen units localized to the AVCN did not respond to the auditory stimuli tried. These units were excluded from the subsequent analyses.

On Group

All units in the On group had a distinct response (often with a high instantaneous rate) at the onset of a CF tone, followed by a marked decrease in the rate of response (sometimes to zero in less than 10 msec.) As in the case of the On-L units of PVCN (Godfrey et al., 1975a), the On type units of AVCN exhibited their phasic character most clearly for tonal stimuli below a certain intensity. For some On units this level was only 10 or 20 dB above the STB threshold. As the stimulus intensity was raised above this level the response became more sustained.

By plotting the mean rate of discharge to CTCF versus the intensity of the tone (CTCF rate functions), the low steady-state rates of the On units are obvious. Some On units have a threshold for CTCF which is considerably higher than that for STBCF. Thus there would be an intensity range over which a response occurs at the onset of a tone, but there is no response in the steady-state (i.e. to CTCF). The size of this threshold difference ranges from zero to more than 60 dB. For many units an explicit CT threshold was not determined during the experiment, but had to be inferred from a level series

at 5 or 10 dB increments. Those units with at least a 10 dB difference between the STBCF and CTCF thresholds were placed in a subgroup of the On units as represented in Figure IV-6 by the On-A and On-G categories. The range of thresholds found for these units is shown in Fugure IV-7. The On units with a threshold difference of less than 10 dB formed the On-P category. The large threshold difference of the On-A and On-G categories delimits these categories from all others, particularly from all "sustained" categories.

From the units that were tested with both CTCF and LTBCF it was found that a low response rate to LTBCF was a sufficient but not a necessary condition to ensure the same for CTCF. Thus although a few units were placed in the On group based on responses to LTBCF, it can be assumed that the responses to CTCF would be consistent.

Over the span of a 25 msec tone burst the discharge rates of all On units were found to decrease markedly, usually to a rate close to zero. A complete profile of the histogram shapes versus the intensity of the STBCF was, in all but a few cases, unique to the On group.

In Figures IV-8, 9 are shown examples of the STBCF responses for the On categories. The On-A units tend to show an Abrupt decrease in the discharge rate following the initial peak, very similar to the On-L units of PVCN (Godfrey et al., 1975a). The On-A unit, B97-9, (Figure IV-8) shows one of the more distinct On responses seen in AVCN. Even at 60 dB above threshold (93 dB SPL) there were only a few responses near the end of the STB stimulation and the CTCF response rate was less than 2/sec. The multiple peaks represent multi-

Figure IV-7 CTCF threshold for the On-A and On-G units

Two measures of threshold are available for the CTCF responses of some of the On-A and On-G units. Both estimates are derived from a level series usually taken at 10 or 20 dB increments. The lower histogram shows a "lower bound" on the CTCF thresholds of 26 units. Plotted with respect to the STBCF threshold are the CTCF levels at which the rate was still less than 1 spike per 10 seconds sampled over a 30 to 60 second interval. The upper histogram shows an "upper bound" on the threshold of 16 units. The CTCF stimulation at the indicated levels elicited a rate less than or approximately equal to 1 spike per second sampled over a 30 to 60 second interval. Dashed lines connect the threshold measures from a given unit.

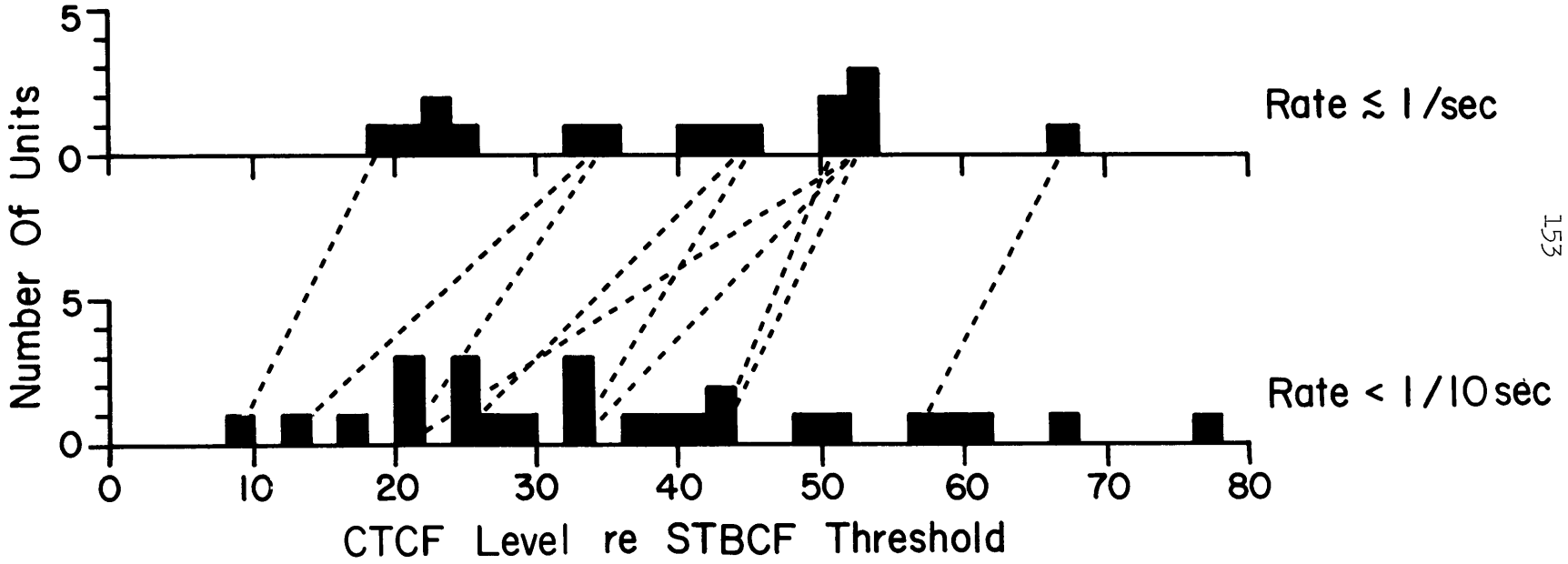
5
0
Number Of Units
Rate ≲ 1/sec
5
0
Rate < 1/10 sec
0
10
20
30
40
50
60
70
80
CTCF Level re STBCF Threshold

Figure IV-8 STBCF response of On-A and On-G units

Each column displays the PST histograms from an intensity series of STBCF stimulation. At the top of each column is given the unit number, CF and STBCF threshold. With each histogram is given the tone burst level with respect to threshold. The bin contents are normalized to instantaneous rate by dividing by the bin width and the number of tone burst presentations. The vertical scales, constant within a column, are given on the upper histogram (in spikes/sec). All PST histograms are based on approximately 300 to 600 tone burst presentations unless otherwise noted. Bin width is 0.25 msec. The above description is applicable to the figures for the other response types. This figure and the next (On-P units) have the added feature of a CTCF rate function at the bottom of each column. The vertical scale on these plots displays rate in spikes/sec and the horizontal scale, CTCF level in dB re the STBCF threshold.

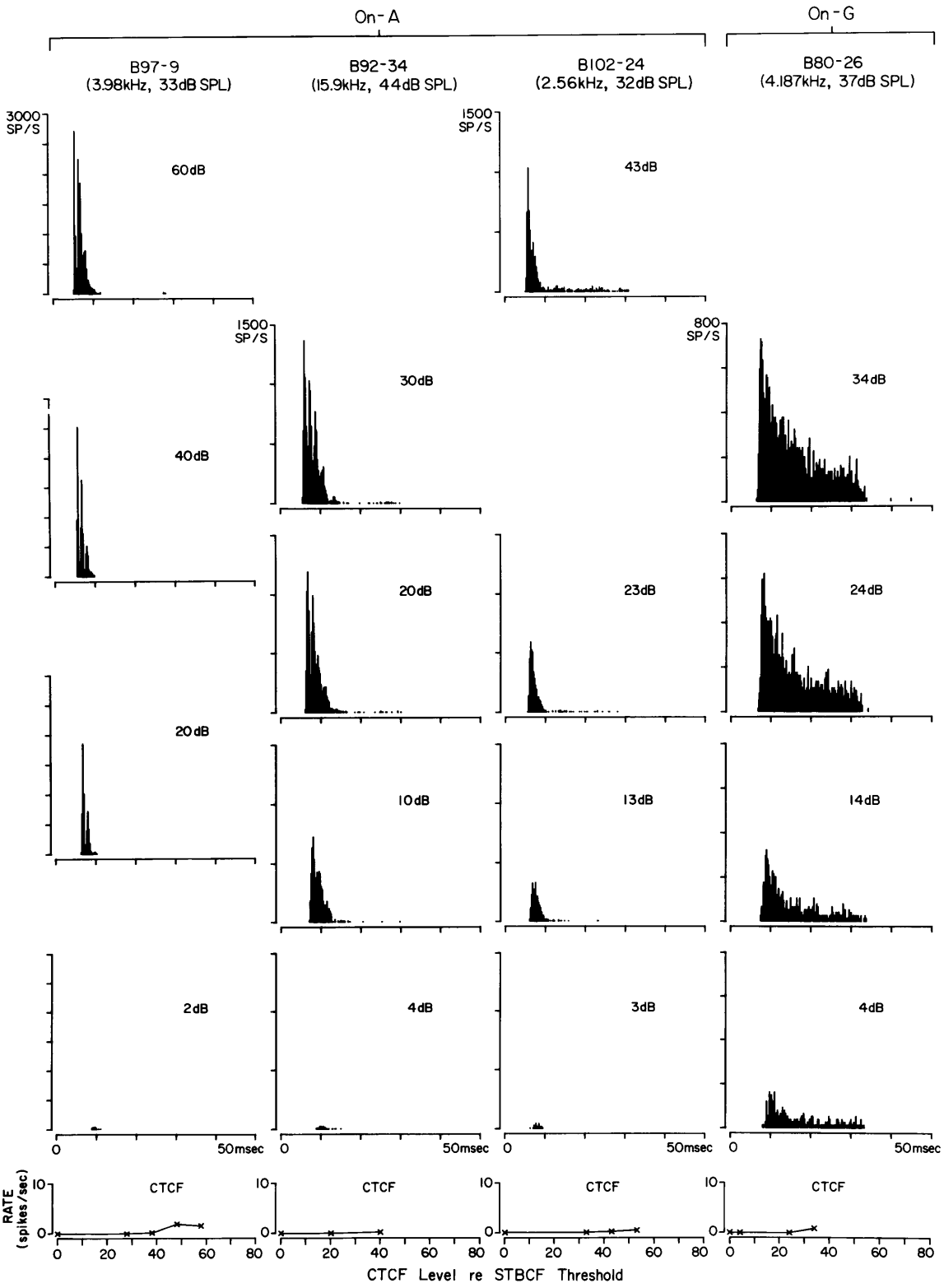
On-A
On-G
B97-9
(3.98kHz, 33dB SPL)
B92-34
(15.9kHz, 44dB SPL)
B102-24
(2.56kHz, 32dB SPL)
B80-26
(4.187kHz, 37dB SPL)
3000 SP/S
1500 SP/S
800 SP/S
60dB
43dB
30dB
34dB
40dB
20dB
23dB
24dB
20dB
10dB
13dB
14dB
2dB
4dB
3dB
4dB
0
50msec
RATE (spikes/sec)
CTCF
CTCF Level re STBCF Threshold

Figure IV-9 STBCF response of On-P units

The format is the same as described in the caption of Figure IV-8.

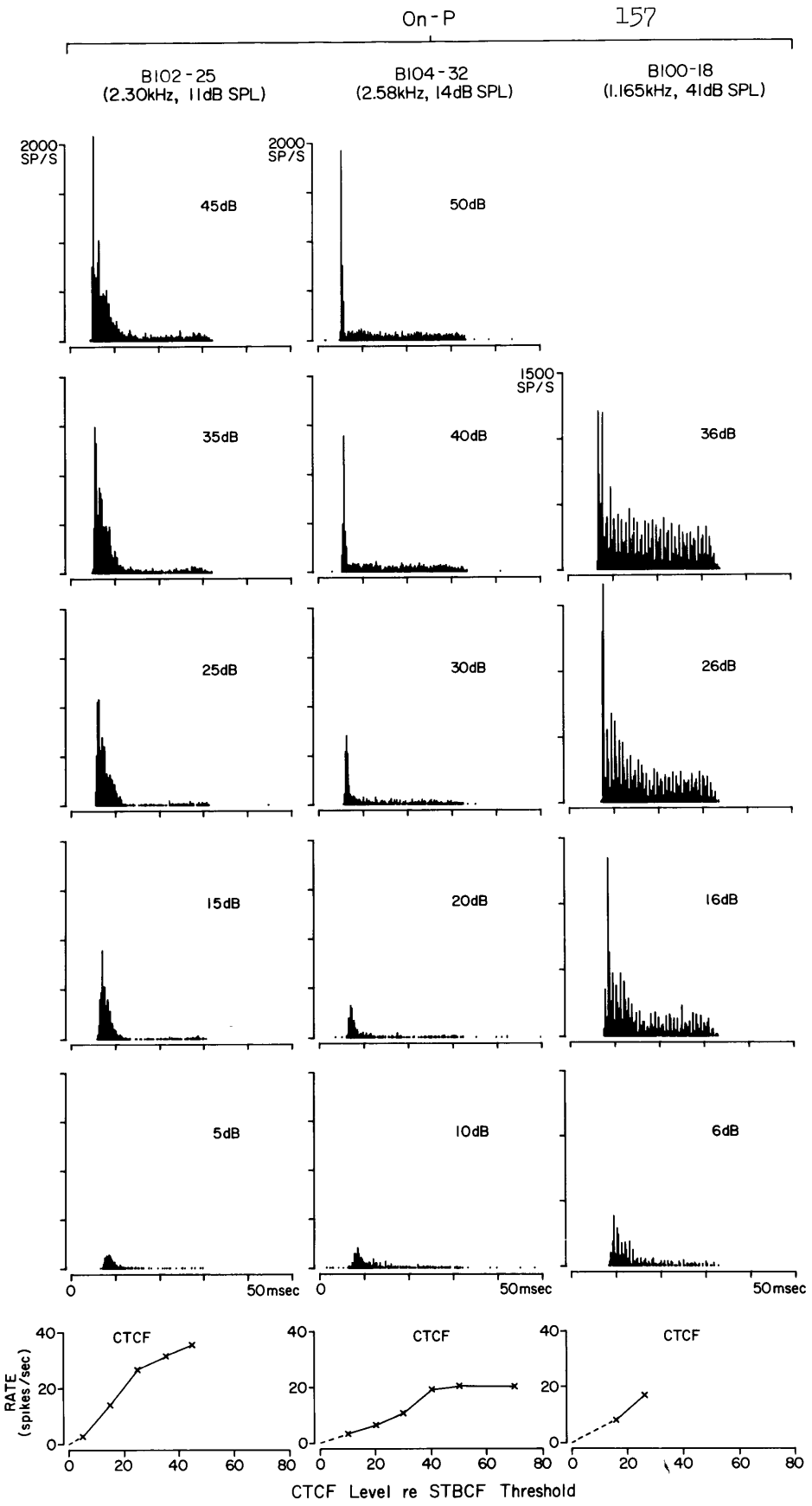
On-P
B102-25
(2.30kHz, 11dB SPL)
B104-32
(2.58kHz, 14dB SPL)
B100-18
(1.165kHz, 41dB SPL)
2000 SP/S
45dB
2000 SP/S
50dB
35dB
40dB
1500 SP/S
36dB
25dB
30dB
26dB
15dB
20dB
16dB
5dB
10dB
6dB
0
50msec
0
50msec
50msec
CTCF
CTCF
CTCF
RATE (spikes/sec)
0
20
40
60
80
CTCF Level re STBCF Threshold

ple discharges to each tone burst. B102-24 illustrates a response without these multiple peaks. The On-G units also have an elevated CTCF threshold but show a more Gradual decrease in rate, a characteristic also seen in the response of some On-P units. The On-G unit, B80-26, represents one of the most gradual decrements found for the On-A,G units.

The On-P units had PST histogram profiles which tended to be more Prolonged than those of the On-A category but there were several examples of On-P units whose STBCF response was as abrupt as some of the On-A units. It is this overlap which maintains the On-P units as part of the On group. Since the units in the On-P category have essentially no difference between the STBCF and CTCF thresholds and since their rates of discharge to CTCF, although exceptionally low, can approach those of some units in the "sustained" categories, it is the shape of the PST histograms of tone burst responses that is crucial in distinguishing the units of the On-P category. The examples in Figure IV-9 show the variety of PST histogram shapes found for the On-P units. B102-25 is similar to the On-A units. B100-18 has one of the most sustained responses found for the On-P units, and like several other similar On-P units it exhibits strong phase-locking at CF.

The three On type categories form an ordered subdivision of the On units, arranged according to the brevity and distinctness of the On response. As is shown in Figure IV-6, 100 units were assigned to the On group and 81 of these were placed in the On categories. Because of a lack of data 19 units were dropped at nodes "f" or "g"; these units were placed in an On-? "category".

The "sustained" categories were subdivided at node "b" (Figure IV-6) according to distinctions represented by three of the response types defined by Kiang et al. (1965b) and Pfeiffer (1966a), Primary-like,Chopper and Pauser. Typical short tone burst level series for these types were shown in Figure II-5.

Pri

Some of the units recorded in the AVCN have a response to STBCF which has the same shape of PST histogram and are therefore assigned to the Primarylike category (Pri). The PST histograms of the Pri units to high frequency (≤ 5 kHz) tone bursts generally have an initial peak followed by a monotonic decay to a rate greater than ¼ of the initial peak (the peak with 0.25 msec bin width). No statistically significent dips (minima) are found in the PST histograms except when low frequency stimuli caused peaks spaced at the period of the stimulus. Units with CF's below about 1.5 kHz were not placed in the Pri category because the strongly phase-locked response could not necessarily be distinguished from the phase-locked response of other response type categories. The response to LTBCF has only a slight peak at the onset and a maintained response for the remainder of the burst. Unit B74-14 in Figure IV-10 shows the typical Pri response profile to STBCF. Unit B97-18 is a Pri unit with one of the more distinct initial peaks and a tendency to exhibit a minimum after the peak.

Figure IV-10 STBCF response of Pri and Pri-N units

The two columns on the left show units in the Pri response type category. B97-18 borders on the Pri-N category which is illustrated by the three units shown on the right. B96-17 exhibits one of the more distinct peaks following the notch. The format is the same as described for Figure IV-8. The histograms for units B97-18 and B72-15 are at 20 dB increments; all others are at 10 dB.

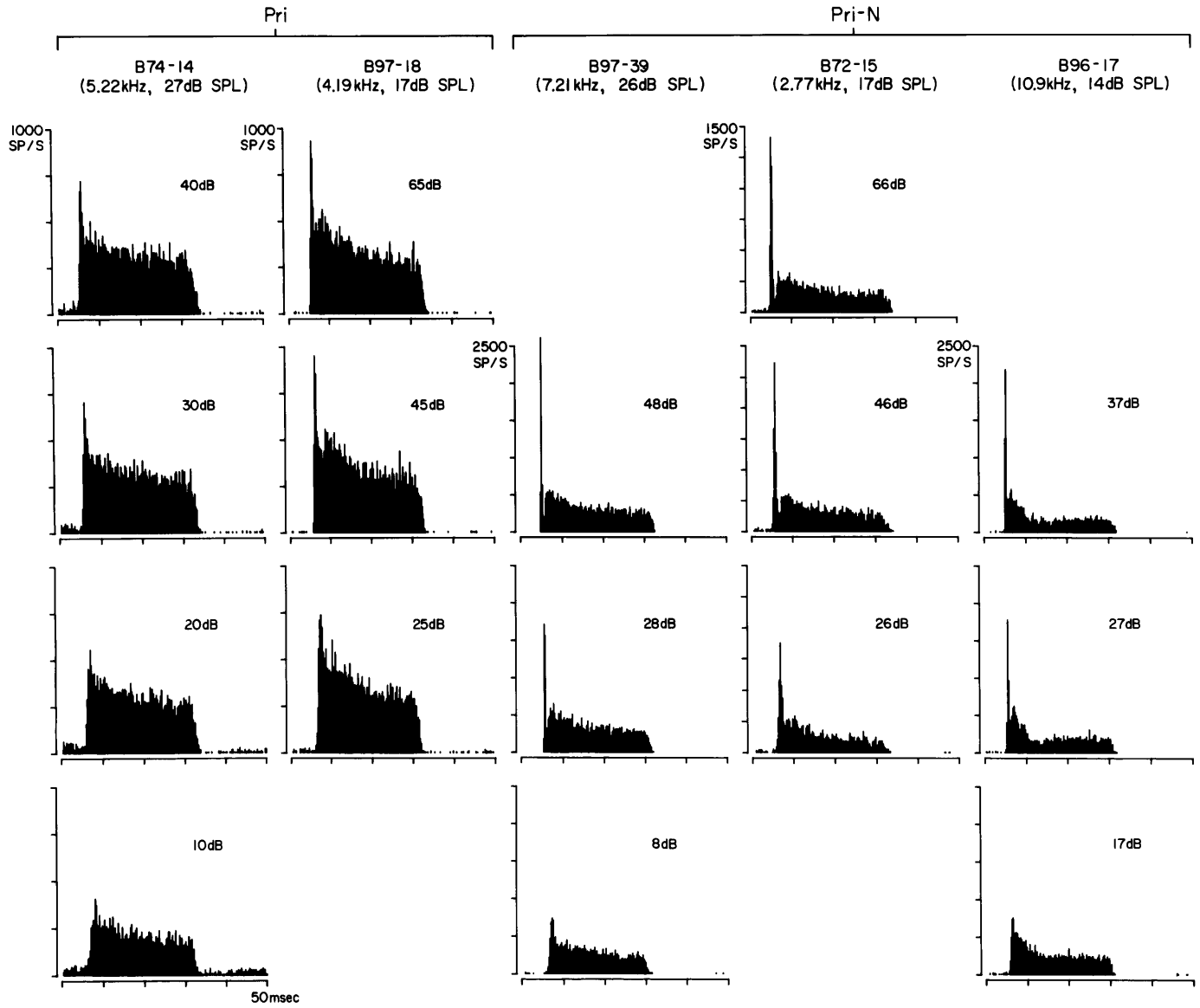
Pri
Pri-N
B74-14
(5.22kHz, 27dB SPL)
B97-18
(4.19kHz, 17dB SPL)
B97-39
(7.21kHz, 26dB SPL)
B72-15
(2.77kHz, 17dB SPL)
B96-17
(10.9kHz, 14dB SPL)
1000 SP/S
1000 SP/S
1500 SP/S
2500 SP/S
2500 SP/S
40dB
65dB
66dB
30dB
45dB
48dB
46dB
37dB
20dB
25dB
28dB
26dB
27dB
10dB
8dB
17dB
50msec

Pri-N

Closely related to the Pri units are the units that have been described as Primarylike with a "notch". Following an initial narrow peak in the PST histogram of the tone burst response there is a narrow dip (see examples in Figure IV-10). The initial peak can attain a much larger instantaneous rate than any of the Pri units and the dip can extend to zero. At half-depth the duration of the dip was never greater than 2 msec and was more usually from 0.5 to 1 msec. It should be obvious that bin width and a sufficient number of tone burst presentations are necessary to be able to detect the notch. The notch was not usually clear for STBCF levels within 20 dB of threshold so that in some cases much higher levels were required to demonstrate the notch. Increases in the level of the tone burst generally sharpened the initial peak and increased the width and depth of the notch.

Pri-LR

Twelve units were found to have a response to STBCF that exhibited a PST histogram shape which was similar to the primarylike shape. The discharge rates, however, were unusually low as is shown for two Pri-LR units in Figure IV-14. The low rates were sustained so that the CTCF responses were also unusually low for a Primarylike unit. The rate versus level functions for CTCF stimulation were, in fact, comparable to those of the On-P units and although three of these units exhibited a response to STBCF that was more peaked at the onset than that of the Pri units, none of these

units had a distinct enough peak to be assigned to the On group. Since these units may represent part of the Pri category, they were called Low-Rate-primarylike (Pri-LR). In sections 4 and 11 some additional properties will be discussed that support keeping these units in a separate category.

Chopper Group

All units in the Chopper group exhibited the chopper pattern to tone burst stimulation at levels more than 10 to 20 dB above threshold. Near threshold the response forms to STBCF are primary-like whereas at higher levels the PST histograms show at least two distinct peaks and in most cases many more. As the tone burst level is increased, the spacing between the peaks generally decreases, while the amplitude and number of the peaks increases. Although some Chopper units can exhibit a PST histogram of the Pri-N form, this shape is usually found for only a small range of tone burst levels. The spacing between successive peaks in a chopper pattern generally increases with time in contrast to the decrease found with many Pauser units. The large first interval followed by smaller spacings or no peaks at all distinguish the pauser pattern from a chopper.

Next to the Pri and Pri-N categories the Chopper categories represent the most populous group recorded in this particular sample of AVCN units. Amongst the Choppers certain differences in response characteristics gave rise to the definition of the Chopper categories. The mean firing rate at which a chopper pattern ap-

peared in the PST histogram was quite variable across units. Some exhibited a chopper pattern at a rate as low as 50 spikes/sec whereas others had to be discharging at a rate approaching 500 spikes/sec to have distinguishable peaks in the PST histogram. The CN units that can have a chopper PST histogram pattern with long intervals between the peaks are relatively frequently found in DCN but very infrequently in most of AVCN. The Choppers which could exhibit the longer intervals were separated from the other Choppers by means of a criterion based on the mean interspike interval at the onset of the chopper response. The Chopper units which exhibited chopper peaks with a mean interspike interval greater than or equal to 5 msec were placed in the Chop-L category. The STBCF responses of two Chop-L units are shown in figure IV-11. The other two Chopper categories did not show a chopper pattern with increasing stimulus intensity until the mean interval was less than 5 msec. The upper row of histograms for the four right-hand columns in Figure IV-11 illustrates two contrasting chopper patterns. The two Chop-S units in that figure exhibit a chopper pattern with gradually diminishing peaks whereas the Chop-T units have a rapid termination of the oscillations. Both of the Chop-T units in this figure have a distinct Chop-T profile of PST shapes. Unit B98-24 has, in fact, one of the more extreme forms particularly at 20 dB above threshold.

In developing a more sensitive criterion to discriminate these two (Chop-S and Chop-T) chopper forms it was found useful to examine more closely the discharge characteristics during the tone burst. The test can be best explained by first examining the Chop-S and

Chop-T response forms with a special type of dot display. In Figure IV-12 the dot displays show the occurrences of the individual spikes in a two-dimensional system which represents with the horizontal coordinate the time of occurrence of the spike with respect to the onset of the tone burst and with the vertical coordinate the length of the interval to the next spike. Superimposed on each of these dot displays is a plot of the mean interval to the next spike, averaged over the 200μsec intervals which correspond to the bins of the PST histograms above the plots. We can see that for the Chop-S unit, there is a gradual increase in the mean interval. The increase, often by as much as a factor of two over the duration of the tone burst, is comparable to that exhibited by most AN fibers or Pri units of the AVCN. The choppers with a gradual change in the mean interval and correspondingly a gradual decrease in the oscillations in the instantaneous rate (PST histogram) were placed in the Sustained chopper response type, Chop-S.

In contrast, the Chop-T unit shows a rapid increase in the mean interval at the time when there is a sudden change in the distribution of interspike intervals. The change from a tightly concentrated cluster of points for each of the first few peaks of the PST histogram to a broad distribution is characteristic of the Chop-T units. The rapid increase in mean interval generally occurs after 2 to 5 spikes (5 to 10 msec); and number of spikes and/or the time span was constant for a given unit. Associated with the rapid increase in mean interval is the sudden loss of peaks in the PST histogram. In extreme cases there is a dip in the PST histogram

Figure IV-11 STBCF response of Chopper type units

The three Chopper response type categories are each represented by two units. The format is the same as described for Figure IV-8.

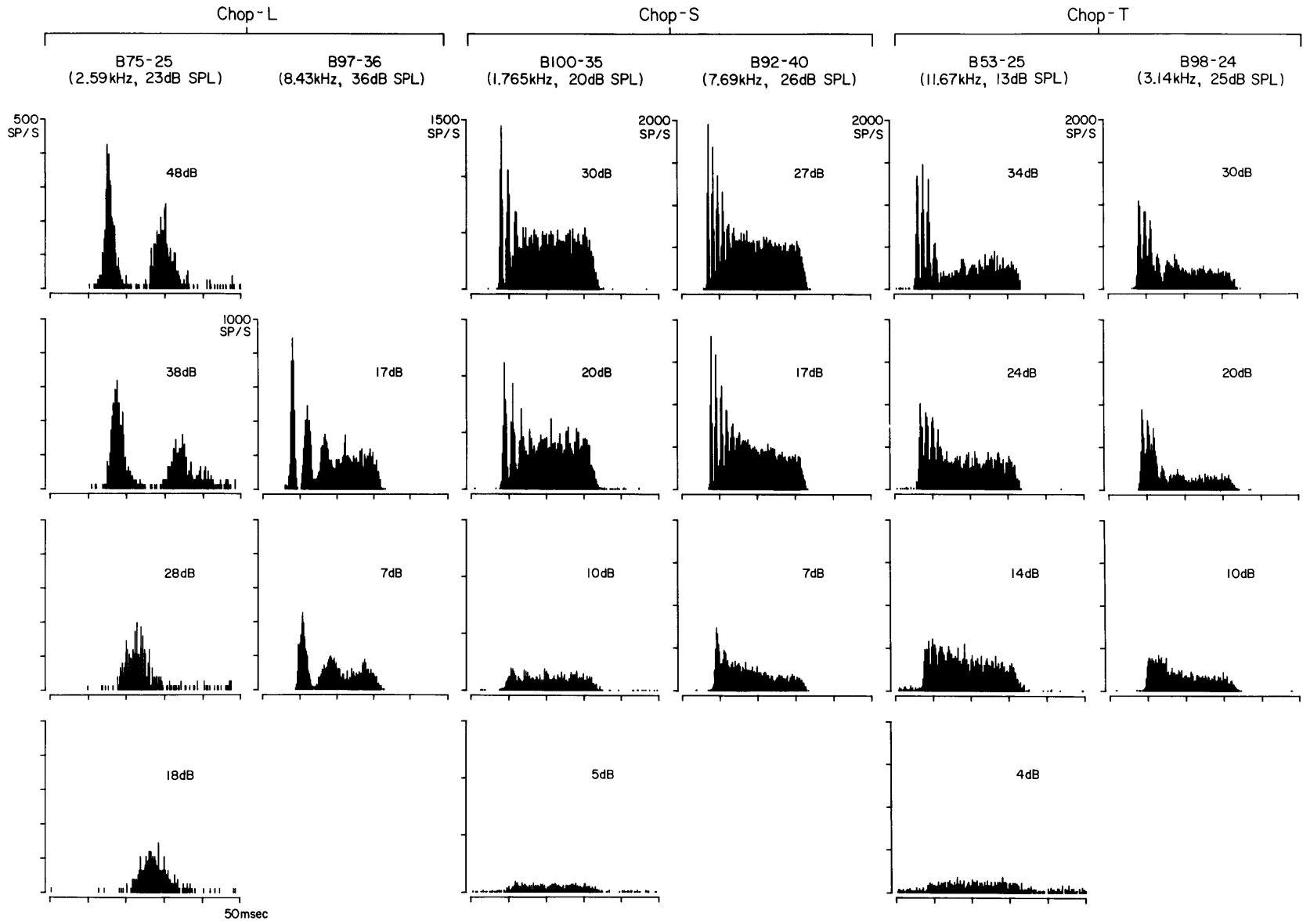
Chop-L
Chop-S
Chop-T
B75-25
(2.59kHz, 23dB SPL)
B97-36
(8.43kHz, 36dB SPL)
B100-35
(1.765kHz, 20dB SPL)
B92-40
(7.69kHz, 26dB SPL)
B53-25
(11.67kHz, 13dB SPL)
B98-24
(3.14kHz, 25dB SPL)
500 SP/S
1000 SP/S
1500 SP/S
2000 SP/S
2000 SP/S
2000 SP/S
48dB
38dB
17dB
28dB
7dB
18dB
30dB
20dB
17dB
10dB
7dB
5dB
34dB
24dB
14dB
4dB
30dB
20dB
10dB
50msec

Figure IV-12 Interspike intervals during STBCF response for Chop-S and Chop-T

The distinction between the Chop-S and Chop-T responses to STBCF stimulation is illustrated by the two sample dot displays. The dots on a 200 x 200 grid represent the time of occurrence of spikes (horizontal axis) and the interval to the next spike (vertical axis). The size of each dot is proportional to the number of spikes that occurred at each grid point during the 600 tone burst presentations. Spike occurrences corresponding to points outside the labelled space are not represented in the dot displays. After about 12 msec post-stimulus time, many spikes of the Chop-T unit are not shown because the "Subsequent Interspike Intervals" were often longer than 10 msec. The PST histograms above the dot displays represent the total number of spikes (including those off the interval scale) in pairs of columns of the dot displays. The mean inter-spike interval for the same pairs of columns is plotted on top of the dot displays. The three smaller histograms to the left of each dot display show the complete PST histograms plus the associated histograms of the mean and the standard deviation of the subsequent interspike intervals.

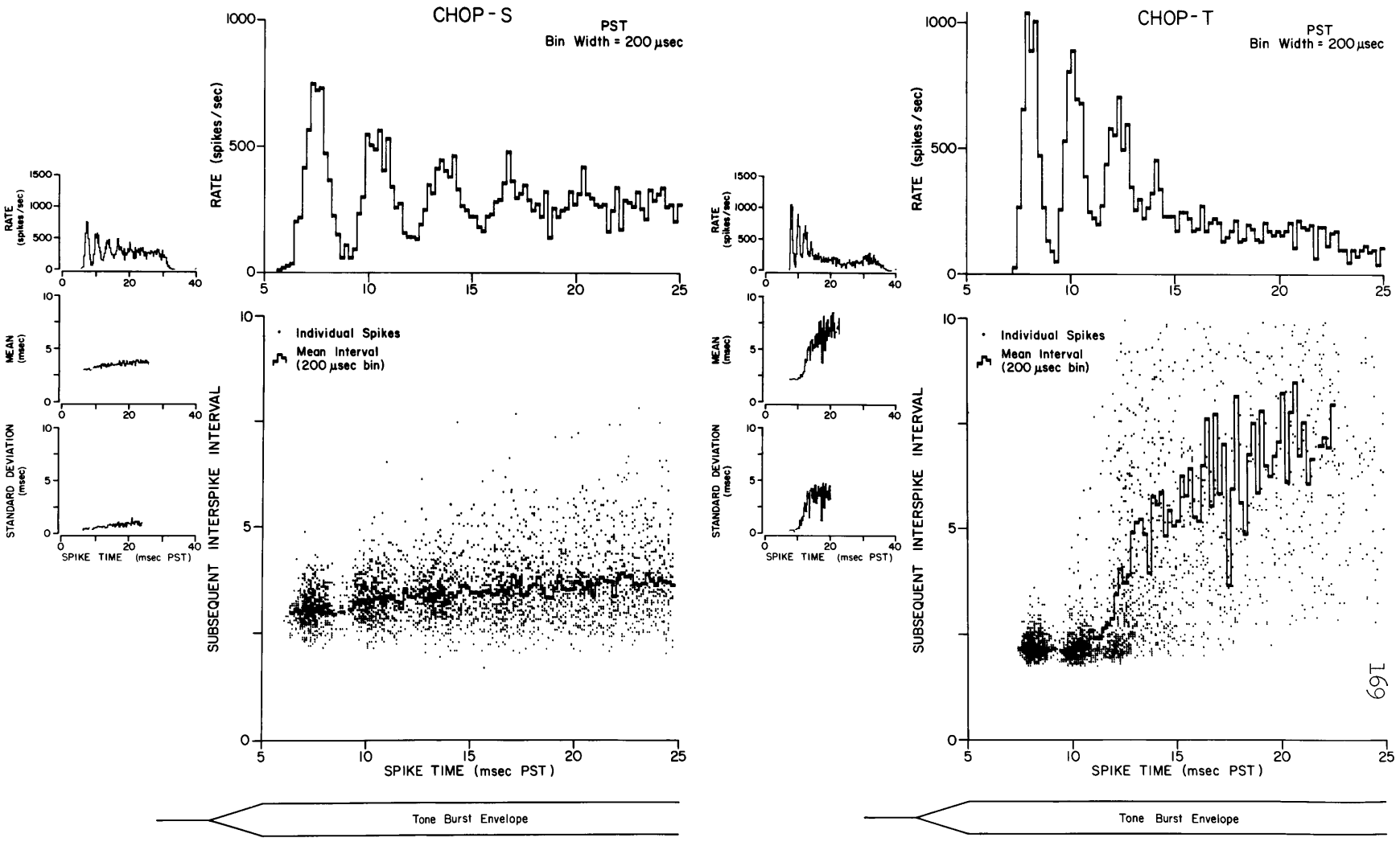
CHOP - S
PST
Bin Width = 200 µsec
RATE (spikes / sec)
1000
500
0
5
10
15
20
25
RATE (spikes/sec)
1500
1000
500
0
0
20
40
MEAN (msec)
10
5
0
STANDARD DEVIATION (msec)
SPIKE TIME (msec PST)
SUBSEQUENT INTERSPIKE INTERVAL
Individual Spikes
Mean Interval
(200 µsec bin)
SPIKE TIME (msec PST)
Tone Burst Envelope
CHOP - T
PST
Bin Width = 200 µsec
RATE (spikes / sec)
SUBSEQUENT INTERSPIKE INTERVAL
Individual Spikes
Mean Interval
(200 µsec bin)
SPIKE TIME (msec PST)
Tone Burst Envelope

Figure IV-13 The Chop-S versus Chop-T distinction

Four examples each are shown of the Chop-S (upper) and Chop-T (lower) categories. For each unit one PST histogram is shown along with the corresponding mean interspike interval plot. The same convention is used for the PST histograms as in Figure IV-8, except the bin width is 0.2 msec. The mean interval histograms were obtained from the INTSTAT program (Methods, section 4.4.2). Only those points based on greater than 10 intervals per 0.2 msec bin were plotted. The mean interval plots were terminated at the first bin for which the mean plus 3 times the standard deviation (not shown) was greater than the time to the end of the response. This condition generally ensures an estimate of the mean that is within a few percent of the estimate that would result had the tone not been turned off.

The histograms for B58-7 are based on 2400 tone burst presentations, B81-17 and B100-17, 1200 and all others 600.

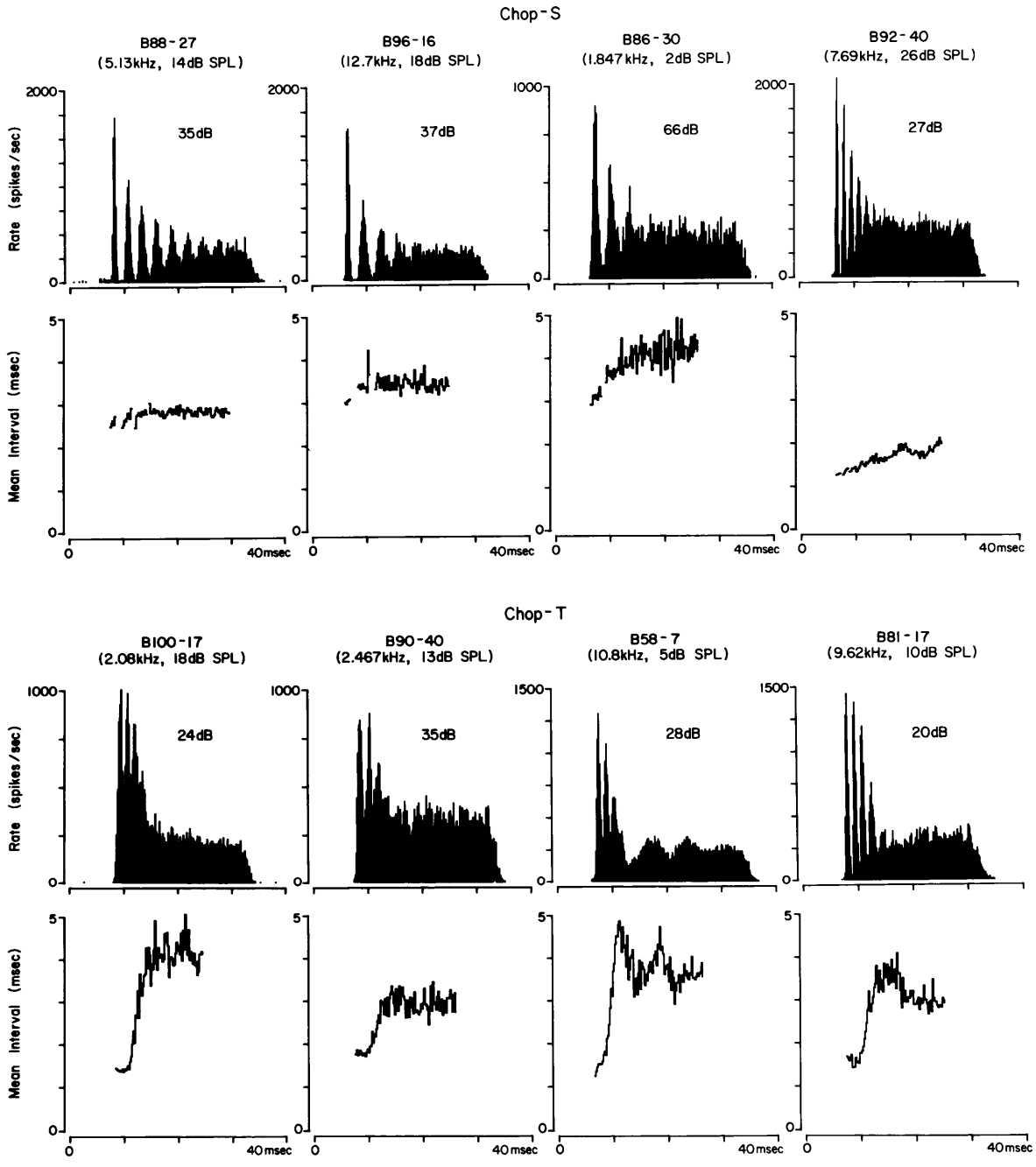
Chop-S
B88-27
(5.13kHz, 14dB SPL)
B96-16
(12.7kHz, 18dB SPL)
B86-30
(1.847kHz, 2dB SPL)
B92-40
(7.69kHz, 26dB SPL)
35dB
37dB
66dB
27dB
Rate (spikes/sec)
Mean Interval (msec)
40msec
Chop-T
B100-17
(2.08kHz, 18dB SPL)
B90-40
(2.467kHz, 13dB SPL)
B58-7
(10.8kHz, 5dB SPL)
B81-17
(9.62kHz, 10dB SPL)
24dB
35dB
28dB
20dB

following the initial peaks. This response type was named Chop-T because of the more Transient nature of the chopping which is restricted to the onset time. A collection of single histograms along with the corresponding mean interval functions from some identified Chop-S and Chop-T units is shown in Figure IV-13. The occurrence of a Chop-T type of response at any intensity was sufficient to qualify a unit for the Chop-T category. In some cases the response was clearly Chop-T at only one of the levels in an intensity series with 10 dB increments. At the levels above and below the optimal level, the response was similar but the change in the mean interval and/or the PST histogram peaks was not as distinct.

A total of 29 units that had a chopper response had to be dropped at either node "c" or "d" because of lack of data; these units were placed in a Chop-? "category".

Pauser

Six of the single units localized to AVCN were found to be Pausers. These units had characteristics similar to those described by Kiang et al. (1965b), Pfeiffer (1966a), and Godfrey et al. (1975b) for Pausers recorded in the DCN. At low intensities of STBCF stimulation a Pauser unit can have a primarylike or chopper PST histogram shape. For levels around 20 dB above threshold, the pause is generally evident. A dip in the PST histogram after an initial peak is considered to be a pause under two conditions:

1. If there are later chopper peaks, the dip must be longer than the interpeak time of the later chopping, or

2. If there is no chopping, the dip must be at least 5 msec long. This qualification helps to avoid mistaking a Pri-N unit for a Pauser. An example of a unit categorized as Pauser is shown in Figure IV-14.

Having described all of the response type categories across the bottom of Figure IV-6, we can now return to node "a" to consider the categories that were excluded from the main "sustained"-"transient" distinction.

Composite

The Composite response type contains 5 units which had a tone burst response that appears to have two components. What will be referred to as component A was somewhat similar to the responses of other units in the AVCN; one was a Chopper form, the others were like the Pri-LR or On type units in that they had an initial peak with a slowly decreasing rate through the short tone burst and little or no response to CTCF. The B component was more stereotyped and formed the defining characteristic of the Composite response type. The B component appeared to consist of a single spike or burst of spikes with a high instantaneous rate, narrow distribution and a latency of about 10 to 15 msec. Two examples of this response type are shown in Figure IV-14. Whether this second component also provided some further discharges beyond the transient burst is, of course, difficult to assess because of the uncertainty caused by the more sustained discharges of the A component.

Figure IV-14 STBCF response of Pri-LR, Composite and Pauser units

The format is the same as described for Figure IV-8.

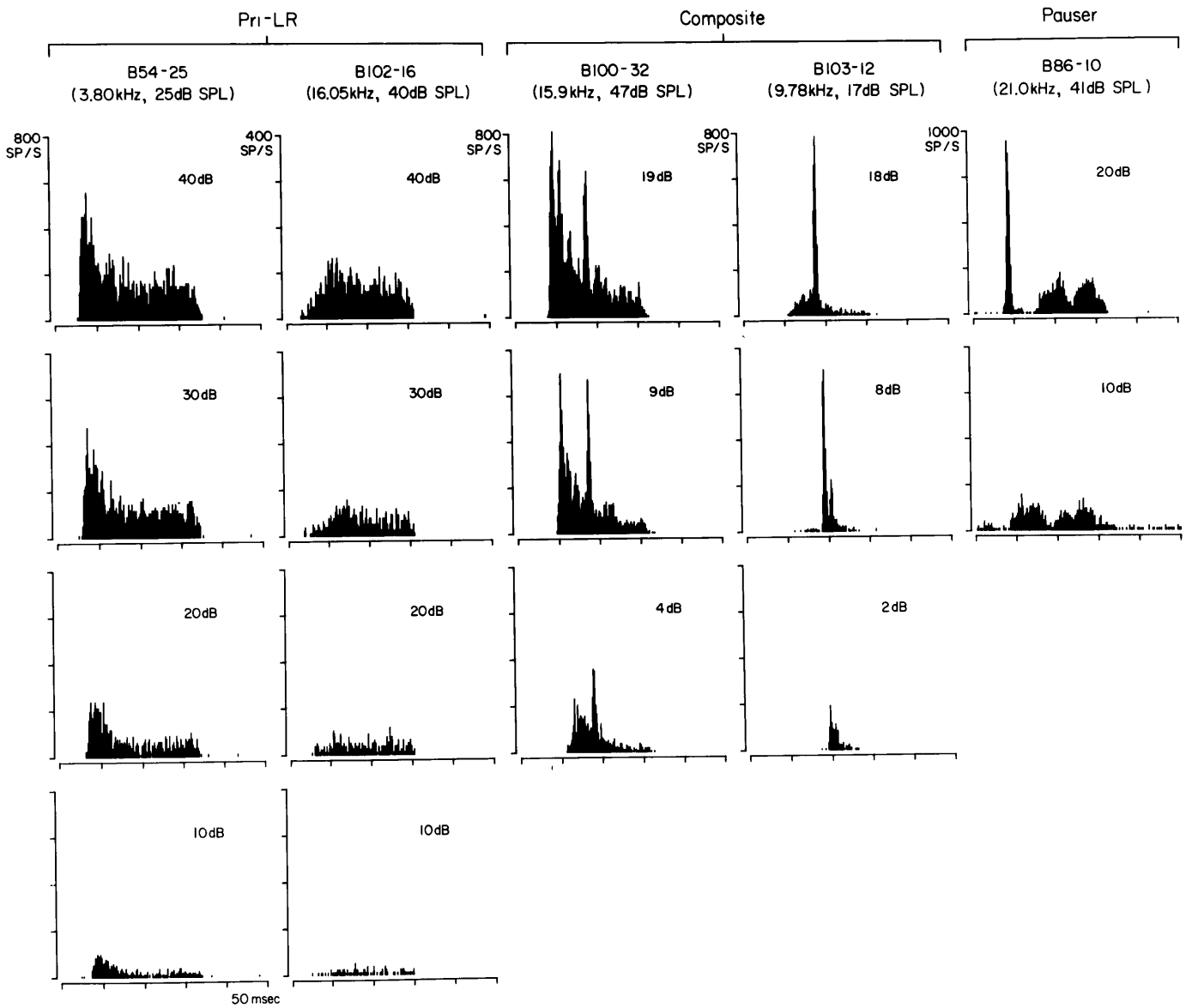
Pri-LR
Composite
Pauser
B54-25
(3.80kHz, 25dB SPL)
B102-16
(16.05kHz, 40dB SPL)
B100-32
(15.9kHz, 47dB SPL)
B103-12
(9.78kHz, 17dB SPL)
B86-10
(21.0kHz, 41dB SPL)
800 SP/S
400 SP/S
800 SP/S
800 SP/S
1000 SP/S
40dB
40dB
19dB
18dB
20dB
30dB
30dB
9dB
8dB
10dB
20dB
20dB
4dB
2dB
10dB
10dB
50 msec

The designation of these late peaks as a separate component is based on the evidence shown in Figure IV-15. In the column on the left we see the effect of the length of the tone burst used to excite a Composite response type, B71-22. At the bottom of the column is shown the response to the standard 25 msec tone burst at CF (STBCF). As the tone burst duration was reduced, the A component was truncated at successively earlier times until as in the 8 msec tone burst example the A component was only a short burst. The B component, however, was relatively stable until the duration became shorter than 5 msec, causing the rising and falling phases of the tone burst to overlap thereby reducing the peak value of the tone burst. The B component, therefore, appears to be a long latency response to the tone burst onset, whereas the A component is a more sustained response with a more normal latency. The next column of Figure IV-15 illustrates the effect of increasing the amplitude of shock pulses delivered in the region of the contralateral superior olivary complex. Single shock pulses delivered just before the tone burst presentations were capable of reducing or even preventing the B component. The A component always appeared to be relatively unaffected. The two columns on the right illustrate a similar effect of central shocks in reducing the late component of a Composite response. In the case of B100-32, a brief shock burst was delivered to the contralateral inferior colliculus preceding the tone burst presentations. These shocks were capable of affecting the B component of the response to all tone burst intensities tried. An intensity series is shown for B100-32 both with and without the

shocks. A similar effect of shocks on the B component of the Composite units was verified for 3 of the 5 units, 2 with shocks to the trapezoid body and 1 with shocks to the IC.

In addition to the effect of the shocks on the B component, contralateral acoustic stimulation was also found to influence the B component. With one of the Composite units, contralateral short tone bursts at the ipsilateral CF reduced the ipsilateral threshold of the B component and/or increased the current level required to reduce the B component.

Unusual

The Unusual category contains 6 units that did not fit into any of the response types defined above. This collection of units is highly heterogeneous and contains such unusual units as one which changed its response characteristics from excitatory to inhibitory during the recording time.

Phase-locked

Although not a true category, the Phase-locked classification was used to represent those units that could not be classified because the STBCF response patterns were dominated by phase-locking.

Each of the main response types used for the AVCN units can be seen to have members that exhibit phase-locking to low frequency tone bursts. Since the response type categories have proven useful in organizing the physiological data, efforts were made to extrapolate the categories to the cases of units with a low CF. Units

Figure IV- 15 Partitioning the tone burst responses of units in the Composite category

The left column (B71-22) illustrates the effect of tone burst duration on the two components of the response. The B component (peaks in center of histograms as indicated by arrows on some histograms) appears to be a long latency response to the tone onset. The level was 6 dB above STBCF threshold. The next column shows the effect of increasing the amplitude of a 50 μsec pulse presented in the contralateral trapezoid body before each 50 msec tone burst. The tone burst level was the same as for the left column. The current in μA is given on each histogram. Unit B100-32 (right-hand columns) illustrates the similar effect obtained when the electric stimulation was delivered in the contralateral inferior colliculus. A STBCF level series was run with and without the presentation of a burst of shock pulses just before each tone burst. The repetition rate was 5/sec for B71-22 and 10/sec for B100-32; all histograms represent a 1 minute sample.

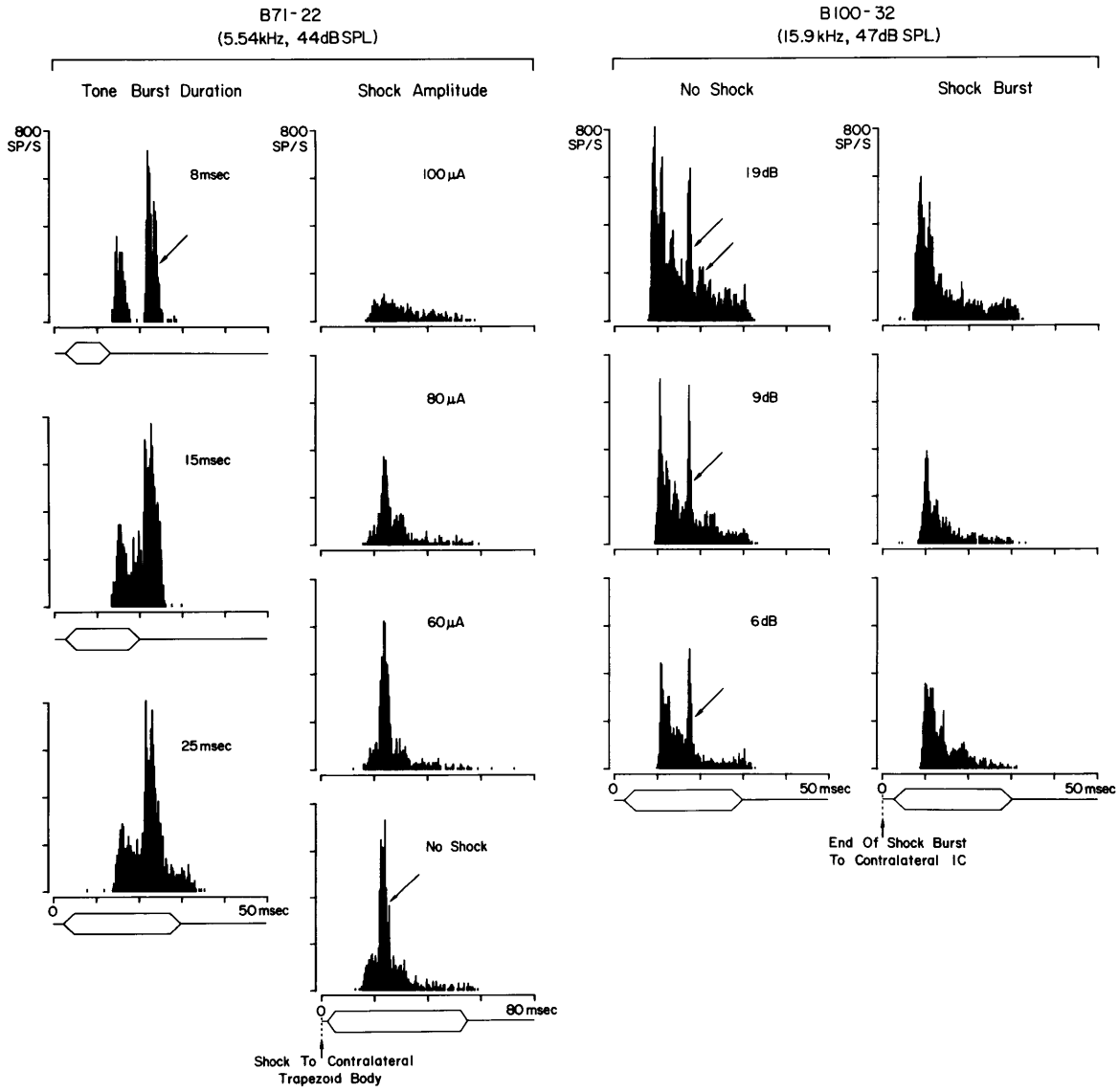
B71-22
(5.54kHz, 44dB SPL)
Tone Burst Duration
Shock Amplitude
800 SP/S
8msec
15msec
25msec
100μA
80μA
60μA
No Shock
0
50msec
80msec
Shock To Contralateral Trapezoid Body
B100-32
(15.9kHz, 47dB SPL)
No Shock
Shock Burst
19dB
9dB
6dB
End Of Shock Burst To Contralateral IC

were placed in the response type categories in spite of the presence of phase-locked peaks in the PST histograms of STBCF response, provided the characteristic pattern(s) could be discerned from the envelope of the phase-locked peaks. For example, if a unit had essentially no response to CTCF ($\leq$ 1 spike/sec) for some intensity range above the STBCF threshold, the unit was assigned to the On group. For some units there was a modulation of the phase-locked peaks suggesting a chopper pattern. By using a tone burst with an asynchronous envelope (i.e., an envelope which is not phase-locked to the sinusoidal stimulus being gated) a chopper pattern was clearly revealed. An example of the use of an asynchronous tone burst, along with tone bursts at a frequency above CF, is shown in Figure IV-17. The response to an asynchronous tone burst was used in classifying only two Chopper units but would be useful in a study focussed on units having CF's below 1 kHz.

4. Relationship of Prepotential and Response Type Categories

In the definition of both the prepotential and response type categories two levels of organization for the physiological data were used; this section introduces yet another level. It is necessary, therefore, to describe these levels more explicitly and to clarify the terminology that will be used. The first level beyond an initial processing of the recordings is the recognition of certain properties such as the presence or absence of a prepotential in the spike waveform or the occurrence of a chopper pattern in

response to tone bursts at a certain frequency and intensity. These properties generally apply to a single observation, such as a single spike waveform, PST histogram or average. The second level is established by the selection of a set of categories to summarize and represent the common profiles of unit behaviour with respect to one or more properties. The response type categories, for example, are based on the sequence of patterns for a level series of STBCF stimulation and the discharge rates to a level series of CTCF stimulation. Since most categorizations are strongly correlated with one particular property, the nomenclature for the categories is often similar to that for the property. Care must be taken, therefore, to distinguish between the names of properties (lower case) and categories (capitalized). Thus, a unit in the Chop-S category can have a primarylike response pattern for STBCF stimulation near threshold but a chopper pattern (of a particular form) at higher stimulus levels. This complete profile is identified as the Chop-S response type. The unit can also be referred to as a Chopper. In the prepotential categorization, the collective name for the units with a prepotential (pp) (i.e., the PP0, PP1 and PP2 units) will be Prepotential units, whereas the PP3 units are those without a pp.

The third level of organization for the physiological data is the definition of "unit types". The objective is for each unit type to represent a class of units having a common profile of characteristics with respect to the "salient" physiological properties and consequently to possibly represent the correlate of one of the cell types. In the attempts to define unit types, the categories

can act as summaries of large segments of the unit physiology. Although a unit type can be based on any physiological property, category or combinations of these, it will usually be based on one or more of the categorization schemes. The most useful categorizations, in terms of organizing the data, were found to be the pp and response type categories. By virtue of this observation these categorizations become major candidates for defining unit types in this study; taken separately and/or together they form a basis for much of the remainder of this presentation. Thus we shall speak of PP1 units, Chop-T units and (PP3, Chop-T) units, the latter representing the intersection of the two categorizations. It will therefore be useful to examine the relationship between these two classifications. A comparison of the pp and response type categories of all units recorded from cats with a VDL of -70 dB or better is presented in Table IV-1.

The top row of Table IV-1, labelled "?", contains the units for which a response type could not be assigned because of a lack of data. The PP1 and PP4 columns represent most of the units in the "?" row. The (PP4,?) units were mainly the poorly isolated units from which reliable recordings were difficult to obtain. We believe that almost all PP1 units are also Primarylike. About three-quarters of the PP1 units are in the "?" row because the tone burst responses of most of the PP1 units were not formally documented with PST histograms. With practice, most Primarylike units can be distinguished from the other types by observing the spike patterns on the oscilloscope. If the unit was clearly identified

Table IV-1 Numbers of units in (PP, Response type)

	PP0	PP1	PP2	PP3	PP4
?	37	320	13	26	357
Pri	19	60	12		
Pri-N		21	34	7	3
Pri-LR			7	4	1
Chop-?				17	12
Chop-L				28	2
Chop-S				57	3
Chop-T				76	3
On-?				13	6
On-A				39	2
On-G				2	
On-P			2	33	3
Pauser				5	1
Composite				5	
Unusual			2	3	1
Phase-locked	6	31	7	16	6

as Primarylike, the recording time was used to study other properties. A series of PST histograms of the response at several intensities of STBCF stimulation was obtained from PP1 units mainly when either the response type or prepotential rating were in question. What is entered in Table IV-1 are the units with histogram documentation of the response. Thus the response type distribution of the units in the PP1 column is biased against the Pri and Phase-locked categories in which most of the 320 units in the (PP1,?) group belong. If a PP1 unit had a STB response that was possibly or obviously of the Pri-N form, a PST histogram was generally computed. The other columns of Table IV-1 were unbiased in this respect since the experimental paradigm was always oriented toward determining the response type for every unit which did not show an obvious pp.

From Table IV-1 it can be seen that there are some strong correlations between the presence of a prepotential and the response pattern to CF tones and tone bursts.

PP0 - The negative pp units (PP0) were found to be limited to the Pri and Phase-locked categories. This is consistent with the interpretation that the negative pp represents responses of the primary neuron. The relatively large number that were not classified was due mainly to the poor isolation of many of these units, a factor which prevented reliable definition during supra-threshold stimulation.

PP1 - The units with a positive pp have response types that are similar to the responses of the AN; that is, Pri, Pri-N and Phase-locked.

PP2 - The response of PP2 units is also similar to that of AN fibers since most of these units fall into the Pri, Pri-N, and Phase-locked categories. However, there is a definite shift toward the Pri-N form as compared with the Pri. Some PP2 units are also found to be in the Pri-LR and On-P categories, both of which have members whose response patterns are somewhat similar to the primarylike form of response. Several of the On-P units had a response which was similar to some of the more extreme Pri-N units in that the PST histogram to STBCF has a very sharp peak (high instantaneous rate) and unusually low rate following this peak. It was this type of On-P unit, such as B104-32 in Figure IV-9, which had a PP2 rating.

PP3 - The units without a pp (PP3) represent almost all of the units with response types that were clearly non-primarylike and the PP3 column has no Pri units. There is virtually no overlap in the response types of the PP1 and PP3 units.

Examining the matrix from the other direction, we see that the Chopper, Pauser, Composite and On (except On-P) units fall entirely into either the PP3 or PP4 categories; that is, they never have an identifiable pp. The Primarylike units (Pri) are almost exclusively units with a pp. The Pri-N response type, however, appears to have a pp rating distribution shifted to the right. Considering the small number of PP2 units and the bias in determining the response types for the PP1 units, the Pri-N response seems to be strongly correlated with the PP2 category. The distribution of pp ratings for the Pri-LR group was one of the

reasons for regarding these units as belonging to a separate group. As expected, the Phase-locked row has units with and without pp's.

* 5. Long Tone Burst Response

Some of the units studied with STBCF stimulation were also tested with long tone bursts at CF (LTBCF). Since the LTB paradigm has a relatively short off-period, it represents a stimulus that is intermediate between the short tone burst and continuous tone stimuli which were used in defining the response type categories. For some units the form of LTBCF PST histogram could be qualitatively predicted from the STBCF and CTCF responses, whereas for others the relatively short off-period between the tone bursts and/or the longer time scale of the LTB revealed an unexpected response.

There are two main purposes in considering the LTBCF responses and in defining categories for the responses. An immediate objective is to compare the AVCN data with the data obtained in the survey of the CN by Pfeiffer (1966a) and in the more detailed study of PVCN and DCN in Godfrey et al. (1975 a,b). Correlations between the LTBCF categories and other properties of the units, particularly the STBCF response, have been shown in the above mentioned studies. The demonstration of similar correlations in this study will serve to relate the present categories to those previously defined. Of more specific interest, however, is the opportunity that the examination of the LTBCF response will provide to test the response type categories; correlations will reinforce the distinctions; lack of correlation may identify possible sub-categories of the present classification scheme.

The methodology in analyzing the response to LTBCF was similar to that used for the STB responses. The units were characterized on the basis of the level dependent sequence of PST histogram shapes to the LTBCF stimulation. Several sequences of shapes were frequently found in the sample of AVCN units. These response profiles to LTBCF were arranged in a set of categories which are similar to those shown by Pfeiffer (1966a).

Examples of the five main categories for LTBCF response are shown in Figure IV-16. The most common form is the Primarylike, characterized by an initial peak in the discharge rate followed by a decline to a relatively constant rate after 50 to 200 msec. The ratio of the initial rate to the final rate was generally less than 2:1 (unit B92-43 in Figure IV-16 exhibited the largest rate change in the Primarylike LTBCF category). For the units with the Primarylike shape of LTBCF response there was a large range of overall discharge rates. Since those units with the lowest rates appeared to correlate with other properties, a tentative subdivision of the Primarylike category has been introduced. The units with a discharge rate of less than 50 spikes/sec at the end of the response to LTBCF (20 to 30 dB above STBCF threshold) were placed in the Low-rate-primarylike category for LTBCF. This criterion segregated about 20% of the units with a primarylike response to LTBCF.

The units of the Dip category are characterized by a temporary decrease in rate following the initial peak. The dip lasts for 50 to 100 msec and is generally present at all stimulus levels more

Figure IV-16 LTBCF response categories

Each column of histograms represents the response to an intensity series of long tone burst stimulation at CF (LTBCF). The stimulus level in dB SPL is given with each histogram. The STBCF threshold is given below each column. Five of the LTBCF categories are illustrated, each with one or two units. B74-14 illustrates the typical Primarylike LTBCF response. The general trend across the figure and even within the pairs of units illustrating one category is for the responses to shift from more sustained to more strongly adapting or phasic. Each histogram has 200 bins over the 1 sec PST interval, a normalized vertical scale (600 spikes/sec maximum) and contains the responses from approximately 60 tone burst presentations (1/sec for 60 sec).

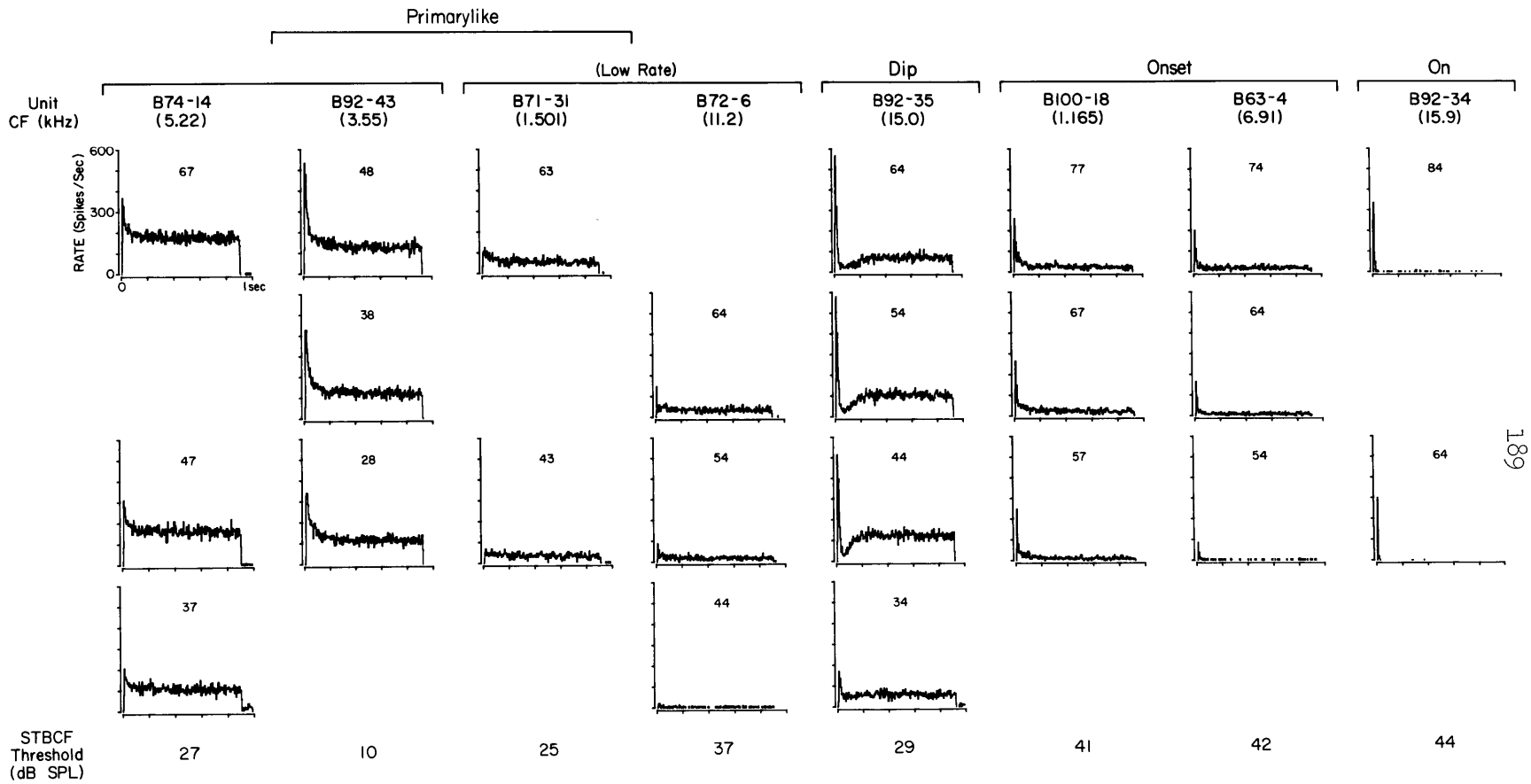
Primarylike
(Low Rate)
Dip
Onset
On
Unit
CF (kHz)
B74-14 (5.22)
B92-43 (3.55)
B71-31 (1.501)
B72-6 (11.2)
B92-35 (15.0)
B100-18 (1.165)
B63-4 (6.91)
B92-34 (15.9)
RATE (Spikes/Sec)
600
300
0
0
1 sec
67
48
63
64
77
74
84
38
64
54
67
64
47
28
43
54
44
57
54
64
37
44
34
STBCF Threshold (dB SPL)
27
10
25
37
29
41
42
44

about 20 dB above threshold. Three units having a Dip response to LTBCF and spontaneous activity were tested with tone bursts having a duration of several hundred msec or longer and an off-period approaching 1 second or more; the discharge rate after the tone was turned off was first depressed below the normal spontaneous rate and then increased to a rate of 2 to 3 times the spontaneous rate. After about 300 msec, the rate had returned to essentially the spontaneous level (An example of this behaviour is shown in Figure IV-19).

The units of the next category in Figure IV-16, Onset, show an abrupt increase in rate followed by a monotonic decline to a constant, low rate over about the final 500 msec of the response to LTBCF. The distinction between the Onset type and the Primarylike, both normal and Low-rate, is the larger change in rate that occurs for the Onset response plus the very low final rate which usually leaves many bins with no spikes after the 60 presentations of the long tone burst. The units of the On category show a more rapid decrease in rate, usually over 10 to 50 msec, and few later spikes. At stimulus levels of 40 to 60 dB above threshold the units of both the Onset and On LTBCF categories usually had a response more like that of the Low-rate-primarylike units.

The final two types of LTBCF form, Chopper and Build-up (not shown in Figure IV-16), are represented by only 1 and 2 units respectively. The Chopper LTBCF response was found for the one unit which had such a long interval between the "chopper peaks" that they were evident in the PST histogram of 1 second full scale

and 5 msec bin width. The two Build-up responses were of the form commonly seen in the DCN. After a relatively long latency, the discharge slowly increased in rate, reaching a plateau at 100 msec or more after the onset of the tone.

Having defined the categorization used to partition the various discharge characteristics shown by the AVCN units, we can now examine correlations with the other aspects of the physiology of the single units. Only the comparison with the pp and STBCF response type categories will be examined in this section; most other correlations can be inferred from this representation. The upper part of Table IV-2 shows the relationship between the LTBCF and the pp categories, the circled entries representing some of the more noteworthy correlations. The PPO and PP1 units are restricted to the Primarylike LTBCF categories and have only one unit each in the Low-rate-primarylike category. The PP2 units again deviate from the pattern of the PPO and PP1 units in having a different distribution in the LTBCF categories. The greater representation of the PP2 units in the Low-rate-primarylike and Onset categories for LTBCF is probably related to the observation in the previous section that the PP2 units, more frequently than the PPO or PP1 units, can have a Pri-LR or On-P response type.

In the lower part of Table IV-2 the LTBCF and the response type (STBCF) categorizations are compared. The Pri, Pri-N and Pri-LR are concentrated in the Primarylike and Low-rate-primarylike categories but with different distributions. The Pri response type is clearly correlated with the Primarylike LTBCF category, whereas

Table IV-2 LTBCF response versus prepotential and response type categories

	LTBCF Response Categories						
	Primarylike	Low-rate	Dip	Onset	On	Chopper	Build-up
PP0	3	1					
PP1	(20)	1					
PP2	20	(8)		(2)			
PP3	37	9	11	29	14	1	2
Pri	(19)	1					
Pri-N	18	(6)		1			
Pri-LR	1	5					
Chop-?	1						
Chop-L	7	1				1	
Chop-S	(14)	1	1				
Chop-T	9	1	(8)	(6)			
On-A				4	(12)		
On-G				1	1		
On-P	1	3	1	(15)			
Pauser	1						(2)
Composite	1		1	2	1		
Unusual	1						
Phase-locked	1			2			
?	6	1					
Totals	80	19	11	31	14	1	2

the Pri-N was more commonly found to have a low rate of discharge and even one unit in the Onset category.

Except for four of the On-P units, all of the On units with LTBCF data are found in the Onset, On and Dip columns. The majority of the On-A units have an On LTBCF response and the majority of the On-P units have an Onset response (These correlations are largely expected from the definitions of the On-A and On-P response type categories.). The On-P category, however, has some units that are not of the Onset and On LTBCF forms. The On-P units and to some extent the units of the other On categories were observed to exhibit a significant reduction in the initial rate as the duty cycle was increased and/or the time between tone burst presentations decreased. The reduction was greater than is found for the On units of the octopus cell area of posterior PVCN (Godfrey, 1971; Godfrey et al, 1975a and unpublished observations). With the initial rate depressed, the response becomes more primarylike as reflected in Table IV-2.

The Chopper units are seen to be largely of the Primarylike LTBCF response form, except for the Chop-T units. The Chop-T row has a significant fraction of the total units in the Onset category and almost all of the units in the Dip category. Pfeiffer (1966a) noted the correlation of the Dip LTBCF response with Choppers, but here we see that in the AVCN, at least, there is a particular type of Chopper that has the Dip form of response. The Dip and Onset forms are consistent with the Chop-T type of STBCF response which has a very high rate of discharge initially (often as high as 500 to 800 spikes/sec averaged over the first few discharges) and then

a rapid decrease in rate. The one unit in the Low-rate-primarylike column indicates that regardless of whether the sustained rate is high or low for the Chop-T units, the initial rate is generally high even with LTBCF.

As previously mentioned, the one Chopper LTBCF unit was a Chop-L unit and the two build-up responses to LTBCF were recorded from units that were Pausers to STBCF. The correlation of Build-up and Pauser categories has been noted for DCN units (e.g., Godfrey et al., 1975b) and thus further emphasizes the similarity of the AVCN Pausers with those found in DCN.

*6. Single Unit Response Area

*6.1 Tone burst responses off CF

A systematic examination of the response patterns to tone bursts at frequencies other than CF was undertaken with a relatively small number of units in this study. However, in determining a tuning curve or even the CF, the response of each unit was observed from the spike pattern as displayed on the oscilloscope. With most units, the only change in response form was the appearance of phase-locked responses for low frequency tone bursts. Figure IV-17 shows the behaviour of the Chopper unit, B105-21, for STB stimulation below, at, and above CF. At CF the chopper PST form is barely discernible, whereas for frequencies above the CF the phase-locking was less prominent and the chopper pattern more obvious. The use of tone bursts at 1kHz shows the chopper pattern which can also be

demonstrated at CF by using a tone burst stimulus with variable phase for the sinusoid being gated.

The tone burst responses of two On-A units are shown in Figure IV-18. The columns on the left (lower frequencies) show, for each unit, the appearance of a phase-locked response that tends to persist throughout the tone burst. Near threshold, however, the "on" behaviour is still evident even though the response pattern becomes more sustained at higher stimulus levels.

For frequencies at which phase-locking does not dominate the response, On units have been consistently observed to maintain an "on" type of response. The sequence of PST histograms shapes for a STB level series may be slightly different for different frequencies but the response still occurred predominantly at the onset. Most of the On units were observed from the audiovisual monitors of the spike discharges to be of the "on" type both at and off CF. Unit B97-9 shown in Figure IV-18 illustrates the small change in response pattern that can occur near the high frequency edge of the tuning curve (upper histograms, CF versus 5 kHz).

In Figure IV-19 is shown an example of a form of response found for several Chop-T units. The use of a tone burst with a duration longer than about 50 msec reveals a "dip" in the PST histograms. After the tone is turned off there is a period with no discharges followed by a period during which the discharge rate is higher than the spontaneous rate. At frequencies above CF it was possible to find frequency-level combinations that produced a rate suppression during the tone and a temporary rate increase after the tone was turned off.

Figure IV-17 Tone burst responses for B105-21 at different frequencies

All histograms are based on STB stimulation for one minute (600 tone burst presentations) and have the same vertical (normalized to spikes/sec) and horizontal scales (200 bins) as labelled on the lower center histogram. Frequency is constant within a column and level constant (within 1 dB) across a row.

The three columns on the left show responses to tone bursts with the envelope synchronized to the sinusoid being gated. The column on the right shows the response to tone bursts at CF with the envelope not synchronized to the sinusoid.

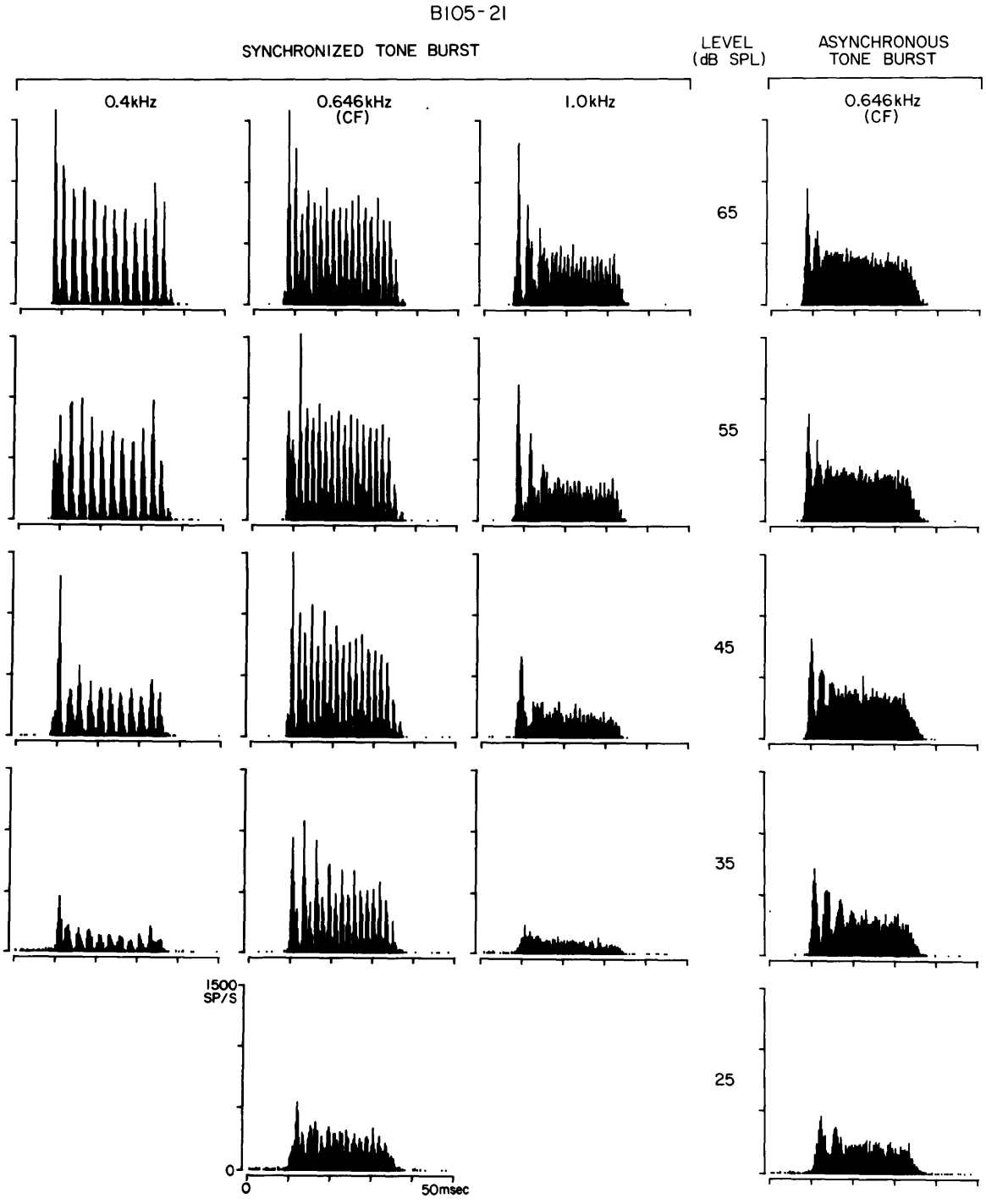
B105-21
SYNCHRONIZED TONE BURST
LEVEL (dB SPL)
ASYNCHRONOUS TONE BURST
0.4kHz
0.646kHz (CF)
1.0kHz
0.646kHz (CF)
65
55
45
35
25
1500 SP/S
0
0
50msec

Figure IV-18 Tone burst responses for two On units at and off CF

The general format is described in the first paragraph of the caption for Figure IV-17. All stimulus levels are within 1 dB of the levels indicated on the right. The tuning curve for B97-9 is shown in Figure IV-24 and for B39-21 is shown in Figure IV-20.

B97-9

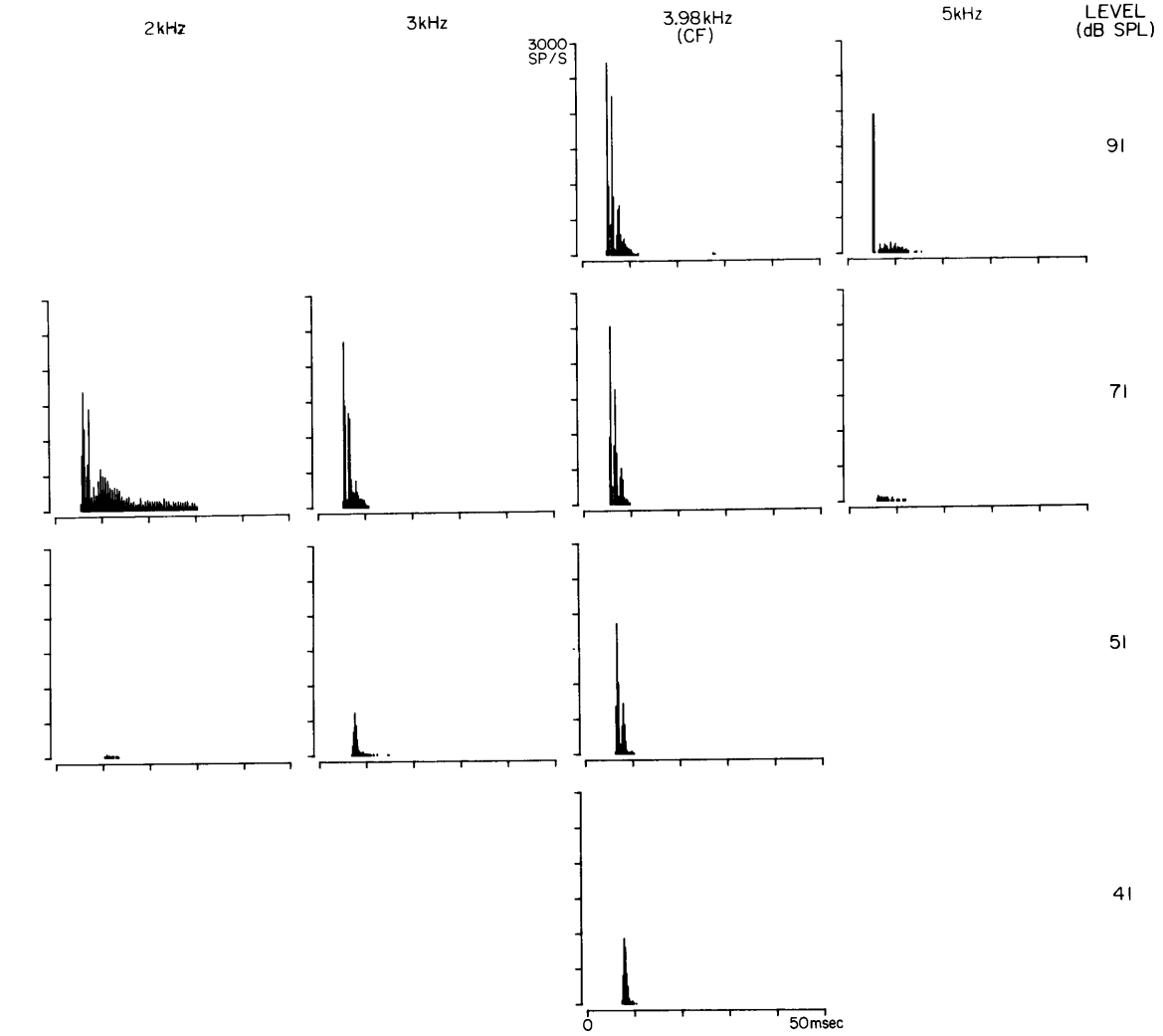
2kHz
3kHz
3.98kHz
(CF)
5kHz
LEVEL
(dB SPL)
3000
SP/S
91
71
51
41
0
50msec

B39-21

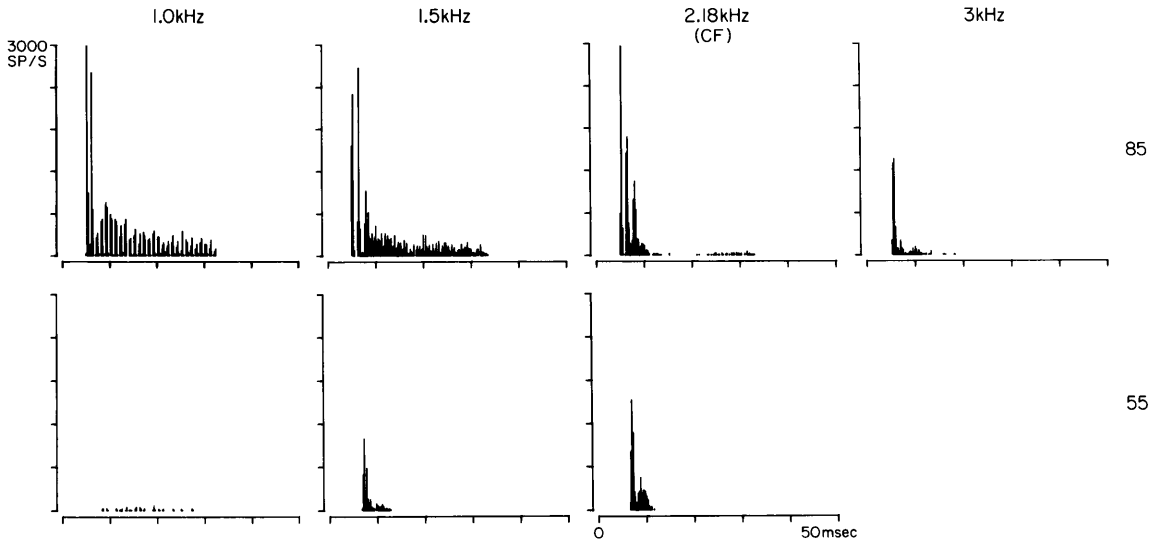
1.0kHz
1.5kHz
2.18kHz
(CF)
3kHz
3000
SP/S
85
55
0
50msec

Figure IV-19 Tone burst responses of B92-35

The PST histograms for three tone burst paradigms are shown as a function of the stimulus level dB SPL (on left). Each column has a constant vertical scale as labelled on the upper histogram. PST histograms for the standard STBCF and LTBCF paradigms shown on the left have 200 bins. The two right-hand columns use 100 bin PST histograms to show the response to 300 msec tone bursts presented once every 4 seconds. The histogram on the right shows the response to the 300 msec TB at 17 kHz.

The CF in kHz and STBCF threshold in dB SPL are given below the unit number.

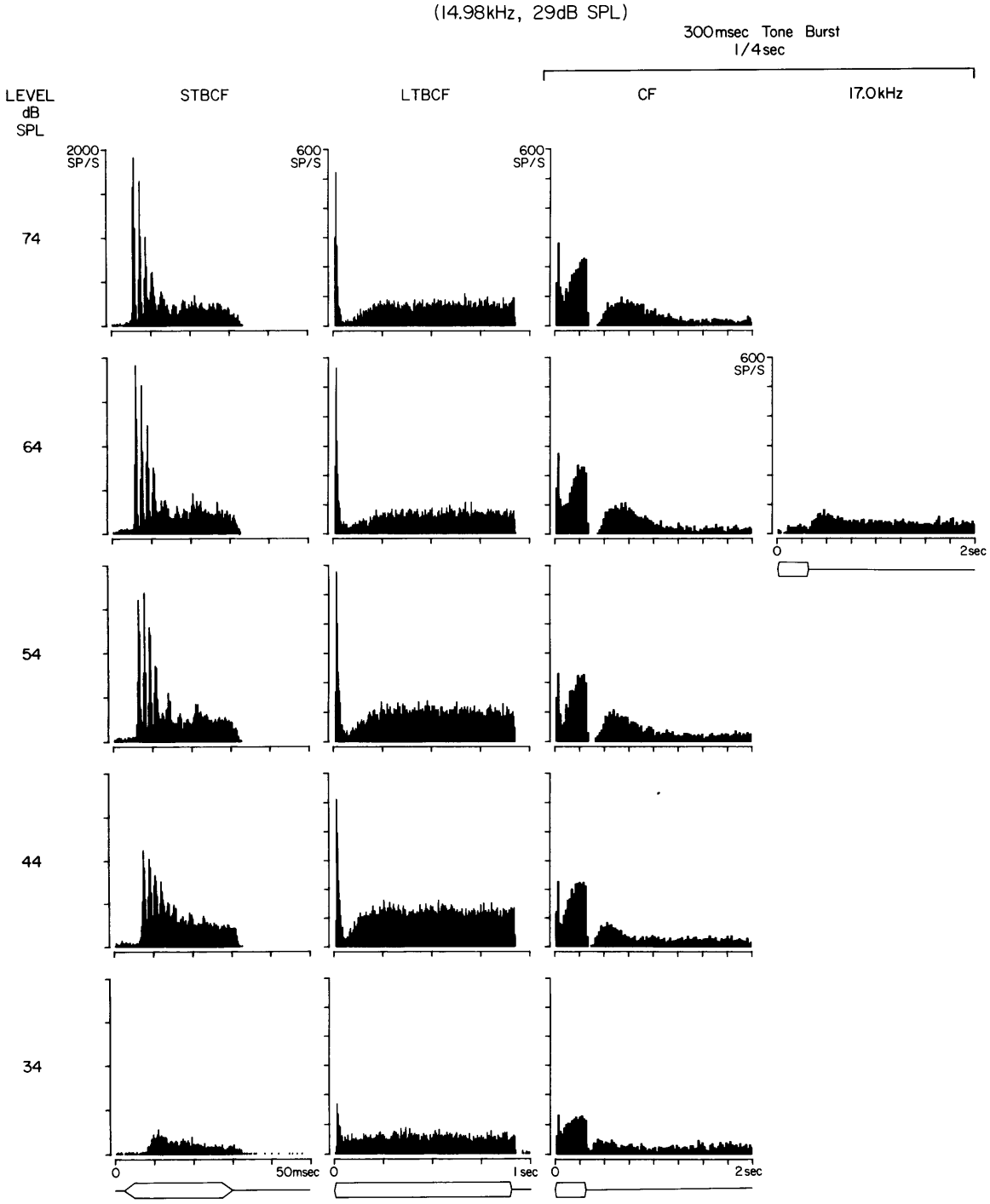
B92-35
(14.98kHz, 29dB SPL)
300msec Tone Burst
1/4sec
LEVEL
dB
SPL
STBCF
LTBCF
CF
17.0kHz
2000
SP/S
600
SP/S
600
SP/S
600
SP/S
74
64
54
44
34
0
2sec
0
50msec
0
1 sec
0
2 sec

* 6.2 Tuning curve

Most of the tuning curves obtained from AVCN units were similar to the range of tuning curves found for auditory nerve units. The only clear deviations from auditory nerve tuning curves were the occasional presence of suppression of spontaneous activity ("inhibitory sidebands") and slightly broader tuning. Inhibitory sidebands were not studied systematically enough to allow any general observations about their occurrence. Most of the non-primarylike units had such a low rate of spontaneous activity that inhibitory sidebands were difficult to demonstrate.

For all of the On, Pauser, Composite and Pri-LR units, the automatic tuning curve program was not used. On both theoretical and empirical grounds an algorithm using single tone burst presentations to decide whether such units are responding is inappropriate. In the case of the units with a positive prepotential and of the units with primarylike characteristics, the automatic procedure was used since comparison of the automatic tuning curves with manually obtained tuning curves failed to reveal any gross differences. There was a tendency for the manual tuning curves to be slightly more sensitive in some cases. Although in later experiments the automatic tuning curves were used routinely for the units in the PPO, PP1, Pri and Pri-N categories, the CF and threshold at CF were still determined manually as a check. The Choppers present a problem in that their response characteristics were usually, but not always, suitable for the automated procedure. Often both methods were used. The automated procedure was used alone only for Choppers

that had a vigorous, short latency response to tone burst stimulation. These units were, in fact, even better suited than the AN single units to the automatic procedure since their low spontaneous activity and steep intensity functions for tone burst produced well defined thresholds.

Two aspects of the tuning curves will be considered, the shape and the threshold at CF. As mentioned above, all of the tuning curves obtained from AVCN units were basically similar to those of AN single units. The shapes varied with CF as the AN tuning curves do. The tuning curves were generally V-shaped around the most sensitive frequency (CF) with a steeper slope above the CF than below, except for the low CF units which could have this reversed. All tuning curves exhibited a single minimum (at CF) except for the high CF units which could have a broad minimum associated with the low frequency "tail" as do AN units (Kiang and Moxon, 1974). The tuning curves obtained from the Prepotential units, i.e., the PPO, PP1 and PP2 units, were indistinguishable from those of AN units. Tuning curves were obtained from only 9 of the (PP2, Pri-N) units. The PP3 units exhibited a wider range of tuning curve shapes than found for the AVCN units with a prepotential or for AN units. In Figure IV-20 is plotted a representative sample of tuning curves from Chopper and On units. The variety of shapes is illustrated by the two On-A units, B97-3 and B75-28 (center of plot), the two On-P units, B65-24 and B104-32 (CF's of about 2 and 3 kHz) and the two Chopper units, B75-29 and B84-28 (CF's of about 4 kHz).

Figure IV-20 Tuning curves of some PP3 units

Sample tuning curves selected to illustrate the range of shapes and thresholds found for On and Chopper units. Each data point represents a threshold determination based on a combination of audio and visual cues.

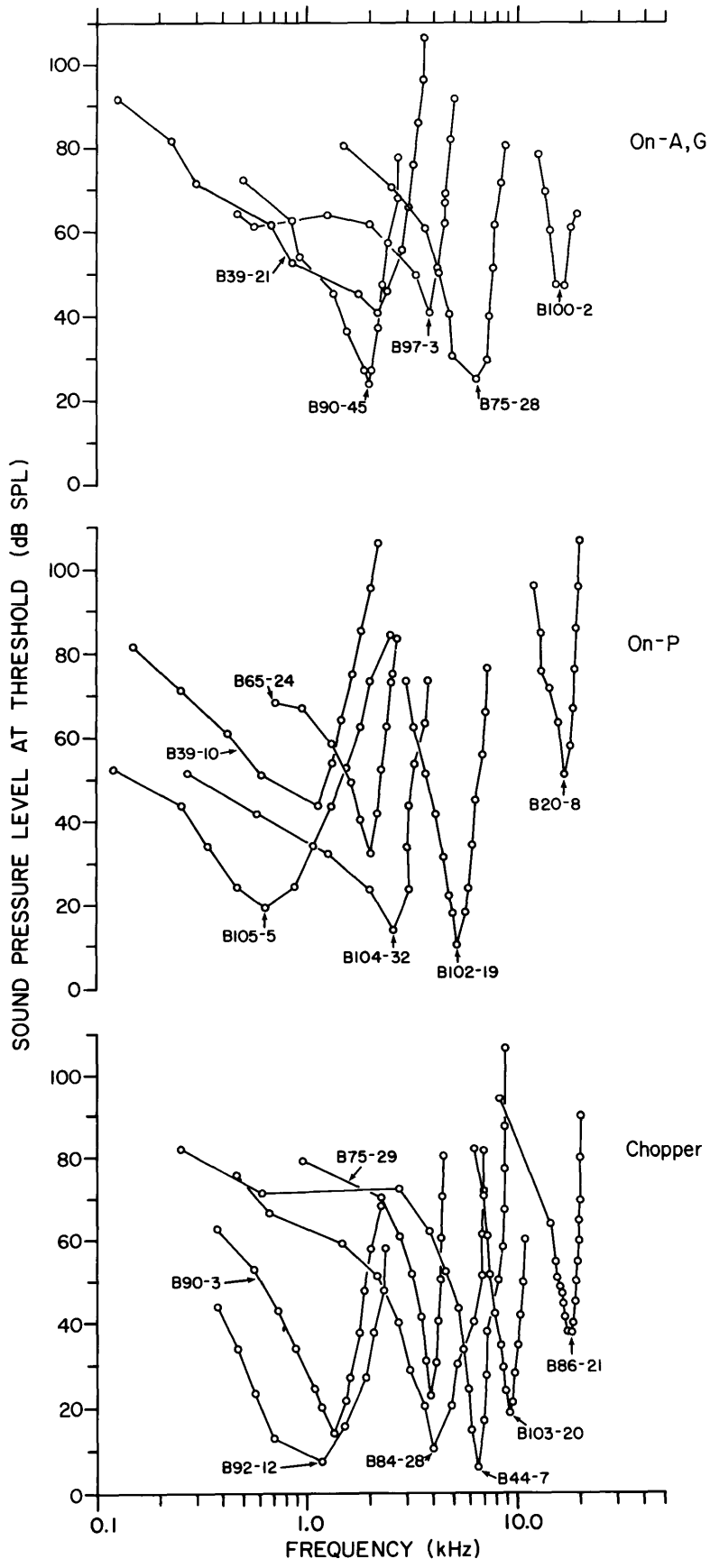
On-A,G
B39-21
B97-3
B100-2
B90-45
B75-28
On-P
B65-24
B39-10
B20-8
B105-5
B104-32
B102-19
Chopper
B75-29
B90-3
B86-21
B103-20
B92-12
B84-28
B44-7
SOUND PRESSURE LEVEL AT THRESHOLD (dB SPL)
FREQUENCY (kHz)
0.1
1.0
10.0
0
20
40
60
80
100

Figure IV-21 Q_{10} as a function of CF

All Q_{10} values were estimated from tuning curves corrected to SPL at the tympanic membrane. At 10 dB above the tip of the tuning curve the width was estimated by linearly interpolating between the available data points. If more than one tuning curve had been determined for a given unit the individual Q_{10} values were averaged. The Q_{10} values for the Prepotential units were all obtained from automatic tuning curves. The values for the Chopper units came from both automatic and manual tuning curves. Since no systematic differences were found in the range of Q_{10} values, the data were pooled. The Q_{10} values for the On units came exclusively from manual tuning curves. The curve 1.6 + 0.7 (CF) was visually fitted to the data of the upper plot and duplicated on the lower plots.

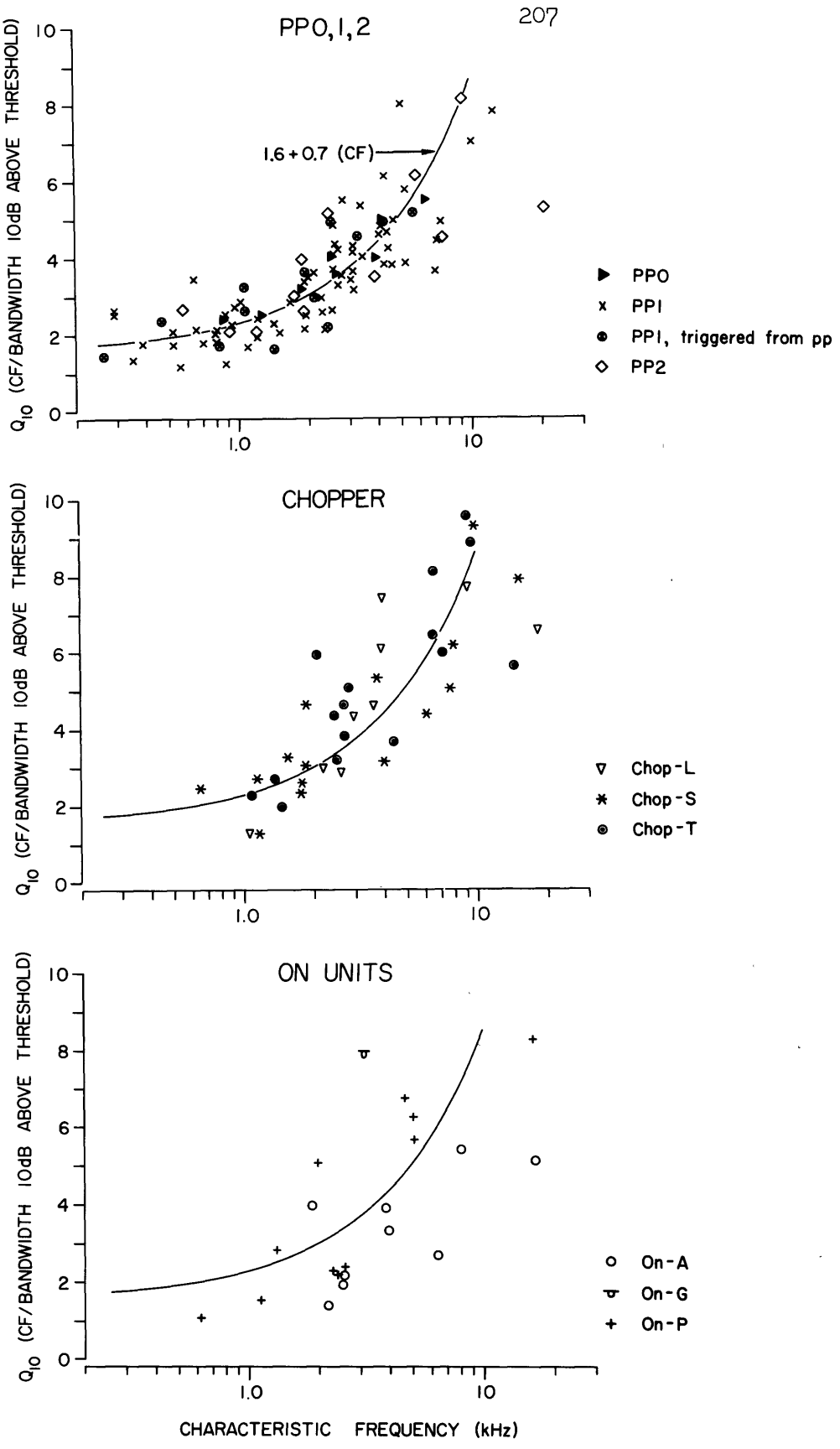
PPO,1,2
1.6+0.7 (CF)
PPO
PP1
PP1, triggered from pp
PP2
CHOPPER
Chop-L
Chop-S
Chop-T
ON UNITS
On-A
On-G
On-P
Q_{10} (CF/BANDWIDTH 10dB ABOVE THRESHOLD)
CHARACTERISTIC FREQUENCY (kHz)
1.0
10
0
2
4
6
8
10

The plots of Q_{10} in Figure IV-21 show how tuning curve width varies as a function of CF for the three main groups of units. The Q_{10} values for the Prepotential units (upper plot) exhibit the same scatter and CF dependence as found for auditory nerve units. Both the Chopper and On units, however, appear to exhibit a larger spread of Q_{10} values than found for the Prepotential units. As was observed for the On units of posterior PVCN (Godfrey et al., 1975a), the On units in AVCN, especially the On-A units, also appear to have Q_{10} values below the range of Chopper and Primarylike units.

*6.3 Threshold at CF

In addition to the variations in the shapes of the tuning curves, there was also a large range of thresholds at CF for the PP3 units. The threshold variations, in some cases, appeared to correspond to overall level shifts of the tuning curve; whereas in other cases, the variations may be related to shape changes.

Although full tuning curves were determined for a relatively small number of units in this study, the stimulus level at the tip of the tuning curve ("threshold") was estimated for most. It is necessary, however, to pool the thresholds from all of the experiments to obtain a statistically significant sample for each unit category. A problem in pooling the threshold data, however, is the variation in overall sensitivity of the different cats. The only available objective measure of this sensitivity is the VDL to clicks which has some limitations as a general measure. In the upper plot of Figure IV-22, the thresholds for units with a clear prepotential (PPO and 1) were plotted with three symbols which

indicate the VDL of the ipsilateral ear at the time of the recording. Although unit thresholds from the three VDL ranges overlap, the upper and lower ranges are relatively disjoint. In order to more convincingly display the greater threshold range found for the PP3 units it was necessary to correct for the variation in peripheral sensitivity. The lower half of Figure IV-22 shows the data points from the upper plot replotted, correcting all thresholds to an equivalent VDL of -80 dB by assuming that VDL correlates directly with threshold. The variability is significantly reduced and the three VDL ranges now superimpose. A detailed examination of the data of Figure IV-22 reveals that the threshold versus CF distributions for several cats with VDL's in the middle range were elevated at CF's above about 2 kHz consistent with their poorer sensitivity but had lower thresholds at CF's below 1 or 2 kHz. Thus the VDL correction worked well in reducing the scatter at CF's above 2 kHz but sometimes increased the scatter below 2 kHz. This effect is not surprising, considering the view that the VDL would be a better measure of the sensitivity of medium and high CF units than the low.

The plots in Figure IV-22 serve as a control for the VDL "correction" of thresholds and as a reference for the similar (VDL "corrected") plots of the PP2 and PP3 units as shown in Figure IV-23. The main effect of the less faithful correspondence between the VDL and the thresholds of units with CF's below about 2 kHz was found to be the presence of thresholds below 0 dB when "corrected" with the VDL. In Figure IV-23, however, our concern is mainly with the upper limits of the distributions for the Chopper and On units. As a

Figure IV-22 The correction of unit thresholds with VDL

The PP0 and PP1 units are used in this figure to illustrate the effect of correcting the thresholds of single units to an equivalent VDL of -80 dB. The thresholds to STBCF stimulation are plotted in the upper plot in sound pressure level (SPL) versus the single unit CF. The three symbols code for the VDL of the ipsilateral cochlea at or close to the time at which the CF and threshold were estimated for each unit. Assuming that VDL is a direct measure of the overall sensitivity of the cochlea, each threshold was corrected by subtracting (80 + VDL). The resulting corrected thresholds are plotted in the lower plot.

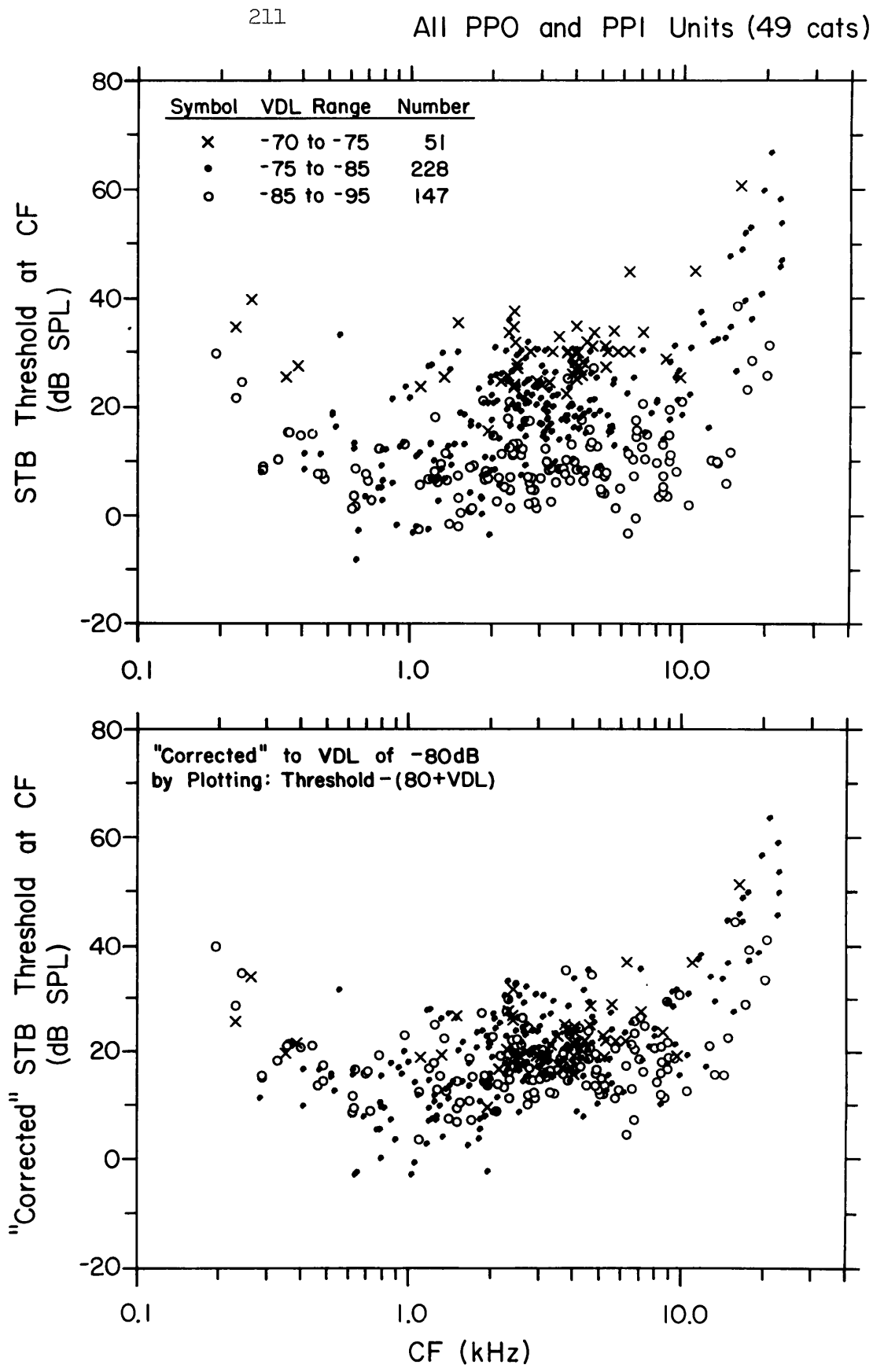
All PPO and PPI Units (49 cats)
Symbol VDL Range Number
× -70 to -75 51
• -75 to -85 228
o -85 to -95 147
STB Threshold at CF (dB SPL)
"Corrected" to VDL of -80dB
by Plotting: Threshold - (80+VDL)
"Corrected" STB Threshold at CF (dB SPL)
80
60
40
20
0
-20
0.1
1.0
10.0
CF (kHz)

Figure IV-23 Threshold versus CF for the PP2 and PP3 units

The "corrected" thresholds to STBCF stimulation are plotted as a function of CF for the PP2 units and for three groups of PP3 units. The correction procedure is described in the caption of Figure IV-22. A three segment approximation to the upper edge of the threshold distribution for Chopper units is also shown on the plot for On units. The threshold data for all plots in this figure came from the same experiments that provided the data for Figure IV-22.

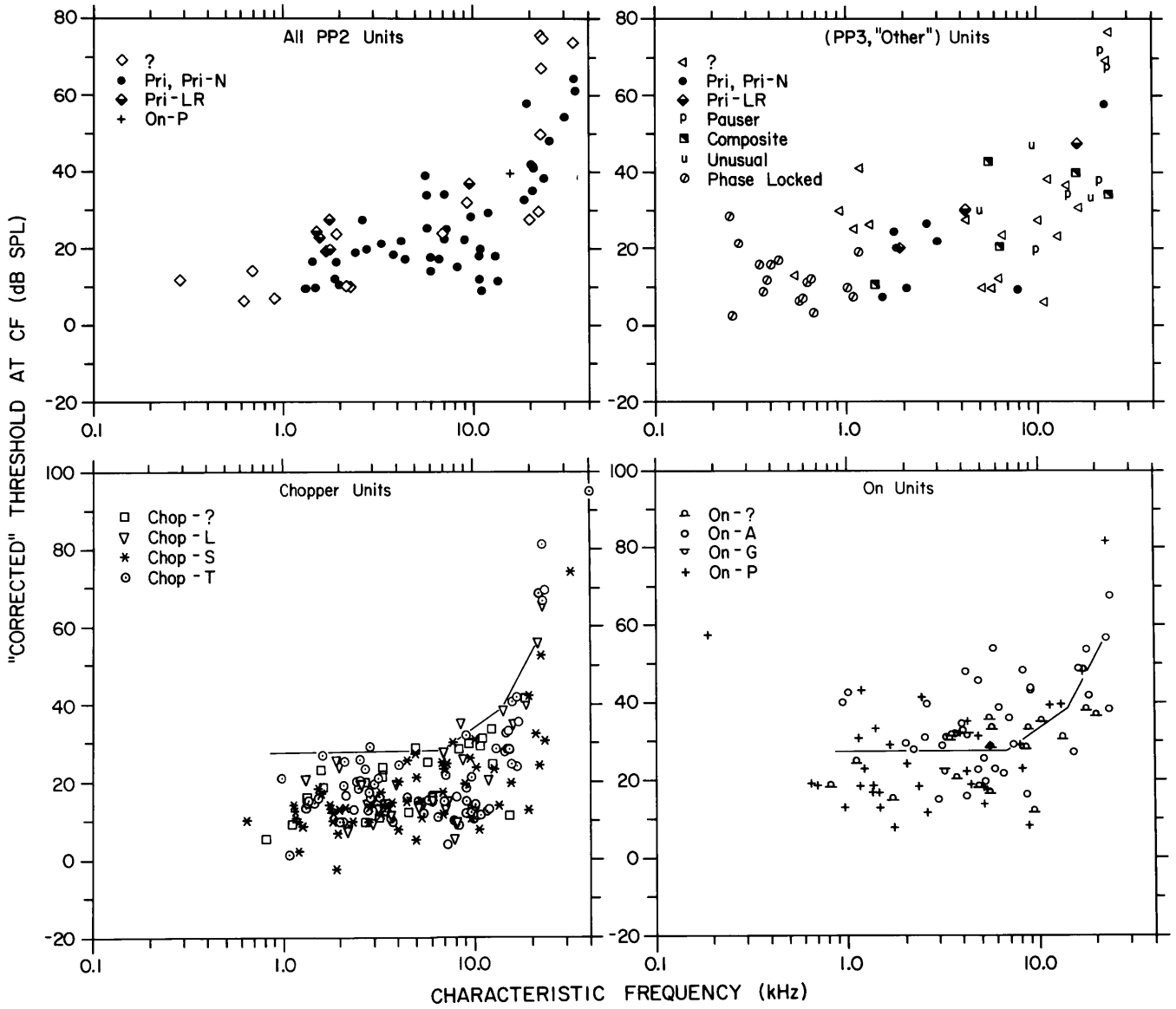
All PP2 Units
?
Pri, Pri-N
Pri-LR
On-P
(PP3,"Other") Units
?
Pri, Pri-N
Pri-LR
Pauser
Composite
Unusual
Phase Locked
Chopper Units
Chop-?
Chop-L
Chop-S
Chop-T
On Units
On-?
On-A
On-G
On-P
"CORRECTED" THRESHOLD AT CF (dB SPL)
CHARACTERISTIC FREQUENCY (kHz)
80
60
40
20
0
-20
100
0.1
1.0
10.0

demonstration of the elevated STBCF thresholds of On units, a three part approximation to the general trend of threshold with CF was selected to cover the frequency range from 0.9 to 20 kHz and to form an upper bound for most of the Chopper unit thresholds. This curve is also drawn on the On unit threshold plot. There are 3 Chopper units above this line and 168 below, whereas there are 43 On units above and 44 below. Although the pooling of data from many experiments is necessary to demonstrate the tendency for the On units, as a whole, to have higher thresholds, it was noted in individual experiments that an On unit adjacent to other unit types with almost identical CF's would often have a threshold that was as much as 20 dB higher.

It is now of interest to ask if this threshold variation within the On group is correlated with some other properties. Table IV-3 summarizes the number of On units above and below the threshold curve in Figure IV-23. In the initial definition of the response type categories which we shall call On-A1 and On-A2. These two categories have been collapsed into the single On-A category for all other purposes. The On-A1 units resembled the On-I units of PVCN; whereas the On-A2 resembled the On-L units (Godfrey et al., 1975a). The On-A1 tended to have a greater difference between the STBCF and CTCF threholds and showed a more rapid cessation of discharge after the tone onset. The progression from the A1 to A2 to P categories represents a transition from a distinct "on" pattern to a response which is marginally "on". Corresponding to this shift Table IV-3 shows that the STBCF threshold varies from being elevated

Table IV-3 Number of units above and below the threshold versus CF curve on Figure IV-23

	Above	Below
On-?	8	11
On-A1	13	1
On-A2	10	9
On-G	1	1
On-P	11	22

Figure IV-24 Comparison of tone burst and continuous tone tuning curves

Tuning curves obtained with STB stimulation are shown with solid symbols and connecting lines; those obtained with CT stimulation are shown with open symbols and dashed lines. Each symbol represents a separate audio-visual threshold discrimination. Beside each pair of tuning curves is the unit number and response type category.

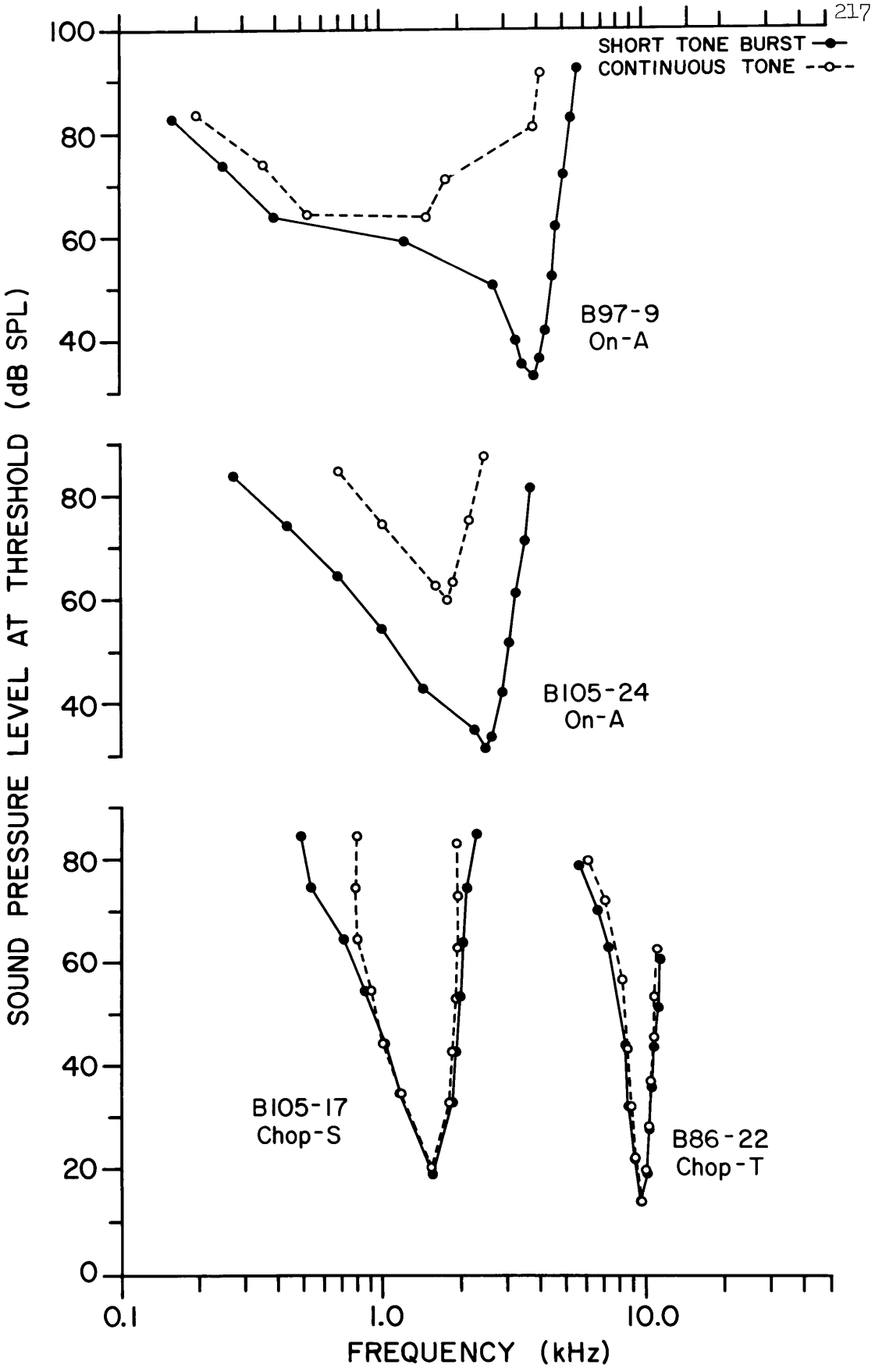
SHORT TONE BURST
CONTINUOUS TONE
B97-9
On-A
B105-24
On-A
B105-17
Chop-S
B86-22
Chop-T
SOUND PRESSURE LEVEL AT THRESHOLD (dB SPL)
FREQUENCY (kHz)
100
80
60
40
20
0
0.1
1.0
10.0

by about 20 dB (or more) to being within the range of the Chopper or Prepotential units.

One of the defining characteristics of the On-A and On-G units is that the continuous tone (CT) threshold at CF is significantly higher than the STBCF threshold. For a few On units, the thresholds to CT and STB were measured at frequencies other than CF. Figure IV-24 shows two such On units at the top and two Chopper units below for comparison. It is already known that the primary units have essentially equal thresholds for CT and STB (Kiang et al., 1965a). A similar observation was made for many of the PPO and PP1 units recorded in AVCN. The On units, B97-9 and B105-24 shown in Figure IV-24, however, exhibit different tuning for the STB and the CT stimuli. At frequencies below about 2 kHz, the On type units begin to develop a more sustained response (phase-locked) and corresponding to this change the CT threshold usually approaches the STB threshold (the STB response of unit B97-9 was shown in Figure IV-18 for two frequencies below CF.).

*7. Click Response

Some aspects of the unit responses to click stimulation appear to be related to the pp and response type categories. The lowest effective click level (i.e. click threshold), the shape of the PST histogram of the responses and the minimum click latency all show correlations with the unit categories. When using extracellular recording, however, the study of click responses in the CN is restricted by the large evoked response that is recorded in most

regions. The evoked response can obscure all but the largest spikes at click levels more than about 20 dB above the thresholds of the more sensitive units. Subtraction of an averaged version of the gross response waveform was useful in recovering some of the marginal units but was not adequate for many others. Demonstrating the lack of response to click stimulation (at levels up to the maximum available) was also hampered by the evoked response.

In individual experiments it was observed that the click threshold was a function of the unit type. As a method of compensating for some of the inter-experimental variation, the click thresholds have been plotted with respect to the units' short tone burst threshold at CF. We thereby obtain a measure of the relative sensitivities to click and tone burst. Figure IV-25 shows the relative click thresholds for four groups of units. The data for the units in the three prepotential categories PP0,1 and 2 (upper plot) all appear to be indistinguishable, falling between 20 and 30 dB over the mid-frequencies. There is a peak near 10 kHz where the spectrum of the 100 μsec click has its first zero. The lower three plots provide a breakdown of the units that do not have a prepotential type of spike waveform. We note that the Chopper and On types exhibit opposite trends when compared to the Prepotential units (summarized by the dotted bands). An underlying correlate of what is revealed in Figure IV-25 is that although many On units have an elevated STBCF threshold (Figure IV-23), their thresholds to a rarefaction click are often closer to the AN thresholds. Conversely, although the Choppers may tend to have lower

Figure IV-25 Click threshold compared to STBCF threshold

Each plot shows the ratio of click threshold to STBCF threshold as a function of the CF of the unit. The ratio is based on the peak voltage delivered to the earphone to produce a just-detectable response to a 100 μsec rarefaction click (RC) and a 25 msec tone burst at CF (STBCF). The (PP3, "Other") plot contains the PP3 units which are not in a Chopper or On response type category. The dotted band in each plot is provided to assist the comparison of the Chopper and On units with the Prepotential units.

The complete, standard symbol set is given on the right.

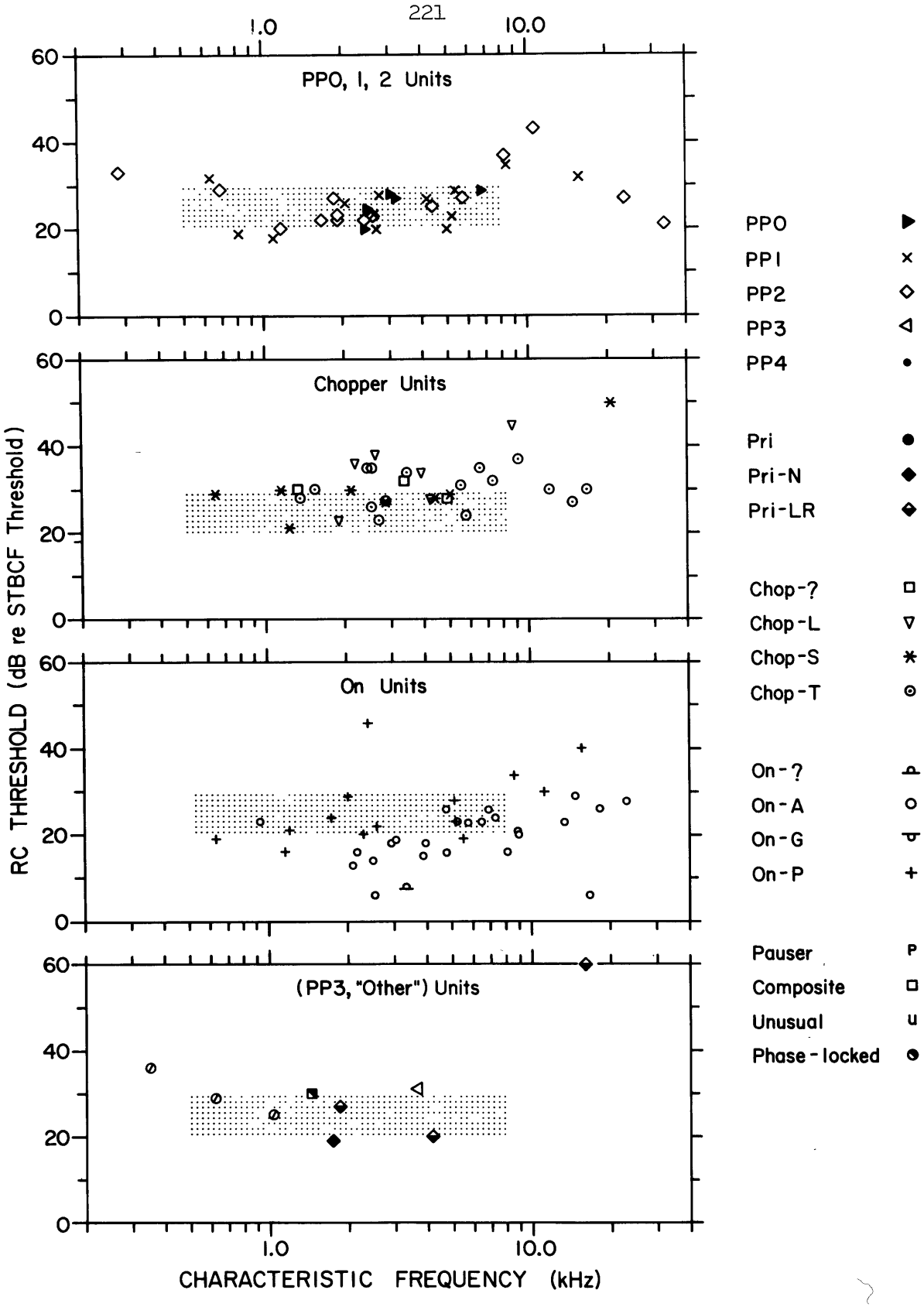
1.0
10.0
PPO, 1, 2 Units
Chopper Units
On Units
(PP3, "Other") Units
RC THRESHOLD (dB re STBCF Threshold)
CHARACTERISTIC FREQUENCY (kHz)
0
20
40
60
PPO
PP1
PP2
PP3
PP4
Pri
Pri-N
Pri-LR
Chop-?
Chop-L
Chop-S
Chop-T
On-?
On-A
On-G
On-P
Pauser
Composite
Unusual
Phase-locked

STBCF thresholds their click thresholds tend to be higher than those of primary units.

The responses of most units change systematically with click level. The form of the response and the type of changes that occur are related to the CF of the unit and the unit type. Units with a CF below about 800 Hz tend to have click responses for which the PST histograms have multiple peaks at intervals of approximately 1/CF and are essentially indistinguishable from those of AN units. In the 1 to 3 kHz range the Prepotential units have a group of peaks spaced at 1/CF. Sometimes the interpeak time after a large peak is a multiple of the basic 1/CF interval, presumably due to refractoriness during the 0.5 to 0.8 msec gap in the PST histogram. The PP2 units, more often than the PP0 or PP1 units, have a PST histogram which has an initial peak with an area close to the number of click presentations (near 1 if normalized). After this peak there is a gap of 0.5 to 0.8 msec followed by a group of very small peaks at an interval of 1/CF. The PP3 units, in contrast, seldom have a complex of CF related peaks, but have 1, 2 or 3 peaks separated by 1.1 to 2 msec. The second and third peaks generally represent second and third spikes in the individual responses to the click. The interval usually shortens with increasing click intensity and increased probability of occurrence of these later spikes. It would seem that additional peaks in multi-peaked PST histograms of the click response of PP3 units represent a repetitive discharge to the input from the AN rather than a faithful representation of the nerve response which would show 1/CF interpeak times. When the CF

is above 5 kHz, the Prepotential units tend to have only 1 peak in the PST histogram as do AN units, whereas PP3 units are about equally divided between 1 and 2 peaks, with a few having 3. The Chop-L units were found to have only 1 spike in response to a click. This behaviour may be the result of the long interval between discharges generally exhibited by these units.

Whenever possible the latency of response to a rarefaction click was followed as a function of click level. Over the first 10 to 20 dB above threshold the latency was generally observed to decrease relatively more than for further increases in level. A "minimum" click latency was assigned to a unit when the latency appeared to be changing less than 0.1 msec for a 10 dB increase in click level. The click level at which the "minimum" latency was obtained was usually at -40 to -20 dB re the maximum click level (i.e., at a click level about 50 dB above VDL). Click latency was measured to the mode of the first discernable peak in the PST histogram of the response to a click presented at 10/sec. In some cases in which there was little or no spontaneous activity and the first spike in the click response occurred at a "constant" latency, the time could be estimated from the oscilloscope display. The plots of "minimum" latency, as shown in Figure IV-26, are organized according to the main unit categories. The latency of response from PP1 units is generally longer than that from PP0 units. According to the interpretation of the PP0 units, these represent action potentials recorded from primary structures and therefore should be about 0.5 msec earlier than the spikes from

Figure IV-26 Click latencies

The plots of latency versus CF represent the time of the earliest response of units to clicks about 20 to 40 dB above threshold. A click latency was assigned to a unit only if the latency versus click intensity relationship changed less than 0.1 to 0.2 msec over the final 10 dB of the intensity series. The circled points in the PPO,1 plot were triggered from the prepotential of PP1 units with a large prepotential and small second component. Approximate latency ranges for the high CF PP1 and PPO units are shown to the right of the data points. In the PP3 latency plot, the Chopper units are represented by solid symbols and the On units by closed symbols. There is one Chop-L unit with a latency of 7 msec.

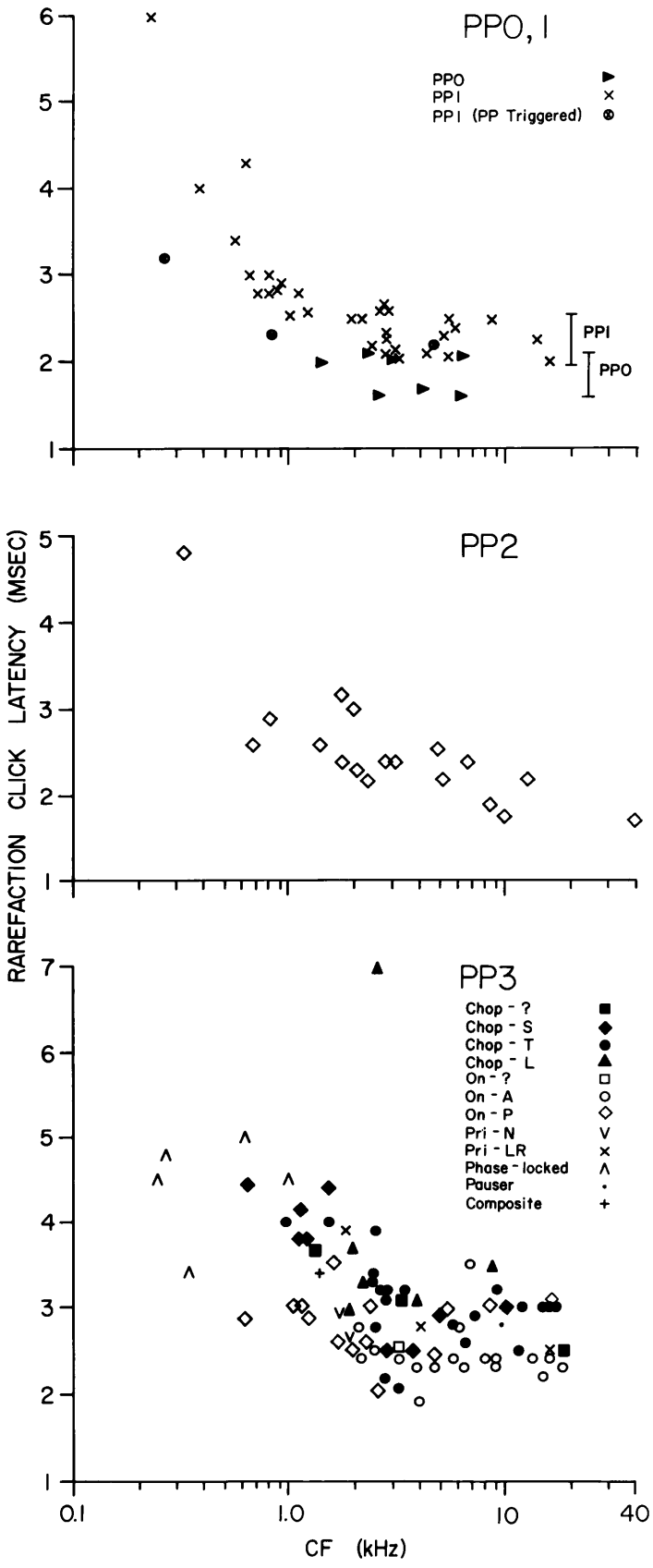
PP0, 1
PP0
PP1
PP1 (PP Triggered)
PP1
PP0
PP2
PP3
Chop - ?
Chop - S
Chop - T
Chop - L
On - ?
On - A
On - P
Pri - N
Pri - LR
Phase - locked
Pauser
Composite
RAREFACTION CLICK LATENCY (MSEC)
CF (kHz)
0.1
1.0
10
40

the CN cells. The three circled PP1 units were actually triggered from the positive prepotential of PP1 units because it was larger than the negative part. These units, therefore, should have a range of latencies similar to that of the PPO units. The PP2 units, in contrast to the PP1 units, have several examples with latencies near the lower edge of the PPO range. It should be noted that the particular PP2 units with the shortest click latencies were recorded in or close to PV (where the auditory nerve enters the CN) whereas the PP1 and the PPO units were recorded in rostral AVCN, mostly AA. This separation of up to 3 mm could represent several tenths of a millisecond of conduction time. The PP3 units exhibit a much greater range of latencies than shown by the PP1 or PP2 units. To a large extent the upper range of latencies for the PP3 units is occupied by Chopper types and the lower range by On types. The On units tend to have slightly longer latencies than the PP1 and 2 units, but with much overlap.

* 8. Steady State Discharges:
Spontaneous Activity and Continuous Tone Response

Both spontaneous discharges and responses to continuous tone stimulation were characterized in terms of the interspike interval statistics. As in the case of tone burst responses, a strong phase-locked component produced by low frequency tones can dominate the interval histogram of a continuous tone response to the point that these units sometimes have to be excluded from the same analysis applied to other units. The period histogram is used to assess the time-varying component introduced by low frequency tonal stimuli.

* 8.1 Spontaneous rate

"Spontaneous activity" is often defined as those discharges that occur when no controlled acoustic stimuli are being delivered to the animal. However, background noise including sounds generated by the animal are difficult to control and can contaminate the "true" spontaneous activity which is internally generated. Several experiments were excluded from the pool of data for spontaneous activity because of known or suspected acoustic contamination.

The average rate of discharge over a 30 or 60 second period was measured for most units. Within each unit category a range of spontaneous rates was found. The ranges, in general, overlap but the detailed distributions are markedly distinct for many categories. Figure IV-27 shows the spontaneous rate distributions and plots of spontaneous rate versus CF arranged according to the prepotential categories.

From the rate distributions we see that PP0 units seem to have low spontaneous rates more often than do PP1 units. Approximately 50% of the PP0 units have rates below 5 spikes/sec whereas only about 10% of the PP1 units have rates below 5 spikes/sec. The PP2 units also show a propensity for lower rates of spontaneous discharge in comparison with the PP1 distribution. The number below 5 spikes/sec is about 30% and the form of the distribution is quite distinct from that of PP1 units since it lacks the peak around 60-75 spikes/sec. More than 70% of the units without a prepotential (PP3) have spontaneous rates less than or equal to 1 spike/sec. The On units are represented entirely by the first bin, most On

Figure IV-27 Spontaneous rate distributions by prepotential category

The data for each of four categories of units are represented by a plot of spontaneous rate versus CF and a histogram of the rate distribution. Only data from experiments with a VDL of -70 dB or better were used. The histogram bin width is 2.5 spikes/sec. The PP3 units with low spontaneous rates are further analyzed in Table IV-4.

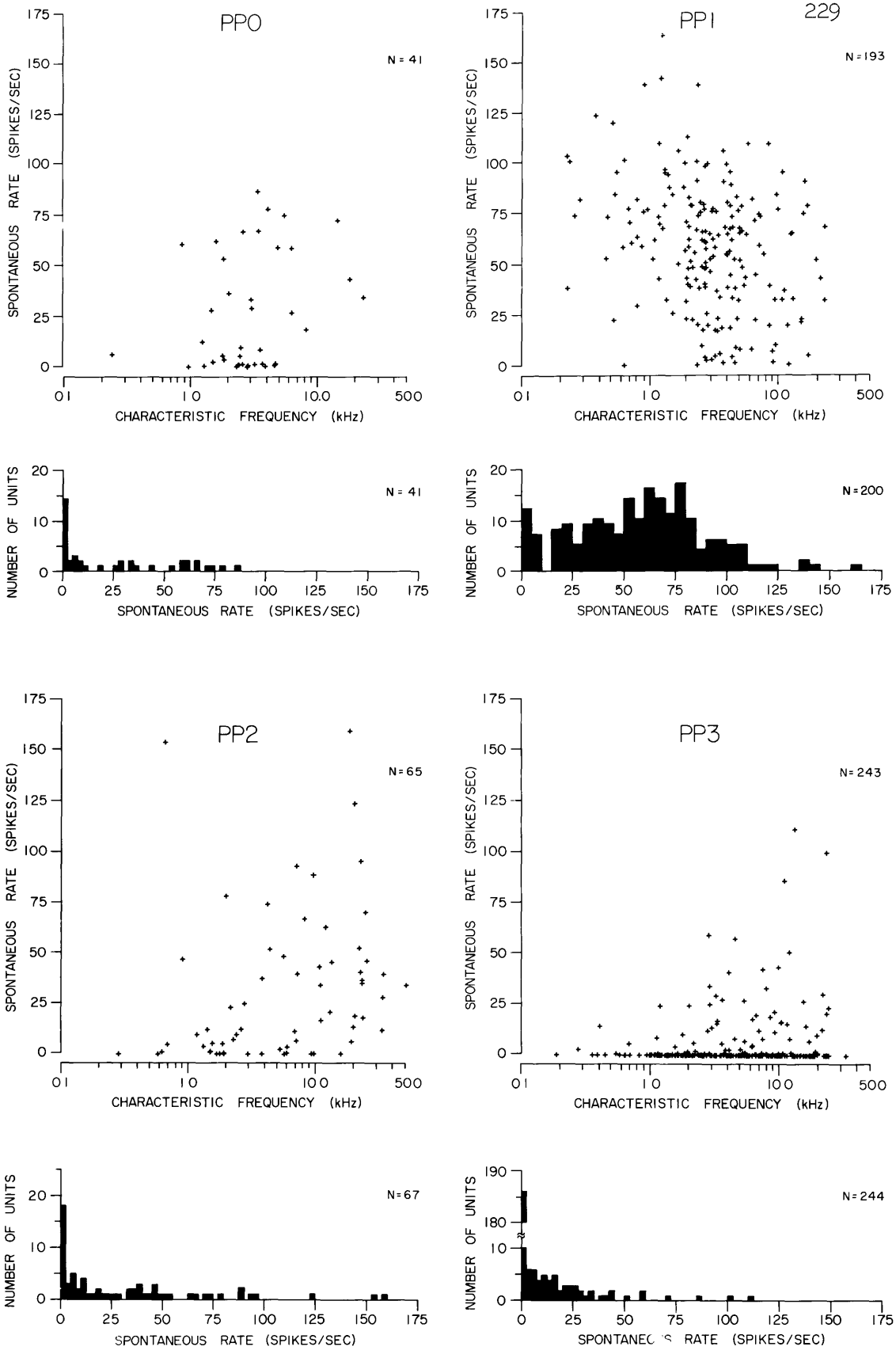
PP0
N = 41
SPONTANEOUS RATE (SPIKES/SEC)
CHARACTERISTIC FREQUENCY (kHz)
NUMBER OF UNITS
SPONTANEOUS RATE (SPIKES/SEC)
PP1
N = 193
N = 200
PP2
N = 65
N = 67
PP3
N = 243
N = 244

Table IV-4 Percentages of units with low spontaneous rates

	Percentage of units with spontaneous rate		Number of units
	≤ .1 spikes/sec	≤ 1 spike/sec	
Pri	4	4	75
Pri-N	4	11	53
Pri-LR	63	75	8
Chop-?	82	91	11
Chop-L	43	57	21
Chop-S	49	60	47
Chop-T	53	66	62
On-?	88	100	8
On-A	97	100	34
On-G	100	100	2
On-P	79	97	29
PP0	7	22	41
PP1	1	2	201
PP2	18	23	62
PP3	59	72	246

units having less than one or two "spontaneous" discharges in 15 to 30 seconds. The highest spontaneous rate found for any unit in the On group was 2.4 spikes/sec. This unit was in the On-P category as were most other On units with spontaneous activity. It is the Chopper units that provide most of the spontaneous rates above 1 spike/sec in the PP3 group. The distribution appears to be unimodal, with the mode near zero spikes/sec.

In order to examine the contributions of various Chopper units to the spontaneous rate distribution the data are replotted in Figure IV-28. The Chop-S and Chop-T units appear to have a similar distribution of rates. The Chop-L units may also be similar.

The units in the posterior cochlear nucleus have spontaneous rates for which the maximum rate at any given CF is an increasing function of CF (Kiang, 1976). The positive prepotential units of rostral AVCN, however, were found to have a distribution of rates which resembles that of the auditory nerve in its independence of CF (Kiang et al., 1965a). It appears from Figure IV-27 that the spontaneous activity of the PPO and PP1 units does not depend on CF. The spontaneous activities of the On units are all low regardless of CF. Focussing on the Choppers, we can see from Figure IV-28 that the maximum spontaneous rates seem to increase with the CF of the units. The evidence is sparse since elimination of the 3 units with the highest rates would change the distribution to one which appeared uniform with CF. It is the units with CF's below 1 kHz that are particularly crucial to demonstrating the trend with CF. Units with a CF below 1 kHz are difficult to identify as Choppers

Figure IV-28 Spontaneous rate for the Chopper units

The upper plot shows spontaneous rate as a function of CF for all units assigned to the Chopper group. The key in the upper left lists the symbols and number of data points for each category. The lower plot shows the distribution of rates for each of the Chopper categories. The bin width is 2.5 spikes/sec.

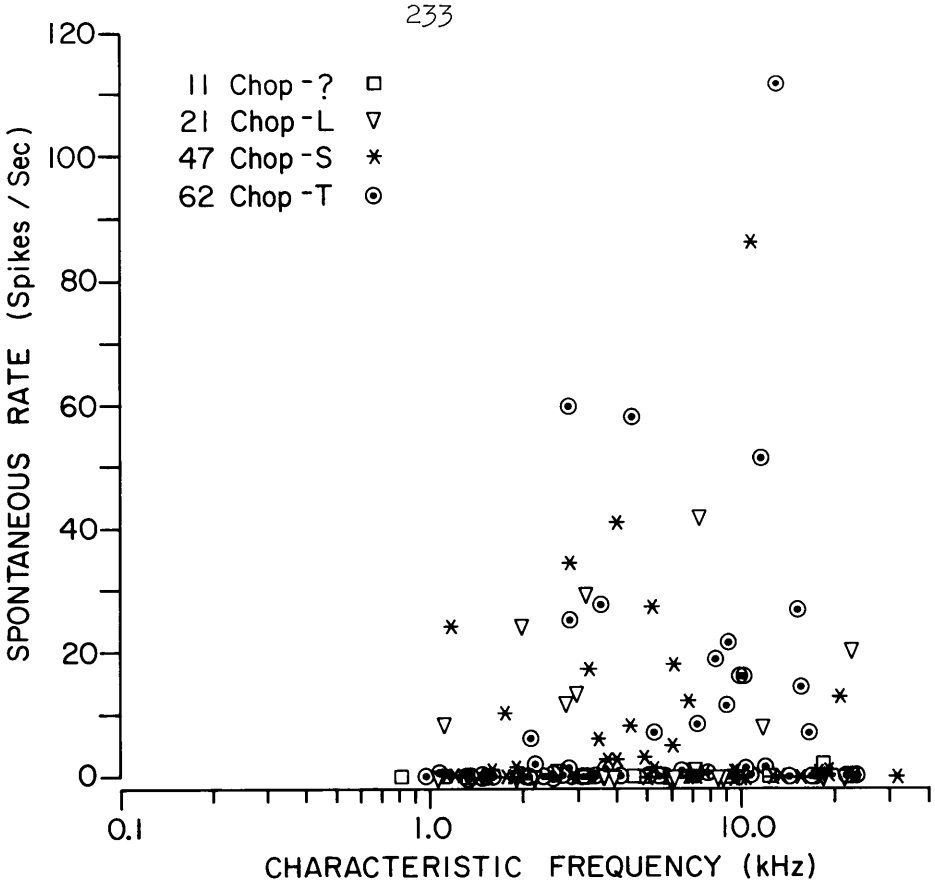
11 Chop-?
21 Chop-L
47 Chop-S
62 Chop-T
SPONTANEOUS RATE (Spikes / Sec)
120
100
80
60
40
20
0
0.1
1.0
10.0
CHARACTERISTIC FREQUENCY (kHz)

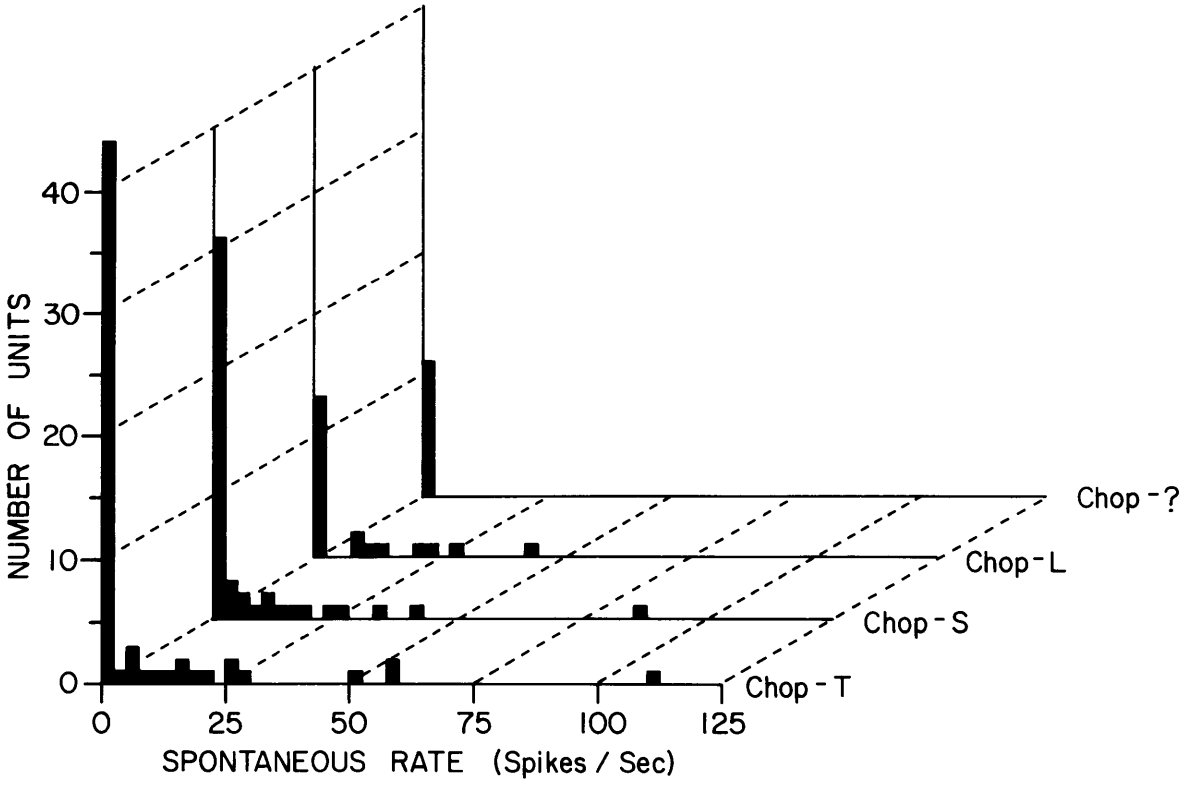
NUMBER OF UNITS
40
30
20
10
0
0
25
50
75
100
125
SPONTANEOUS RATE (Spikes / Sec)
Chop-?
Chop-L
Chop-S
Chop-T

because of phase-locking. Without a non-primarylike response pattern, a PP3 unit could always be a unit with a very small prepotential. The PP2 units, however, also appear to have a similar CF dependence for the maximal spontaneous rate. The only exception in the present data is unit B100-27 with a CF of 0.66 kHz. This unit was recorded in the rostral part of the AVCN whereas most of the PP2 units were located in caudal AVCN.

* 8.2 CTCF rate functions

The discharge rate versus level functions for CTCF stimulation ("rate functions") were determined for some of the well-isolated units. With most units, the "threshold" of the rate function is comparable to its STBCF threshold, but as is shown in Figure IV-7, can be elevated by as much as 80 dB for the On-A and On-G units. The rate generally increases rapidly for the first 20 to 40 dB above "threshold" then either remains approximately constant or decreases for further increases in level. For some On units, however, the rate was still increasing uniformly at 60 to 80 dB above the "threshold". A similar behaviour has been observed for some On-L units in the octopus cell region of the PVCN (Godfrey et al., 1975a).

Sample rate functions are shown in Figure IV-29 for units in the PP1 and PP2 categories, as well as the main components of the PP3 category, the Chopper and On groups. The data in these plots have been checked against the partial data obtained for other members of each category.

Attention is drawn to the large range of slopes and maxima exhibited by the various curves in each plot. The rate functions of PP1 units resemble those of AN units. Corresponding to the large range of spontaneous rates commonly found for PP1 units, the curves appear to be shifted vertically. The change in rate from spontaneous to the maximum is generally in the range of 30 to 100 spikes/sec. The PP2 units, however, appear to have more variety in the shapes of the rate functions including a more pronounced non-monotonicity for some units. The sample of PP2 units was taken from those localized to the posterior division, that is, subdivisions PD and PV of Brawer et al. (1974), in order to exclude the small number of PP2 units found in the anterior division which appear to have rate functions more like those of the PP1 units. The Chop-S units, in contrast to all other unit categories, generally have much steeper slopes, and large changes in discharge rate. The spontaneous rates of Chop-S units are usually low as are those of the other PP3 units. Most of the curves for the Chop-S units lie above those of the Chop-T units. A line from the origin to 100 spikes/sec at 20 dB approximately segregates the rate functions of these two Chopper categories. The generally lower rates of the Chop-T units may be related to the rate decrease during the STBCF response of the Chop-T units. The little data available on Chop-L units were included for completeness. The curves for the On units are, as expected, below those of almost all other units. Most of the On-A units lie along the baseline with only a few rising above

Figure IV-29 CTCF rate functions

Discharge rate is plotted as a function of the continuous tone level re the STBCF threshold. Each plot represents a particular group of units. The PP2 unit plot includes data from only those PP2 units localized to the posterior division (PD and PV). The PP3 units are represented by the major non-primary-like response type categories. Each data point was based on at least a 30 second sample. The spontaneous rates are shown at the vertical scale and are connected to the point at the lowest tone level. All plots have the same vertical scale.

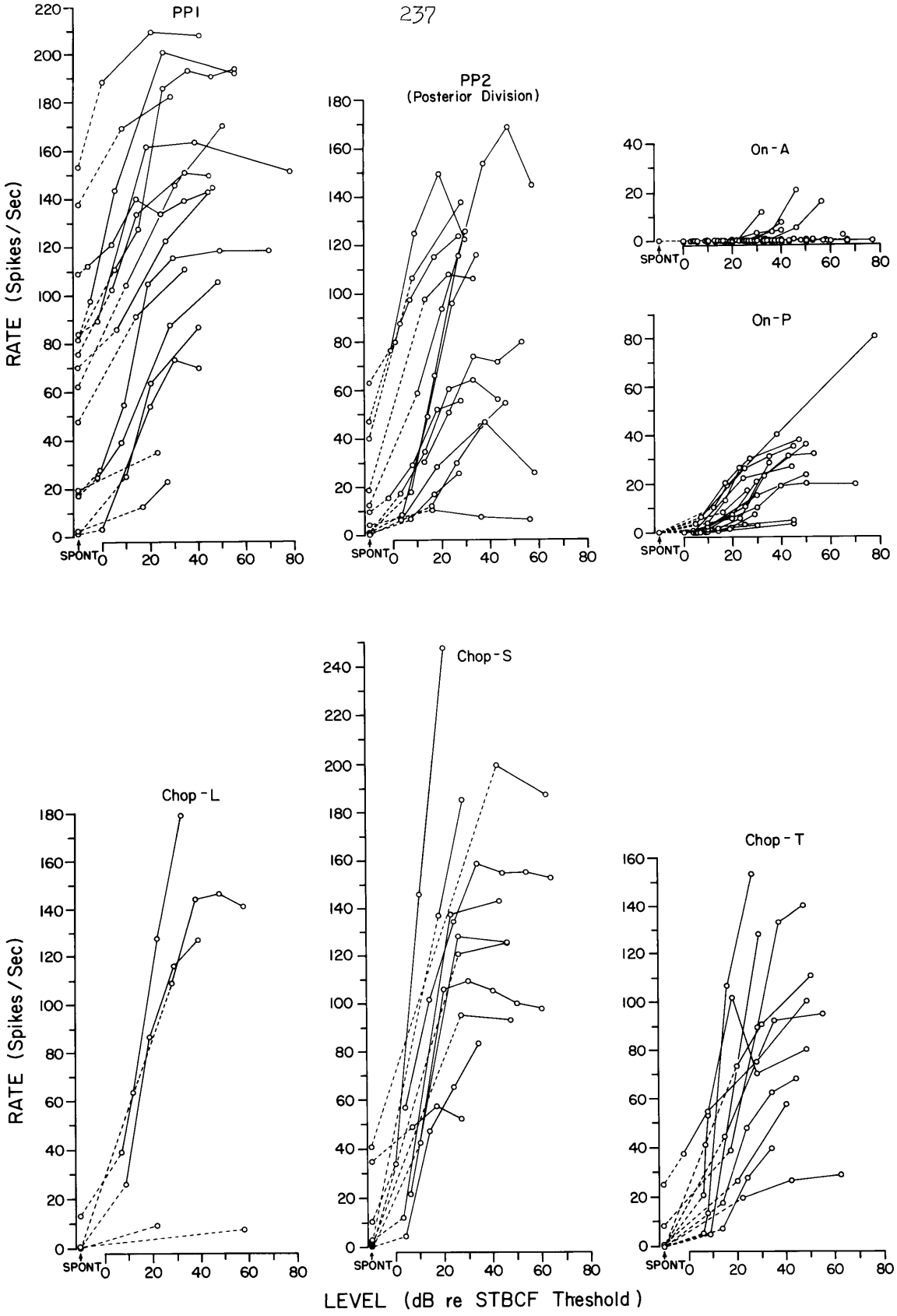
PP1
PP2
(Posterior Division)
On-A
On-P
Chop-L
Chop-S
Chop-T
RATE (Spikes/Sec)
LEVEL (dB re STBCF Threshold)
SPONT

1 spike/sec. The slopes for the On-P units are all below 1.2 spikes/sec/dB and the rates generally saturate at 10 to 40 spikes/sec.

* 8.3 Interval histogram shape

When the spontaneous or continuous tone driven rate of a unit was greater than about 5 spikes/sec, an interval histogram (IH) was usually computed. Correlations of the shape of the IH with other properties of the units have been reported in several studies of the CN (Pfeiffer and Kiang, 1965; Goldberg and Brownell, 1973; Godfrey et al., 1975a,b) and the superior olivary complex (Guinan et al., 1972a). Similar observations were made for the present data, and will be discussed in order to show how the IH shape is related to the unit categories developed in this study. Each IH was characterized by four measures of the shape whenever the sample size was adequate. In order of increasing minimum sample size required, the measures were: (1) mean interval (or its inverse, average rate), (2) mode, (3) width at 1 decade below the height at the mode and (4) the shape of the histogram beyond the mode (the "decay"). The first three parameters will be considered together because it is in a three-dimensional space defined by these parameters that certain shape variations can be demonstrated. Two two-dimensional projections of this space will be used to illustrate the relationship of these measures to the unit categories.

Figure IV-30 shows plots of Mode-versus-Rate and Mode-versus-Width for three groups of IH's. The line (mode x rate) = 1, shown as a solid line, represents equality of the mode and the mean inter-

val, a condition which is approached as the IH becomes more symmetric. The IH's of the spontaneous activity of most AVCN units have modes that are much smaller than the mean interspike interval. The dashed lines in the Mode-versus-Rate plots represent a less symmetric condition which was included to assist comparison of the plots. For the Mode-versus-Width plots there are no theoretical bounds on the location of the data points, but it is in this plot that the irregular ("Poisson") and regular ("Gaussian") IH shapes defined for the SOC data in Guinan et al. (1972a) segregated most distinctly. The partitioning of the (mode, width) plane shown on the plots as a dotted line is consistent with the separation that exists in data from the superior olivary complex. This partitioning is included here to contrast the upper left ("Gaussian") versus lower right ("Poisson") quadrants. These two regions correspond approximately to the upper right versus lower left on the Mode-versus-Rate plots.

We can now make some observations regarding the three groups of data shown in Figure IV-30. The upper pair of plots is based on the IH's of the spontaneous activity of PPO, PP1, and PP2 units. This plot is included here mainly for comparison with that of the PP3 units represented in the lower plots. Note that all points in the Prepotential unit plots lie below the dotted lines. As with AN data, the Prepotential units of AVCN have a mode around 8 to 10 msec for the very low rates and asymptotically approach 1 to 2 msec for high rates.

The PP3 units are, however, much more varied. For PP3 units with spontaneous activity above 5 to 10 spikes/sec, there are two

Figure IV-30 Indices of the shapes of interval histograms

The shapes of three groups of interval histograms (IH) are considered separately in this figure: (1) spontaneous activity of the units with a pp (PP0, PP1 and PP2), (2) spontaneous activity of the units without a pp (PP3) and (3) the CTCF driven activity of the PP3 units. The measurements taken, whenever possible, from each IH were: (a) average rate, (b) mode of the IH, and (c) width of the IH at the bin height equal to one-tenth of the average bin contents around the mode.

The left-hand column contains plots of mode versus rate and the right-hand column contains plots of mode versus width. The modes and widths are given to the nearest 1 or 0.5 msec. The symbols used in this figure come from the standard set (see Figure IV-25) except that PP3 units which were not assigned to a response type category are represented by an additional dot within the left-pointing triangles. The solid line in the mode versus rate plots represents equality of the mode and mean interval (mode x rate = 1). The dashed line on the mode versus rate plots was drawn to emphasize the tendency of the Chop-L (downward triangles) and Pauser (P) type units to have IH's with (mode x rate) close to unity. The dashed line in the mode versus width plots was drawn to match the separation between the "Gaussian" and "Poisson" units of Guinan et al. (1972a).

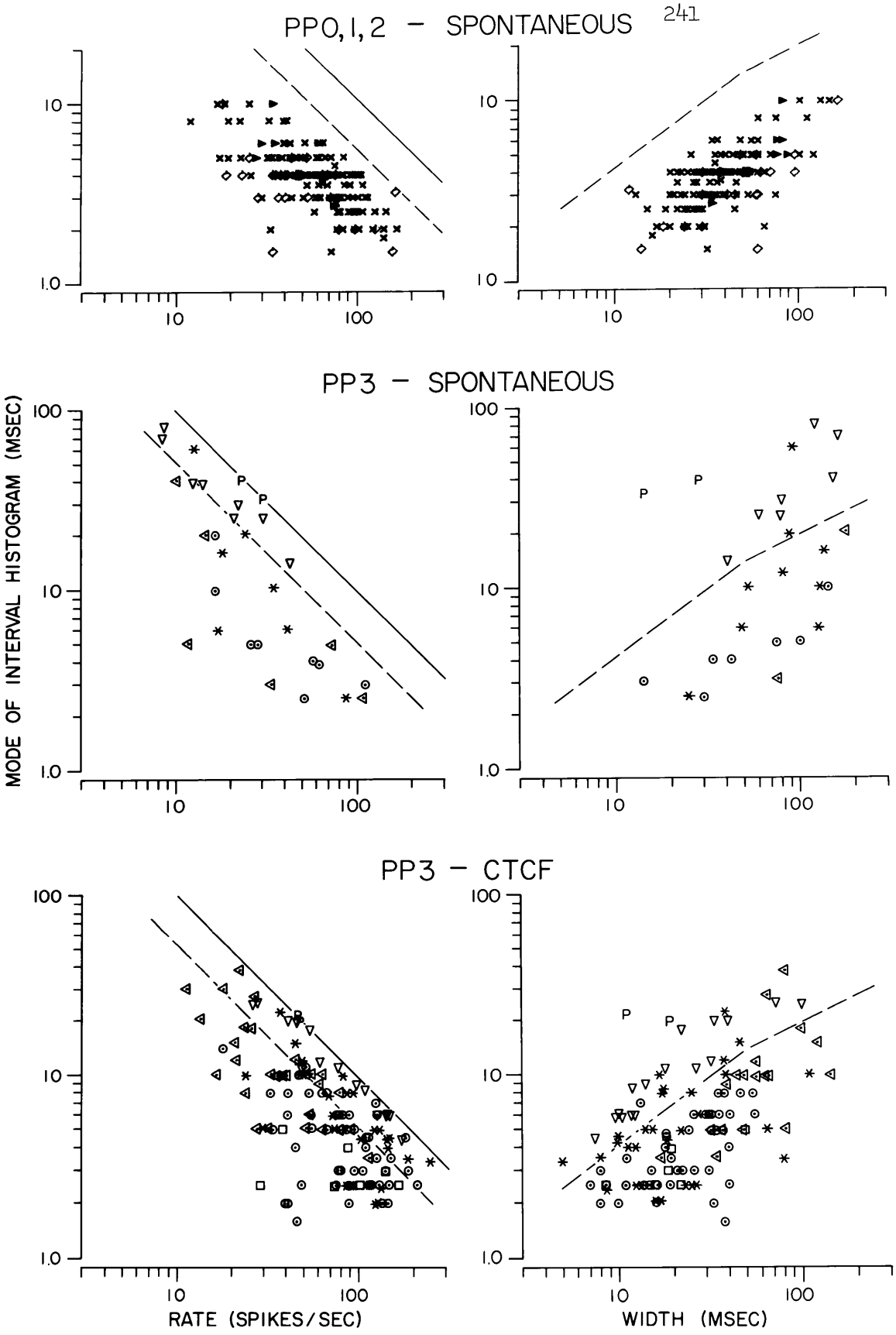
PP0, 1, 2 – SPONTANEOUS
PP3 – SPONTANEOUS
PP3 – CTCF
MODE OF INTERVAL HISTOGRAM (MSEC)
RATE (SPIKES/SEC)
WIDTH (MSEC)
100
10
1.0
P

response types that are never found below the dotted lines. The two Pauser units which had highly symmetric IH's serve as reference points on the plots. Between the Pausers and the dotted lines are found all of the Chop-L units. The one Chop-S unit above the dotted lines was very close to being categorized as Chop-L. Thus for spontaneous activity the (mode, width, rate) space appears to subdivide into three zones: "Poisson" region with Prepotential units as well as most Chop-S and Chop-T units; an intermediate region with Chop-L units; and a highly symmetric region with the Pausers.

The two plots at the bottom of Figure IV-30 show similar data for CTCF responses of the PP3 units. As was true for spontaneous activity, the Pauser and Chop-L points are located entirely above the dotted lines. As the discharge rate increases with increasing stimulus level, the points for each "Gaussian" unit follow a trajectory parallel to the dotted lines; that is, the IH's would be almost identical if normalized by the rate (Pfeiffer and Kiang, 1965). For the other types of Choppers and the Prepotential units, the mode changes less than the rate so that the "rate-normalized" mode (mode x rate) increases with increasing discharge rate. These units, therefore, move closer to the dotted line in the mode versus rate plots as the CTCF level is increased. The trajectory for many PP3 units crosses the dotted line. Those of the Prepotential units that cross, do so only in the lower part of the plots.

Another aspect of the IH shape is the decay from the mode. Since the decay of the IH's of most AVCN units is close to exponen-

tial, the histograms were displayed with a logarithmic vertical scale. Pfeiffer and Kiang (1965) found it useful to distinguish three categories for the shape of the decay:

(i) straight, Exponential (E)

(ii) convex up, Faster-than-Exponential (FE), or

(iii) concave up, Slower-than-Exponential (SE).

A slight rounding at the mode was not considered to be convex up; rather the histogram had to display a definite curvature over a decade or more change in bin height. Figure IV–31 shows examples of IH's from each of these categories along with the associated hazard functions.

The hazard function, defined in the caption of Figure IV-31, is a constant, greater than zero for a true exponential decay. Corresponding to the initial portion of an IH (up to the mode) there is an increase in the hazard function, but from the point at which the IH has an exponential decay the hazard function will be constant for all longer intervals. An IH with a "true" faster-than-exponential decay should rise monotonically beyond the mode. If a constant value is attained the decay would of course be exponential from that point. Similarly, a "true" slower-than-exponential should decrease monotonically for all intervals more than a small increase beyond the mode. From Figure IV-31 we see that for the IH's that are beyond the mode, the hazard functions are essentially constant and for the IH's that are FE, the hazard function has a positive slope beyond the mode. When the mode is short (less than about 20 msec) there is a distinct slope change at the mode, whereas

Figure IV-31 Interval histogram decay shapes

The three columns represent the categories: Slower-than-Exponential (SE), Exponential (E) and Faster-than-Exponential (FE). For each histogram a hazard function was computed, smoothed and normalized to probability P at the mode of the histogram (dashed line). The hazard function, obtained by dividing the contents of each bin by the contents of that bin plus all subsequent bins, provides a measure of the probability of discharge during the time span of the bin, given that the unit has not discharged up to that interval (bin). The upper two histograms in each column are considered to be typical examples of the categories. The lower histograms are less typical. B98-24 (SE) exhibits a rapid transition from a Slower-than-Exponential curvature (decrease in the hazard function) to a straight exponential decay. Both B86-20 (E) and B84-28 (FE) are examples of long mode histograms. With each histogram is given the unit number, whether the activity was spontaneous or driven and the total number of spike triggers in the histogram.

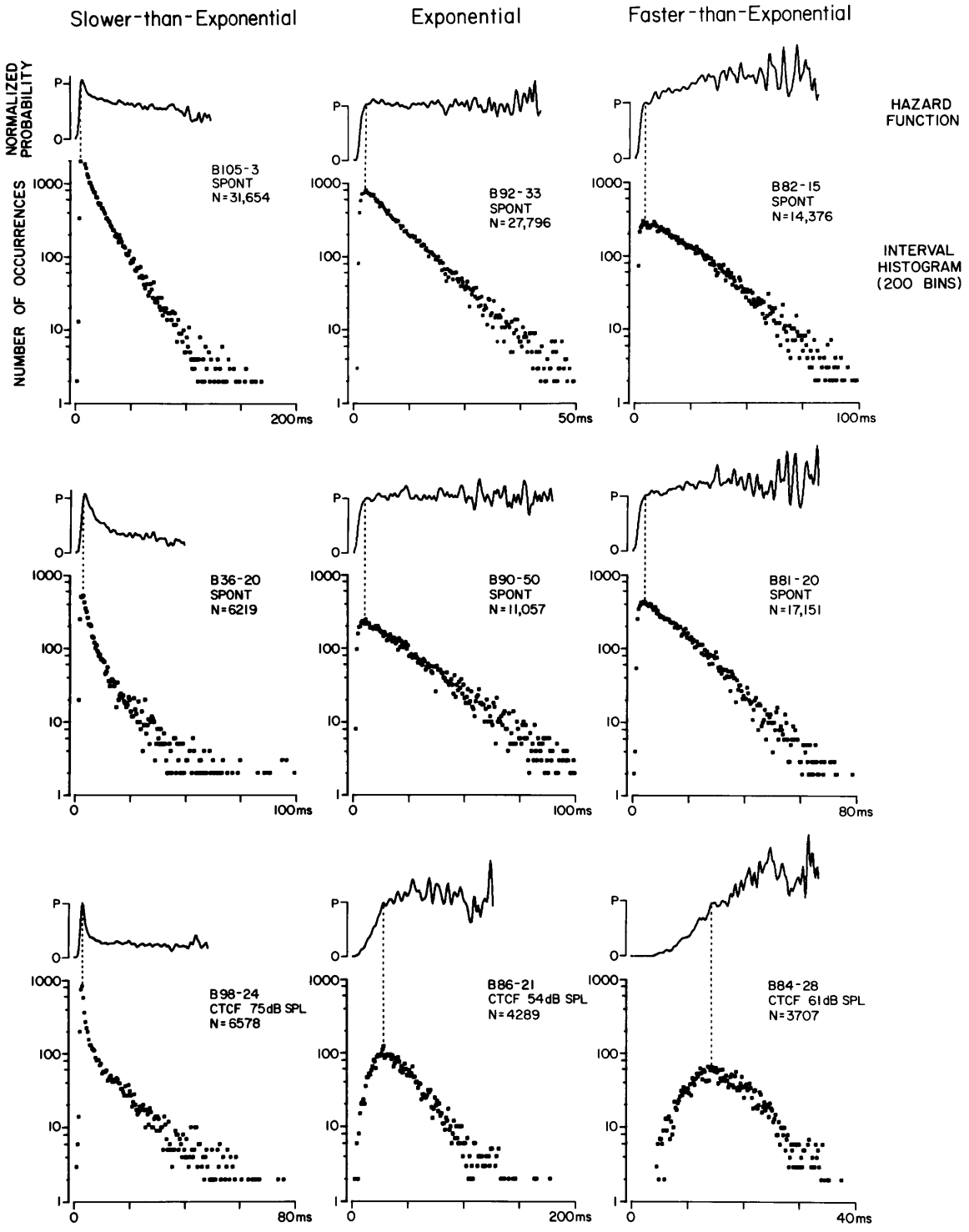
Slower-than-Exponential
Exponential
Faster-than-Exponential
NORMALIZED PROBABILITY
NUMBER OF OCCURRENCES
HAZARD FUNCTION
INTERVAL HISTOGRAM (200 BINS)
B105-3
SPONT
N=31,654
200ms
B92-33
SPONT
N=27,796
50ms
B82-15
SPONT
N=14,376
100ms
B36-20
SPONT
N=6219
100ms
B90-50
SPONT
N=11,057
100ms
B81-20
SPONT
N=17,151
80ms
B98-24
CTCF 75dB SPL
N=6578
80ms
B86-21
CTCF 54dB SPL
N=4289
200ms
B84-28
CTCF 61dB SPL
N=3707
40ms

when the mode is long, the IH's with FE decay show only a small slope change at the mode. The IH's that are SE have a peaked hazard function with a distinct decrease beyond the mode.

Some of the IH's classified as FE or SE appeared to have an exponential decay after the first 1 or 2 decades down from the mode. The small number of intervals usually represented in this range prevents a definite conclusion for most units. A few units did, however, exhibit a transition close enough to the mode so that the available data were adequate to show that the hazard function was essentially constant; the histogram of unit B98-24 is one of the clearer examples.

For many of the units, the discrimination of the three decay shapes was difficult. A straight line fit to the part of the IH beyond the mode (by a least-mean-square-error criterion) often helped to discriminate a deviation from linearity. Hazard functions were also used in some cases. When examined as a function of increasing CTCF level, the decay shape of some units changed, moving, generally to the right in Figure IV-31. For the majority of units, however, the decay was of one form at most levels more than about 20 dB above threshold; the unit was then assigned to a decay shape category.

Table IV-5 summarizes the shape of decay for spontaneous and CTCF driven activity. The upper part of the table shows a breakdown by prepotential category and the lower by the relevant response type categories. The two Pauser units (not included) had symmetric IH's with an FE decay and all but one of the Composite

Table IV-5 Decay from mode of IH

	Spontaneous activity			CTCF driven activity		
	SE	E	FE	SE	E	FE
PP0		1	13		1	3
PP1		62	80		5	26
PP2	1	24	4	1	15	2
PP3	6	27	3	6	34	24
Pri-N	2	18	10	2	8	5
Chop-L		7	1		2	3
Chop-S		8			8	7
Chop-T	4	4		5	12	6

units, like the On units, had no spontaneous activity and very low rates of response. From Table IV-5 it can be seen that only a small number of units was found to have an SE decay and that these units are in the Pri-N and Chop-T response type categories. Thus, the SE decay appears to provide another distinction between the Chop-S and Chop-T units. Two of the PP2 units that are in the E category for spontaneous activity had decays that were almost of the SE form but did not have sufficient curvature. In this regard, the PP2 units differ from the other units with a prepotential. The relative frequency of the FE decay for spontaneous activity progressively decreases down the categories in Table IV-5. Most of the PPO units, about half of the PP1 units and about 15% of the PP2 units are in the FE category. The three PP3 units with FE decay for spontaneous activity had a long mode, symmetric or "Gaussian" IH (one of which is the Chop-L unit shown below) instead of the short mode, FE IH found for the Primarylike units. The Chop-S and Chop-T categories have no members with spontaneous activity that have a FE IH.

The distribution of decay shapes for CTCF driven activity differs from that for spontaneous activity in one major way; the FE category is relatively larger in all categories except probably the PP2 and Pri-N. When the PP1 units were stimulated and the mean interval decreased, a curvature near the mode became relatively more important in determining the shape of the histogram. With the Choppers the combination of their relatively long modes and high rates of discharge to CTCF made the IH relatively symmetric which was generally correlated with an FE decay.

* 9. Low Frequency Tone: Synchrony

* 9.1 Continuous tone

Response to continuous tone was recorded for many of the single units encountered in AVCN. Whenever the frequency of the tone was less than 5 kHz, a period histogram was computed as a test for periodic components in the instantaneous rate of discharge of the unit. As described in Methods, Section 4.4.3, the magnitude and phase of the fundamental and second harmonic terms of a Fourier series representation of the period histogram were computed. From the fundamental coefficient is obtained a commonly used measure of synchrony, S, which has been called the "synchronization index" or "vector strength" (Goldberg and Brown, 1969; Anderson et al., 1971; Lavine, 1971; Goldberg and Brownell, 1973; Johnson, 1974). For each tone frequency, the objective was to examine the synchronization index as a function of stimulus level up to the level at which the synchronization index saturated. The data to be presented come mainly from units with a CF of less than 5 kHz. Units with higher CF were not generally studied with low frequency tonal stimuli because of the high stimulus levels required. At these high levels one frequently sees progressive damage to the cochlea, large gross responses recorded by the microelectrode and stimulation of units by higher harmonics in the acoustic stimulus. Other reasons for avoiding high levels of sound stimulation include subtle effects of gross responses or electrical cross-talk on the shape of the period histogram as discussed in Methods, Section 4.4.3. Special

Figure IV-32 Period histograms of the responses to a 2 kHz tone

Each column shows period histograms computed from responses to a continuous tone level series. At the top of each column is given the unit number, the prepotential and response type categories of the unit and the stimulus frequency. Just above each histogram is given the rms sound pressure level at the tympanic membrane in dB SPL. The horizontal scales represent one period of the stimulus (T) with zero phase corresponding to the positive-going zero-crossing of the oscillator voltage. The vertical scale is given in spikes/sec on the upper histogram of each column. B104-32 had a CF of 2.58 kHz; all other units in this figure were stimulated at CF. The histograms for B84-30 and B104-32 were derived from 30 sec samples of the response; all others were from 60 sec samples.

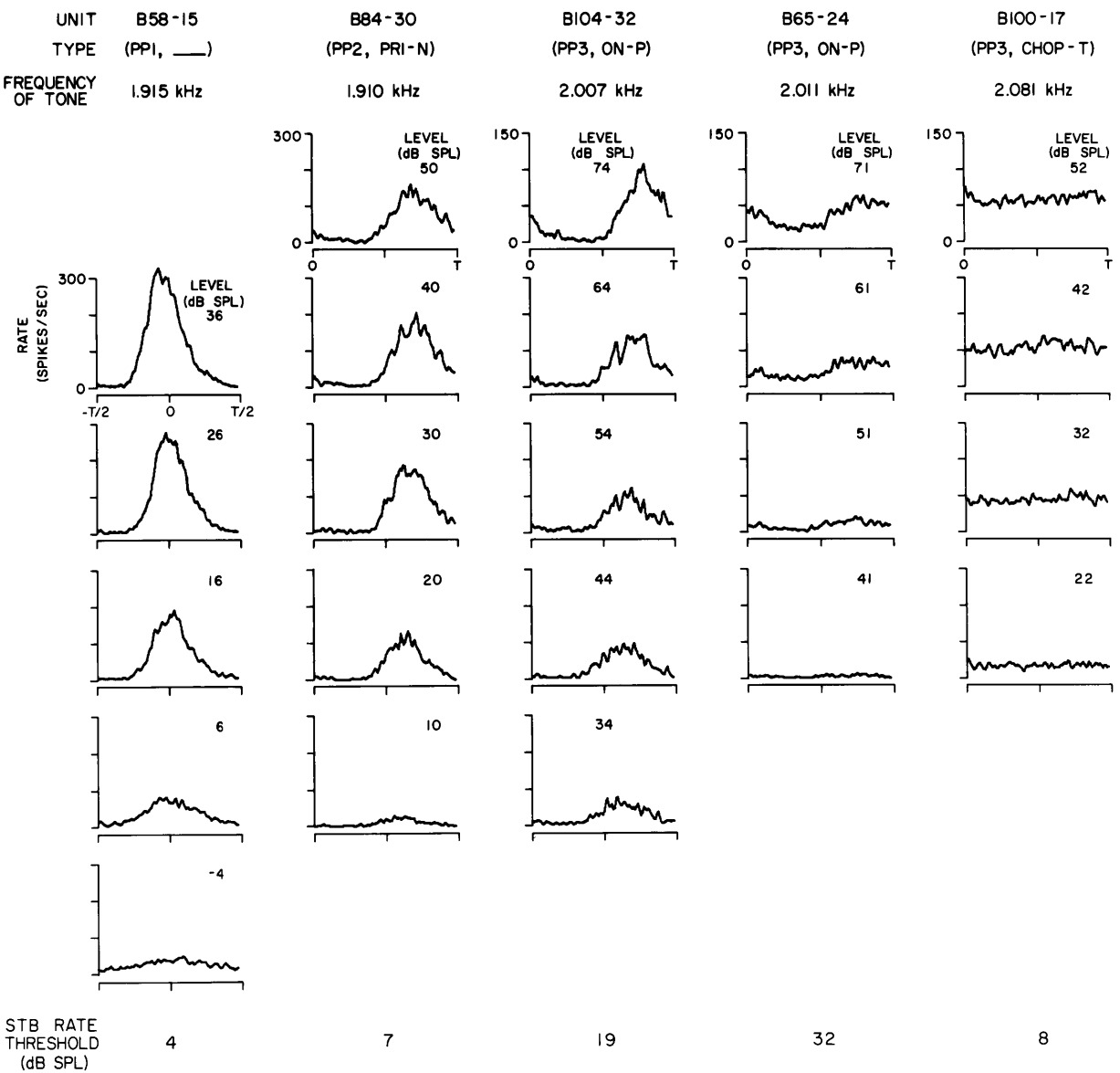
UNIT
TYPE
FREQUENCY OF TONE
B58-15
(PP1, ___)
1.915 kHz
B84-30
(PP2, PRI-N)
1.910 kHz
B104-32
(PP3, ON-P)
2.007 kHz
B65-24
(PP3, ON-P)
2.011 kHz
B100-17
(PP3, CHOP-T)
2.081 kHz
RATE (SPIKES/SEC)
300
0
-T/2
0
T/2
T
LEVEL (dB SPL)
36
26
16
6
-4
50
40
30
20
10
150
74
64
54
44
34
71
61
51
41
52
42
32
22
STB RATE THRESHOLD (dB SPL)
4
7
19
32
8

attention was paid to this problem in the experiments. Although most of the data on synchrony were taken at the CF of the unit, some were taken at frequencies below CF and a small amount at frequencies above CF. Since no trend with CF could be found, all data will be considered together. Tonal stimulation at frequencies below the CF must, however, be used routinely to study low frequency phase-locking of most units assigned to a response type category since the units in the AVCN cannot generally be categorized when the CF is less than 1 to 2 kHz.

As a tone was raised in level from below threshold to 30 to 40 dB above threshold, the shapes of the period histograms were observed to change in characteristic ways depending on the frequency of stimulation and the unit type. Example level series are shown in Figure IV-32 for a representative set of units each stimulated with a tone at approximately 2 kHz. Plots of the synchronization index computed from these histograms are shown in Figure IV-34. For all units with a clear prepotential (PP0 and PP1) and many with a variable or small prepotential (PP2), the form of the period histograms and the variation with level were consistent with AN data (e.g., Johnson, 1974). The synchrony begins to increase at 10 to 20 dB below the rate threshold, rises to a maximum, and either remains constant or, for low frequencies in particular, decreases. The decrease was always associated with a growing second harmonic component. The dynamic range was similar to AN starting at 10 or 20 dB below the rate threshold and extending to 10 to 30 dB above. For On units and some of the Pri-N units with very low spontaneous

rates, the synchrony measure is maximum at only a few dB above the rate threshold and decreases or remains approximately constant with increasing level. This decrease in the value of S was not associated with an increasing second harmonic component but is attributable to increases in the average discharge rate which were greater than the increases in the peak-peak modulation. The lower plots in Figure IV-34 have level plotted in dB SPL which emphasizes the relationship of the On type synchrony function for B65-24 to the Primarylike form. Although B65-24 has its maximum synchrony just above threshold, the stimulus level is actually so high that most Primarylike units with a similar CF have already reached their maximum synchrony.

Previous reports on the synchronization of discharges for units in the CN describe a large range of synchronization (e.g., Moushegian and Rupert, 1970a,b; Lavine, 1971; Goldberg and Brownell, 1973). Moushegian and Rupert classified units as "phase-lockers" and "non-phase-lockers" with an intermediate group of "quasi-phase-lockers". Any examination of synchrony, however, must take the frequency of the stimulus into account. The choice of a 2 kHz stimulating frequency for the units in Figure IV-32 was made to emphasize the differences between the unit types. The PP1 unit has spontaneous activity and exhibits a synchronized discharge below threshold (for an increase in discharge rate to STBCF). Most of the other unit types in the AVCN that do not have much spontaneous activity exhibit a synchronized response only for levels above the STBCF threshold. In the case of Choppers, the

Figure IV-33 Period histograms of the responses to an 800 Hz tone

The format is the same as in Figure IV-32. B105-21 had a CF of 646 Hz; the other two units were stimulated at CF. All of the histograms were computed from 30 sec data samples.

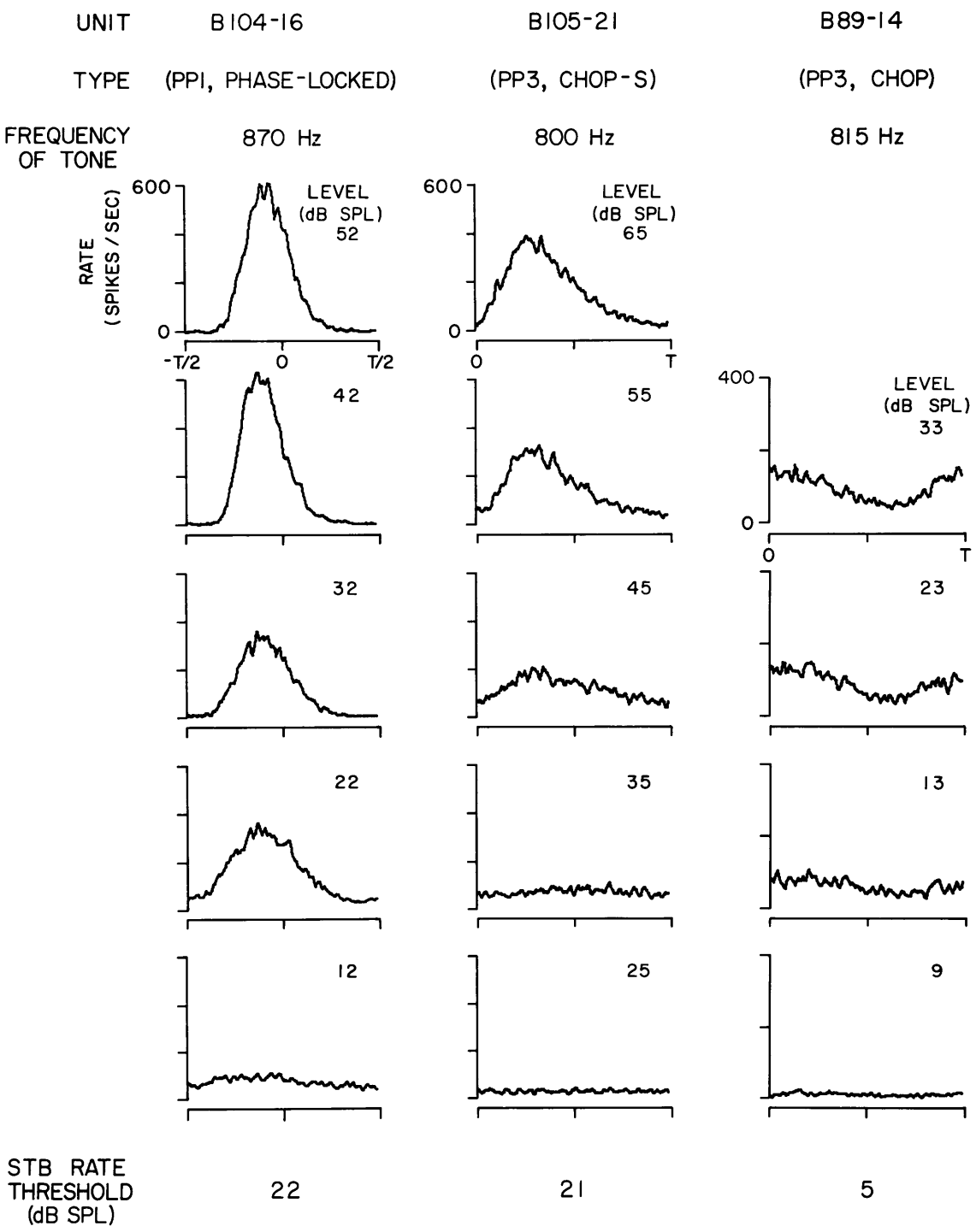
UNIT
B104-16
B105-21
B89-14
TYPE
(PPI, PHASE-LOCKED)
(PP3, CHOP-S)
(PP3, CHOP)
FREQUENCY OF TONE
870 Hz
800 Hz
815 Hz
RATE (SPIKES / SEC)
600
0
LEVEL (dB SPL)
52
42
32
22
12
-T/2
0
T/2
65
55
45
35
25
T
400
33
23
13
9
STB RATE THRESHOLD (dB SPL)
22
21
5

Figure IV-34 Discharge rate and synchronization index as a function of continuous tone level

Data points in the right-hand plots correspond to the period histograms in Figure IV-32. The left-hand plots are associated with Figure IV-33. The upper two plots of each column show the discharge rate in spikes/sec and the synchronization index plotted as functions of the tone level in dB re the STB threshold at the same frequency. The bottom two plots show synchronization index plotted as a function of the tone level in dB SPL.

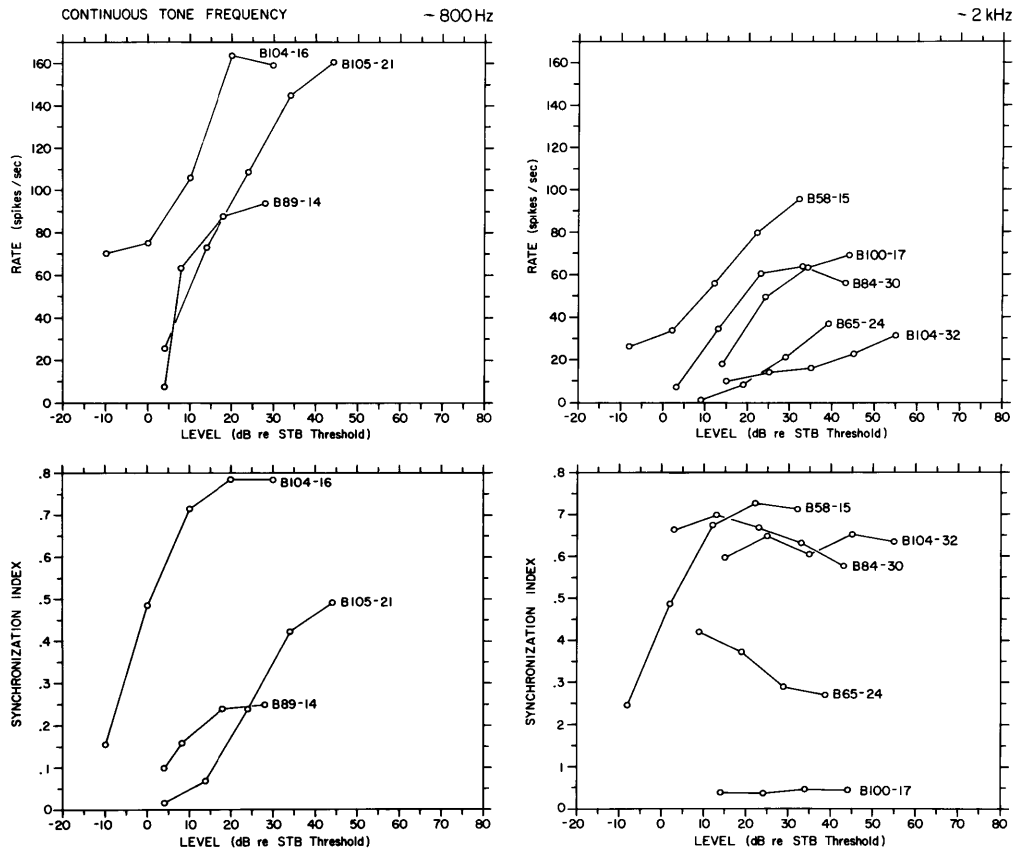
CONTINUOUS TONE FREQUENCY
~ 800 Hz
~ 2 kHz
RATE (spikes / sec)
SYNCHRONIZATION INDEX
LEVEL (dB re STB Threshold)
B104-16
B105-21
B89-14
B58-15
B100-17
B84-30
B65-24
B104-32

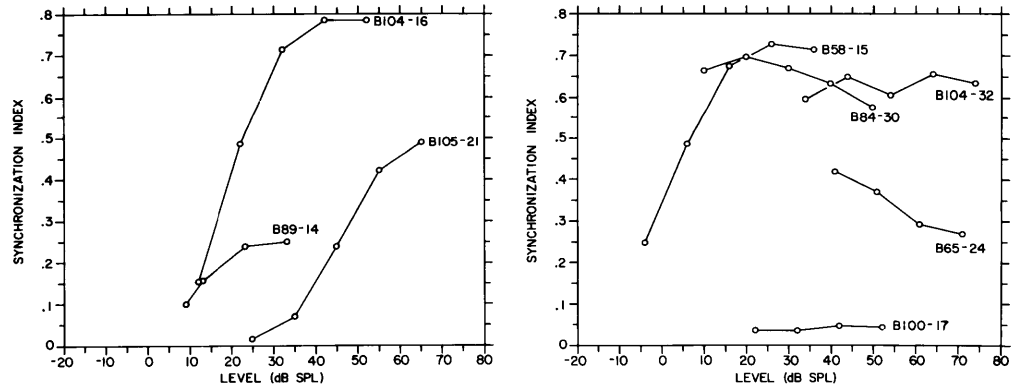
SYNCHRONIZATION INDEX
LEVEL (dB SPL)
B104-16
B105-21
B89-14
B58-15
B84-30
B104-32
B65-24
B100-17

synchronization index often increases only slowly with increasing stimulus level. The On units more closely resemble the PP1 units in terms of their maximum synchronization. Units B84-30 and B104-32 are examples that show how the Pri-N and On units (particularly the On-P units) have similar synchrony versus level behaviour.

When the stimulus frequency is below 800 Hz, the period histograms of most units in AVCN are largely indistinguishable from those of AN units. The units used in Figure IV-33 illustrate a comparison of a PP1 unit with two Chopper units. These Choppers represent the typical range of synchrony found for the Choppers at 800 Hz. The synchrony level functions are also shown in Figure IV-34.

In order to facilitate comparison of the dependence of synchrony on stimulating frequency for the different unit types, we shall use one parameter from the synchrony versus level functions, namely the maximum value of the synchronization index. For most PPO and PP1 units the form of the level dependence is highly stereotyped except for the occasional unit which exhibits "peak-splitting" (Johnson, 1974). The maximum value, therefore, provides a good characterization of the PPO and PP1 units. The other unit types are often similar to the Primarylike units (as shown in Figure IV-34). The level functions may, however, have a more extended dynamic range (some Choppers) or a very abrupt rise followed by a gradual decrease over a broad range (most On units and some PP2 units). A maximum S value (S_{max}) was assigned to a particular level series when there were at least two suprathreshold levels at which the synchronization indices were approximately equal. The

On units usually had to be exempted from this criterion because the S versus level functions of many On units have a different form from that of most other units; when the discharge rate was more than a few spikes/sec S was maximal or close to it and with further increases in stimulus level S decreased. From the level series at 10 dB increments, the level closest to the rate threshold usually gave the maximum synchronization index value. Figure IV-35 shows the frequency dependence of S_{max} for four groups of units. The connected points for one unit intermingle with single points for other units pointing to a lack of CF dependence for S_{max}. The upper left plot shows the S_{max} data from the PPO and PP1 units. The data for the AVCN units with a clear prepotential (PPO and PP1) have been replotted in Figure IV-36 to allow a direct comparison with the S_{max} data for auditory nerve obtained by Johnson (1974). The straight line on this plot was chosen by Johnson to approximate the frequency dependence above 1 kHz. To a large extent the CN and AN data superimpose. Attention is drawn, however, to two units which fell significantly below the AN data. Both of these units had large, well-isolated spikes with clear positive prepotentials, a normal synchrony dependence on level and a clearly defined maximum value of the synchronization index. The S_{max} values are, however, about one-half of the expected value at the particular frequencies used. The only property of these two units that was unusual was a small change in rate from spontaneous activity to the maximum driven rate.

Figure IV-35 Level-maxima of synchronization index for AVCN units

The level-maxima of synchronization index are plotted as a function of the frequency of continuous tone stimulation. Each point represents data from a particular unit for a particular stimulus frequency. The lines connect points from the same unit (usually the point at the highest frequency is at CF). The data are organized into four groups according to the prepotential and response type categories. The number of units contributing to each of the plots is, in clockwise order beginning with the Prepotential units, 70, 11, 41, and 13.

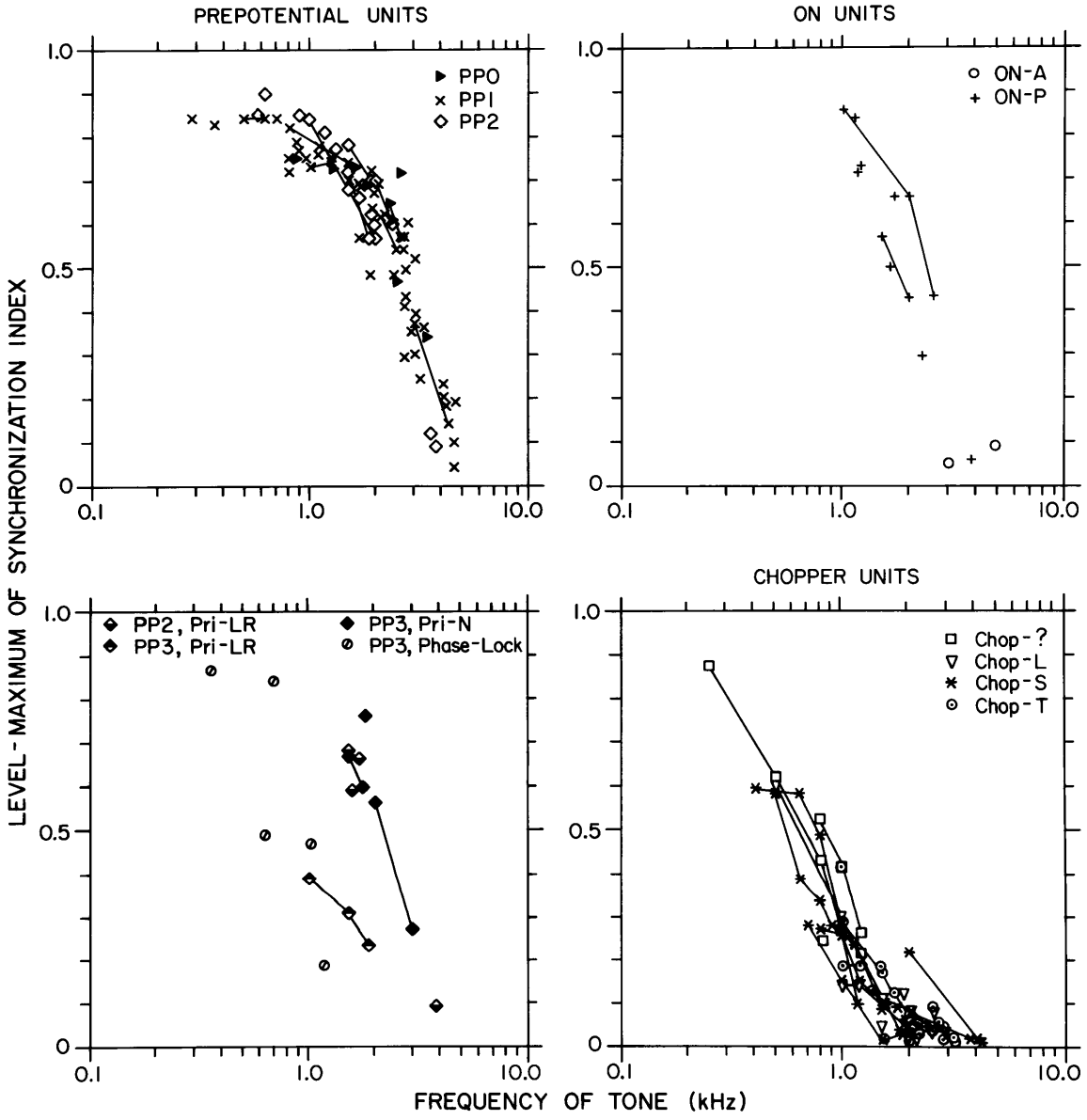
PREPOTENTIAL UNITS
PP0
PP1
PP2
ON UNITS
ON-A
ON-P
PP2, Pri-LR
PP3, Pri-LR
PP3, Pri-N
PP3, Phase-Lock
CHOPPER UNITS
Chop-?
Chop-L
Chop-S
Chop-T
LEVEL-MAXIMUM OF SYNCHRONIZATION INDEX
FREQUENCY OF TONE (kHz)
1.0
0.5
0
0.1
1.0
10.0

Figure IV-36 Level-maxima of synchronization index; comparison of PPO and PP1 units with auditory nerve units

The open circles represent the estimated maxima of synchronization index obtained by Johnson (Figure 4.4, 1974) from auditory nerve recordings. The other data points were obtained from AVCN recordings of PPO (filled triangles) and PP1 (x) units. Each point represents the maximum of the synchronization index exhibited in a continuous tone level series with 10 dB increments. A maximum was assigned to a level series if saturation was indicated by the lack of a difference larger than 0.02 between two successive points at the highest stimulus levels.

Each data point on the plot represents a particular unit, tone frequency combination. Stimulation was not necessarily at CF. The PPO data come from 9 units; the PP1 data from 46 units; The line 1-f/6 was fit to the auditory nerve data between 1 and 5 kHz by Johnson (1974).

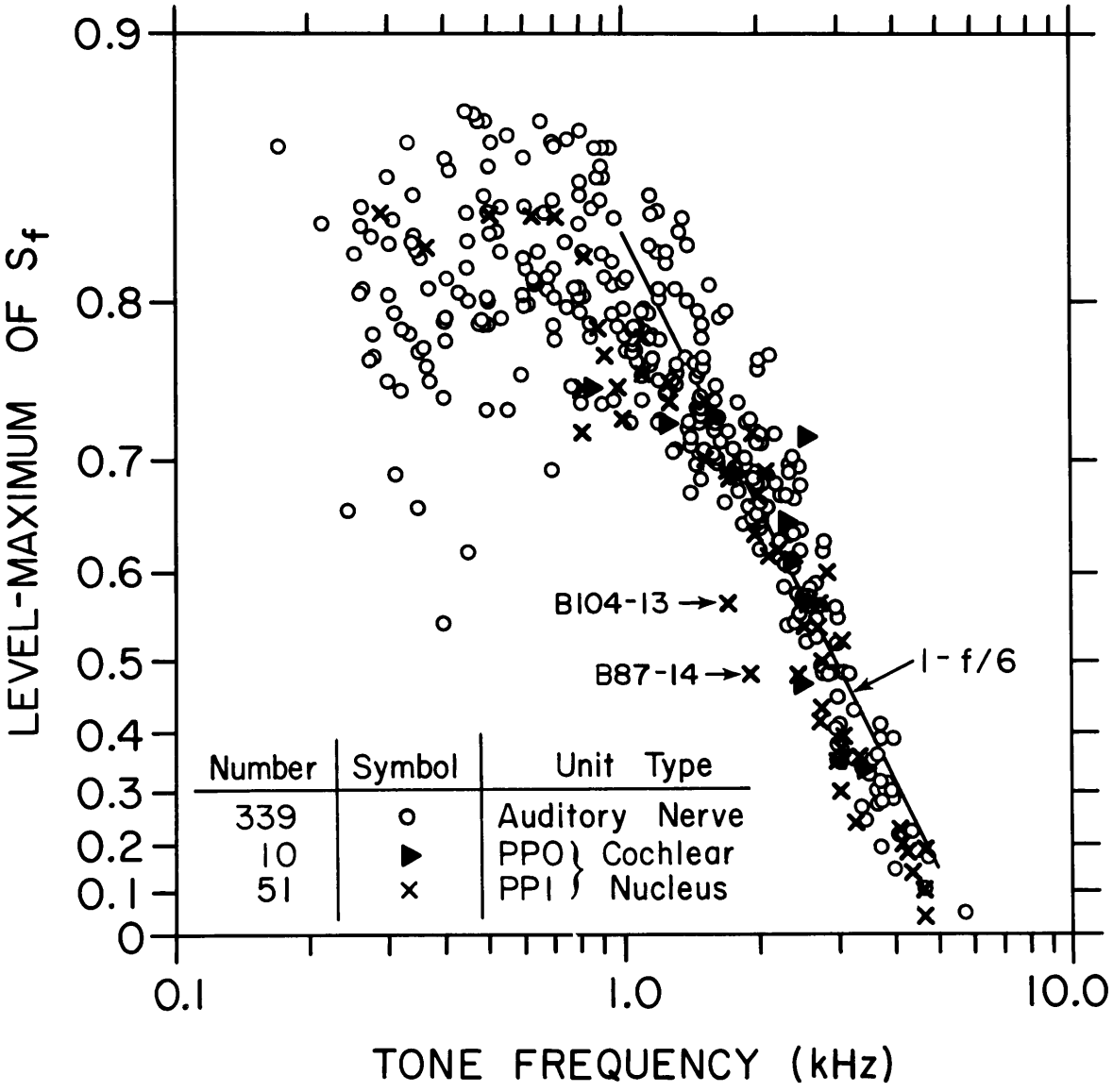
LEVEL-MAXIMUM OF S_f
0.9
0.8
0.7
0.6
0.5
0.4
0.3
0.2
0.1
0
0.1
1.0
10.0
TONE FREQUENCY (kHz)
B104-13
B87-14
1 - f/6
Number | Symbol | Unit Type
339 | o | Auditory Nerve
10 | ▶ | PPO } Cochlear
51 | x | PPI } Nucleus

Returning to Figure IV-35 we can now compare the other units of AVCN to the PPO and PP1 units. The S_{max} data on the units with a small prepotential are plotted along with the PPO and PP1 units in the upper left of Figure IV-35. Although most of the data points from the PP2 units falls in the range of PPO and PP1 units, a few PP2 units were found to have higher synchrony values. The lower spontaneous rates of the PP2 units may be related to this finding for even the auditory nerve units have been shown to have a tendency for the S_{max} values to be inversely related to the spontaneous rates of the units (Johnson, 1974).

For the units without a prepotential (PP3) the maximum synchrony values span a larger range than is found for PPO or PP1 units. When S_{max} is plotted against the frequency of stimulation, two groups become obvious. The partitioning appears to parallel the two major response type categories for the PP3 units. Figure IV-35 shows separate plots for the Chopper and On units. We note, however, that the On unit plot consists almost entirely of On-P units, a result largely of the definition of the categories since the On-A and On-G units often have elevated CT thresholds even at low frequencies. The S_{max} values of all of the On type units studied with low frequency continuous tone were equal to or higher than the range of S_{max} values defined by the PPO and PP1 units.

The S_{max} values for Choppers show quite a different behaviour. When the frequency of the tone was above 1 kHz, the S_{max} values were all below the corresponding values for PPO or PP1 units. The change from auditory nerve form resembles the effect of a low-pass

filter with a pole at about 300 to 400 Hz. Because of the range of S_{max} values for AN and Chopper units the two groups are clearly separate only for frequencies above about 1 kHz. The two Chopper units shown in Figure IV-33 illustrate the range of synchrony at 800 Hz and included is a Primarylike unit for comparison. The form of the S_{max} values in Figure IV-35 indicates that although Choppers can have low S_{max} values above 800 Hz, below 500 Hz they probably are within the primary range.

The PP3 units with the response types other than Chopper and On and the Pri-LR units that are PP2 and PP3 are represented in the fourth plot in Figure IV-35. The (PP2, Pri-LR) units are within the S_{max} range exhibited by the Prepotential and AN units whereas the (PP3, Pri-LR) unit is below this range and on the upper edge of the range for Choppers.

No single unit data from the AVCN was found to be inconsistent with the view that at a sufficiently low frequency all units would exhibit phase-locking that would produce a synchronization index within the primary range. Above 800 Hz the Choppers are differentiated from PPO, PP1, PP2, and probably from On units by their significantly lower synchrony.

* 9.2 Low frequency tone burst

The responses to low frequency tone bursts as well as continuous tones can be synchronized to individual cycles of the sound pressure waveform. Neither the discharge rate nor the degree of phase-locking during the transient and sustained portions of the

of the response need to be the same. The discharge rate, for example, usually decreases significantly from the transient to the steady-state condition.

In order to obtain a measure of the synchrony during STB, period histograms were computed from the last half of the response to 25 msec tone bursts (STB) used for the PST computations. The limits of a 12 msec window used to select the spikes for the period histogram were chosen to exclude the initial transient response (about the first 10 msec) and the final few milliseconds of the response. The position of the window was found to be non-critical provided that the initial one or two sharply time-locked spikes were excluded. From the period histograms, the synchronization index was then computed (S_{STB}).

All units with both STB and CT responses recorded for frequencies below 5 kHz were reprocessed to obtain the period histograms for both conditions. An example of this comparison is shown in Figure IV-37. The shapes of the two period histograms shown for the STB and CT stimulation are similar despite the 2 to 1 ratio in discharge rates. The synchronization indices computed from these period histograms are shown as the circled points in the plot below. At the example level of 34 dB SPL and at the other levels tested with both STB and CT, the synchronization index for STB is larger.

A total of 51 units was stimulated with STB and CT at one or more frequencies to obtain 69 pairs of synchrony versus level plots. The relationship between these pairs of plots appeared to be a constant vertical separation at all levels more than about 10 dB above

synchrony threshold, i.e., over the rising portion of the synchrony level function and in the saturated region. Just as for B105-21, the difference was usually small. At the bottom of Figure IV-37, the difference between the synchronization indices at each level is plotted as a function of the CT synchronization index.

As a summary of the synchrony differences and a demonstration of the consistency of these small differences, Figure IV-38 shows plots of synchrony difference versus continuous tone synchrony. Various stimulus intensities are represented in this data, although mainly levels near saturation of the synchronization index.

Just as the S_{max} versus frequency plots separated into at least two groups, Chopper versus non-chopper, the plots in Figure IV-38 partition in the same way. The Chop-?, Chop-S and Chop-T categories all contributed to Figure IV-38 and each type had consistently larger synchronization during the STB, whereas the other unit types (which have higher CT synchrony values above 800 Hz) showed a smaller change in synchrony and the change was in the direction of an increase with time following tone onset. Although the consistency of the effect within any group and the opposite effects exhibited by different groups both suggest that these observations are significant, such small differences must be interpreted cautiously.

A methodological implication of this comparison of STB and CT synchrony arises in connection with the use of STB responses instead of CT to evaluate the synchrony of a particular unit. For the Pri, Pri-N, and On units, it appears that the synchronization indices for STB and CT are very close. For the Choppers, however,

Figure IV-37 Change in synchronization index for B105-21: STBCF to CTCF

The upper half of the figure is divided into two columns: the left for tone burst, the right for continuous tone. Responses to a 60 second presentation of CT were used to compute a period histogram whereas only the discharges during the 12 msec interval indicated on the sample PST histogram were used to compute a period histogram for the short tone burst (STB) responses. Two sample period histograms for STB and CT at 34 dB SPL are shown in the figure. Both were synchronized to the positive-going zero-crossing of the oscillator voltage. The horizontal scales represent one period (T) and the vertical scales are in spikes/sec. The synchronization indices computed from these two period histograms (S_{STB} and S_{CT}) are indicated by the circled points on the synchrony-level functions. A "synchrony change" was defined as the difference in synchronization indices, $S_{CT} - S_{STB}$. The bottom plot shows the synchrony change for B105-21 plotted as a function of the steady state (CT) synchronization index, S_{CT}.

B105-21 CF TONE: 646Hz

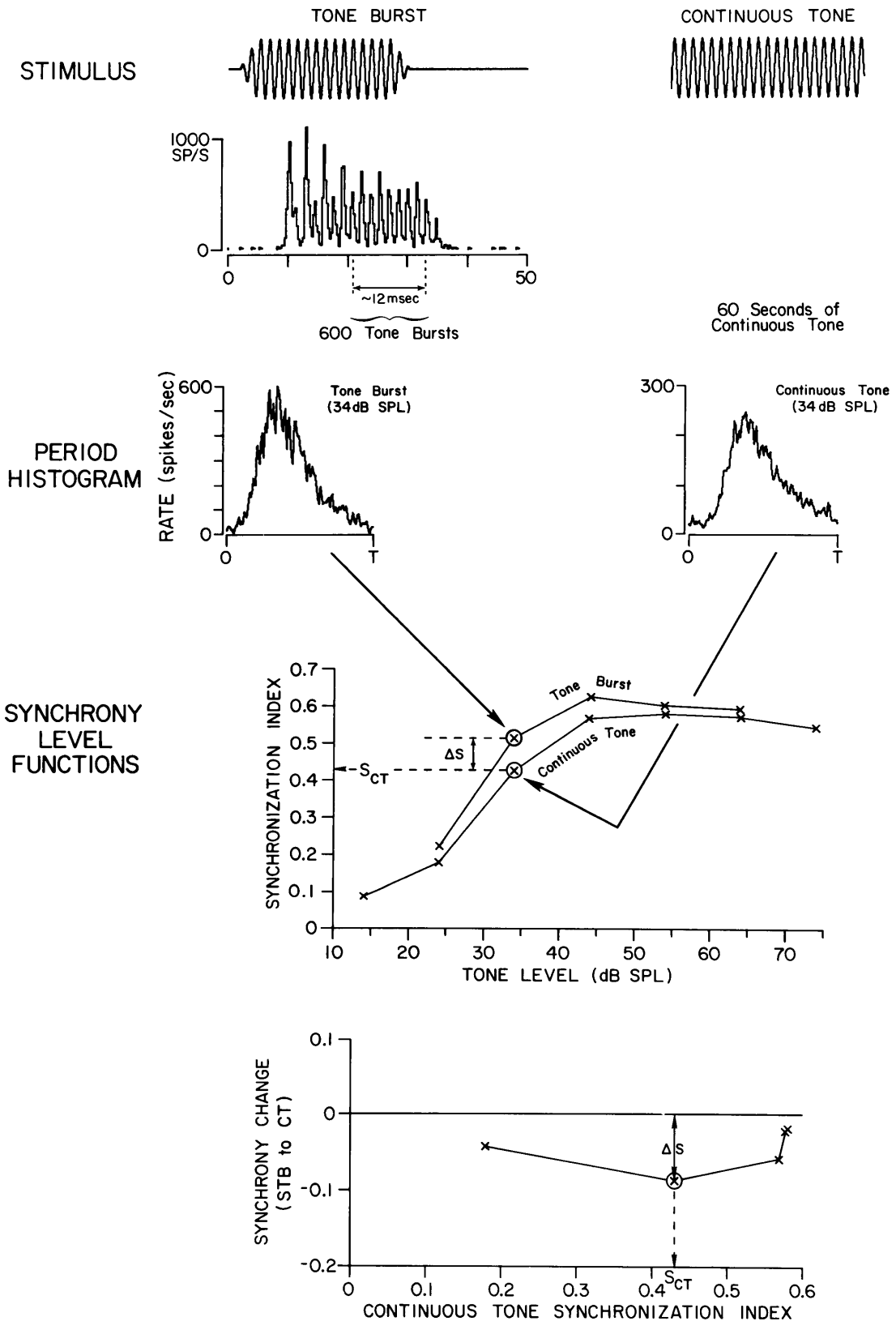

Figure IV-38 Synchrony changes

The change in synchronization index, $S_{CT} - S_{STB}$, is plotted as a function of the steady-state synchrony measure, S_{CT}. Each isolated point or connected sequence of points represents a separate (frequency, unit) combination with a data point for each stimulus level at which both S_{STB} and S_{CT} were determined. The stimulus frequency was usually at CF. The number of units and number of (frequency, unit) pairs represented in each plot are:

Plot	number of units	number of (frequency, unit) pairs
Prepotential units	15	17
(PP3, "Other") units	9	9
Chopper units	23	37
On units	4	6

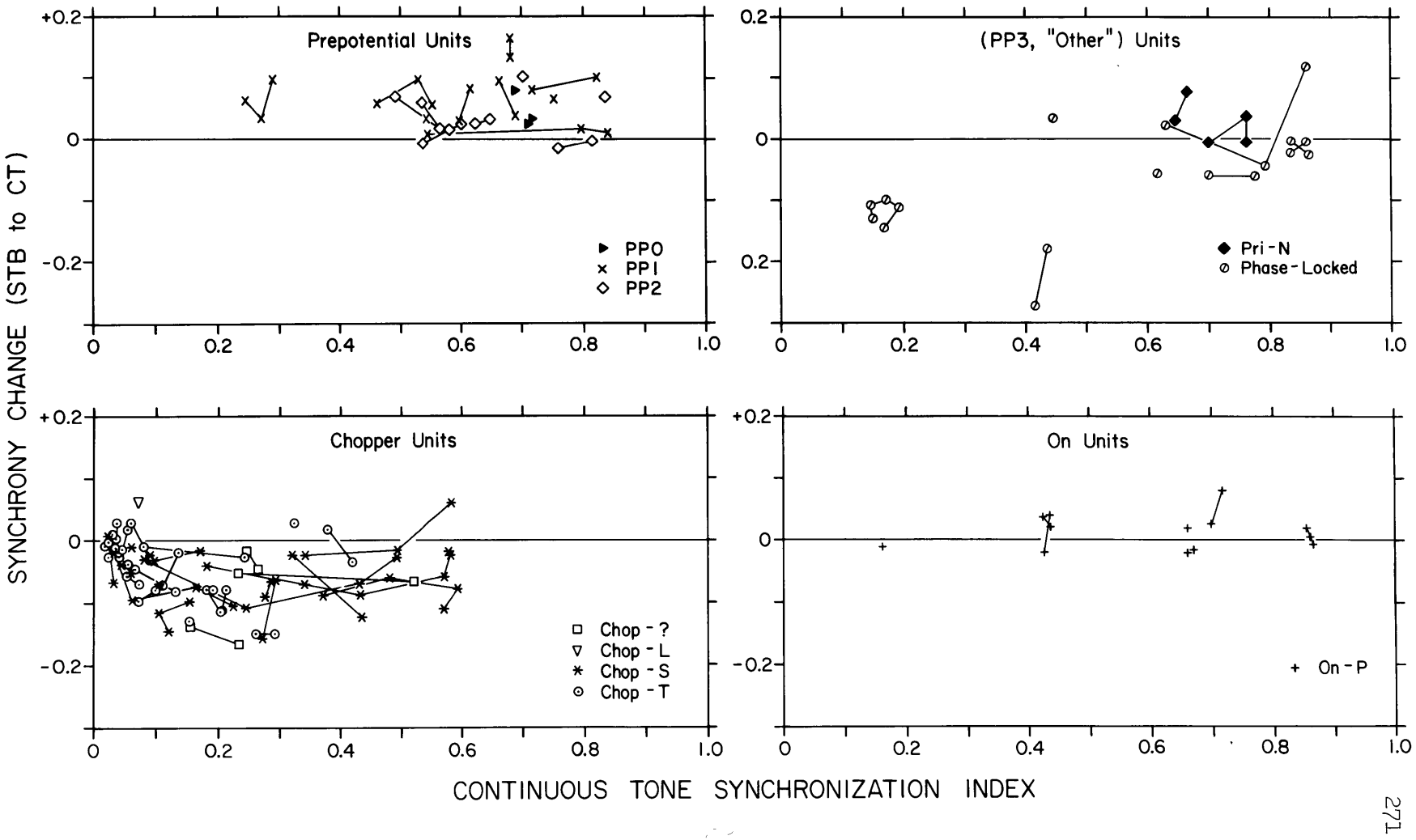
Prepotential Units
PP0
PP1
PP2
(PP3, "Other") Units
Pri-N
Phase-Locked
Chopper Units
Chop-?
Chop-L
Chop-S
Chop-T
On Units
On-P
+0.2
0
-0.2
0.2
0.4
0.6
0.8
1.0
SYNCHRONY CHANGE (STB to CT)
CONTINUOUS TONE SYNCHRONIZATION INDEX

STB stimulation results in greater synchrony than does CT and can therefore provide only an upper bound on synchrony to CT. Chopper units without CT data were accordingly used to check and were found to be consistent with the finding of section 9.1, that Choppers have lower S_{max} values than the PPO or PP1 units at frequencies above 1 kHz.

10. Localization

10.1 General

As was described in Methods, section 5.6, the principle in mapping single unit locations into the CN block model was to preserve relative position within the subdivisions. The description of the location of each unit was then recorded in two ways. A total of 1171 units localized to AVCN were assigned a location within the block model coordinate system. The less complete description of unit location, namely specification only in terms of the subdivision in which the unit was located, is available for 1188 units. Given the uncertainties of unit locations and subdivision boundaries, any unit within 1 block model unit (80 μm) of a subdivision boundary was first labelled for the subdivision in which it was most probably located and secondarily for the adjacent region. The Granular region presents special problems because it forms a thin layer over most of the AVCN surface which can be only a few block model units thick. Thus units localized to the Granular region are somewhat uncertain in their real location since the layer is often thinner than the error limits on localization. Superficial localizations depend strongly on the entry point of the electrode track which is not as dependable a reference point as that provided by lesions made deeper into the nucleus.

The spatial distribution of units reveals some possible sampling biases in the pooled data. These biases could have their origin in (a) the placement of the microelectrode passes, (b) the possible

Figure IV-39 Spatial distribution of the units recorded in the AVCN

The AVCN subdivisions serve as an anterior-posterior measure of unit location (upper plot) and the sagittal coordinate within the block model measures lateral-medial position (lower plot). For comparison, the corresponding distributions of AVCN subdivision volumes in the block model are provided. The distributions for units are shaded with dots. Volumes are not corrected for tissue shrinkage.

Taking into account the variations in cell density from AA (very dense) to PV (sparse), the discrepancy in the two distributions at the top is reduced.

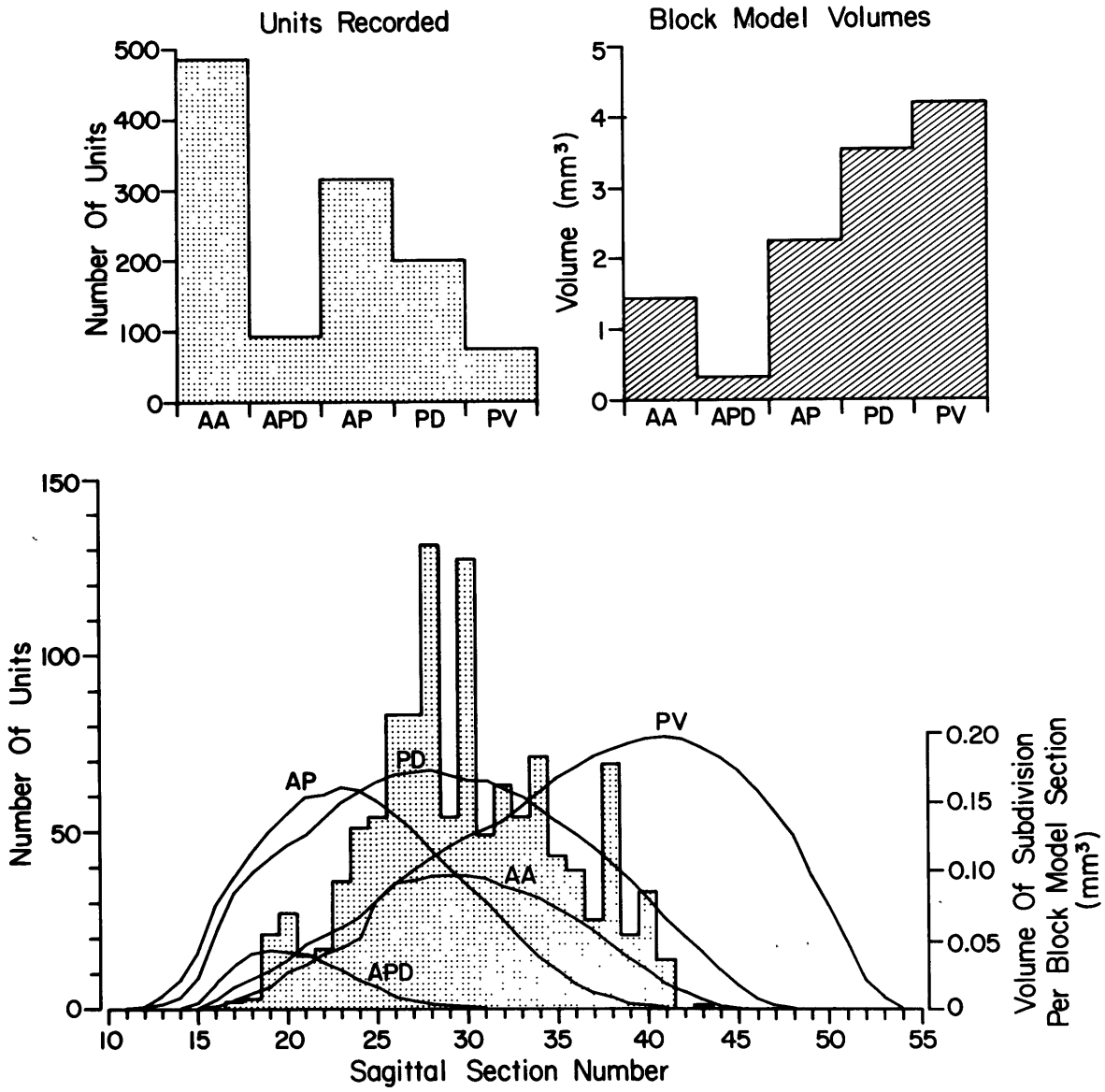
Units Recorded
Number Of Units
500
400
300
200
100
0
AA
APD
AP
PD
PV
Block Model Volumes
Volume (mm³)
5
4
3
2
1
0
AA
APD
AP
PD
PV
150
100
50
0
Number Of Units
PV
PD
AP
AA
APD
0.20
0.15
0.10
0.05
0
Volume Of Subdivision Per Block Model Section (mm³)
10
15
20
25
30
35
40
45
50
55
Sagittal Section Number

sampling biases of the microelectrode and search stimulus and (c) regional variations in cell density. The unit distributions in the AVCN are characterized by the plots in Figure IV-39. The upper histogram displays the rostro-caudal dimension in terms of the AVCN subdivisions. The strong bias toward rostral AVCN has a clear basis in (a) and (c) above; many more passes were made in rostral AVCN and the cell density of AA is obviously greater than in PV. As will be shown below, AA has a large proportion of one unit type, thus in order to obtain a significant sample of the less common types in AA requires a large total sample of units. The lower half of Figure IV-39 shows the lateral to medial distribution of single units plotted as a function of the sagittal section from the block model to which the units were localized. For comparison with the distribution of the AVCN subdivisions, the corresponding volume distributions obtained from the block model are plotted. Since the units were localized mainly to AA, AP and PD, we see that the lateral-medial sampling was probably reasonably representative. In PV, however, the most lateral portion which has a very low cell density was not sampled. The rapid decrease in sampling near the lateral and medial limits results mainly from a bias against recording from the edges of the nucleus because of the difficulty of using tangential passes and the small number of units recorded from such a short pass. The very lateral passes are also difficult to localize because of poorly defined tracks and lesions in the short passes.

For most of the physiological data the spatial distributions of

the unit properties appear to be adequately described in terms of the subdivisions. Each of the parameters examined was encoded in a set of symbols and plotted on drawings of the block model sections. The standard planes, sagittal, transverse, and horizontal, were used as needed to obtain a three-dimensional appreciation of the particular distribution. In all but a few cases which will be considered in the final part of this section, no significant positional variation in unit characteristics could be distinguished within any subdivision other than those correlated with CF variation within the subdivision.

10.2 Tonotopic organization

The CF was determined for over 88% of the single units in the present data. Among the units assigned a location within the block model, there were 1050 with a CF estimate. The CF data are useful as a check on the reliability of the localization procedure and the pooling of data from many experiments. We would expect the individual CF values to exhibit a systematic dependence on position within AVCN, conforming to the general tonotopic pattern previously described by Rose et al. (1957, 1959). Localization errors or inter-animal variations could disrupt this pattern. The CF's for all 1050 units were plotted on a set of block model sections and the data from individual passes compared with the general trend. Figure IV-40 shows every fifth section of the sagittal series with the CF data from that section and from an adjacent section superimposed. The results are generally satisfactory in that only a few examples of "misplaced" CF

Figure IV-40 Characteristic frequencies of units localized to selected sagittal sections

On the sagittal sections spaced 5 block model units (400 μm) apart are plotted the CF's of units localized to the particular section shown and an adjacent section. All CF's were rounded to the nearest tenth of a kHz if below 1 kHz and to the nearest integer kHz if above. In some cases the density of units required that the CF of a unit be plotted up to 2 block model units from its assigned location. The sections are shown in outline with only the subdivision PV delimited. Section S20 is the most medial in this sequence and S40 the most lateral. The subdivisions for these sections are shown in Figure IV-41.

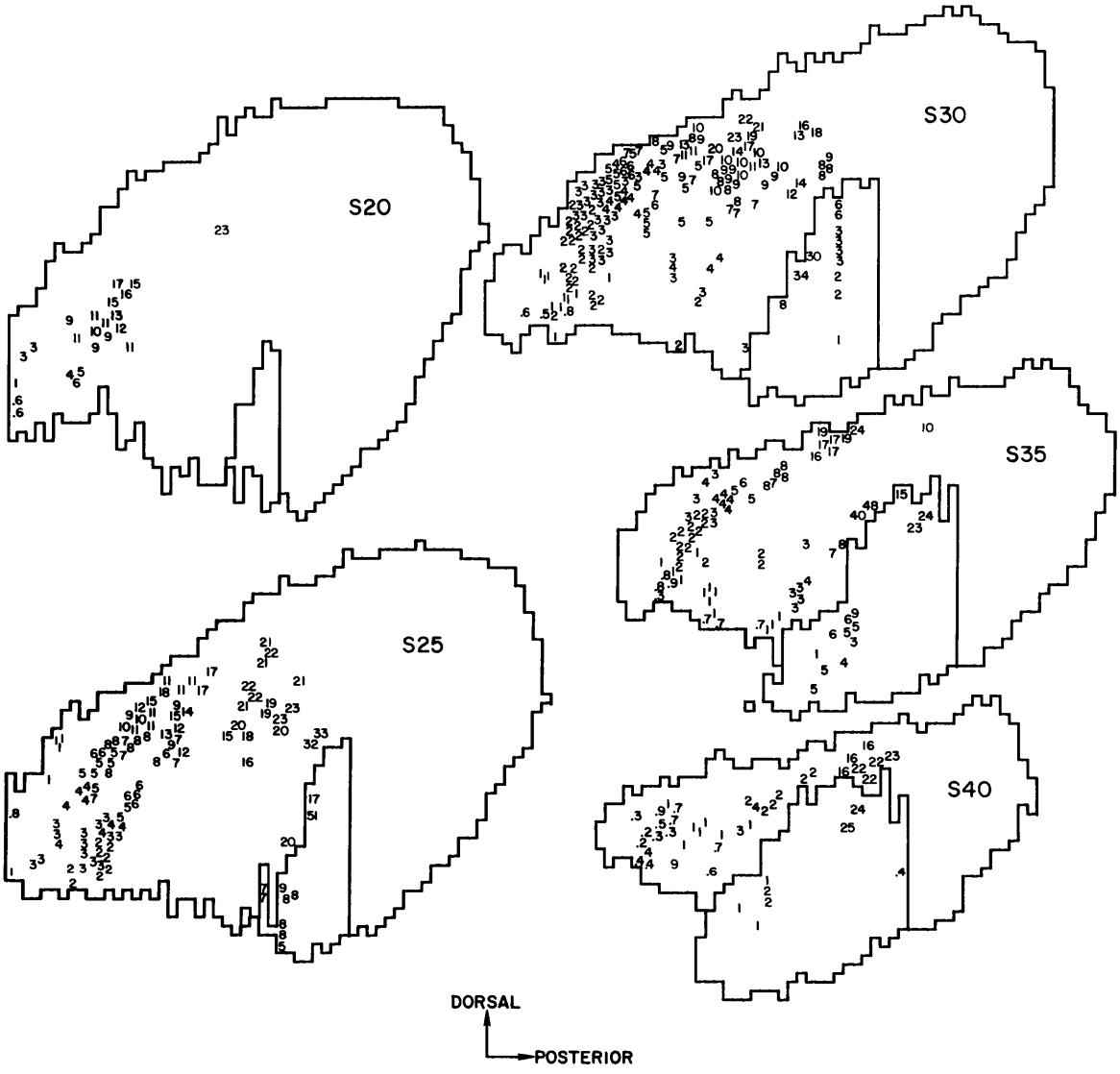
S20
S30
S35
S25
S40
DORSAL
POSTERIOR

values were found and these were generally located within 2 or 3 block model units of the average positions of similar CF values.

Although the general tonotopic organization of the CN was described almost two decades ago (Rose et al., 1957), a detailed presentation of the CF organization of the subdivisions of the CN is still not available. In spite of the fact that the data gathering techniques of this study were not overtly designed to study tonotopic organization, some information can be obtained from the results. From the point of view of the subdivisions, the CF distributions are of concern since the small size of some of the subdivisions in the CN make it highly likely that some will not contain a full representation of the CF range. As a representation of the tonotopic organization in the AVCN it was decided to estimate the shape of three constant CF surfaces having separations of two octaves. The three CF values chosen were 0.8, 3 and 12 kHz. The individual CF's were plotted on the complete set of transverse, horizontal and sagittal block model sections. Figure IV-40 shows some of this data as plotted on sagittal sections. The units localized to the indicated sections plus an adjacent section are superimposed to increase the unit density.

In order to obtain a consistent set of lines for the three views and take advantage of the different perspectives obtained from the three planes, a computer program was used to initially define the CF surfaces by tracing estimated lines of constant CF from the sagittal series and then to interactively alter the surfaces until the CF lines as viewed on each plane of sectioning conformed with the trends exhibited through the particular series of sections.

The lines of constant CF were transferred to a set of block model sections which included the subdivision boundaries. Figure IV-41 shows every fifth section over the ranges that had CF data in AVCN. The precise shape of these lines should not be taken too seriously as the data are often sparse. The particular curvature of a line may depend on the data from a single pass. The sections in Figure IV-40 are the same as the sagittal series used in Figure IV-41 in order to facilitate comparison.

The subdivision, PV, was not included in the estimation of the CF surfaces because of the small number of units localized within it. Although most of these units had CF's which appeared to fit the trends seen in the adjacent PD, some units were markedly deviant. A striking example of this form of deviation was provided by two units with CF's around 22 kHz situated between units with CF's around 1.5 kHz. As far as could be assessed, these "isolated" high CF units were not recorded from primary afferents. In support of this view are observations that the spike waveforms did not have the characteristics of the narrow spike waveforms of the PPO units and that two of these high CF units were antidromically activated by electrical stimulation in the contralateral trapezoid body. An additional problem in drawing the CF lines near PV was the presence of high CF's (20 kHz and above) dorsal to PV in even the most lateral sections sampled. Ventral to these high CF units there must be an exceptionally steep CF gradient because of the low CF values found in ventro-lateral VCN. It may be that these two observations on the distribution of very high CF units

Figure IV-41 Surfaces of constant CF in AVCN

Every fifth section (400 μm) from the standard planes of the block model is used to illustrate the estimated surfaces of constant CF. The surfaces are for 0.8 kHz, 3 kHz and 12 kHz. The surfaces were estimated only over the regions defined by the symbols; i.e., the termination of a CF line is not significant except where it intersects the edge of the CN.

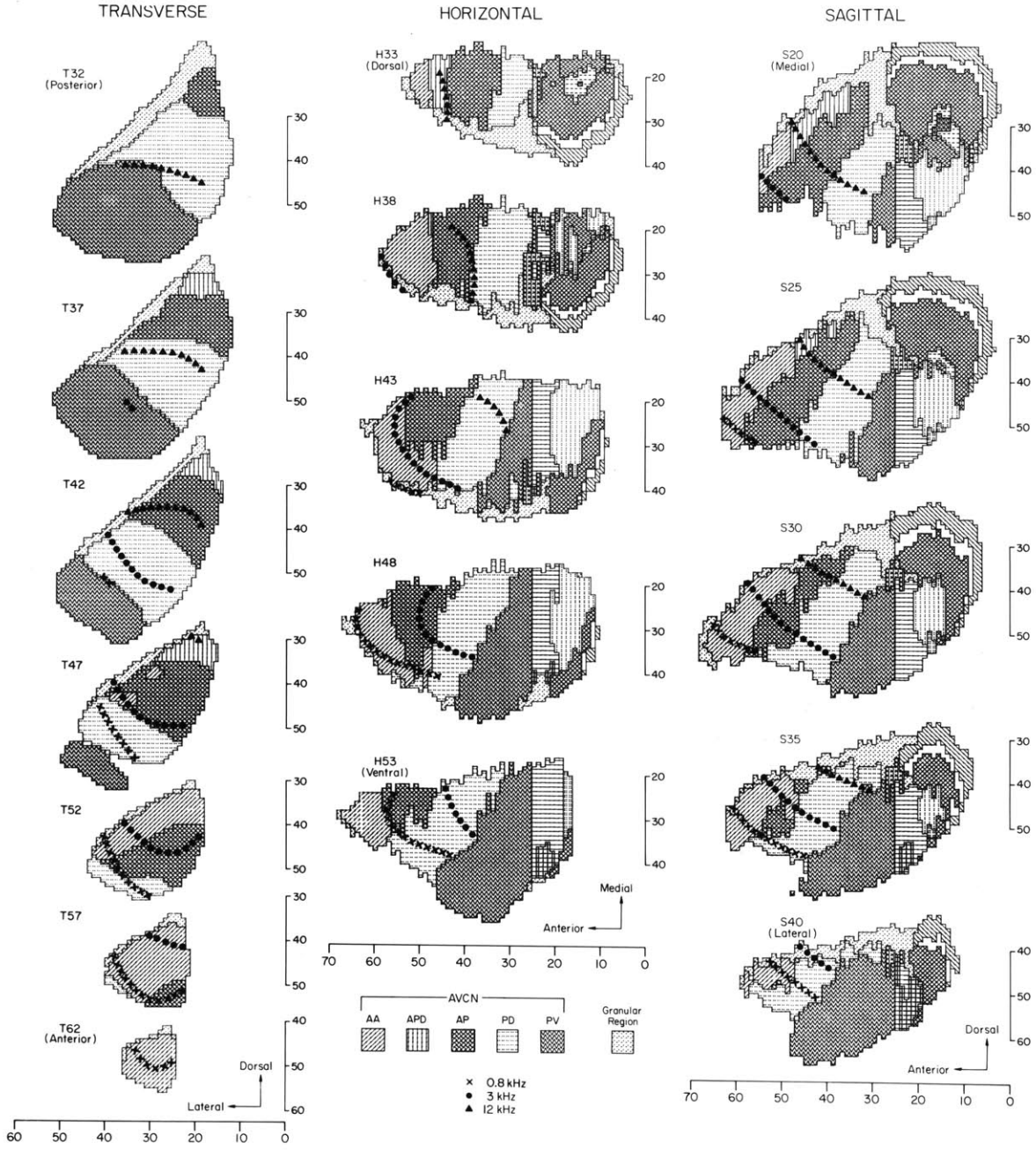
TRANSVERSE
HORIZONTAL
SAGITTAL
T32 (Posterior)
T37
T42
T47
T52
T57
T62 (Anterior)
H33 (Dorsal)
H38
H43
H48
H53 (Ventral)
S20 (Medial)
S25
S30
S35
S40 (Lateral)
Dorsal
Lateral
Medial
Anterior
AVCN
AA
APD
AP
PD
PV
Granular Region
0.8 kHz
3 kHz
12 kHz

are related. Perhaps there are two CF "systems" in and around PV, one which is continuous with the adjacent PD, AP pattern and another with very high CF's over the dorso-lateral surface of PV and in some cases penetrating into it. Some examples of the high CF units in and around PV can be found in the sample of sagittal sections shown in Figure IV-40.

From the three sets of block model sections it is possible to visualize the approximate CF surfaces in AVCN. A surface of constant CF in AVCN, particularly the mid-frequencies, approximates a plane surface which is tilted so that it intercepts a sagittal section at an angle 45^{o} from the horizontal, running in the approximate direction of the ascending branch of the AN. This plane intercepts a transverse section at an angle of 45^{o} from the horizontal, running almost perpendicular to the upper or dorso-lateral surface of the CN.

As was stated earlier, one of the objectives in estimating the CF distribution was to relate tonotopic organization to the subdivisions of the AVCN. A number of observations can now be made. The AA to APD border is very close to the 12 kHz CF surface throughout the AVCN. Based on both the 12 kHz surface and the individual unit data, AA and APD appear to have disjoint CF ranges, intersecting at about 10 kHz. The ventral and lateral borders of AP can be seen in Figure IV-41 to follow closely the 0.8 kHz surface. Also the narrowing of AP as it approaches this surface means that very few units in AP could have CF's close to or below 1 kHz. The subdivision PD, by contrast, appears to have a uniform representation of the CF range. The

units in PV probably span the full CF range although there may be a disproportionate representation of high CF's. The dorsal part of AP and PD just adjacent to the granular cell region is presumably the region of the small cell cap (Osen, 1969b); this region appears to have exclusively high CF's, with many units in the 15 to 30 kHz range.

10.3 Prepotential categories

There are two main reasons for examining the spatial distribution of units with a prepotential. The first is to test the hypothesis that units having a prepotential correlate with cells that receive end-bulbs. If the hypothesis is true the physiological data will also provide an estimate of the distribution of cells with the large endings. The strong correlation that the Prepotential units exhibit with the Pri and nearly primarylike categories (Pri-N and Pri-LR) enables the locations of units with "Primarylike" response to be examined.

The data base for the distribution of the prepotential categories consists of all units localized to an AVCN subdivision or a part of the granule cell region adjacent to the AVCN. Seventeen "non-auditory" units were eliminated (none of them was found to have a prepotential). Table IV-6A summarizes the number of units placed in each of the pp categories. The right-hand column represents the units localized to the granule cell region adjacent to the AVCN. Since the electrodes used in these recordings probably do not record isolatable spikes from either granule cells or the relatively small axons in the granule

Table IV-6 Prepotential categories versus AVCN subdivisions

(A) Unit totals

	AA	APD	AP	PD	PV	G
PP0	30	6	13	1	3	
PP1	283	24	82	5	2	1
PP2	8	4	13	26	20	1
PP3	56	7	109	103	20	9
PP4	103	34	87	75	25	15
Total	480	75	304	210	70	26

(B) Percentages

PP0	8	15	6	1	7	
PP1	75	58	38	4	4	
PP2	2	10	6	19	44	
PP3	15	17	50	76	44	
Sample size	377	41	217	135	45	

(C) Percentages

PP1	82	69	40	4	5	
PP2	2	11	7	19	48	
PP3	16	20	53	77	48	
Sample size	347	35	204	134	42	

cell layer, the units localized to the granule cell layer probably represent cells located adjacent to the granule cell region. Omitting the PP4 category which represents the units for which a decision could not be made and converting the numbers to a percentage within each subdivision we obtain Table IV-6B which summarizes the distribution of the pp categories for well-isolated units. Since the PPO category probably represents recordings from endings of the auditory nerve rather than CN cells, the tabulation in Table IV-6B should therefore be presented without PPO units. This is provided in Table IV-6C which tabulates the percentages of PP1, PP2 and PP3 units. The PP3 units represent, by definition, the units which probably do not have a prepotential, but also according to the correlations shown in section 4, they represent the units with other than "Primarylike" response characteristics. We can see from Table IV-6C that the number of PP3 units is lowest in AA and highest in PD. Both AP and PV contain approximately equal numbers of units with a pp (PP1 and PP2) and without a pp (PP3). The other aspect of the distributions summarized in Table IV-6C is the shift in the ratio of PP1 to PP2 units from the anterior division (AA, APD, AP) to the posterior division (PD, PV). In the anterior division the balance is in favour of the PP1 units especially in AA, and is reversed for the posterior division, especially PV.

10.4 Response type categories

This section will present aspects of the spatial distribution of

the response types that are adequately described in terms of the AVCN subdivisions. The location of all units assigned to a subdivision is summarized in Table IV-7. The "?" row, which contains the units not assigned to a response type category, represents many of the PP1 ("Primary-like") units. As was explained in section 4, the Pri and Pri-N response types were identified in a biased manner so that interpretations based on relative numbers of these units must be made with caution. Through the correlation of the Prepotential units with the units in the Pri, Pri-N, and Pri-LR response type categories it is possible, however, to infer the distributions of these units. If we consider a generalized primarylike response (Pri, Pri-N and Pri-LR) "Primarylike", these units will have essentially the distribution of the Prepotential units as summarized in the previous section. However, as was noted in Section 4, there is a tendency for PP1 units to correlate with Pri units and PP2 with Pri-N. Just as the PP1 to PP2 ratio changes through AVCN, rostral to caudal, so also does the Pri to Pri-N ratio. An unbiased demonstration of this shift is not available, but the estimated percentage of "Primarylike" units in AA with the Pri-N form is about 10%. (This figure applies, of course, only to the units with CF greater than about 2 kHz since the "notch" of the Pri-N response cannot generally be distinguished when there is strong phase-locking.) In PV the Pri-N response type predominates but a significant fraction (perhaps as large as $\frac{1}{4}$) of the units do not exhibit a "notch" in their STBCF response.

From Table IV-7 it can be seen that any region <u>may</u> contain members of each response type. The zero entries cannot be taken as a definitive demonstration of a lack of representation because of the small

Table IV-7 Response type categories versus subdivisions

	AA	APD	AP	PD	PV	G
Pri	56	5	14	4	6	
Pri-N	10	5	10	21	16	
Pri-LR	3		6	2		
Chop-?	4	5	4	8	2	
Chop-L	2		6	9	8	2
Chop-S	5		7	34	6	1
Chop-T	12	4	47	13		1
On-?	7		4	3		1
On-A	6		20	11		
On-G						
On-P	11		13	8	2	
Pauser			3			3
Composite	1		1	2		1
Unusual			3			2
Phase-locked	37			19	1	1
?	320	44	138	66	26	14
Totals	474	63	276	200	67	26

sample size for the columns containing the zeroes. Although there do not appear to be any cases of complete segregation of a response category to a single subdivision there are some distinct regional variations.

The non-primarylike units fall into 2 main groups (Chopper and On) and several minor types which for convenience can be considered as a third group. The Chopper and On groups are both relatively cohesive since the members have many common properties. The members of the third group, namely Pauser, Composite, and Unusual, even taken collectively, constitute only a small proportion of the units recorded in AVCN. For the On and Chopper groups, there is a rostro-caudal variation in the relative populations. There is an increasing proportion of On units along the caudal to rostral dimension of the AVCN. It is in the more rostral subdivisions of the AVCN that On units become prominent. In terms of absolute percentages in each subdivision we must, of course, consider the number of non-primarylike units in each subdivision. Thus although the On to Chopper ratio becomes almost 1 in AA, the total of both groups remains much smaller than the "Primary-like" units in AA.

From Table IV-7 it can be seen that the relative numbers of units in the Chopper types are a function of the AVCN subdivision. In subdividing the Choppers, those which did not show chopping with a mean interval of 5 msec or longer fell into two categories, the Chop-S (sustained) and Chop-T (transient). An anatomical validation of the Chop-S versus Chop-T distinction lies in comparing the numbers of units

in these categories for the anterior and posterior divisions. The ratios of Chop-S to Chop-T are 12 to 63 for the anterior division and 40 to 13 for the posterior. In addition, the long interval Choppers (Chop-L) may be more strongly represented in PV. The sample, however, is small. Another way of demonstrating an anatomical correlate of the Chop-L units will be presented in section 10.7.

10.5 Long tone burst

The distribution of the LTBCF response categories can be largely predicted by a chain of previously described correlations. In particular, the relationship of the LTBCF types to the pp categories and (STBCF) response types can be used to predict much of the location of the LTBCF forms. Table IV-8 contains the regional distributions of LTBCF types: part A for the PP1 units, B for the PP2 units and C for the PP3 units. The PP0 units, which are not shown because of the small sample, are essentially Primarylike to LTBCF just as the PP1 units are. The PP2 and PP3 units, however, exhibit much more variety in their LTBCF response. From the correlation of the response type categories with the LTBCF categories and with subdivisions, it is not unexpected that most of the LTBCF types are found in each subdivision. Many of the Primarylike in Table IV-8C are from the Chopper units; many of the On and Onset from the On units. The Build-up category, however, is probably an LTBCF category that is restricted to a small region of the AVCN. The distribution of the Pauser response type with which the Build-up LTBCF response is correlated will be described later.

Table IV-8 LTBCF categories versus AVCN subdivisions

		AA	APD	AP	PD	PV	G
(A) PP1	Primarylike	13	1	3			
	Low-rate	1					
(B) PP2	Primarylike	1	1	3	12	1	
	Low-rate	2		1	3	2	
	Onset				2		
(C) PP3	Primarylike		1	12	15	7	1
	Low-rate	2		3	3		
	Onset	7	1	8	6	2	1
	On	3		10	3		
	Dip	1		3	7		
	Chopper			1			
	Build-up			1			1

The Dip LTBCF category exhibits a distribution which was not anticipated from the other correlations. The Dip units were shown in section 5 often to be in the Chop-T category. As noted in the previous section, Chop-T units are found mainly in the anterior division. However, those Chop-T units in the Dip LTBCF category are located mainly in PD. Considering the smaller sample size for PD and that one of the AP localized Dip units was actually at the AP-PD border, we see that the ratio of Dip responses in PD to those in AP could be as large as 8:1. Further evidence that the Chop-T units in PD differ from those of the anterior division will be presented in the next section.

10.6 Interval histogram shape

Some aspects of the IH shape parameters were examined for correlation with AVCN subdivisions. Although most of the correlations are accounted for by correlations with the pp or response type categories, one unexpected observation was noted in connection with some of the Chop-T units. Of the 13 units with an SE decay of the IH, 10 were Choppers, 9 were categorized as Chop-T and the other unit was Chop-?. Thus most of the units with an SE decay were of the Chop-T response type. In a previous section, the Chop-T units were shown to be located mainly in the anterior division. From these correlations it was expected that the units with an SE decay would be located mainly in the anterior division. Of the 10 Choppers referred to above, 1 was located in AA near AP, 2 in AP, 1 on the AP-PD border and 6 in PD. We find, therefore, that there may be at least two types of

Chop-T unit. One type is concentrated in the anterior division and has IH's with E or FE decay and Primarylike (normal or Low-rate) response to LTBCF. A second type of Chop-T unit is located mainly in the posterior division (perhaps only in PD) and has a SE decay in the IH and/or a Dip LTBCF response.

We note also that two of the units with SE decay that were not in the Chop-T response type were Pri-N and also located in the posterior division (PD and PV).

10.7 Location of non-primarylike response types

Except for the CF's, all of the preceding data concerning unit locations have been presented in terms of the anatomical subdivisions defined by Brawer et al. (1975). Each aspect studied has been examined for correlations that do not fit the subdivision partitioning. The prepotential and response type categories, in particular, were plotted onto the full series of transverse, horizontal and sagittal block model sections and these representations examined for other patterns. Most of the regional variations in the density of the physiological categories appear to be adequately described by the subdivisions. The response type categories apply, of course, only to the regions of the AVCN with CF's above about 1 to 1.5 kHz.

The complete three-dimensional distributions of all response type categories, except Pri and Pri-N, are shown in Figure IV-42. The Pri and Pri-N categories are not included in the figure because, as was explained in section 4, the identification of the Pri and Pri-N units

Figure IV-42 Block model locations of units other than Pri and Pri-N

This figure shows the location of all units assigned to a response type category other than Pri or Pri-N and recorded from cats with an ipsilateral VDL of -70 dB or lower. The block model sections are from the horizontal series. Proceeding down each column and from left to right (from H25 to H63) the contour drawings represent successively more ventral sections. The location of each unit is indicated with a mnemonic symbol at, or adjacent to, the block model coordinate to which it was localized. At the upper left of each drawing is the horizontal coordinate number for the section. All sections are truncated at coordinate 20 on the transverse scale (shown at the top of each column). The sagittal coordinates for the sections are defined by the Sagittal 30 scale mark to the right of each section (on dashed line). Medial is up and posterior to the right. The particular AVCN subdivisions on a section can be determined by extrapolating from the coded horizontal sections in Figure IV-41 and from the labelled sections (25, 38, 55, 63). The symbols used are as follows:

Chop-?	C	On-?	O	Pauser	Ⓩ
Chop-L	Ⓛ	On-A	A	Composite	Ⓔ
Chop-S	S	On-G	G	Unusual	U
Chop-T	T	On-P	P	Pri-LR	|
				Phase-locked	+

The circled symbols were used for units that are located near the periphery of AVCN (and along PV-PD border). The granule cell regions are shaded with diagonal arrays of dots.

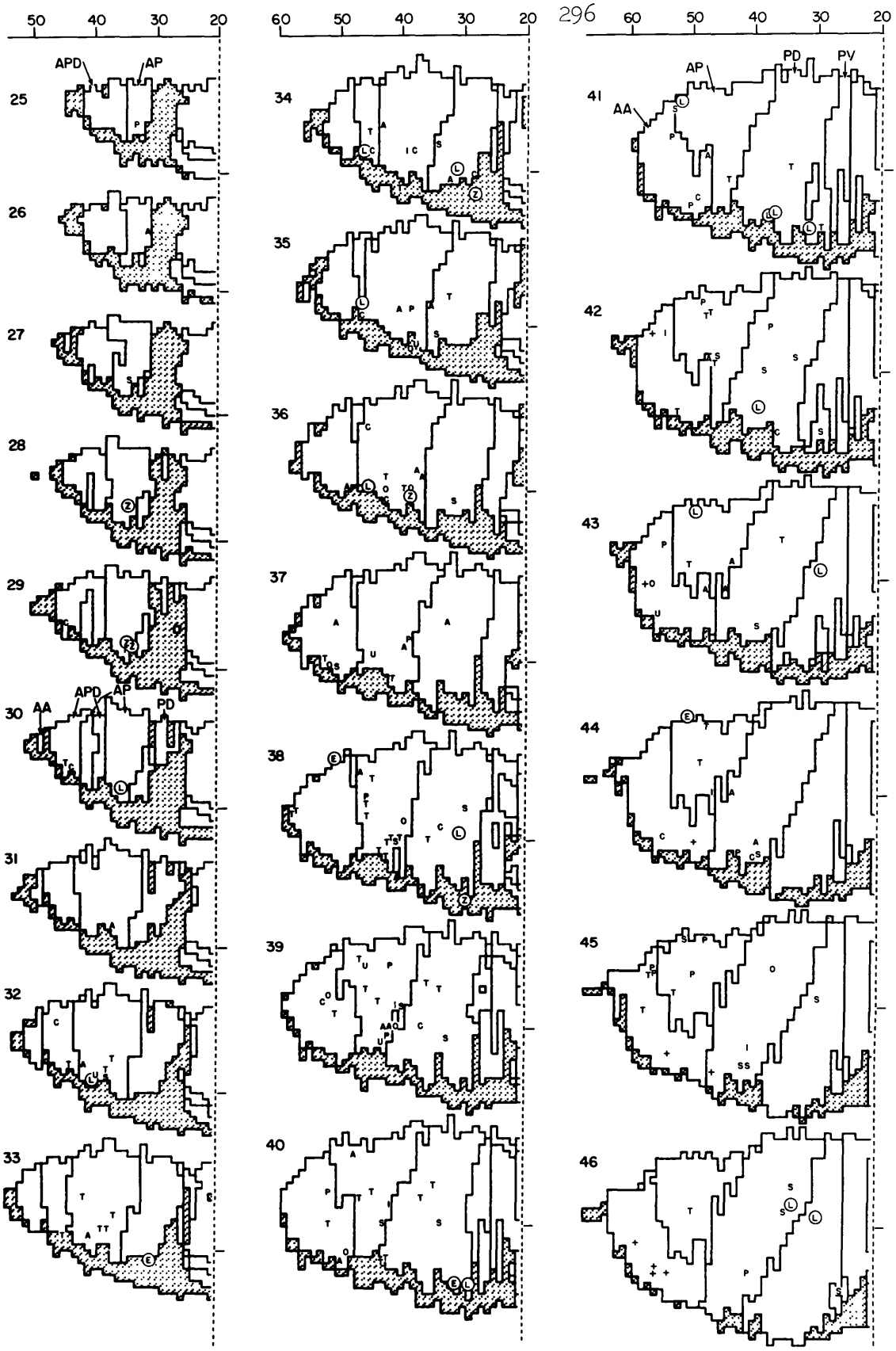
50 40 30 20
APD
AP
25
26
27
28
29
AA
30
31
32
33
60 50 40 30 20
34
35
36
37
38
39
40
60 50 40 30 20
PD
PV
41
42
43
44
45
46

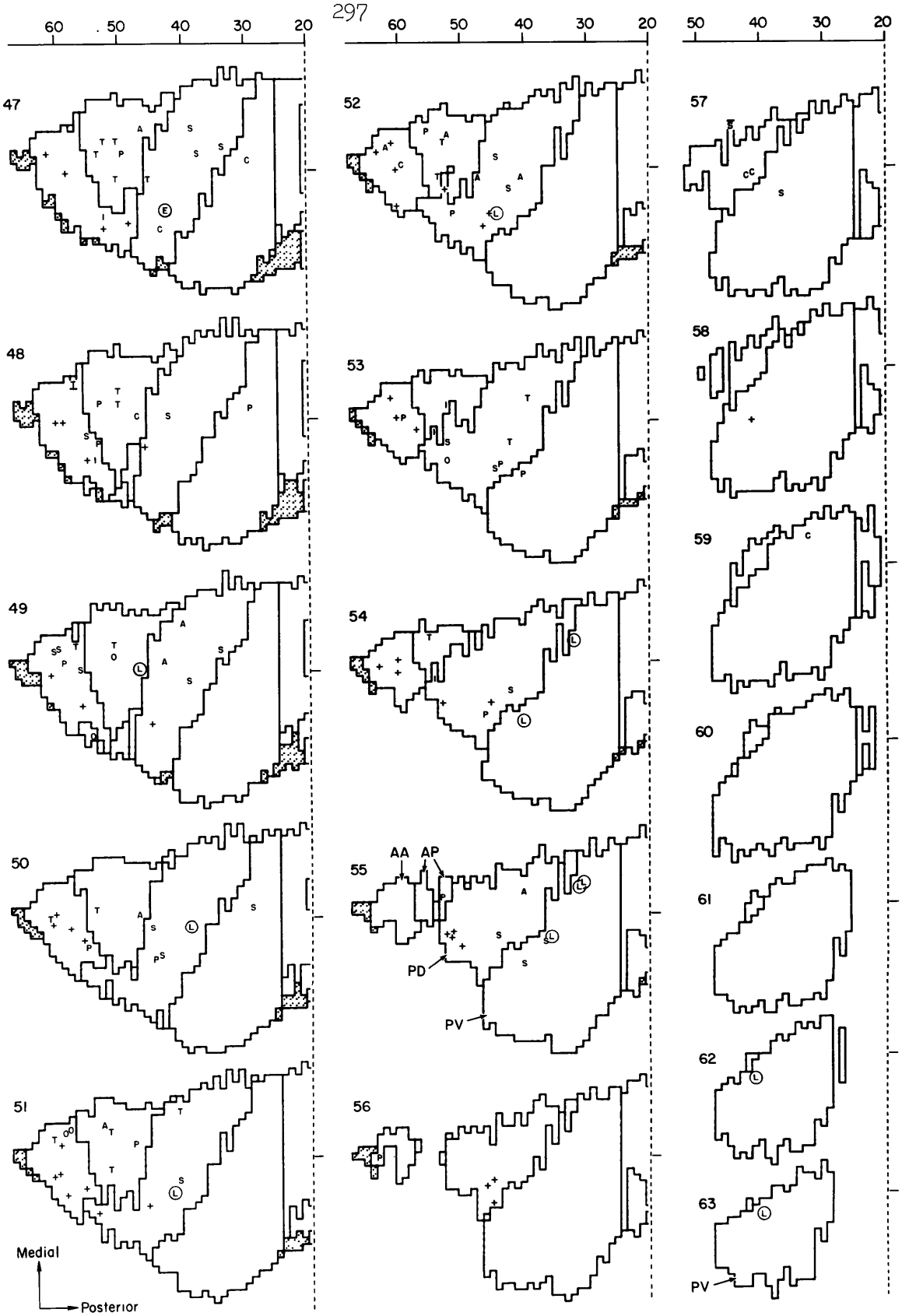
60
50
40
30
20
47
48
49
50
51
52
53
54
55
56
57
58
59
60
61
62
63
AA
AP
PD
PV
Medial
Posterior

was performed with PST histograms mainly for the uncertain cases; thus, the samples for the Pri and Pri-N categories are biased. The distribution of the Prepotential units (mainly Pri and Pri-N units) appeared to be documented by the breakdown by subdivision. There were many Prepotential units in and around AA but there were some even in the most dorsal portions of AP and PD.

The response type categories that appear to have distributions that do not conform with the subdivisions of the AVCN are shown in Figure IV-42 as circled letters. These categories, Chop-L, Pauser and Composite, are frequently located near the dorsal, medial and lateral surfaces and also along the region of the PV-PD border. An exception to this trend is the Chop-L unit in section H49 (at the AP-PD border). The units in the Unusual category also tend to lie near the perimeter of the AVCN. Some of the circled units appear concentrated in the postero-dorsal part of AVCN just adjacent to the granule cell region which lies over PV and between AVCN, DCN and PVCN. This region corresponds to Osen's small cell cap (Osen, 1969b). Furthermore these circled units appear to match, in location and relative density, the small cell distribution shown by Osen in her diagrammatic sections from sagittal, horizontal and transverse series (Osen, 1969b; see also the sagittal section shown in Figure II-2.).

11. Response to Trapezoid Body Shocks

Electrical stimulation in the region of the contralateral superior olivary complex was tried in 33 experiments. The main objective of electrical stimulation in the CNS was to activate antidromically cells in the AVCN by electrically stimulating their axons as they course through the contralateral trapezoid body. This stimulus will be referred to as trapezoid body shocks (TBS).

Shock pulses of controlled current levels were delivered at various electrode depths while the microelectrode recordings were scrutinized for a response during a 5 to 20 msec period following the shocks. Four types of response were observed and interpreted to be either:

1. Antidromic,
2. Synaptically mediated, presumably via descending inputs to CN or recurrent collaterals of CN axons which project into the trapezoid body,
3. Acoustically mediated responses produced by low frequency sound 5 to 10 msec after the shock, or
4. Inhibition of responses to acoustic stimuli. Inhibition of spontaneous activity was never observed for the particular parameters of stimulation and processing that were used. Single shocks delivered at 10/ sec were never observed to produce an obvious reduction of the spontaneous discharge rate either in the overall rate or during a PST histogram of 4 to 20 msec duration except for a brief (1 or 2 msec) reduction of discharges immediately following a response discharge. On only a few occasions were shock bursts used in combination with

long duration PST histograms to test for small changes in the spontaneous rate which might have occurred during or after the shock stimulation. No effect was found.

Of the categories of shock effect defined above, the antidromic response was by far the most commonly observed. Some discussion of categories (2) through (4) will be given in a later section, so it is only necessary here to describe how they were distinguished. Category (4) which involves inhibitory effects is obviously distinct from the others since they all reflect excitation. Category (3) occurred only with low CF units, resembled a delayed click response with multiple peaks in a PST histogram of the discharges and could be masked with a broad-band noise stimulus. Both categories (3) and (4) were easily distinguished from an antidromic response. Category (2) responses, however, can be confused with those of category (1). The best test to discriminate category (2) from category (1) responses is the long minimum interval between an orthodromic and an antidromic discharge as compared to the shorter minimum interval between orthodromic or antidromic spike pairs. The phenomenon of spike collision annihilation for any antidromic spike initiated before a preceding orthodromic spike would have passed the stimulation site will be referred to as the ortho-antidromic spike collision test. In practice, very few units did not exhibit the spike collision phenomenon, there being only three units in category (2).

The spike collision test is not a fool-proof demonstration of the antidromic nature of a response. Theoretically snyaptic activation

via recurrent collaterals of CN neurons with axons passing through the trapezoid body could exhibit an ortho-antidromic interaction due to a collision of action potentials on the axons of the cells which provide excitatory collaterals to the cell being recorded. Use of spontaneous activity or low level continuous tone response reduces the probability of a synchronized discharge of both the cell being recorded and the neurons providing the recurrent contacts. Furthermore, an interaction may simply be due to an orthodromic refractory effect. When the ortho-antidromic interaction time approaches the refractory period of the axon and/or soma, the test results are inconclusive. For instance, some AVCN units have an antidromic latency that is less than 0.5 msec. The interaction time is then on the order of 1 msec which could be simply a refractory effect. As an additional control, the minimum interval between a pair of shock activated discharges of many units was measured. Figure IV-43 shows a plot of the ortho-antidromic interval versus the latency of the presumed antidromic response. Below is a plot of the minimum interval between the spikes produced by a pair of shocks. Although there is a tendency for units with a latency around 0.5 msec to have a shorter interval between successive spikes, the interval is often marginal for the collision test. However, the very short latency of these units almost precluded the possibility of of any synaptic activation via a synapse with a synaptic delay as long as 0.5 msec even disregarding any conduction time to the CN.

Not all shock responses were tested for their antidromic nature by a collision interaction. The collision test was considered the

best criterion and was used as a standard against which the other criteria were validated. All statements that will be made concerning antidromic responses produced by stimulation in the contralateral trapezoid body have been checked with data on units with collision test data. The criteria of a sharply defined current threshold and a stable latency with less than about 0.1 msec change from threshold to at least 2X threshold were always satisfied. The additional property of 1:1 response to high rate shocks (200 to 800/sec) was noted for many units. The probability of a synaptically mediated response being included in this data is considered to be very low. Only 3 units were found to fail the collision test. These units had latencies that were all greater than 2 msec, fluctuating at current levels near threshold, and a decreasing function of current level. These responses were regarded as being synaptically mediated.

11.1 Antidromic response

The questions as to which units project out of the CN, as opposed to being inter-neurons, and where these projections terminate are crucial in any description of the role of the CN. By recording in the trapezoid body (at the midline) Brownell (1975) found single unit activity resembling responses recorded in the AVCN. Since his sample was largely lacking in units of the non-primarylike types seen in AVCN, it may be that these types do not project out of AVCN (or at least not to the midline). However, sampling biases of the electrodes are another explanation. A limitation of recording from the trapezoid body is that the units cannot be related to cells in the various

Figure IV-43 Comparison of ortho-antidromic and shock pair interaction times with the latency of antidromic responses

Both plots show data from units presumed to be antidromically activated by shock pulses delivered to the contralateral trapezoid body. The times were measured at the half-amplitude point on the leading edge of the spikes and estimated to the nearest 0.1 msec. The upper plot displays the minimum time between an orthodromic spike (spontaneous or acoustically activated) and the response to a suprathreshold trapezoid body shock (TBS) plotted as a function of the latency to an isolated shock pulse. The solid line (broken only for data points) represents the situation in which the orthodromic time is equal to 2 times the latency. The lower plot shows the minimum time between the responses to a pair of suprathreshold shocks plotted as a function of the latency to a single shock. The dashed line, which is the same as the one in the upper plot, is an upper bound to the shock pair times and separates the data points of the two plots.

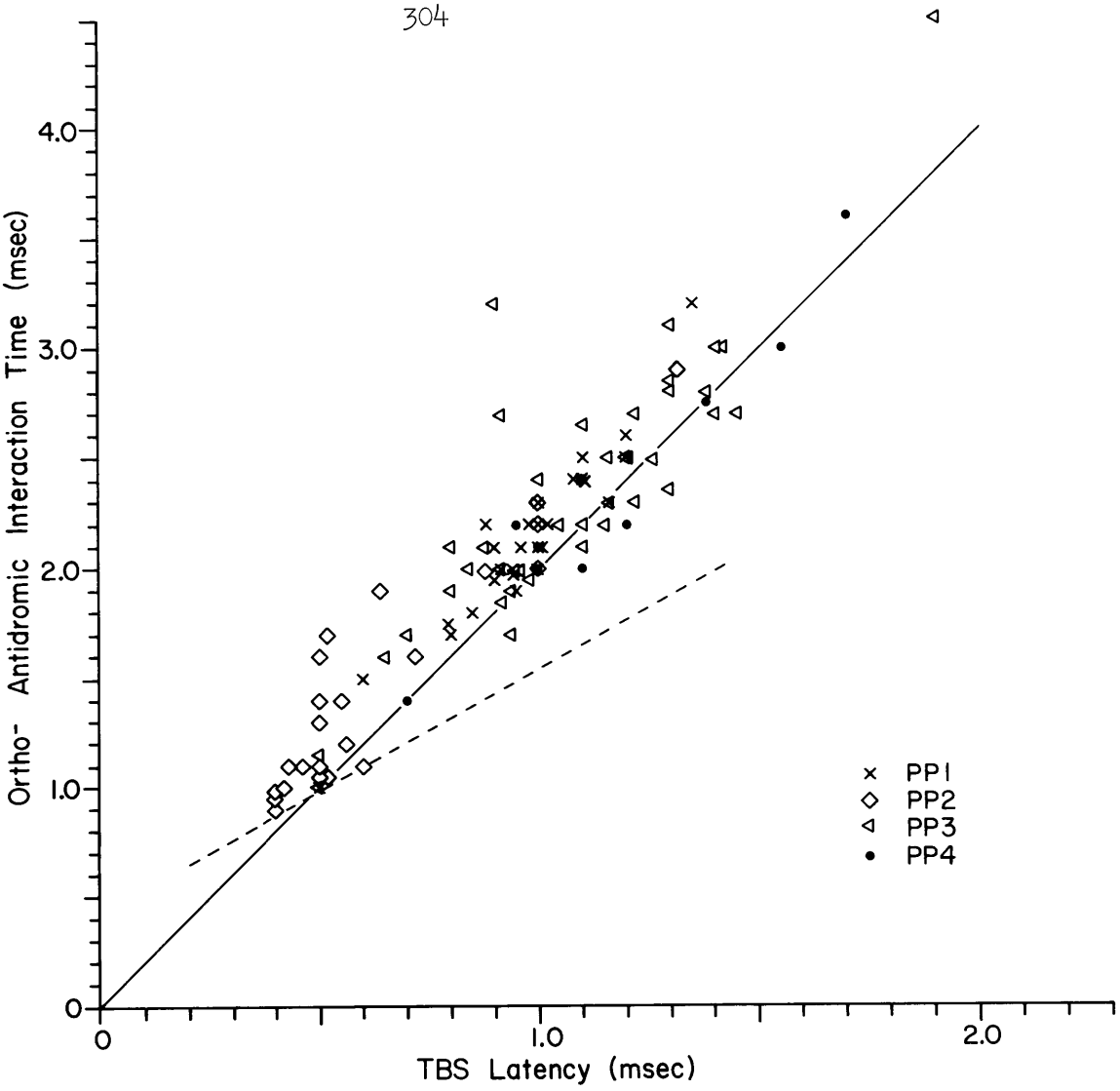
Ortho- Antidromic Interaction Time (msec)
4.0
3.0
2.0
1.0
0
0
1.0
2.0
TBS Latency (msec)
PP1
PP2
PP3
PP4

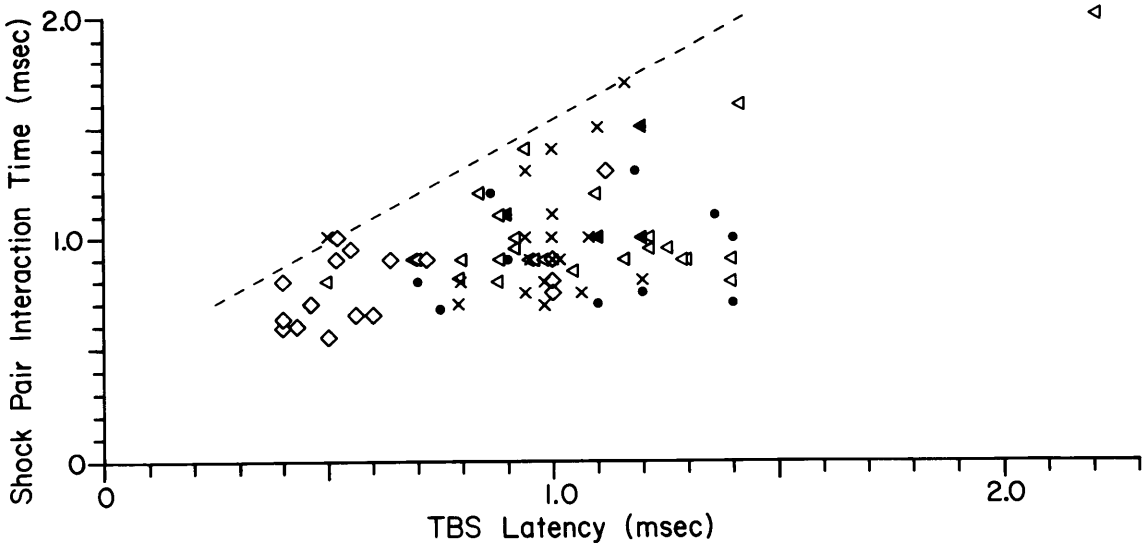
Shock Pair Interaction Time (msec)
2.0
1.0
0
0
1.0
2.0
TBS Latency (msec)

subdivisions of the CN. In this section we shall examine the characteristics of the antidromic response elicited by TBS, since this type of experiment can give decisive information on which units project out of the AVCN.

11.1.1 Unit types

In all of the major categories defined for the AVCN units, except for the PPO units, there are at least some units that were antidromically stimulated. Any category without an antidromically stimulated member was such a small category that the lack cannot be regarded as statistically significant. Some figures on the frequency of demonstrating an antidromic response are tabulated in Table IV-9 for some of the main categories of units used for the AVCN data. These figures must be interpreted with caution. They represent only the percentage for which a response could be clearly identified under the particular conditions of the experiment and are influenced by the care taken in searching for the response. It is probable that many unit responses were not found simply because their thresholds for electric stimulation were high enough that a gross response obscured the single unit action potentials. There was considerable variability between experiments and between passes within an experiment, the success ratio ranging from near zero to almost 80%. The overall average for most categories is close to 30%, being significantly higher for the PP2 units and the Chop-? category (marked with asterisks).

The stimulating electrode was generally placed in the region of

Table IV-9 Units responding to TBS

	Number of units with a response	Total number of units in the experiments	Fraction that responded
PP1	79	361	0.22
PP2	33	62	0.53 *
PP3	88	249	0.35
PP4	88	306	0.29
Pri	27	71	0.38
Pri-N	31	54	0.58 *
Pri-LR	5	10	0.50 *
Chop-?	14	25	0.56 *
Chop-L	3	24	0.13 ←
Chop-S	13	40	0.33
Chop-T	27	66	0.40
On-?	2	12	0.17
On-A	9	31	0.29
On-P	11	23	0.48 *
Pauser	2	3	
Composite	1	4	
Phase-locked	17	46	0.37

the contralateral MSO. If we assume that the conditions of the experiment ensure that neural elements on the ipsilateral (to the CN) side of the brain could not be activated directly by the shocks, then we may conclude that all of the major single unit categories defined for the AVCN have at least some members that correspond to cells with projections that cross the midline. The discussion in Methods, section 2.2, giving the current-distance relationship for the stimulating electrodes provide support for the view that the shock pulses probably would not have stimulated axons on the opposite side of the brain. Even a monopolar electrode under the particular conditions of pulse duration and distance to the midline would have a safety factor of about 4 at a current level of 100 μA. From estimates of the change in the current-distance relationship from a monopolar to bipolar configuration we obtain a relationship with a safety factor of 2 to 3 or better at currents as high as 1 mA.

From the experiments with a 2 mm or larger separation between the stimulating electrode and the midline, we find that all major groups of units in the AVCN (PP1, PP2, PP3; Pri, Pri-N, Pri-LR; Chop-L, Chop-S, Chop-T; On-A, On-P; Pauser and Composite) are represented in the sample of units that were stimulated with current levels of 100 μA or less.

11.1.2 Antidromic latency

Within any group of units there is a range of latencies for antidromic responses. Among the sources of this variation would be

factors related to the types of neurons, different lengths of axons to the cell soma in the CN, and experimental variations in the placement of the stimulating electrode. No discernible correlation of antidromic latency with the variation in distance from the midline could be found in plots of latency versus sagittal coordinate in the block model. Another parameter of the units that may be correlated with the conduction time for antidromic response is the CF of the units. CF has a positional relation to the CN through tonotopic organization and may have a functional relation. In Figure IV-44, the latency of antidromic response is plotted as a function of the CF of the units. Since no CF related latency variation can be seen in the data of Figure IV-44, it seems reasonable to pool the latency data over all CF's for the subsequent analysis.

Most of the physiological parameters discussed in this thesis have shown correlations with the major categorizations of units (prepotential category, response type category, and AVCN subdivision localization). The latency of response to trapezoid body shocks also shows such correlations. As stated previously, the main objective in examining the latency of the antidromic responses is to relate the AVCN recordings with the different components of the trapezoid body, simplistically viewed as made up of three groups, large, medium, and small diameter axons.

Three populations of units illustrate the proposed association of the TBS latencies with the anatomical components of the trapezoid body. The latency distributions of these groups are displayed in

Figure IV-45. Each plot in this figure represents the latencies of units in groups defined by the pp categories and the AVCN subdivisions. Some of the variance in the latencies of any group of units results from the pooling of data. The segregation of the groups was often more distinct in the individual experiments but pooling is necessary to obtain a representation sample for each group. A key reference point in Figure IV-45 is a distinct group of units found in the posterior division. The PP2 units in PV and often those in PD were usually in the Pri-N response type category and in general had the shortest antidromic latencies of all units. Latencies in the 0.4 to 0.6 msec range are almost limited to the (PP2, Pri-N) or (PP2, Phase-locked) units of PV and PD. The largest axons of the trapezoid body are associated with the globular cells of the CN. Since the largest axons would have the fastest conduction velocities, it is consistent that the location of the short latency TBS responses corresponds to the globular cell distribution (in PD and PV). The distribution in Figure IV-45 represents the PP1 units located in the most rostral subdivision of AVCN. Because of the large sample of units from AA, this group is one of the largest with TBS data. The latencies are obviously distributed about 1 msec which is the next longer, common latency after the 0.5 msec latency of the PP2 units of the posterior division. The PP1 units of AA are one of the most likely groups to contribute axons to the medium diameter population of the trapezoid body. The PP1 units form a major component of the units in rostral AVCN which appears to be a source of the medium diameter axons (Warr, 1966). It is

Figure IV-44 TBS latency as a function of CF

The latencies of presumed antidromic responses to the TBS stimulation are plotted as a function of CF for three groups of units, PP1, PP2 and PP3 plus PP4. The horizontal lines through the plots are provided to illustrate the lack of CF dependence. The PP3 plus PP4 plot has a different vertical scale from the others.

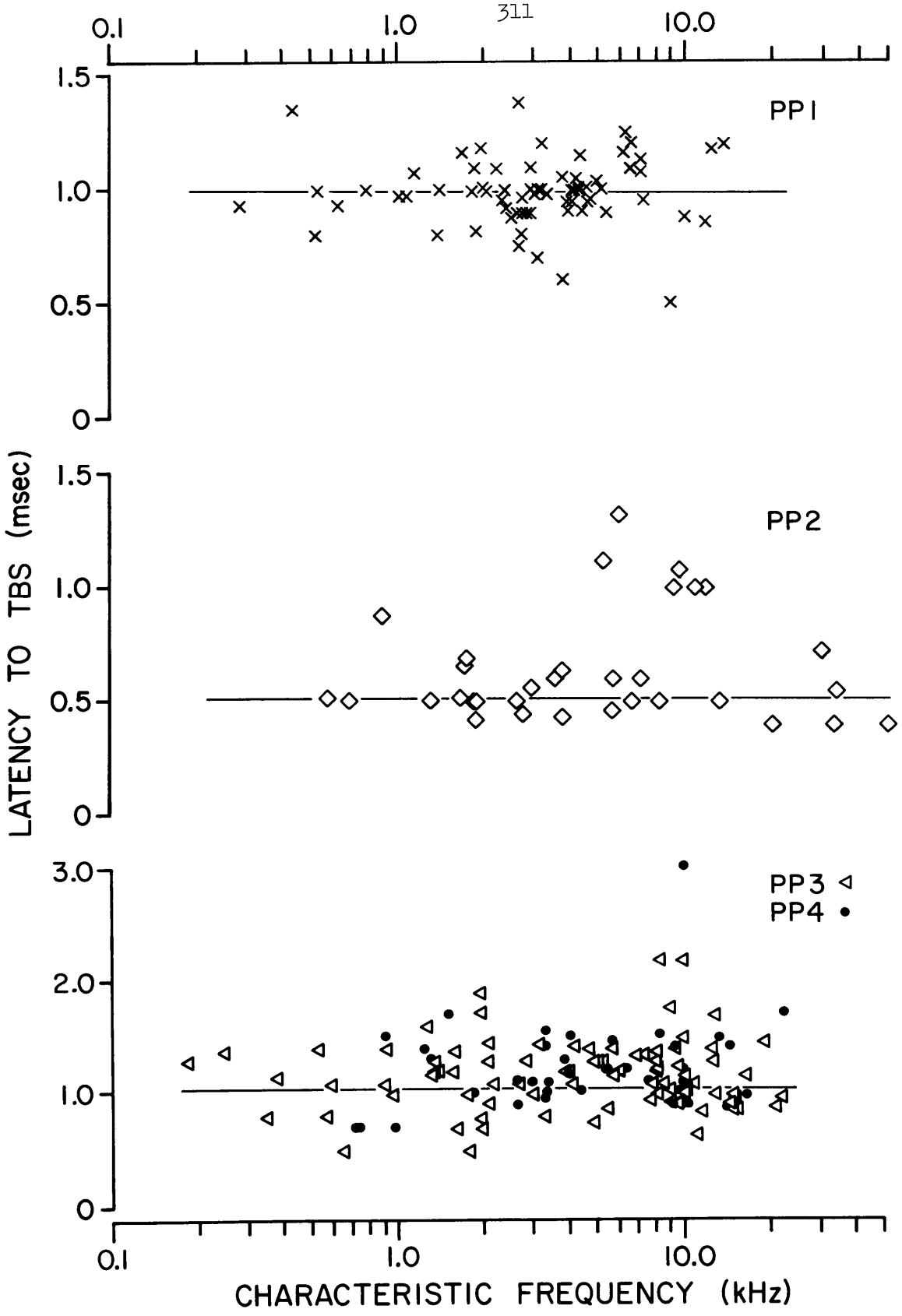
0.1
1.0
10.0
1.5
1.0
0.5
0
PP1
PP2
PP3
PP4
3.0
2.0
LATENCY TO TBS (msec)
CHARACTERISTIC FREQUENCY (kHz)

Figure IV-45 TBS latency distributions according to AVCN subdivision and prepotential category

Histograms of the latency of response to TBS are arranged in a matrix with the AVCN subdivisions represented by the columns and the prepotential categories by the rows. The solid black portion of each histogram represents responses that were shown to be antidromic by the spike collision test. The other units represented in each distribution are presumed antidromic responses that satisfied the less strict criteria of (a) sharply defined threshold, (b) stable latency over a factor of 2 in current levels above threshold, (c) ability to respond to each shock in high rate stimulation. Latency was measured from the onset of the electrical pulse to the half-amplitude point on the leading edge of the dominant peak of the spike. Data from experiment B103 were excluded because the stimulating electrode was at the midline.

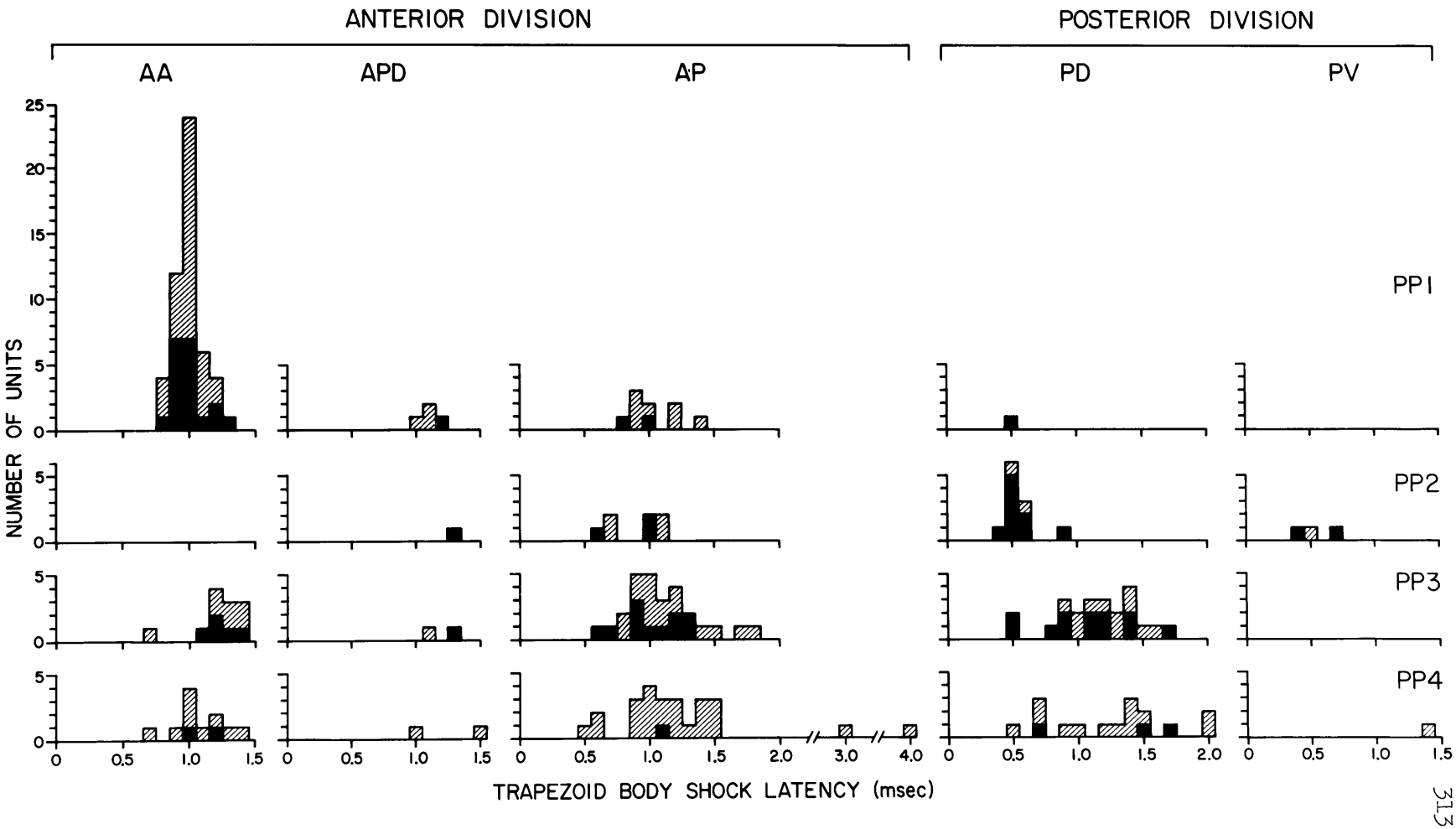
ANTERIOR DIVISION
POSTERIOR DIVISION
AA
APD
AP
PD
PV
PP1
PP2
PP3
PP4
NUMBER OF UNITS
TRAPEZOID BODY SHOCK LATENCY (msec)

also consistent that the shock evoked response recorded at most sites in AVCN shows two prominent peaks, one at 0.5 msec and the other at 1.0 msec, the times at which spikes are most likely to occur for the PP2 units (in PD and PV) and the PP1 units (in AA). (These peaks occurred earlier in experiment B103 when the stimulating electrode was placed at the midline instead of in the contralateral MSO.) Later components of the evoked response were generally small and indistinct - never as well defined as the first two peaks. One possible candidate for the cells of origin of the fine diameter axons in the trapezoid body is the PP3 units of AA. Warr (1966) found degeneration in the trapezoid body after making lesions in the rostral AVCN. The PP3 units in rostral AVCN generally had longer latencies than PP1 units.

Assuming for the moment that the PP2 units of PV and PD and the PP1 units of AA correlate with cells having the large and medium diameter axons, respectively, we shall now examine the complete array of latency distributions for the pp categories and subdivisions (Figure IV-45). Among the PP1 and PP2 units we can see the transition from a latency of 0.5 msec to a latency of 1 msec, with the units localized to AP exhibiting a mixture. The PP3 units, particularly in AP and PD cover a range of latencies that contains range of the PP1 units and approaches the values of PP2 units. The PP3 units with the shortest latencies may even be "PP2 units" for which the pp was too small to be identified. As we shall see later some of the PP3 units with a short latency have an On-P response which is similar to the Pri-N response. But even without these units there is a significant number of PP3 units

with latencies of 0.7 to 0.9 msec. The PP3 groups also have a number of units with latencies which are longer than the majority of the PP1 units. The distributions for the PP4 units might be expected to contain units from all of the other groups. The PP4 plots, however, show a disproportionate number of units with latencies longer than 1 msec. Many of these units were not verified by the collision test to be antidromically activated because the spikes were too small.

Having shown that the prepotential categories provide some ordering of the TBS latency data, we shall now examine the influence of the response type categories. Figure IV-46 shows TBS latencies according to the response type category and the localization to either the anterior or posterior division of the AVCN. The distinction between anterior and posterior divisions is made to demonstrate the group of "Primarylike" units in PV and PD that exhibit very short antidromic latencies. The dashed lines in both plots are provided to emphasize the latencies that are shorter than those of the PP1 units. In the anterior division we find two response types which have latencies below the dashed line. Both of these categories, the Pri-LR and On-P, have some members in the PP2 as well as PP3 prepotential categories. Their latencies are between the shortest latencies of the (PP2, Pri-N) units and the longer latencies of the majority of the (PP3, non-primarylike) units.

Among the Chop and On type units there appears to be no significant difference in latency except for the On-P units, as noted above. Each of the Chop and On response types have a distribution of TBS

Figure IV-46 TBS latencies for the response type categories

Both plots show the latency of presumed antidromic responses to shock pulses delivered to the trapezoid body. The latencies were measured from the onset of the electrical pulse to the half-amplitude point on the leading edge of the dominant peak of the spike. Filled circles represent antidromic responses that passed the spike collision test; the X's represent responses satisfying the less stringent criteria. The dashed lines serve to emphasize the "short" latency responses. Data from experiment B103 was not included because the electrode placement was unusually close to the CN.

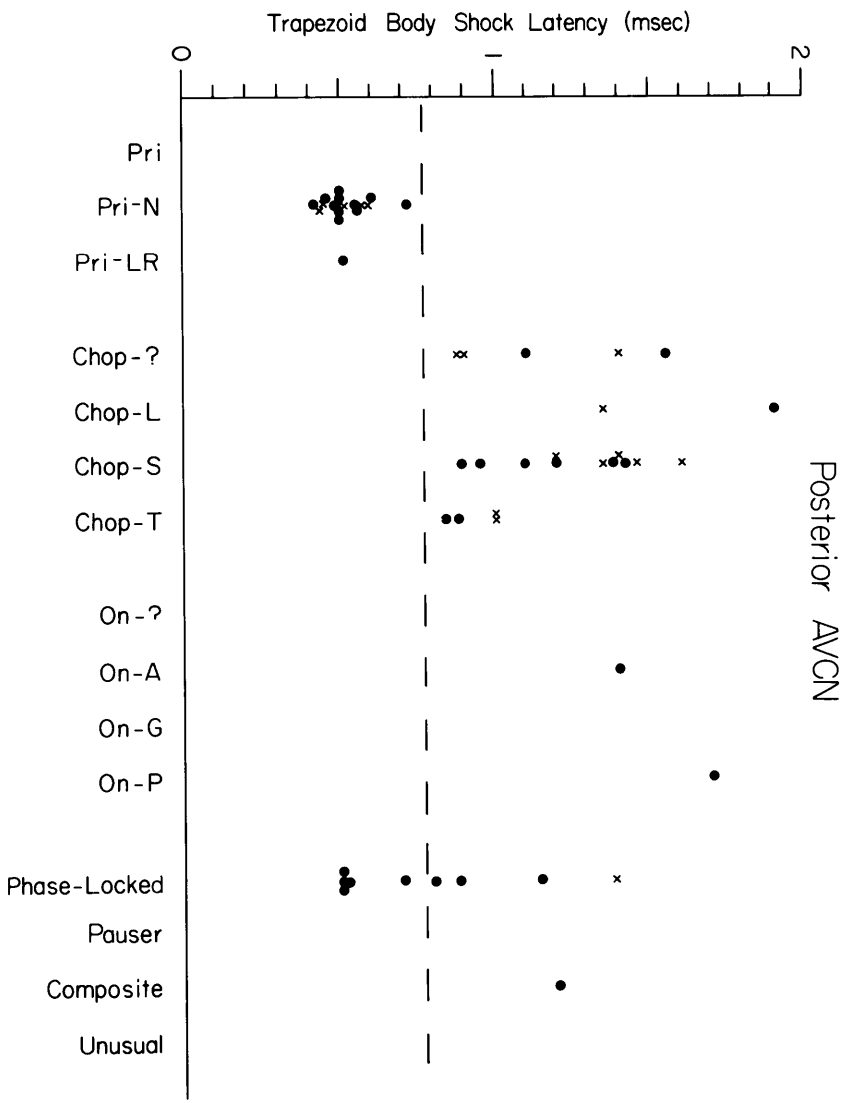
Trapezoid Body Shock Latency (msec)
0
1
2
Pri
Pri-N
Pri-LR
Chop-?
Chop-L
Chop-S
Chop-T
On-?
On-A
On-G
On-P
Phase-Locked
Pauser
Composite
Unusual
Posterior AVCN

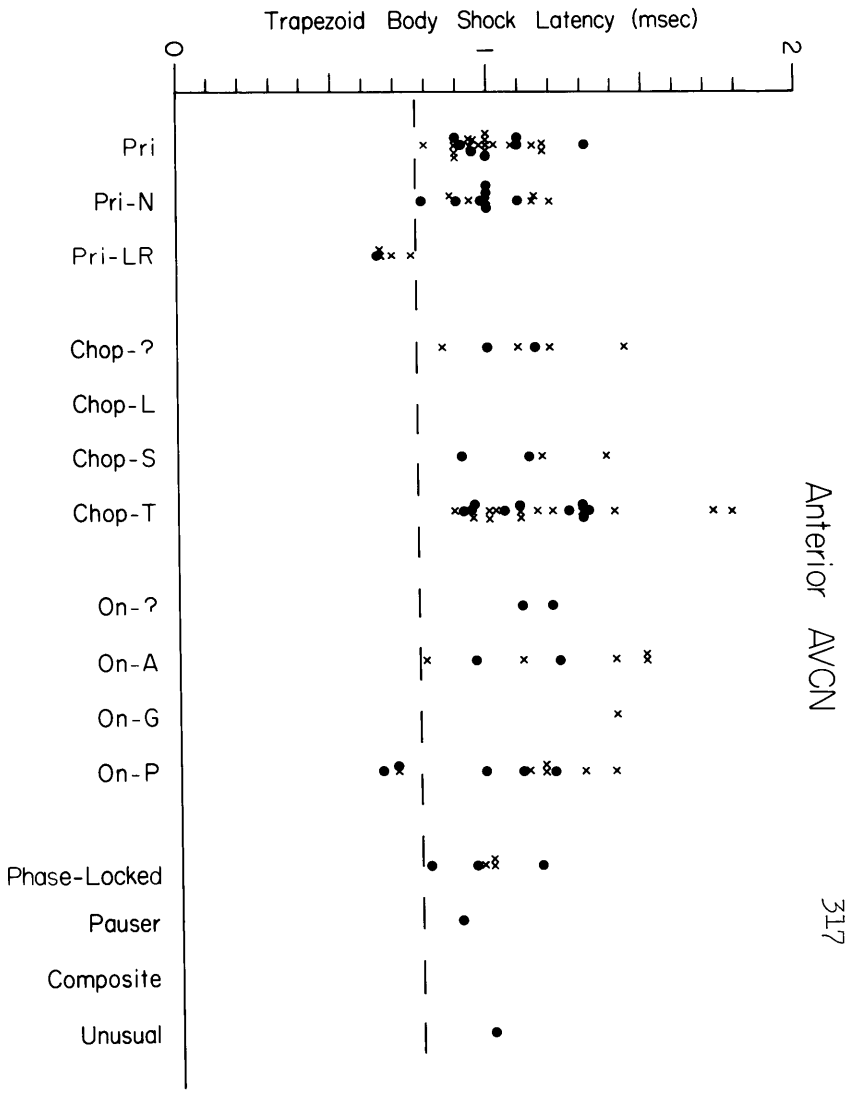
Trapezoid Body Shock Latency (msec)
0
1
2
Pri
Pri-N
Pri-LR
Chop-?
Chop-L
Chop-S
Chop-T
On-?
On-A
On-G
On-P
Phase-Locked
Pauser
Composite
Unusual
Anterior AVCN

antidromic latencies that overlaps with that of the PP1 or Pri units. Almost all of the non-primarylike types, however, have some members with latencies of 1.2 msec or longer. The Chop-T and On-P units have latencies shorter than 1 msec (the mean latency for PP1 units). Two of the Pauser units recorded in this study were electrically stimulated. One was localized to dorsal AP and is included in Figure IV-46; the other was localized to the edge of the AVCN in the granule cell layer. Both units had a latency near 0.9 msec.

Two additional observations on the TBS latencies bear on the uniformity of the response type categories. The Pri-LR units are distinguished from the Pri category on the somewhat arbitrary basis of the lower discharge rate. Figure IV-46, however, shows that the Pri-LR units have systematically shorter latencies than the Pri or PP1 units, thereby providing further support for making the distinction. The other observation is that the On-P category has a rather large range of antidromic latencies and may represent two categories. Some On-P units have been noted to be similar to Pri-N units whereas others are obviously similar to the On-A units; these similarities may represent the type of discrimination that will be necessary to resolve these subcategories.

11.2 Non-antidromic responses

The data regarding shock responses that were not antidromic are summarized in Tables IV-10 and IV-11. As would be consistent with

Table IV-10 Non-antidromic response to trapezoid body shock

Unit	PP	CF (kHz)	Response type	Location	Latency (msec)
B79-16	3	23.1	On-A	AP	2.5 to 3
B91-6	3	14.3	Chop-?	?	3 to 5
B103-13	3	9.31	Chop-S	DCN to AVCN boundary	2 to 2.5

Table IV-11 Suppression of tone burst responses produced by trapezoid body shock

Unit	PP	CF (kHz)	Response type	Location	Response to shock ?
B57-25	3	8.1	On-A	AP	Yes (?)
B59-18	3	0.93	On-A	AA	Yes (Antidromic)
B79-16	3	23.1	On-A	AP	Yes (not Antidromic)
B92-42	3	5.66	On-A	PD	Yes (Antidromic)

a synaptically mediated discharge, the TBS response of each of the units in Table IV-10 had a highly variable latency that decreased and became more stable with increasing current amplitude. The units that exhibited a suppression of responses following TBS stimulation are listed in Table IV-11. None of these units had spontaneous activity and the normal tone burst response was just at the onset (On-A). The TBS caused either a partial or complete elimination of the response to STBCF. In some cases an antidromic response was also present at the current level that elicited the suppression of responses. For unit B59-18 the suppression occurred at current levels both above and below the unit's antidromic threshold. For unit B79-16, there was a non-antidromic response to the TBS followed by a suppression of tone burst responses. Electrical stimulation also resulted in decreases in the discharges of Composite response type units to tone burst stimulation (see Figure IV-15). They were not included in Table IV-11 because of the different form of the effect; only the second component of the response was affected by the TBS.

11.3 Location of stimulating electrode

The stimulating electrode track was determined in the 30 cats with histology available for the contralateral trapezoid body. The lateral-medial variation of the tracks was relatively small since most passes were directed toward the MSO, the main exception being the midline pass in experiment B103. The rostral-caudal positions of the tracks were specified in terms of the point at which the electrode passed through

or came closest to the MSO. Figure IV-47 (left) summarizes the paths of all of the electrode tracks that were histologically verified. As a reference for the electrical stimulation sites in the trapezoid body, a parasagittal cross-section through the trapezoid body was reconstructed for three of the experimental cats at the typical distance of the stimulation sites from the mid-plane (2 mm). Since the MSO was the main landmark used for locating the stimulating electrodes, the outline of the MSO was also projected onto the reference plane. The individual tracks shown in Figure IV-47 (left) are drawn at the nominal angle of the electrode with respect to the ventral surface of the brain and at a position that would have it cross the projected outline of the MSO at the histologically verified position relative to the rostral and caudal limits of the MSO. Attempts to correlate CF, prepotential category, response type category, or rostral-caudal position in the CN with the rostral-caudal location of the stimulating electrode revealed no discernible patterns for the antidromically activated units.

The dorsal-ventral location of the stimulating electrode, however, did influence the unit types that could be stimulated at low current levels. As was described in the Background chapter, the three fiber groups of the trapezoid body are roughly layered across the trapezoid body with a dorsal to ventral arrangement of the components. The dorsal-ventral dimension, however, is the least well specified in an absolute sense because of the difficulty in establishing a reference point in the region of the superior olivary complex.

In most experiments, movement of the electrode was observed to

Figure IV-47 TBS: localized electrode tracks and minimum current sites

The plot on the left shows a summary of all histologically verified tracks of stimulating electrodes. Each line represents one or more tracks as indicated by the experiment number(s) listed at the top of each line. The MSO and trapezoid body outlines represent "averages" from three experimental cats of: (1) the trapezoid body outline at a sagittal plane 2 mm from the midline and (2) the outline of the MSO projected onto this sagittal plane. These outlines were reconstructed from histological sections in the plane of the stimulating electrode (55° from the ventral surface of the brain). The sections were aligned by assuming the ventral surface of the brain to be a straight line in the relevant region.

The right hand plot shows the estimated locations at which the current required to stimulate an AVCN unit was minimized to a current amplitude of 100 μA or less. The procedure used to estimate the stimulation sites is described in the Methods, section 5.7 (see also Figure III-11). The stimulation sites are shown by means of symbols indicating the unit category for the unit stimulated. The symbols are from the standard set (see e.g., Figure IV-25).

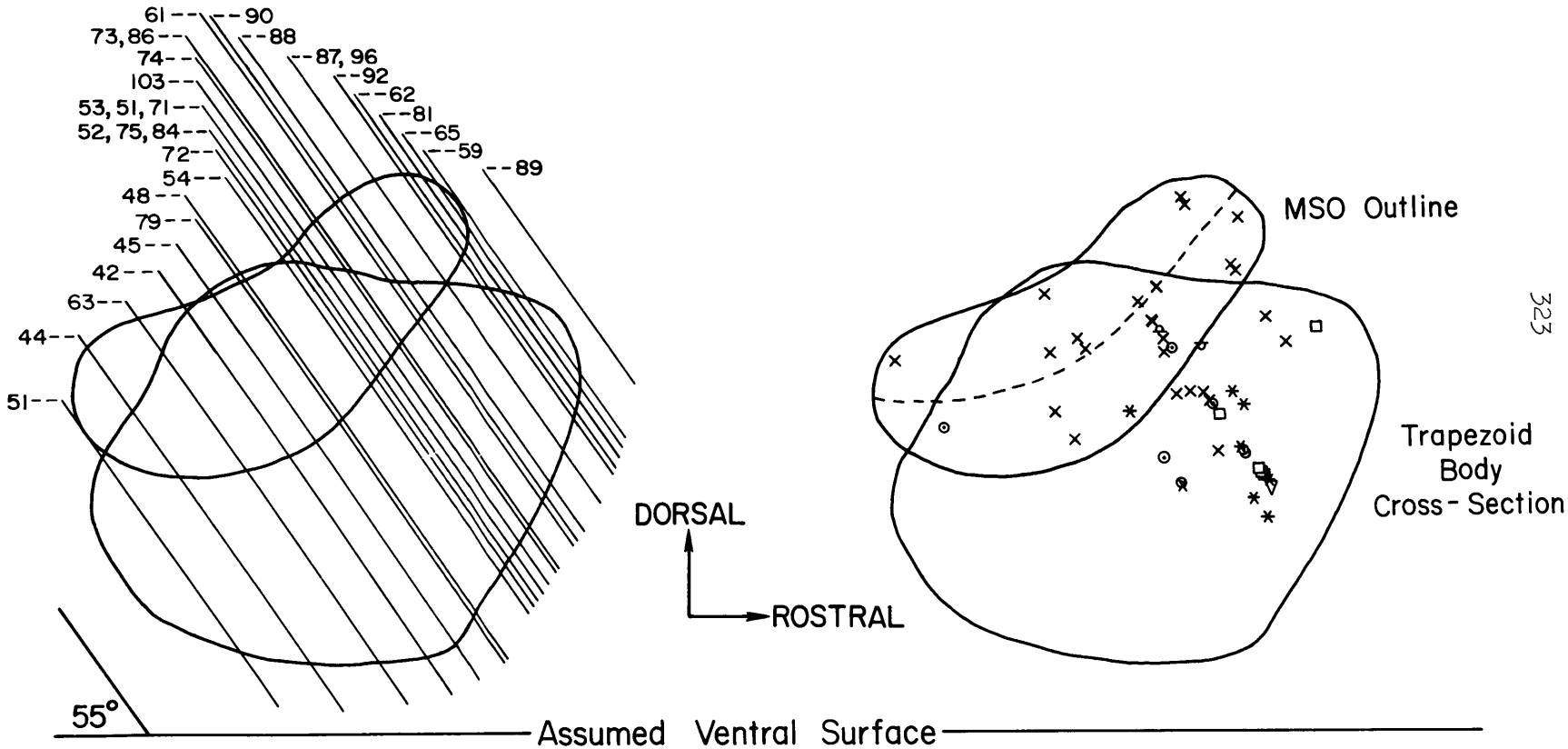
All Stimulating Electrode Tracks
61
90
73, 86
88
74
87, 96
103
92
53, 51, 71
62
52, 75, 84
81
72
65
54
59
48
89
79
45
42
63
44
51
55°
DORSAL
ROSTRAL
Assumed Ventral Surface
Minimum Current Sites
MSO Outline
Trapezoid
Body
Cross-Section

cause reversible changes in the gross potentials evoked by a single shock pulse. With a shock amplitude of 100 to 200 μA, dorsal locations of the stimulating electrode elicited a waveform with a clear peak at 1 msec (negative polarity relative to the headholder); as the electrode was advanced to successively more ventral locations, the peak at 1 msec gradually diminished in size as a peak at 0.5 msec developed. Often the peak at 0.5 msec became larger than the peak at 1 msec. With further advancement of the electrode both peaks decreased with the peak at 0.5 msec decreasing less rapidly. Occasionally some later peaks developed for mid to ventral locations of the stimulating electrode. The electrode depths at which these various peaks were maximal were found to correlate with the locations at which minimum current was required to antidromically stimulate different unit types. In particular the PP1 units were often stimulated with minimum current at the dorsal locations and the PP2 units at more ventral locations. PP3 units were stimulated over most of the middle range of depths. In the pooled data of Figure IV-47 (right) which used the gross response "cross-over" point to plot minimum current threshold locations, the trend is only roughly present. This figure represents the stimulating sites from 11 experiments which had histology of the track and an estimate of the "cross-over" location. The plot is restricted to those units activated by shocks of 100 μA or less. The PP1 and Pri units are found near the level of the MSO. PP3 and Chopper units tend to lie below the MSO. Some PP2 units situated below the level of the ventral edge of the MSO were not represented in this plot because of the high current levels

required to stimulate these particular units.

11.4 Conduction velocity

With the antidromic conduction times available it is possible to estimate the axonal conduction velocities. There are, however, several difficulties which should be stated at the outset. First, the velocity will be an average value. Any attempt to relate it to axon diameter must take into account the change in velocity along the course of the axon. Expansion of the axon as it leaves the soma and any reductions in axonal size as a result of collateral branching can change the axon characteristics. A second problem is the uncertainty in the estimation of the axonal length from the CN to the contralateral superior olivary complex. Finally, when a latency as short as 0.5 msec is to be measured, the latency estimate is significantly affected by such aspects as the position on the spike waveform used for the measurement, the time required for the shock to produce a propagating action potential in the axon and invade the structure which gives rise to the recorded spike. The latencies were measured to the nearest 0.05 msec at the half-amplitude point on the leading edge of the spike. The spike first leaves the baseline about 0.05 to 0.07 msec before this time. We could probably easily justify subtracting 0.1 msec from the measured latencies in estimating conduction velocities. For units with a latency of 0.5 msec this change would represent a 20% reduction in latency.

Considering the uncertainties in the axon length, only one

estimate of the average length for all experiments, except for B103, will be used. For 25 experiments an average distance could be measured from the histological material. The measurement was taken from the middle of the lateral-medial extent of the CN to the midline following the center of the trapezoid body, then from this point to the stimulating electrode track. The CN to midline measure was always based on the contralateral side because the ipsilateral CN was removed for histological preparation. The measured distances, without corrections for shrinkage, ranged from 10 to 13.6 mm with an average of 11.6 mm. Applying a correction for shrinkage (20%) to the trapezoid body we obtain an average axon length of 14 mm for the experimental (TBS) situations. From the estimates of conduction time and distance we obtain a velocity of 35 m/sec for the PP2 units of posterior AVCN and of 16 m/sec for the PP1 units of anterior AVCN.

12. Response to Inferior Colliculus Shock

The experiments in which shock stimuli were delivered in the region of contralateral MSO showed that at least some members of all the major physiological categories of the AVCN single units were antidromically stimulated from this site. It was next decided to test the most distant site of CN projection, the contralateral IC. The type of electrode and stimulus parameters were the same as used for the trapezoid body stimulation experiments. In several of the 9 experiments more than one penetration of the CNIC was made. All of the tracks made by the stimulating electrode passes were shown histologically to pass

through some part of the CNIC in approximately a horizontal plane. The tracks were located preferentially in the ventral half of the CNIC with some close to the ventral surface. Almost the entire lateral-medial extent of the CNIC was penetrated by at least one of the various stimulating electrode passes.

A striking difference from the experiments in which the trapezoid body was stimulated, was the lack of a gross response following current pulses with an amplitude of 100 μA to 1 mA. As described in section 11.3, the trapezoid body stimulation gave rise to a gross response which had negative peaks at 0.5 and 1 msec latencies and on a few occasions broader, lower amplitude components at longer latencies. The evoked-response during IC shock experiments was so small in rostral AVCN that it was usually difficult to see without averaging. In posterior AVCN the gross response was somewhat more noticeable but this may have been simply because the electrode was closer to DCN which always exhibited a large gross response. Throughout AVCN, therefore, shock stimuli to the contralateral CNIC could be set at a relatively high current level as a search stimulus without a gross response obscuring the spikes. Many units with very small spikes were noted during the IC shock experiments probably because the lack of an evoked response allowed small spikes to be distinguished.

In the 9 experiments involving shock stimuli to the contralateral CNIC, 105 units were found to respond to a single shock. Two of these units had latencies which were variable when the current level was set near threshold and exhibited a monotonically decreasing dependence

on current level until a stable, shorter latency was attained. These two units plus a third which responded with a highly variable latency to a burst of shocks will be excluded from the subsequent discussion since they were probably activated synaptically. An additional 13 units were localized to DCN and PVCN. The 89 units from the AVCN that responded to shocks in the CNIC exhibited a wide range of physiological properties and were distributed throughout AVCN. The dispersion of these 89 units over the many categories limits somewhat the conclusions to be drawn from this data. The most striking finding, however, was the total lack of PP1 units from the units that were antidromically activated from the contralateral CNIC. In 9 passes histologically confirmed to have recorded units in AA (and AP) and 5 others in AP only, no PP1 units were stimulated by shocks to the contralateral CNIC. During these experiments 52 PP1 units were carefully checked for a response while the stimulating electrode was moved across the rostral-caudal limits of the IC and current levels up to 1 to 2 mA were used. Interspersed between the non-responsive PP1 units were many units which did respond to the CNIC shocks. As was mentioned above, there were many units whose spikes were too small to permit a determination of the response type or pp category. Of 47 PP3 units that were carefully tested, 24 responded to the shocks. Although a negative result in such an experiment cannot, in principle, be conclusive, the consistency with which the PP1 did not respond and the intervening PP3 and PP4 units often did respond is compelling. During these experiments a variety of stimulating electrode locations were tried in the CNIC

and all gave similar results. It is somewhat uncertain as to whether the PP2 units of posterior AVCN can be antidromically stimulated from the contralateral CNIC. Five PP2 units were carefully tested. Four could not be stimulated, the fifth exhibited an unusual response. This unit responded at either 6 or 8 msec latency depending on the current level; when the collision test was applied the response to the shock did not go from 100% response to 0% over the usual 0.1 to 0.2 msec change in interval between the orthodromic and antidromic spikes, but was instead more gradual. The shock response eventually did fail, however, suggesting that it may be an antidromic response after all.

Units that showed antidromic responses to the CNIC shocks are plotted in the latency histograms of Figure IV-48. The units that satisfied the collision test are represented by shaded squares. The shortest latencies, 1.15 to 1.8 msec, were found mainly in DCN and for an AVCN Pauser. It is interesting to note that the large gross response recorded in DCN had a negative peak at about 1.5 msec after the shock. The distribution of latencies for the AVCN (and PVCN) units peaks around 2 to 2.5 msec and falls off toward 3 to 4 msec. There may be another group at about 6 msec. With units at 10 and 12 msec latencies we see that there is a 10:1 ratio in the possible conduction times between the CN and the contralateral CNIC.

Also contained in the histograms of Figure IV-48 are the response types of the units that responded to the shocks. There is one or more representatives of each of the Chopper types, the On-? and -P types and the Pauser type ; except for the Pauser, each of the above response

Figure IV-48 Response to inferior colliculus shocks

Latency distributions are plotted for three groups of units stimulated by shocks to the contralateral inferior colliculus. The upper plot contains data for units localized to AA, the middle plot the rest of the units localized to the AVCN, and the bottom plot units localized to the DCN. Latencies were measured from the onset of the electrical pulse to the half-amplitude point on the leading edge of the dominant peak of the spike. Each block in the histograms is coded for response type categories using the standard symbol set (see, e.g., Figure IV-25). Shading indicates the responses that were verified to be antidromic with the spike collision test. The other (unshaded) responses were probably also antidromic.

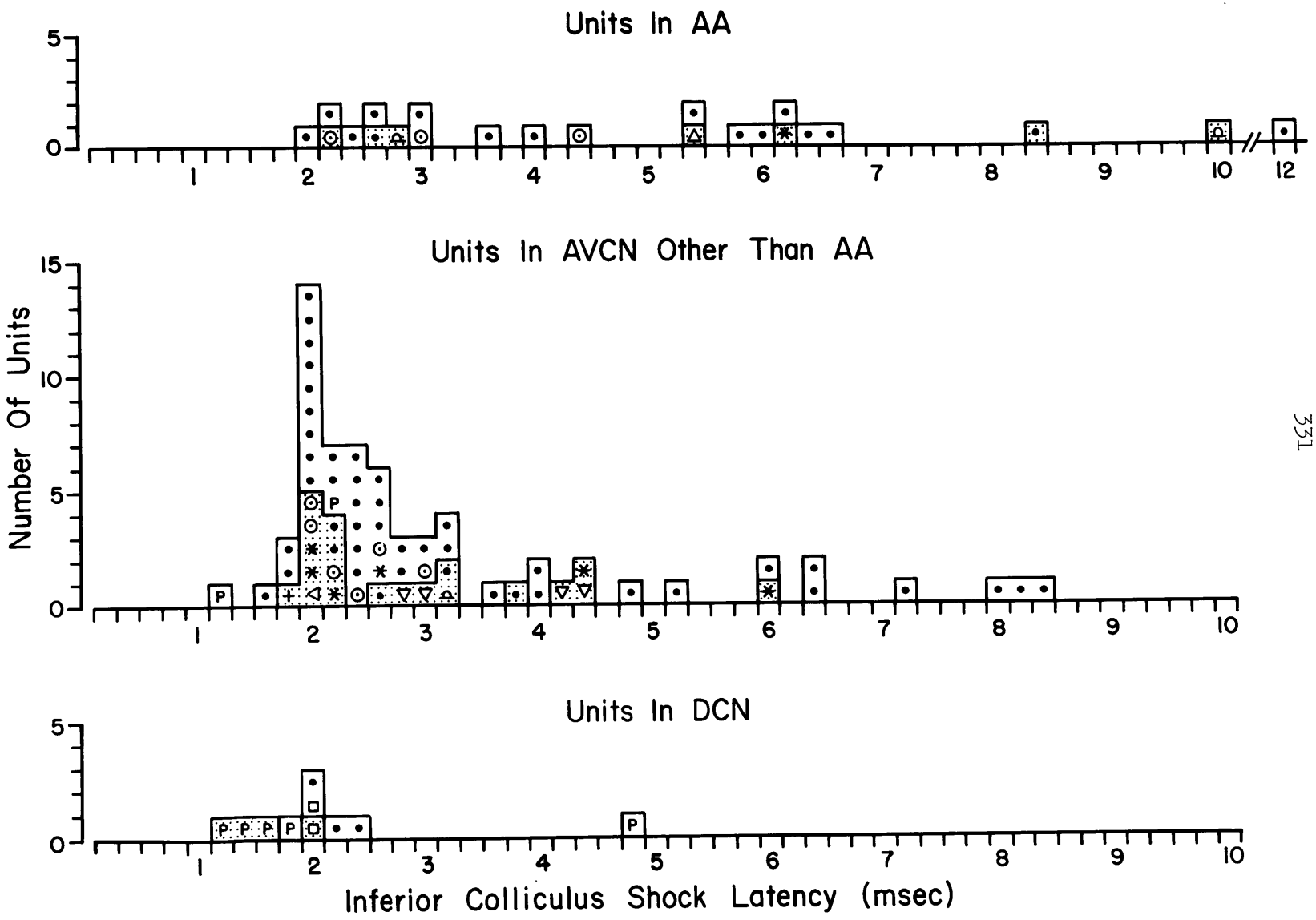
Units In AA
5
0
1
2
3
4
5
6
7
8
9
10
12
Units In AVCN Other Than AA
Number Of Units
15
10
5
0
P
1
2
3
4
5
6
7
8
9
10
Units In DCN
5
0
P P P P
P
1
2
3
4
5
6
7
8
9
10
Inferior Colliculus Shock Latency (msec)

types had at least one unit that was confirmed by the collision test to be antidromically stimulated. Two Composite units were shown to have the late component depressed by the CNIC shock in the same manner as documented for trapezoid body shocks (see section 3 and Figure IV-15).

The locations within the CN of units that responded to the shocks to the CNIC are probably determined more by the particular microelectrode passes than by any inherent regional distribution. The units appear in the present data to be uniformly distributed throughout the AVCN. The localized units which responded to shocks in the contralateral IC were distributed as follows:

1. AA 25
2. APD 1
3. AP 12
4. PD 13
5. PV 13.

CHAPTER V

DISCUSSION

Most of the discussion will focus on an attempt to integrate the current anatomical and physiological observations of AVCN. The organization will therefore differ from that of the Results chapter and as a consequence much of the data will not be discussed specifically, although most will be considered as they contribute to the development of particular ideas.

1. Prepotential Units

It appears to be possible to recognize the extracellular signs of bushy cell discharges by the presence of a prepotential before the spike. If one accepts the evidence that the prepotentials correlate with the activity of end-bulbs, then, the presence of a prepotential would identify a unit as being a cell that receives an end-bulb. Brawer and Morest (1975) and Lorente de Nó (1976) claim that the end-bulbs of the AVCN appear to contact only bushy cells. If this is so, then the presence of prepotentials would also correlate with bushy cell activity.

1.1 Prepotentials as end-bulb responses

The association of pp's with end-bulbs is directly supported by evidence from the PP1 units of rostral AVCN. The PP2 units, located mainly in the posterior division, represent a consistent extrapolation of the argument based on the PP1 units. Pfeiffer (1966b) suggested

that the pp was of presynaptic origin mainly because of his observation that the pp persists after the negative spike, thought to be postsynaptic, was eliminated by moving the microelectrode. Li and Guinan (1971) provided more direct proof of the presynaptic origin of the pp in the MNTB by demonstrating that the antidromic invasion of the "complex waveshape" units interacts with the spike but not with the pp. Similar experiments were performed in the present study of AVCN units with similar results.

The end-bulbs in the AVCN are reported to arise from AN fibers and therefore the time patterns of prepotentials, particularly the negative pp units (PPO), should resemble those of AN fibers, as indeed they do. The discharge patterns to STBCF for the PPO units were either Pri or Phase-locked. The distribution of the rates of spontaneous activity for the PPO units closely resembles that of the AN. The latencies of prepotentials in response to clicks are similar for the PPO and PP1 units and are shorter than the latencies of the negative (postsynaptic) component of PP1 units. When a short current pulse is delivered to the cochlea the spike discharges of AVCN and PVCN units have latencies of 0.9 to 1.5 msec whereas the pp's of the PPO and PP1 units have latencies of 0.5 to 0.6 msec. This latter range is only a few tenths of a millisecond longer than the latency of the auditory-nerve fiber responses recorded in the internal auditory meatus (Moxon, 1967).

Based on the evidence outlined above, we suggest that probably all pp's originate from the large endings of the auditory nerve. In the recordings from rostral AVCN we note that the prepotentials:

(1) are relatively large (usually within an order of magnitude of the postsynaptic spike).

(2) appear to be unitary in size and shape, and

(3) are followed by a postsynaptic spike with a stable latency of about 0.6 msec (a delay consistent with a chemical synapse).

The only PP1 units that showed a latency variation greater than about 50 msec were the exceptionally small number of units with a second component that fractionates as shown by Pfeiffer (1966b) and in Figure IV-2 (such behavior in some cases at least appeared to be the result of injury of the cell by the microelectrode).

Thus for the PP1 units and possibly for the PP2 units, a unitary event at an end-bulb appears to result in a pp and is generally associated with the discharge of the postsynaptic cell. The latency of the postsynaptic spike with respect to the pp is so short and stable as to suggest that coincident with the PP is a dominant synaptic input capable of discharging the cell without the need for summation of inputs. Further support for this conclusion comes from a comparison of the physiological properties of Prepotential units in regions known to have different sizes of large endings. In the MNTB, the very large calyces apparently give rise to large pp's with a stable 1 to 1 relationship between the pp and spike (Li and Guinan, 1971; Guinan et al, 1972a,b). In AA, where the end-bulbs of Held are smaller than the calyces, some of the spike waveforms of the Prepotential units are similar to those of units in MNTB but most have a smaller pp. In PV, where the modified end-bulbs are noticeably smaller, the pp's are often

detectable only by averaging and in the few cases when individual pp waveforms could be seen, the latency between the pp and the spike was often variable (suggesting a less effective synaptic input to the cell). Thus the different amplitudes of prepotentials parallels the different sizes of endings in each of the regions, and both seem to correlate with the effectiveness of the ending in producing a post-synaptic spike discharge.

Having concluded that the pp's represent the discharges of end-bulbs, we still need to ask whether end-bulb activity must necessarily produce detectable prepotentials. Such a question depends in part on the sensitivity of detecting prepotentials. Almost 90% of the PP1 units in AA were identifiable without the use of special pre-spike displays or averaging. Only 1 in 40 of the Prepotential units in AA had a pp so small that averaging was required for identification (i.e., PP2). From the distribution of pp sizes found for units in AA, it appears unlikely that any unit with a pp would have been mistakenly categorized as PP3. In the more posterior subdivisions the ratio of PP2 to PP1 units increases until in PV it is strongly in favor of units with a small pp. In PV, it is less certain that all pp units would be identified as such, and, in fact, some units that probably should have been placed in the PP2 category may well have been assigned to the PP3 category. Based on the correlation of PP2 unit identification with their other properties, it is estimated that probably less than 10% of the possible PP2 units could have been classified as PP3. Thus we can see that the full sensitivity of the tests for the presence of a pp is required for only a small percentage of Prepotential units.

If an end-bulb or a complex of synchronously activated endings has an excitatory influence that is sufficiently effective to produce a strong correlation of the discharge of the postsynaptic cell with each spike input to the ending, then it is easy to see how the spike waveform of that cell would exhibit a pp. If the effect of the endings is inhibitory or only weakly excitatory, however, a pp would not be expected. All of the categories for Prepotential units (i.e., PP0, PP1 and PP2) implicitly assume an excitatory role for the structure that produces the pp, since, by definition, a pp precedes a spike (PP1 and PP2 units) or at least a diminutive "spike" (some PP0 units).

In the MNTB and sometimes in AA there is a large extracellular potential associated with an end-bulb; the discharges of these endings can be individually distinguished (i.e., isolated) so that displays and computations can be triggered from them. In these cases, it is possible to verify that strong inhibitory effects are not produced by end-bulbs. They are found to be either excitatory with a postsynaptic spike approximately 0.6 msec after each discharge of the end-bulb or else there is no following discharge as can occur when the postsynaptic cell has been injured by the microelectrode.

For many Prepotential units in the AVCN and particularly those in the posterior division, the extracellular potentials from end-bulbs are so small that a positive correlation with a postsynaptic spike is required to identify the pp. Under these conditions, it is not possible to test directly for an inhibitory effect of an end-bulb. Indirect evidence, however, supports the extrapolation that all end-bulbs are excitatory. Shock stimulation of the cochlea, which would

presumably discharge all end-bulbs, was not found to produce an immediate suppression of discharges for AVCN units other than a refractory period after each discharge. In posterior AVCN, the end-bulbs contact bushy cells, which are probably the same as Osen's globular cells. The globular cells are the probable source of the large diameter axons in the trapezoid body. The correlation in PV of units having a pp (PP2) with units having the short antidromic latencies suggests that at least one end-bulb on each globular cell is excitatory.

Do some end-bulbs have such a weak influence on the discharges of the postsynaptic cell so as to not result in a pp? This question cannot be conclusively answered at present. Whether end-bulbs are qualitatively different in effect or merely form a continuum with the boutons is unknown. The small end-bulbs commonly found in posterior AVCN, however, provide a test situation. In PV and PD the (modified) end-bulbs still appear to produce detectable prepotentials for most of the "Primarylike" units. Thus, except possibly for some unusually small or ineffectual end-bulbs, most are probably detected by the pp tests.

The correlation of the pp categories with the response type categories provides further evidence that Prepotential units constitute a distinctive population that corresponds to cells receiving end-bulbs. From the large number of synaptic contacts that each end-bulb forms with the AVCN cells (Lenn and Reese, 1966), we might expect that the discharges of the end-bulb(s) would dominate the discharge pattern of the postsynaptic cell. Thus the fact that units with a

large pp have primarylike discharge patterns is only to be expected. The response of units with a small pp is also primarylike or else close to it (Pri-N, Pri-LR and a few On-P that have a response which is similar to some of the Pri-N units). What is more, the converse appears to be true. Essentially all units with a generalized primary-like response (Pri, Pri-N, some Pri-LR and, of course some Phase-locked) had a pp. The small number of units that represent exceptions to the exclusive association of Prepotential units with a generalized primarylike response can be viewed as minor deviations. For example, (1) there were PP3 units that probably should have been PP2, (2) the Pri-N response form represents a small, predictable change from Pri when the convergence ratio for end-bulbs increases (see section 1.3, paragraph 2), and (3) the few PP2 units in the On-P category have the primarylike with a "notch" response pattern but with a very low rate after the "notch."

1.2 Prepotentials as inputs to bushy cells

Do end-bulbs contact only bushy cells? This final step in the association of pp's with bushy cells is an anatomical issue which has been tentatively answered affirmatively (Brawer and Morest, 1975; Lorente de No, 1976). Some physiological observations reinforce this view. In AA where most cells are bushy cells (large spherical cells) 85% of the units studied had a pp and at least half of the exceptions were localized to sites within several block model units of the borders of AA. Furthermore, the results from electrical stimulation of the IC suggest that the Prepotential units of the rostral AVCN do not

project to the contralateral CNIC. Since there is anatomical evidence (Adams, 1976) that cells receiving end-bulbs in rostral AVCN do not project to the contralateral IC, the association of the pp with the end-bulb and bushy cell seems established, at least for the rostral part of the AVCN.

In several anatomical studies the globular cells of caudal AVCN (PV, PD) have been implicated as being the origin of the large axons in the trapezoid body which give rise to the calyciform endings in MNTB (Harrison and Warr, 1962; Harrison and Irving, 1965; Osen, 1969b). The discharge patterns presumed to be recorded from the calyces have been shown in Guinan et al. (1972a, b) to be of the Pri-N and Pri forms except when the pattern is obscured by Phase-locked responses. The PP2 units in PV and PD have the same response characteristics, so that the globular cells are most likely the target cells of the modified end-bulbs in the posterior AVCN. Since Osen's globular cells are probably bushy cells, the Prepotential units are again linked with bushy cells receiving end-bulbs. It is concluded, therefore, that with the possible exception of PP0 units, the Prepotential units represent recordings from bushy cells. By elimination, then, most PP3 units are probably recorded from stellate cells.

The Prepotential units (bushy cells) are not, however, a homogeneous population throughout AVCN. The PP1 versus PP2 distinction, although defined somewhat arbitrarily, appears to correlate with location in AVCN in a manner that fits with the end-bulb versus modified end-bulb distinction suggested by Brawer and Morest (1975).

In the rostralmost part of AVCN (AA) the Prepotential units are essentially all of the PP1 type, whereas in the posterior extreme

(PV) the Prepotential units are mainly PP2 (see Figure V-1). The shift in the unit distribution from PP1 to PP2 on moving posteriorly might be gradual but the change from AP to PD suggests a rapid transition in the region of the boundary between the anterior and posterior divisions. In fact, given the estimated ratios and the inherent errors in unit localization, the ratios may be as high as 10:1 in favor of PP1 in AP and 10:1 in favor of PP2 in PD. Paralleling this change in the size and reliability of the pp is the abrupt change in antidromic latency from 1 msec for the PP1 units of the anterior division to 0.5 msec for the PP2 units of the posterior division. This is a change which is consistent with the PP1 units in AA representing Osen's large spherical cells and the PP2 units in PV and PD representing Osen's globular cells. The large spherical cells probably provide many of the dorsally located, medium diameter axons in the trapezoid body (Warr, 1966), whereas the globular cells probably provide most if not all of the large diameter axons (Harrison and Warr, 1962; Harrison and Irving, 1966; Osen, 1969b). The small number of Pri-LR units, found mainly in or near AP, may represent an intermediate variety of bushy cell, since the antidromic latencies for these cells were intermediate between those of the Prepotential units in the AA and PV subdivisions.

1.3 Prepotential units as primarylike units

Although almost all PP1 and PP2 units exhibit a generalized primarylike response, some of the PP1 and many of the PP2 units had discharge characteristics that were distinguishable from those of AN

Figure V-1 Regional distribution of unit types

(A) Relative representation of PP1, PP2 and PP3 categories in the four main subdivisions of the AVCN.

(B) Estimated distribution of response types. The "Pri" category, based on the correlation of pp units with primarylike response types, is given by the ratio of the number of (PP1 + PP2) units to the number of (PP1 + PP2 + PP3) units. The remaining fraction of each subdivision is divided among the Chopper group, the On group, and the "other" types (Pauser, Composite, Unusual).

(C) The relative numbers of Chopper and On units.

(D) The relative numbers of Chop-S and Chop-T units. The anterior and posterior subdivisions were combined to increase the sample of units. There may be a variation within each division but the small number of units precludes such a conclusion.

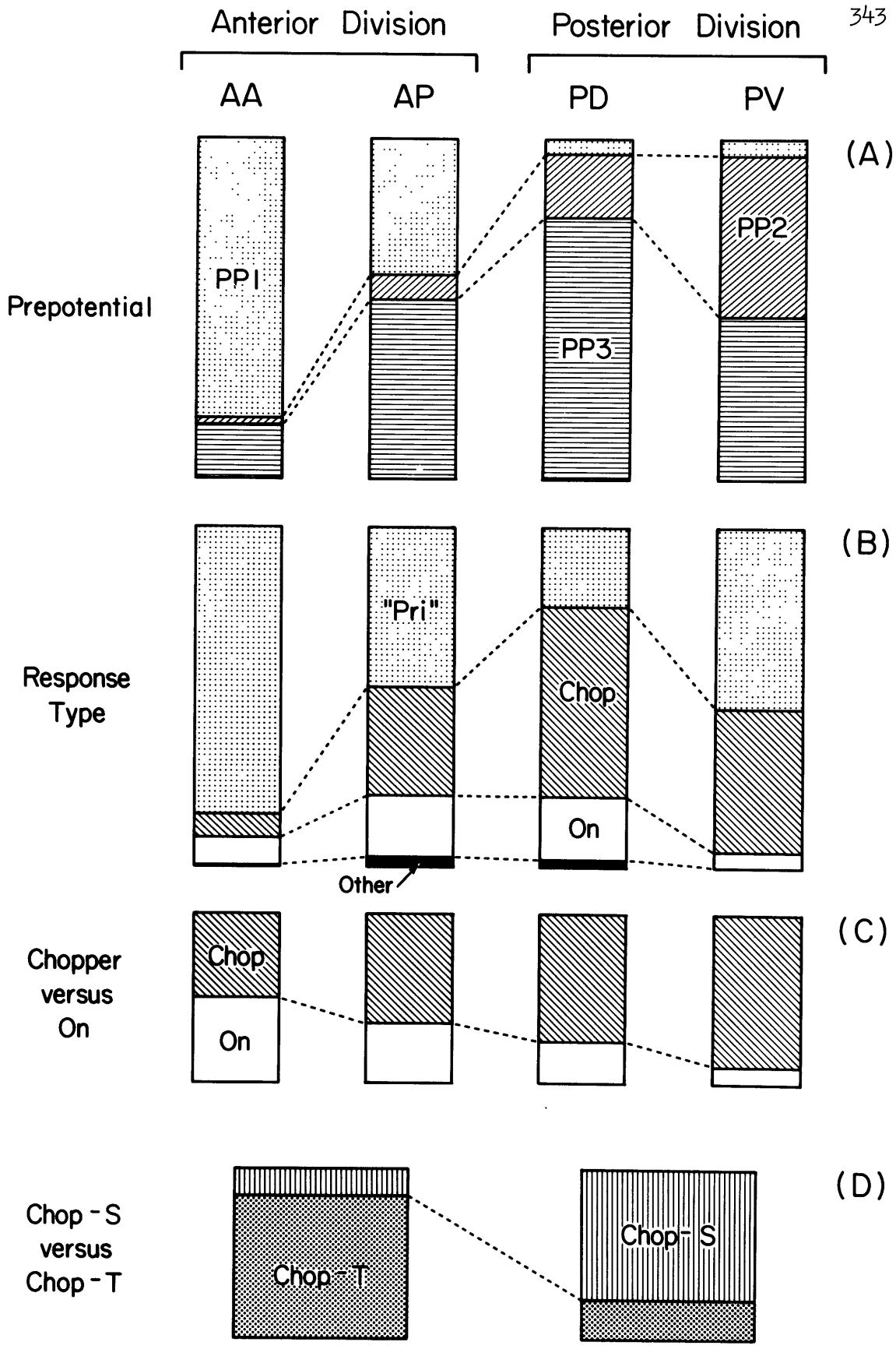
Anterior Division
Posterior Division
AA
AP
PD
PV
(A)
Prepotential
PP1
PP2
PP3
(B)
Response Type
"Pri"
Chop
On
Other
(C)
Chopper versus On
Chop
On
(D)
Chop - S versus Chop - T
Chop - T
Chop - S

units. It may well be that more extensive examinations of the responses will reveal further differences.

Approximately 10% (maybe as many as 20%) of the PP1 units have a Pri-N response to STBCF. It is conceivable that a small percentage of AN units might exhibit a "notch" in PST histograms of their response to STB. The occurrence of the Pri-N response form, however, is fully consistent with the proposed interpretation of the physiology of bushy cells. Based on the anatomical descriptions that several end-bulbs terminate on a bushy cell and the physiological evidence that each of these endings is probably capable of discharging the cell, the resulting activity of the cell would be expected to reflect the summated or superposed activity of the AN fibers providing the end-bulbs. A "notch" appears in PST histograms when the first spike of the response occurs with a probability close to 1 in a time interval about equal to the cell's refractory interval. The refractory period is then evident in the PST histogram as a gap or "notch" after the initial peak. When the summated input activity to a bushy cell is sufficiently large, the first spike will occur over a narrow time range and a "notch" will appear. On the basis of typical PST histograms of AN responses to tone burst (e.g., Kiang et al., 1965a), it can be shown that the convergence of only 2 to 4 AN fibers with average to above average discharge rates could produce a Pri-N response. The sizes and probably the number of end-bulbs terminating on a bushy cell varies along the rostral-caudal dimension of the AVCN, so that in AA there may be only 1 or 2 end-bulbs per cell, whereas in PV the number would be larger. Paralleling this variation in the afferent

input, the change in the relative frequency of Pri and Pri-N units is a consistent physiological correlate.

One of the few other examples of a distinguishable deviation from AN characteristics shown by individual PP1 units was the low maximum synchronization index found for two PP1 units. These two units, recorded in different experiments, had an additional common property of a very small (negligible) change in discharge rate for the continuous tone stimulation.

Other deviations of the characteristics of PP1 units from those of AN units were found only by examining the population distributions with respect to particular parameters. For example, very few PP1 units have rates of spontaneous activity below 5 spikes/sec whereas a significant fraction of AN units do (Kiang et al., 1965a; Kiang et al., 1970, 1976). In addition, probably a larger percentage of PP1 units have spontaneous rates over 50 spikes/sec than do AN units. Since the discharges of PP1 units are always preceded by a pp, any speculation as to the significance of the spontaneous rate distribution of the PP1 units must account for their spontaneous activity in terms of the discharges of end-bulbs. Molnar and Pfeiffer (1968) suggested that the rate distribution could be explained by the effects of superposing discharges of 2 or 3 AN fibers as could conceivably be produced by the convergence of 2 or 3 end-bulbs onto each cell. An alternative explanation is that the AN fibers with the lowest spontaneous rates might represent a separate population of AN fibers (Kiang et al., 1976) that either do not form end-bulbs on the cells of the PP1 units (i.e., the bushy cells of AA and some in AP and APD) or else provide

end-bulbs always in combination with the AN fibers with higher spontaneous rates. If there is only one end-bulb per cell in rostral AVCN (Lorente de Nó, 1976) then we must at least entertain the possibility that the low rate AN fibers do not provide end-bulbs in rostral AVCN.

The discharge characteristics of most PP2 units can be readily distinguished from AN discharges. Some PP2 units were found to have the Pri profile to STBCF but most exhibited a "notch" (Pri-N). In addition, two PP2 units were categorized as On-P. These two units are extreme examples of a variant of the Pri-N form in which the initial peak is very sharp and the later activity exhibits an unusually low rate. Two Pri-N units had a Slower-than-Exponential (SE) decay from the mode of their IH's of spontaneous activity. One of these had a small pp in its pre-spike average and was categorized as PP2; the other may have had an extremely small pp in the average.

In terms of the population distributions of properties, the PP2 units showed several deviations from the AN characteristics. Many more of the IH's of PP2 units had an Exponential decay than either the PP0 or PP1 units. In order to have a basis for comparison with AN units, the data of Walsh et al. (1972) were reprocessed in the same manner as the CN data. The AN IH's showed about equal numbers of units with Exponential and Faster-than-Exponential decay. This ratio is the same as found for the PP1 units, but markedly different from that of the PP2 units which have a strong bias toward Exponential.

The lack of low-CF PP2 units with high rates of spontaneous discharge is similar to most other unit types (PP1 and PP0 units

excluded) in the CN (Results, section 9.1; Kiang, 1976) and MNTB (Guinan et al., 1972a, b). The similarity with MNTB is expected because of the correlation of the PP2 units of PD and PV with the globular cells.

From his recordings in the trapezoid body Brownell (1975) has suggested that some Primarylike units in the CN would show single tone suppression of spontaneous activity (i.e., inhibitory sidebands). He found that more units localized to the region of the large diameter population in the trapezoid body exhibited inhibitory sidebands (eight units out of the ten units tested) than did those in the medium diameter population (one unit out of the eight units tested). The association of the large diameter axons with the globular cells suggests the frequent occurrence of inhibitory sidebands for PP2 and Pri-N units in PV and PD. Three (PP2, Pri-N) units in the present study were tested for inhibition at frequencies above CF. The inhibition of spontaneous activity was found. Because of the heterogeneity of the large diameter population region of the trapezoid body, however, it may be that the units with inhibitory sidebands found by Brownell were recorded from axons of medium or small diameter, which presumably would not have originated from globular (bushy) cells. Van Gisbergen et al. (1975a) found 12 units in caudal AVCN with (1) a "sustained" response to tone bursts at CF and (2) either inhibitory sidebands or else a spontaneous rate which was too low to test for suppression. Most of these units had a chopper response pattern at CF. Since Brownell (1975) used long-duration tone bursts and 5 msec bin width in his PST histograms the majority of the AVCN Choppers (all Chop-T

and Chop-S and probably some Chop-L) would appear to be primarylike. Thus it is difficult to know if the units Brownell (1975) found to have inhibitory sidebands were the projections of globular cells.

2. PP3 Units

If Prepotential units are recorded from bushy cells, most of the units without a prepotential probably represent the stellate cells. A small number of PP3 units probably have a pp which is so small that it was not identified by the tests; for example, most if not all of the (PP3, Pri-N) units should probably be classified as PP2 units. Although PP3 units are found in all subdivisions of AVCN as are both stellate cells and bushy cells, the relative numbers of PP3 units vary over a 5:1 range as shown in Figure V-1.

Approximately 15% of the units recorded in the AA subdivision did not have a demonstrable pp. These PP3 units were found to have non-primarylike responses whenever testable. Kiang et al. (1965b) described only primarylike responses in rostral AVCN. Goldberg and Brownell (1973) noted several "atypical" units in the "large spherical cell zone." Although many of the PP3 units localized to AA were within about 3 block model units of the borders, there were some units localized to the central portion of AA.

The central subdivisions of the AVCN, AP and PD, have large proportions of PP3 units. AP probably has a higher percentage than is given in the present summary because of localization errors and uncertainty at the border with AA. Interleaving of the large clustered cells of AA with the paler staining smaller and more dispersed cells

of AP is common in the border region between AA and AP. As a consequence a smooth boundary line invariably leaves some "AA cells" in AP. These narrow protrusions of "AA cells" probably account for a higher Prepotential unit percentage in AP than would have been obtained had the study been conducted at the level of localizing individual cells. As is shown in Figure V-1, the PP3 unit representation in PD is the highest with AP and PV both having about 50%.

The paucity of PP3 units in AA is consistent with the paucity of stellate cells. In the other subdivisions the larger percentages of PP3 units are consistent with the extensive mixing of stellate and bushy cells (Brawer et al., 1974).

2.1 Response types

Within the PP3 category we find a wide range of response types. The response types followed the general organization described by Kiang et al. (1965b) and Pfeiffer (1966a) except that the On and Chopper groups, which contain most of the PP3 units are further subdivided.

The identification of certain units as On units parallels the tonic/phasic or sustained/transient distinction made in earlier studies of the CN (e.g., Kiang et al., 1965b; Pfeiffer, 1966b; Radionova, 1971; Møller, 1969; Caspary, 1972; Godfrey et al., 1975a, b). The phasic nature of some AVCN units can be as striking as that of units recorded in the octopus cell region (Osen, 1969b) of PVCN by Godfrey et al. (1975a). Unit B97-9, for example (Figure IV-18), had a vigorous and succinct response much like that of the On-L units of PVCN and even

approaching the form of On-I units. Compared to the On-I units most of the On units of the AVCN have a less vigorous response which decreases more distinctly as the silent period between stimuli is reduced. LTBCF, for example, often elicited only a weak response to the onset and click presentations at only 100/sec showed a marked reduction in response. Many of the On units of posterior PVCN can sustain response rates of 500 to 800/sec for clicks (Godfrey, 1971).

The On categories defined for the AVCN On units order them according to the succinctness of the response and the range of stimulus levels over which the transient response is found. Tone burst thresholds were related to this ordering so that when the response was more succinct and the continuous tone threshold more elevated, the STB threshold also tended to be more elevated. This behaviour suggests that the mechanism responsible for the "on" response (i.e., the high threshold to sustained tonal stimulation) also raises the threshold to the initial transient.

The Chopper units have many properties that distinguish them from the "Primarylike" and On units. Several previous studies, however, have probably misclassified many of the Chopper units in the AVCN as Primarylike, because of excessively large bin widths or too few stimulus presentations to reveal the chopper pattern (e.g., Evans and Nelson, 1973a; Goldberg and Brownell, 1973; Brownell, 1975; Britt and Starr, 1976). Failure to identify the Choppers has led to unnecessary confusion in the relationship of the response categories to the: (1) units with and without prepotentials, (2) degree of phase-locking of different

units, and (3) probably, also, the occurrence of inhibitory sidebands.

The identification of different types of Chopper and On units is a new aspect of this examination of the AVCN. Both the Chopper and On types show correlations with other physiological properties and the Chopper types have different spatial distributions within the AVCN. Except for Pausers, the Chop-L units had the most regular spontaneous activity of all AVCN units. This observation is consistent with the regularity ("Gaussian") of spontaneous activity for the long interval choppers found by Guinan (Type D, Guinan et al., 1972a) in the superior olivary complex. The Chop-S versus Chop-T distinction will probably be applicable to other parts of the CN. The Chop-S units are the commonly cited "typical chopper" with a short interval, but the Chop-T form is found in the PVCN at least (an example is shown in Godfrey et al., 1975a).

The Pauser and Composite response types were found infrequently but whenever they did occur their responses were distinctive. The Pausers were basically as described for the DCN (Kiang et al., 1965b; Godfrey, 1975b) and were located in a region just ventral to the granule cell region separating the AVCN and the DCN. Although it is conceivable that units recorded in DCN could have been erroneously localized to the AVCN, the "buffer" region afforded by the granule cell layer makes such an error seem unlikely. The Composite response type, which has an exceptional form of response to tone bursts, has not been previously described for the CN. The response pattern of the Composite units resembles the PST histogram chosen to illustrate category G in the study of the superior olivary complex by Guinan et al. (1972a).

2.2 Anatomical correlates of PP3 units

Returning to the question of the anatomical correlates of the non-primarylike (PP3) units, we note that there are a large number of physiological types and a small number of cell types. In the Brawer et al. (1974) scheme, there are three cell types with which the various PP3 units could be associated, stellate cells, giant cells, and small cells. A fourth possibility, the granule cells, is unlikely because of the large tip size of the electrodes (around 5 μm in diameter). Whether the electrodes can record single unit activity from the small cells is uncertain. The relatively small number of giant cells that are seen in the AVCN (Osen, 1969b; Brawer et al., 1974) may be the source of the Pausers because these units were recorded in the postero-dorsal portion of the AVCN where the giant cells are located and because most of the giant cells are located in the DCN (Osen, 1969b) where many units have a Pauser response (Godfrey et al., 1975b).

Based on the currently defined cell types, the stellate cell and maybe the small cell are left to account for the Chopper and On types and possibly the Composite category. The anatomical basis of these response type categories may lie in the existence of (1) different forms of primary innervation to certain stellate cells, (2) several types of stellate cells and/or (3) a variation in the non-primary (intrinsic or efferent) inputs to the cells. Lorente de Nó (1976) has described different types of AN fibers which have different central terminations; it remains, however, to find out more details concerning the particular cells innervated and the modes of termination. A partitioning of the present stellate cell type is suggested by the

number of cell types Harrison and Irving (1965) described in the rat AVCN. The third factor is also a strong possibility (Cant and Morest, 1975). In fact, variations in the presence or lack of inhibitory inputs to the stellate cells could account for much of the variation seen for the different response types in the Chopper and On groups. This suggestion is based on the observation that the essential distinctions between most of the response types of the PP3 units (Chop-S, Chop-T and On-A, On-P) are based on the rapidity and completeness with which the response to a tone burst ceases after the initial few discharges. Not only do these variations show a correlation with other physiological properties but we find a systematic shift in the distribution of these types throughout the AVCN. As shown in Figure IV-1, the ratio of On to Chopper units and the ratio of Chop-T to Chop-S units are both higher in AA and AP than in the posterior division; i.e., the PP3 units in anterior AVCN are more likely to exhibit a sudden drop in discharge rate shortly after the beginning of the response to a tone burst (at CF).

The posterior division is not without such units and may in fact be the main location of a particular form of Chop-T unit located only in PD; namely the Chop-T with a Dip type of LTBCF response and/or SE decay in the IH's. Units with this same profile are also found in PVCN (unpublished observations; unit DG57-33 shown in Figure 4 of Godfrey et al., 1975a). Inhibitory influences are suggested in the generation of this response type. A conclusion of two modelling studies (Fetz and Gerstein, 1963; Molnar and Pfeiffer, 1968) was that they could not obtain IH's with an SE decay when only excitatory inputs were

applied to the model neuron, whereas with addition of inhibitory inputs the SE decay was easily realizable (Fetz and Gerstein, 1963). The correlation of the SE decay with the Chop-T (particularly in PD), the broad dip in the response to LTBCF and the sudden increase in the interspike interval 5 to 10 msec after the onset of responses to STBCF, all suggest the involvement of inhibitory input to these units.

If we compare the physiological data with the anatomical description of the AVCN provided by Osen, instead of that provided by Brawer et al. (1974), we find different correlations and conflicts. The small spherical cell region (AP) has both PP1 units and a large representation of Chopper and On units. It is not easy to suggest what the "small spherical cell" corresponds to in either the physiological data of this study or the anatomical description of Brawer et al. (1974). Although some of the PP1 units localized to AP may be units that should be associated with AA, PP1 and PP2 units are found throughout AP and must be considered in any description of this region. As is shown in Figure V-1, AP has about 50% PP1 units and slightly more Chopper than On type units in the PP3 population. Many of the "Other" units are located in dorsal AP which is probably not part of Osen's small spherical cell region. According to the physiology, the small spherical cell region is heterogeneous (as suggested in Brawer et al., 1974). Goldberg and Brownell (1973), however, found the units in the "small cell zone" to have mainly a primarylike response similar to the "large cell zone"; this view is contradicted by the present study. As has been mentioned previously their "primarylike" units probably include the Chop-S and Chop-T units. The anterior of the multipolar,

globular cell region (PD) has a large number of Choppers with a maintained discharge to a tone burst (Chop-S and Chop-L). As Godfrey et al. (1975a) observed from PVCN and some AVCN data, the regions with many multipolar cells have a large number of Chopper type units. According to van Gisbergen et al. (1975a) "most" of the 12 "AS" and "A(S)" type units localized to the globular cell region (PD and PV) exhibited "chopping." The correlation of the Prepotential units with large spherical cells and globular cells was noted in the discussion of the Prepotential units. The large percentage of PP3 units in PD (Figure IV-1) suggests a larger representation of the multipolar cell in this region than was shown by Osen in her diagrammatic summary plots (for example, Fig. 6 versus Fig. 7 in Osen, 1969b). The distribution of small cells shown by Osen (e.g. Figure II-2) matches with the locations of the response types shown by circled symbols in Figure IV-42 (Pauser, Composite, and Chop-L). The giant cells in the region of the small cell cap may account for some of the correlation.

3. Correlations with Axon Properties

The anatomical data needed to correlate axon diameters in the trapezoid body with the particular cell types in the CN is at present sketchy. The globular cells in PD and PV are almost surely associated with the largest axons and the rostral two-thirds of AVCN is probably the source of many medium and fine diameter axons (Warr, 1966). The relationship of the medium and fine diameter axons to the various cell types of AVCN is, however, uncertain. Since many small cells project to the contralateral IC (Adams, 1976), presumably via the trapezoid

body, it is probably reasonable to assume that by a simple size relationship the small cells would be the source of at least some of the fine fiber component of the trapezoid body. As was described in connection with the discussion of the Prepotential units, the large and medium diameter axons are probably those associated with the antidromic latencies of 0.5 and 1 msec, respectively, when stimulated from the region of the contralateral MSO. We note that many of the PP3 units can also have latencies as short as 1 msec. Thus if the PP3 units are stellate cells, some stellate cells probably have an average axon diameter that is close to that of the bushy cells that are located in rostral AVCN. From the sites in the trapezoid body requiring minimum current to antidromically stimulate PP3 units it appears that many of their axons were located ventral to the axons of the PP1 units. If so, many of the PP3 units probably project via medium diameter axons in the mixed or large diameter regions. Brownell (1975) did note a few non-primarylike units in his mixed and large diameter regions and expressed the view that these units were probably recorded from axons finer than normally recorded. Again, the 5 msec bin widths of his PST histograms would have prevented Brownell from identifying most Chopper and Pri-N type units.

The PP3 units, however, are probably not associated only with the medium diameter axons because their distribution of latencies is broader than that for the PP1 units. The On-P and Chop-T units, in particular, exhibited a tendency to have latencies shorter than those of PP1 units. In addition, some PP3 units exhibited latencies longer than the PP1 units and may, therefore, be the source of the finer axons in the trapezoid body. The latencies, however, are not as long as

would be expected from the ratio of axon diameters at the midline (van Noort, 1969; Brownell, 1975; Warr, 1976). The ratio of the diameters of the medium and fine axons is about 2 or more. Assuming a linear relationship between diameter at the midline and antidromic latency, we would expect the cells with fine axons to have latencies of 2 msec or longer to the TBS stimulation since the medium diameter axons have a latency of 1 msec.

The relative absence of units with latencies longer than 2 msec could be explained by hypothesizing that the fine axons originate from small cells which were seldom recorded. Even if the activity of the small cells could be isolated, the spikes would probably be smaller than from the larger cells so that the chances would be poor of discriminating a response to the shock stimulation because the large gross responses would obscure the spikes. When the stimulating electrode was located in the contralateral IC the gross response to a shock was generally so small that it did not interfere with discrimination of spike responses. This lack of gross response and the use of the shock stimulation as a search stimulus are possibly the reasons for the relatively frequent finding of latencies longer than 4 msec. The figure of 4 msec is used because: (1) the distance from the CN to the contralateral MSO is about half of the distance to the contralateral IC, (2) the latency of the medium diameter axons is about 1 msec from the contralateral MSO and would be about 2 msec from the IC (if the axon diameter and hence conduction velocity remained the same), and (3) the fine axons should have latencies double (or more) those of the medium diameter axons (assuming linear relation of diameter to velocity). That

many latencies to IC shock were more than double those to TBS may also be the result of lower conduction velocities due to a reduced axon diameter after branching.

4. Extracellular versus Intracellular Recording

Extracellular recording techniques were selected for this study rather than intracellular because of the experimental advantages of: (1) the more stable recording situation in which a unit can be studied for an extended period (many hours) and in which there is probably less damage to the cell (as judged by the stability of discharge properties), (2) the selectivity of the large tipped electrodes for cell body recordings rather than fibers, and (3) the simultaneous extracellular recording from the end-bulbs and postsynaptic cell bodies in the AVCN. With the objective to interrelate the anatomy and physiology of the AVCN, however, extracellular recording imposes some limitations stemming from the necessity to make the comparisons only in terms of spatial distributions. The accuracy with which a recording site can be localized is a limiting factor especially for small regions such as APD. But even in relatively large regions for which localization accuracy is not a limitation, the sampling biases of the microelectrode can influence the relative numbers of various unit types. This issue, for example, was relevant to the possible representation of the small cells in the data presented in this study.

For those regions or subdivisions in which there are several cell types, a potentially serious limitation of extracellular recording is an inability to resolve which of the possible cell types is giving rise

to the various unit types recorded there. A comparison of the relative numbers of the various unit types and cell types in each region can, in fortuitous situations, provide hypotheses as to the association of the physiological and anatomical descriptions of each region. In some cases it is possible to use a process of elimination if certain cell types occur in other regions and/or to take advantage of unique properties such as end-bulbs (pp) or distinctive axon diameters or projections (antidromic responses).

The use of intracellular recording, on the other hand, allows dye-marking of the individual cells. Not only is the location of the cell revealed but in some cases the full dendritic structure is demonstrated, thereby allowing the morphology of the cell to be related to the categories established in Golgi studies. Microelectrode sampling biases would still be present with intracellular recordings but the direct correlation with anatomy would provide a control. The current state-of-the-art for intracellular recording and dye-marking, however, includes many potential artifacts and limitations. Without the preknowledge of an extensive extracellular study, these artifacts can be difficult to identify.

There is one study of the CN (in the kangaroo rat) in which an attempt was made to dye-mark individual cells from which responses were recorded (Caspary, 1972). As was noted by Godfrey et al. (1975a), the current levels for dye ejection used by Caspary were excessive and could easily have resulted in erroneously non-specific marking. Caspary's use of a relatively long tone burst (150 to 240 msec) with only 30 presentations make it likely that short interval Chopper units could

have been misidentified as Primarylike. How Caspary in his description of the chopper response can assume, a priori, that a Chopper cannot be "phase-locked" or even "phase-related" is incomprehensible and is contrary to what has been shown in this thesis. It also appears that Caspary has evaluated units with respect to their synchrony to tonal stimuli at CF and then lumped all units together regardless of CF. The inclusion of units with CF's above 5 kHz only obscures the overall statistics with many units that are "non-phase-lockers" by virtue of their high CF.

In Caspary's data only 4 units were localized to the large spherical cell area. All were "non-phase-lockers." Three of these units had the onset type of "primarylike" response and the other unit was a "pauser." Compared to the description of rostral AVCN (AA) given in this thesis and by Goldberg and Brownell (1973), Caspary's results are surprising. However, closer examination can possibly resolve some of the discrepancies. Caspary's 4 units had CF's above 1.5 kHz which may explain the "non-phase-locker" description considering that his tests were based on IH's rather than period histograms. Caspary's primarylike-onset units have an initial peak as little as 40% above the sustained rate, and so could be either Pri or Pri-N or even an On-P or Chop-T type, all of which have PST histograms with a peak, a dip and then later activity (although all are difficult to confuse with a Pauser as originally defined by Kiang et al., 1965b and Pfeiffer, 1966a).

The single dye-marked "small spherical cell" had a response classified as primarylike-onset. From the appearance of the PST

histograms it might have belonged to the present On-P category. This unit which had a CF of 475 Hz was "phase-locked." Thirteen of the 18 units in the small spherical cell area had CF's below 2 kHz and yet 12 of the 18 units were "non-phase-lockers"; this is difficult to explain in terms of the cat data reported here.

The single dye-marked "globular cell" was classified as a "pauser" but could easily have been a Pri-N unit considering the definition used by Caspary for "pausers." The complete lack of Choppers from the VCN in Caspary's data is difficult to explain on grounds other than the technical ones described above or the less plausible concept of a species difference for the cellular responses in spite of the anatomical similarities which allow Caspary to describe the CN and its cells in terms of Osen's anatomical scheme.

5. Phase-locked Responses

The phase-locked or synchronized discharge of CN units to low frequency tonal stimuli has been examined in several studies (e.g., Lavine, 1971; Moushegian and Rupert, 1970; Goldberg and Brownell, 1973). Lavine (1971) provides the only data with plots of synchronization index as a function of the frequency of stimulation. In his data we see the systematic decrease with increasing frequency and a hint that there may be different groups of units, although the establishing of groups would be difficult to justify from such a small sample of units. Moushegian and Rupert, and Caspary speak of units categorized as "phase-lockers," "phase-related" or "quasi-phase-lockers" and "non-phase-lockers" in the VCN of kangaroo rat. It is not at all obvious

that what they are speaking of are units which exhibit properties as shown by Lavine or whether some of the variation they speak of is due to the use of different frequencies (since they use the CF as the stimulating frequency) for each unit.

From maximum synchrony data there are two major groups of units in the AVCN, the Prepotential units (plus a small number of On units) and the Choppers. The Prepotential units are generally indistinguishable from AN units in the level dependence of synchronization index and the maximum synchrony versus frequency relationship, whereas the Choppers generally differed from the Prepotential units at frequencies above about 800 Hz (above 6 kHz all units are equivalent again since none show synchrony). The maximum synchrony data for the Choppers are best characterized as having a lower "cut-off frequency" above which the Choppers fall off more rapidly than do the Prepotential units.

On units, characterized by their lack of response to continuous tone, usually exhibit a vigorous response to low frequency continuous tone. This response is probably brought about by the synchronous activity of the AN fibers which provides transient, synchronized inputs to the cells. It is possible, therefore, that the On units would exhibit either a highly synchronized response or no response at all.

There is in the synchrony data further evidence that the primarylike responses in the AVCN may not always be an exact replica of AN discharge patterns. Two PP1 units had synchronization indices and rate versus level functions that were unlike those of AN fibers. There was also a Pri-LR unit without an identifiable pp which had a maximum synchronization index versus frequency plot that placed it within the Chopper unit range.

Such a unit could be an unusual "Primarylike" unit or a "Chopper" with such a low rate of response that it did not exhibit its chopping.

No units in AVCN had synchronization indices near zero for frequencies below 1 kHz. Lavine (1971) found such units in DCN. Moushegian and Rupert (eg, 1970) report some units with very low synchronization at frequencies below 500 Hz in the VCN of kangaroo rat.

6. Characteristic Frequency Representation

The tonotopic organization of the AVCN is basically a ventro-lateral to dorso-medial ordering of units with a CF sequence from low to high (Rose et al., 1959). We have not found any obvious discontinuities at the subdivision borders as are seen at the border between the VCN and DCN. Goldberg and Brownell (1973) similarly noted the continuity of CF's at the border between the large and small spherical cell regions. The CF lines shown in Figure IV-41 suggest that CF's above 10 to 12 kHz are not found in AA (large spherical cell region). This upper limit agrees with a similar limit (10 kHz) found by Goldberg and Brownell (1973) for the "large cell zone" and may also be correlated with Brownell's observation (Brownell, 1975) that his sample of the medium diameter population in the trapezoid body had an upper limit of 12 kHz. We also found that APD had CF's above 10 to 12 kHz. The surface for CF's of 0.8 kHz is just outside the latero-ventral limit of AP. Since AP narrows as it approaches this limit, it has very little volume for units with a CF below 1 kHz. This situation is consistent with the small number of Phase-locked units in AP. Goldberg and

Brownell (1973) described the "small cell zone" to have CF's from 0.25 to 27 kHz; localization uncertainty and/or a difference in the criteria for the small spherical cell region might account for this difference. Although the discrimination of the lateral limit of AP is usually difficult, there is a ventro-lateral region where AA and PD are in contact excluding AP. It is interesting that plots versus CF for the "small cell zone" in Goldberg and Brownell (1973) show only units with CF's of 1 kHz and above.

The upper limit on CF's for units in AA agrees with the prediction of Osen (1970) that the large spherical cell region would not receive input from the AN fibers originating from the most basal regions of the cochlea. The lower limit for AP, however, conflicts with her prediction that the small spherical cell region receives input from the whole range of the cochlea. Osen (1969a) also suggested that the large spherical cells project to both MSO's whereas the small spherical cells project to the ipsilateral LSO. The "mainly low CF" and "mainly high CF" descriptions of AA and AP substantiate similar observations on the tonotopic organization of the MSO and LSO (Tsuchitani and Boudreau, 1966, 1967; Boudreau and Tsuchitani, 1968, 1970; Goldberg and Brown, 1968; Guianan et al., 1972b). Guinan et al. (1972b) also noted that LSO units with CF below 1 kHz had different responses than units with CF's above 1 kHz. The CF's found for APD indicate that if the cells in APD are part of the projections to the LSO and MSO from the spherical cell region, then they are more likely involved with the LSO because of its high CF's.

Although the present experiments were somewhat biased against isolating units with a CF out of the general trend, such units were

found in and around PV. In the region above PV where the AVCN, PVCN, DCN and the large invagination of the granule cell layer converge, the "tonotopic organization" appears to be quite complex and may even be multivalued in some regions. Rose et al. (1959) noted reversed CF sequences (ie, ascending CF for successively more ventro-rostral locations) in the region between the DCN and AVCN. No sequences along either a single pass or in pooled data of this study provided clear evidence of a reversed CF sequence.

The estimation of the CF of units responsive to frequencies above 10 kHz can be complicated by resonances in the acoustic system and by "tails" of high CF units (Kiang and Moxon, 1974) which can produce tuning curves with multiple minima. The CF of units dorsal to PV were generally above 10 kHz with many above 20 kHz even in very lateral positions. Units with CF above 10 kHz were also found more ventrally, sometimes between units having a much lower CF. Godfrey (1971) noted that an orderly CF sequence is found in the DCN and PVCN but that this may not be the case for the interstitial nucleus (PV). Several examples were found in this study which suggest that there may be two CF patterns in PV, one continuous with that in the rest of the AVCN and PVCN, the other having much higher CF's and continuous with the pattern in the region dorsal to PV. The unusual, high CF units in PV may be related to an innervation by fibers similar to the dorsally directed collateral system described by Feldman and Harrison (1969) in the rat CN.

7. Projections to the Inferior Colliculus

No group of units was shown to be significantly lacking in members antidromically stimulated by the TBS stimulation. When the stimulating

electrode was located in the contralateral IC, however, none of the PP1 units recorded could be stimulated, whereas many intermixed PP3 units were antidromically stimulated. For the units localized to AA there was a very broad distribution of latencies (from 2 to 12 msec). Although many of the units in this sample had very small spikes and so could not be verified by the collision test to be responding antidromically to the shocks, the responses did satisfy the less strict criteria for antidromic response. The lack of PP1 units and the long latencies of some of the units that did respond appear to be consistent with the finding by Adams (1976) that in and around AA many cells and probably no bushy cells are labeled with horseradish peroxidase after injection in the contralateral IC. Negative evidence from either technique alone is inconclusive, but the combined results are very suggestive that in rostral AVCN the PP1 units (bushy cells) do not project to the contralateral CNIC. Whether bushy cells in the other parts of the AVCN project to the contralateral IC is much less certain because of the small sample.

Warr's observation (Warr, 1966) that the medium diameter axons of the trapezoid body continue to the contralateral IC appears to contradict the suggestion that PP1 units do not project there since these axons are generally thought to arise from the "spherical cells." An alternative explanation, that some of the medium diameter axons arise from stellate cells, is supported by the observation that many of the PP3 units had antidromic latencies of about 1 msec to TBS and some exhibited latencies of 2 msec to IC shock (the path length from contralateral IC being approximately twice that from the contralateral MSO).

8. Bushy Cell versus Stellate Cell Projections

A large fraction of the units recorded in the AVCN had either a "Primarylike" or Chopper response type. The projections of these units to the higher centers appear to be different (eg., PPl units do not project to contralateral IC) and suggest an independent representation of these two types in higher centers. Ascertaining the sites of projection may prove difficult since both appear to project via the medium diameter axons of the trapezoid body. There is, however, a physiological difference between the Prepotential units and the Chopper units; namely, maximum synchrony. In the frequency range from 2 to 4 kHz the Choppers of the AVCN have essentially no synchrony whereas the Prepotential units have a significant synchrony. Units in the higher centers that exhibit synchrony in this frequency range probably receive inputs either directly or indirectly from the Prepotential units (or some of the On units when the stimulus levels are high enough to stimulate them). It would be useful to obtain systematic data on maximum synchrony versus frequency for units in the higher centers.

SUMMARY

1. Extracellular recordings of the discharges of single units in the AVCN were characterized according to several physiological properties. Based on histological preparations the recording sites for most units were mapped onto a model cochlear nucleus which shows the subdivisions of Brawer et al. (1974).

2. The proposed organization of the anatomical and physiological categories of the AVCN is presented in a summary table. The anatomical data is represented by: (1) the cell types of two studies, one based on Golgi preparations, the other based mainly on cell body stains, and (2) whether the cell type receives end-bulbs of Held terminals or just boutons from the auditory nerve. The relationship of these morphological categories to the major physiological categories and to projections from the AVCN is shown on the right. Particular aspects of this table are dealt with in the remainder of the SUMMARY.

3. Prepotentials, associated with the spike waveforms of certain units in the AVCN, are concluded to result from the invasion of an end-bulb by an action-potential conducted by the parent auditory nerve fiber. Single action potentials arriving at an end-bulb appear to be capable of discharging the postsynaptic cell.

4. Units with prepotentials are found throughout the AVCN. Prepotentials exhibit a range of sizes and shapes. Narrow, predominantly

Table A Proposed correlations of anatomical and physiological categories

ANATOMICAL CATEGORIES			PHYSIOLOGICAL CATEGORIES		PROJECTIONS		
Cell Types		Auditory Nerve Endings	Prepotential Category	Response Pattern to Tone Burst	Axon Diameter in Trapezoid Body	Across the Midline	Contra-lateral Inferior Colliculus
Brawer et al. (1974) (Golgi)	Osen (1969b) (Nissl)						
		end-bulb	fast, negative prepotential (PPO)	Primarylike	- no projections -		
	large spherical	end-bulb	large positive prepotential (PP1)	Primarylike	medium	yes	no
bushy	small spherical (?)						
	globular	modified end-bulb	small prepotential (PP2)	Primarylike with notch (& Primary-like)	large	yes	?
stellate	multipolar	bouton	no prepotential (PP3)	Chopper & On	medium (larger & smaller)	yes	yes
giant	giant	bouton	"	Pauser (?)	?	yes (?)	?
small	small	bouton	?	?	small (?)	yes (?)	yes (?)

negative prepotentials may be recorded from the primary axon, peripheral to the formation of an end-bulb. Large positive prepotentials characterize most of the units in the most rostral subdivision (AA), whereas in the posterior AVCN, prepotentials are generally smaller and many appear at a variable latency with respect to the postsynaptic spike.

5. Units with a prepotential have response patterns that can be placed in different categories. However, all of these categories are essentially "Primarylike". Conversely, most "Primarylike" units were found to have a prepotential.

6. It is suggested that Prepotential units represent recordings from the neurons called bushy cells by Brawer et al. (1974). These cells receive the end-bulb of the Held terminals.

7. Based on the interpretation of antidromic latencies, the Prepotential units of rostral AVCN are suggested to be the source of medium diameter axons in the trapezoid body. The Prepotential units of caudal AVCN are interpreted to be the source of the largest axons. In rostral AVCN, the Prepotential units (bushy cells), probably correspond to Osen's large spherical cells; in caudal AVCN, they correspond to Osen's globular cells.

8. The relative frequency of units exhibiting prepotentials is a function of the rostral-caudal position in the AVCN. The rostral extreme (AA) has the highest density of Prepotential units, the caudal extreme (PV) the next highest and PD the lowest. This variation is consistent with the distribution of bushy (or large spherical and

globular) cells.

9. Most units with non-primarylike response patterns were categorized into two groups, Chopper and On. The ratio of these two groups is almost one in the rostral AVCN and shifts in favor of Choppers in the caudal subdivisions.

10. Three sub-categories of Chopper units were defined for AVCN units. These three types exhibit different spatial distributions.

11. All units in the AVCN that were stimulated with tones having a frequency below 2 kHz were found to exhibit phase-locking. Maximum synchrony versus frequency data for all but a few Prepotential units matched comparable data from auditory nerve units. The available On unit data also matched. All Chopper units plus a few other units without a prepotential had maximum synchrony values in a range which deviates from auditory nerve data for frequencies above about 800 Hz.

12. For most units tonal stimuli were used to determine the frequency for which the unit was most sensitive (characteristic frequency, CF). Surfaces of constant CF were determined for the AVCN and compared with the anatomical subdivisions of Brawer et al. (1974). The rostral subdivisions exhibit limited CF ranges: AA has CF's below 10 to 12 kHz, APD has CF's above 10 to 12 kHz and AP probably has no units below 800 Hz and very few below 1 kHz. PD appears to have units representing the full CF range. The organization in PV is somewhat uncertain; it appears that units with CF's differing by more than a decade can be

adjacent.

13. Antidromic activation of single units by means of electrical stimulation near the contralateral medial superior olivary complex demonstrates that probably each unit category in the AVCN has some members that project across the midline.

14. Units in many categories were antidromically activated by stimulation in the contralateral inferior colliculus. Since Prepotential units in rostral AVCN were not stimulated, it is inferred that bushy cells in rostral AVCN do not project to the contralateral inferior colliculus.

15. Many units with a non-primarylike response were shown to have antidromic latencies equal to those of the Prepotential units in AA which presumably provide medium diameter axons in the trapezoid body. It is suggested, therefore, that many stellate cells, as well as spherical cells, project via medium diameter axons. The axons of stellate cells, however, probably exhibit a wider range of diameters. The axons of most stellate cells may lie ventral to those of the large spherical cells.

ABBREVIATIONS

AA	AVCN subdivision; anterior division, anterior part
ab	ascending branch of auditory nerve
AN	auditory nerve
AP	AVCN subdivision; anterior division, posterior part
APD	AVCN subdivision; anterior division, posterodorsal part
AVCN	anteroventral cochlear nucleus
BW_{10}	bandwidth at 10 dB above most sensitive point
cc	cubic centimeter
CC	condensation click
CF	characteristic frequency
Chop-L	"Long interval" Chopper response type category
Chop-S	"Sustained" Chopper response type category
Chop-T	"Transient" Chopper response type category
Chop-?	unspecified Chopper response type category
cm	centimeter
CN	cochlear nucleus
CNIC	central nucleus of the inferior colliculus
CNS	central nervous system
CT	continuous tone
CTCF	continuous tone at CF
db	descending branch of the auditory nerve
dB	decibel
DCN	dorsal cochlear nucleus

E	Exponential, category for IH decay
FE	Faster-than-Exponential, category for IH decay
FFR	frequency following response
G	granular region of cochlear nucleus
Hz	Hertz
IC	inferior colliculus
kHz	kiloHertz
kg	kilogram
KCl	potassium chloride
LMSE	least-mean-square-error
LSO	lateral superior olivary nucleus
LTB	long tone burst (900 msec duration, 1/sec)
LTBCF	LTB at CF
mA	milliAmpere
mg	milligram
MIH	mean-interval histogram
mm	millimeter
MNTB	medial nucleus of the trapezoid body
msec	millisecond
MSO	medial superior olivary nucleus
mV	milliVolt
OCB	olivocochlear bundle
On-A	"Abrupt" On response type category
On-G	"Gradual" On response type category
On-P	"Prolonged" On response type category
On-?	unspecified On response type category

PD AVCN subdivision; posterior division, dorsal part

pp prepotential

PP0, PP1, etc. prepotential categories

Pri Primarylike response type category

Pri-N Primarylike with a notch response type category

Pri-LR Low-rate-primarylike response type category

PST poststimulus time (histogram)

PV AVCN subdivision; posterior division, ventral part (also called interstitial nucleus)

PVCN posteroventral cochlear nucleus

Q_{10} CF divided by BW_{10}

RC rarefaction click

rms root-mean-square

S synchronization index

SE Slower-than-Exponential, category for IH decay

sec second

SIH histogram of standard deviation of intervals

SNB short noise burst (25 msec duration, 10/sec)

SOC superior olivary complex

SPL sound pressure level (reference level of 0.0002 dynes/cm^2)

STB short tone burst (25 msec duration, 10/sec)

STBCF STB at CF

TB tone burst

TBS trapezoid body shock

TC tuning curve

VCN ventral cochlear nucleus

VDL	visual detection level
μm	micrometer
μsec	microsecond
μA	microAmpere
μV	microVolt

REFERENCES

Adams, J. C. (1976). Types of cells in the cochlear nucleus that project to the inferior colliculus in the cat. Anat. Rec. 184: 340.

Aitkin, L. M., D. J. Anderson, and J. F. Brugge (1970). Tonotopic organization and discharge characteristics of single neurons in nuclei of the lateral lemniscus of the cat. J. Neurophysiol. 33: 421-440.

Anderson, D. J., J. E. Rose, J. E. Hind and J. F. Brugge (1971). Temporal position of discharges in single nerve fibers with the cycle of a single-wave stimulus: frequency and intensity effects. J. A coust. Soc. Am. 49:1131-1139.

Barnes, W. T., W. W. Magoun and S. W. Ranson (1943). Ascending auditory pathways in the brain stem of the monkey. J. Comp. Neur. 79:129-152.

Bean, C. P. (1974). A theory of microstimulation of myelinated fibers. Appendix in C. Abzug, M. Maeda, B. W. Peterson and V. J. Wilson (1974). Cervical branching of lumbar vestibulospinal axons. J. Physiol. (Lond.) 243: 499-522.

Boudreau, J. C. and C. Tsuchitani (1970). Cat superior olive S-segment cell discharge to tonal stimulation. In: Contributions to Sensory Physiology. Vol. 4, W. D. Neff (Ed.), Academic Press, New York, pp. 143-213.

Brawer, J. R. and D. K. Morest (1975). Relations between auditory nerve endings and cell types in the cat's anteroventral cochlear nucleus seen with the Golgi method and Nomarski optics. J. Comp. Neur. 160:491-506.

Brawer, J. R., D. K. Morest and E. Kane (1974). The neuronal architecture of the cochlear nucleus of the cat. J. Comp. Neur. 155: 251-300.

Britt, R. and A. Starr (1976). Synaptic events and discharge patterns of cochlear nucleus cells. I. Steady-frequency tone bursts. J. Neurophysiol. 39:162-178.

Brownell, W. E. (1975). Organization of the cat trapezoid body and the discharge characteristics of its fibers. Brain Res. 94: 413-434.

Cant, N. B. and D. K. Morest (1975). Axonal types in the anteroventral cochlear nucleus (AVCN) of the cat: A Golgi study. Fifth Annual Meeting of the Society for Neuroscience.

Caspary, D. (1972). Classification of subpopulations of neurons in the cochlear nuclei of the kangaroo rat. Exp. Neurol. 37: 131-151.

Comis, S. D. and W. E. Davies (1969). Acetylcholine as a transmitter in the cat auditory system. J. Neurochem. 16:423-429.

Comis, S. D. (1970). Centrifugal inhibitory processes affecting neurones in the cat cochlear nucleus. J. Physiol. (Lond.) 210:751-760.

Comis, S. D. and I. C. Whitfield (1968). Influence of centrifugal pathways on unit activity in the cochlear nucleus. J. Neurophysiol. 31: 62-68.

Dowben, R. M. and J. E. Rose (1953). A metal-filled microelectrode. Science 118: 22-24.

Evans, E. F. and P. G. Nelson (1973a). The responses of single neurons in the cochlear nucleus of the cat as a function of their location and the anaesthetic state. Exp. Brain Res. 17:402-427.

Evans, E. F. and P. G. Nelson (1973b). On the functional relationship between the dorsal and ventral divisions of the cochlear nucleus of the cat. Exp. Brain Res. 17:428-442.

Feldman, M. L. and J. M. Harrison (1969). The projection of the acoustic nerve to the ventral cochlear nucleus of the rat. A Golgi study. J. Comp. Neur. 137: 267-294.

Fernández, C. and F. Karapas (1967). The course and termination of the striae of Monakow and Held in the cat. J. Comp. Neur. 131:371-386.

Fetz, E. E. and G. L. Gerstein (1963). An RC model for spontaneous activity of single neurons. M.I.T. Quart. Prog. Rpt. No. 71: 249-257.

Gerstein, G. L., and N. Y. S. Kiang (1960). An approach to the quantitative analysis of electrophysiological data from single neurons. Biophys. J. 1: 15-28.

Gesteland, R. C., B. Howland, J. Y. Lettvin, and W. H. Pitts (1959). Comments of microelectrodes. Proc. I.R.E. 47: 1856-1862.

Gisbergen, J. A. M. van, J. L. Grashuis, P. I. M. Johannesma, and A. J. H. Vendrik (1975a). Spectral and temporal characteristics of activation and suppression of units in the cochlear nuclei of the anaesthetized cat. Exp. Brain Res. 23:367-386.

Gisbergen, J. A. M. van, J. L. Grashuis, P. I. M. Johannesma, and A. J. H. Vendrik (1975b). Neurons in the cochlear nucleus investigated with tone and noise stimuli. Exp. Brain Res. 23:387-406.

Godfrey, D. A. (1971). Localization of single units in the cochlear nucleus of the cat: An attempt to correlate neuronal structure and function. Ph.D. Dissertation, Dept. of Physiology, Harvard Univ., Cambridge, Mass.

Godfrey, D. A., N. Y. S. Kiang and B. E. Norris (1975a). Single unit activity in the posteroventral cochlear nucleus of the cat. J. Comp. Neur. 162:247-268.

Godfrey, D. A., N. Y. S. Kiang and B. E. Norris (1975b). Single unit activity in the dorsal cochlear nucleus of the cat. J. Comp. Neur. 162:269-284.

Goldberg, J. M. and P. R. Brown (1969). Response of binaural neurons of dog superior olivary complex to dichotic tonal stimuli: some physiological mechanisms of sound localization. J. Neurophysiol. 32:613-636.

Goldberg, J. M. and W. E. Brownell (1973). Discharge characteristics of neurons in anteroventral and dorsal cochlear nuclei of cat. Brain Res. 64:35-54.

Greenwood, D. D. and N. Maruyama (1965). Excitatory and inhibitory response areas of auditory neurons in the cochlear nucleus. J. Neurophysiol. 28: 863-892.

Guinan, J. J., Jr., B. E. Norris and S. S. Guinan (1972a). Single auditory units in the superior olivary complex I: Responses to sounds and classifications based on physiological properties. Int. J. Neurosci. 4:101-120.

Guinan, J. J., Jr., B. E. Norris and S. S. Guinan (1972b). Single auditory units in the superior olivary complex II: Locations of unit categories and tonotopic organization. Int. J. Neurosci. 4:147-166.

Harrison, J. M. and R. Irving (1965). The anterior ventral cochlear nucleus. J. Comp. Neur. 124: 15-42.

Harrison, J. M. and R. Irving (1966). The organization of the posterior ventral cochlear nucleus in the rat. J. Comp. Neur. 126: 391-402.

Harrison, J. M. and W. B. Warr (1962). A study of the cochlear nucleus and ascending auditory pathways of the medulla. J. Comp. Neur. 119: 341-379.

Held, H. (1893). Die centrale Gehorleitung. Arch. Anat. u. Physiol. 201-248.

Hilali, S. and I. C. Whitfield (1953). Responses of the trapezoid body to acoustic stimulation with pure tones. J. Physiol. (Lond.) 122:158-171.

Hochfeld, P. R. (1973). Binaural interactions in the cat's cochlear nucleus. Thesis, Dept. of Electrical Engineering, M.I.T., Cambridge, Mass.

Irving, R. and J. M. Harrison (1965). Origin of the large fiber component of the trapezoid body of the rat. Anat. Rec. 151: 458.

Johnson, D. H. (1974). The response of single auditory-nerve fibers in the cat to single tones: synchrony and average discharge rate. Ph.D. Dissertation, Dept. of Electrical Engineering, M.I.T., Cambridge, Mass.

Kiang, N. Y. S. (1965). Stimulus coding in the auditory nerve and cochlear nucleus. Acta Oto-Laryng. 59: 186-200.

Kiang, N. Y. S. (1968). A survey of recent developments in the study of auditory physiology. Ann. Otol. Rhinol. Laryngol. 77: 656-675.

Kiang, N. Y. S. (1975). Stimulus representation in the discharge patterns of auditory neurons. In: The Nervous System, Donald B. Tower, Editor-in-chief. Vol 3: Human Communication and Its Disorders. Raven Press, New York. pp. 81-96.

Kiang, N. Y. S. (1976). Personal communication.

Kiang, N. Y. S., T. Watanabe, E. C. Thomas, and L. F. Clark (1965a). Discharge patterns of single fibers in the cat's auditory nerve. Research Monograph No. 35. M.I.T. Press, Cambridge, Mass.

Kiang, N. Y. S., R. R. Pfeiffer, W. B. Warr, and A. S. N. Backus (1965b). Stimulus coding in the cochlear nucleus. Ann. Otol. Rhinol. Laryngol. 75: 463-485.

Kiang, N. Y. S., M. B. Sachs, and W. T. Peake (1967). Shapes of tuning curves for single auditory nerve fibers. J. Acoust. Soc. Am. 42: 1341-1342.

Kiang, N. Y. S., E. C. Moxon and R. A. Levine (1970). Auditory-nerve activity in cats with normal and abnormal cochleas. In: Sensorineural Hearing Loss, G. E. W. Wolstenholme and J. Knight (Eds.), Churchill, London. pp. 241-273.

Kiang, N. Y. S. and E. C. Moxon (1974). Tails of tuning curves of auditory-nerve fibers. J. Acoust. Soc. Am. 55: 620-630.

Kiang, N. Y. S., D. A. Godfrey, B. E. Norris and S. E. Moxon (1975). A block model of the cat cochlear nucleus. J. Comp. Neur. 162:221-246.

Kiang, N. Y. S., M. C. Liberman and R. A. Levine (1976). Auditory-nerve activity in cats exposed to ototoxic drugs and high-intensity sounds. Ann. Otol. Rhinol. Laryngol. (In press).

Klinke, R., G. Boerger and J. Gruber (1969). Studies on the functional significance of efferent innervation in the auditory system: afferent neuronal activity as influenced by contralaterally applied sound. Pflügers Arch. ges. Physiol. 306: 165-175.

Koerber, K. C., R. R. Pfeiffer, W. B. Warr, and N. Y. S. Kiang (1966). Spontaneous spike discharges from single units in the cochlear nucleus after destruction of the cochlea. Exptl. Neurol. 16: 119-130.

Lavine, R. A. (1971). Phase-locking in response of single neurons in cochlear nuclear complex of the cat to low-frequency tonal stimuli. J. Neurophysiol. 34:467-483.

Li, R. Y-S. and J. J. Guinan, Jr. (1971). Antidromic and orthodromic stimulation of neurons receiving calyces of Held. M.I.T. Quart. Prog. Rpt. No. 100:227-234.

Lenn, N. J. and T. S. Reese (1966). The fine structure of nerve endings in the nucleus of the trapezoid body and the ventral cochlear nucleus. Amer. J. Anat. 118: 375-390.

Lorente de Nó, R. (1933a). Anatomy of the eighth nerve III. general plans of structure of the primary cochlear nuclei. Laryngoscope. 43: 327-350.

Lorente de Nó, R. (1933b). Anatomy of the eighth Nerve. the central projection of the nerve endings of the internal ear. Laryngoscope. 43: 1-38.

Lorente de Nó, R. (1937). The sensory endings in the cochlea. Laryngoscope 47: 373-377.

Lorente de Nó, R. (1976). Ann. Otol. Rhinol. Laryngol. (In press).

Mast, T. E. (1973). Dorsal cochlear nucleus of the chinchilla: excitation by contralateral sound. Brain Res. 62:61-70.

Mast, T. E. (1970). Binaural interaction and contralateral inhibition in dorsal cochlear nucleus of the chinchilla. J. Neurophysiol. 33: 108-115.

McDonald, D. M. and G. L. Rasmussen (1971). Ultrastructural characteristics of synaptic endings in the cochlear nucleus having acetylcholinesterase activity. Brain Res. 28:1-18.

Møller, A. R. (1969). Unit responses in the rat cochlear nucleus to repetitive, transient sound. Acta Physiol. Scand. 75: 542-551.

Molnar, C. E. and R. R. Pfeiffer (1968). Interpretation of spontaneous spike discharge patterns of neurons in the cochlear nucleus. Proc. I.E.E.E. 56:993-1004.

Morest, D. K. (1968). The collateral system of the medial nucleus of the trapezoid body of the cat, its neuronal architecture and relation to the olivo-cochlear bundle. Brain Res. 9: 288-311.

Moushegian, G., A. Rupert, and R. Galambos (1962). Microelectrode study of ventral cochlear nucleus of the cat. J. Neurophysiol. 25: 515-529.

Moushegian, G. and A. L. Rupert (1970a). Response diversity of neurons in ventral cochlear nucleus of kangaroo rat to low-frequency tones. J. Neurophysiol. 33:351-364.

Moushegian, G. and A. L. Rupert (1970b). Neuronal response correlates of cochlear nucleus: evidence for restrictive and multiple parameter information transfer. Exp. Neurol. 29:349-365.

Moxon, E. C. (1967). Electric stimulation of the cat's cochlea: a study of discharge rates in single auditory nerve fibers. Masters Thesis. M.I.T., Cambridge, Mass.

Moxon, E. C. (1973). Personal communication.

Noort, J. van (1969). The structure and connections of the inferior colliculus. Van Gorcum & Corp., Assen.

Osen, K. K. (1969a). The intrinsic organization of the cochlear nuclei in the cat. Acta Oto-Laryng. 67: 352-359.

Osen, K. K. (1969b). Cytoarchitecture of the cochlear nuclei of the cat. J. Comp. Neur. 136: 453-484.

Osen, K. K. (1970). Course and termination of the primary afferents in the cochlear nuclei of the cat: an experimental anatomical study. Arch. Ital. Biol. 108: 21-51.

Pfalz, R. K. J. (1962). Centrifugal inhibition of afferent secondary neurons in the cochlear nucleus by sound. J. Acoust. Soc. Am. 34: 1472-1477.

Pfeiffer, R. R. (1966a). Classification of response patterns of spike discharges for units in the cochlear nucleus: tone-burst stimulation. Exptl. Brain Res. 1: 220-235.

Pfeiffer, R. R. (1966b). Anteroventral cochlear nucleus: waveforms of extracellularly recorded spike potentials. Science 154: 667-668.

Pfeiffer, R. R. and N. Y. S. Kiang (1965). Spike discharge patterns of spontaneous and continuously stimulated activity in the cochlear nucleus of anesthetized cats. Biophys. J. 5: 301-316.

Pirsig, W. (1968). Regionem, Zelltypen and Synapsen im ventralen Nucleus cochlearis des Meerschweinchens. Arch. Klin. Exp. Ohr, Nas., Kehlk. Heilk. 192:333-350.

Pirsig, W. and R. K. J. Pfalz (1967). Neurone im Nucleus cochlearis ventralis, die von homolateral durch elektrischen Reiz an der Schneckenbasis windung erregt wurden: Zentrifugale Hemmung durch kontralaterale Beschallung (Meerschweinchen). Arch. klin. exp. Ohr.-, Nas.-,u. Kehlk.-Heilk. 189: 135-157.

Powell, T. P. S. and W. M. Cowan (1962). An experimental study of the projection of the cochlea. J. Anat. 96: 269-284.

Powell, T. P. S. and S. D. Erulkar (1962). Transneuronal cell degeneration in the auditory relay nuclei of the cat. J. Anat. 96: 249-268.

Radionova, E. A. (1971). Two types of neurons in the cat's cochlear nucleus and their role in audition. In: Sensory Processes at the Neural and Behavioral Levels, G. V. Gershuni (Ed.), Academic Press, New York. pp. 135-155.

Ranck, J. B., Jr. (1975). Which elements are excited in electrical stimulation of mammalian central nervous system: a review. Brain Res. 98: 417-440.

Ramón y Cajal, S. (1909). Histologie du système nerveux de l'homme et des vertébrés. Maloîne, Paris.

Rasmussen, G. L. (1931). Macrotome for cutting brains into blocks of uniform thickness and at any desired angle. Anat. Rec. 48: 61-62.

Rasmussen, G. L. (1946). The olivary peduncle and other fiber projections of the superior olivary complex. J. Comp. Neur. 84: 141-219.

Rasmussen, G. L. (1960). Efferent fibers of the cochlear nerve and cochlear nucleus. In: Neural Mechanisms of the Auditory and Vestibular Systems, G. L. Rasmussen and W. E. Windle (Eds.), Thomas, Springfield, Ill. pp. 105-115.

Rasmussen, G. L. (1967). The efferent connections of the cochlear nucleus. In: Sensorineural Hearing Processes and Disorders. Graham (Ed.), Little Brown and Co., Boston. pp. 61-75.

Reese, T. S. (1966). Fine structure of nerve endings in the ventral cochlear nucleus of normal and expermental animals. Anat. Rec. 154: 408-409.

Rodieck, R. W., N. Y. S. Kiang, and G. L. Gerstein (1962). Some quantitative methods for the study of spontaneous activity of single neurons. Biophys. J. 2: 351-368.

Romand, R. (1976). Personal communication.

Rose, J., R. Galambos and J. R. Hughes (1957). Tonotopic organization of frequency sensitive neurons in the cochlear nuclei of the cat. Anat. Rec. 127: 358.

Rose, J., R. Galambos, and J. R. Hughes (1959). Microelectrode studies of the cochlear nuclei of the cat. Bull. of the John Hopkins Hospital. 104: 211-251.

Rose, J. E., J. F. Brugge, D. J. Anderson and J. E. Hind (1967). Phase-locked response of low-frequency tones in single auditory nerve fibers of the squirrel monkey. J. Neurophysiol. 30: 769-793.

Rose, J. E., L. M. Kitzes, M. M. Gibson and J. E. Hind (1974). Observations on phase-sensitive neurons of the anteroventral cochlear nucleus of the cat: nonlinearity of cochlear outputs. J. Neurophys. 37: 218-253.

Rupert, A. L. and G. Moushegian (1970). Neuronal responses of kangaroo rat ventral cochlear nucleus to low-frequency tones. Exp. Neurol. 26:84-102.

Sando, I. (1965). The anatomical interrelationship of the cochlear nerve fibers. Acta Oto-Laryngol. 59: 417-436.

Starr, A., and J. S. Wernick (1968). Olivocochlear bundle: effects on spontaneous and tone-evoked activities of single units in cat cochlear nucleus. J. Neurophysiol. 31: 549-564.

Stotler, W. A. (1963). Patterns of innervation of the cochlear nucleus complex of the cat. Anat. Rec. 145: 289.

Stotler, W. A. (1949). The projection of the cochlear nerve on the acoustic relay nuclei of the medulla. Anat. Rec. 103: 561.

Svaetchin, G. (1951). Analysis of action potentials from single spinal ganglion cells. Acta Physiol. Scand. 24, Suppl. 86:23-57.

Terzuolo, C. A. and T. Araki (1961). An analysis of intra-versus extracellular potential changes associated with activity of single spinal motoneurons. Annals N. Y. Academy of Sciences 94: 547-558.

Tsuchitani, C. and J. C. Boudreau (1964). Wave activity in the superior olivary complex of the cat. J. Neurophysiol. 27: 814-827.

Tsuchitani, C. and J. C. Boudreau (1966). Single unit analysis of cat superior olive S-segment with tonal stimuli. J. Neurophysiol. 29:684-697.

Tsuchitani, C. and J. C. Boudreau (1967). Encoding of stimulus frequency and intensity by cat superior olive S-segment cells. J. Acoust. Soc. Am. 42:794-805.

Walsh, B. T., J. B. Miller, R. R. Gacek and N. Y. S. Kiang (1972). Spontaneous activity in the eighth cranial nerve of the cat. Intern. J. Neurosci. 3:221-236.

Warr, W. B. (1966). Fiber degeneration following lesions in the anterior ventral cochlear nucleus of the cat. Exptl. Neurol. 14: 453-474.

Warr, W. B. (1969). Fiber degeneration following lesions in the posteroventral cochlear nucleus of the cat. Exptl. Neurol. 23: 140-155.

Warr, W. B. (1972). Fiber degeneration following lesions in the multipolar and globular cell areas in the ventral cochlear nucleus of the cat. Brain Res. 40: 247-270.

Warr, W. B. (1976). Personal Communication.

Webster, D. B., R. F. Ackerman and G. C. Longa (1968). Central auditory system of the kangaroo rat Dipodomys merriami. J. Comp. Neur. 133:477-494.

Wiederhold, M. L. and N. Y. S. Kiang (1970). Effects of electrical stimulation of the crossed olivocochlear bundle on single auditory-nerve fibers in the cat. J. Acoust. Soc. Am. 48: 950-965.